TRACKING AND CONTROL IN MULTI-FUNCTION RADAR

by

Joseph Mackay Butler

A thesis submitted to the University of London for the Degree of

Doctor of Philosophy in Electronic Engineering

Department of Electronic and Electrical Engineering

University College London

August 1998

ABSTRACT

The phased array multi-function radar is an effective solution to the requirement for simultaneous surveillance and multiple target tracking. However, since it is performing the jobs usually undertaken by several dedicated radars its radar time and energy resources are limited. For this reason, and also due to the large cost of active phased array antennas, it is important for the strategies adopted in the control of the radar to be efficient. This thesis investigates and develops efficient strategies for multi-function radar control and tracking. Particularly the research has focused on the use of rotating array antennas and simultaneous multiple receive beam processing.

The findings of the research challenge the traditional view that three or four fixed (static) array faces is the best antenna configuration for a multi-function radar system. By developing novel methods for the comparison of systems utilising different antenna configurations it is shown that a rotating array multi-function radar performs the surveillance function with a greater efficiency in its use of radar time than a static array system. Also, a rotating array system benefits from the ability to distribute the radar resources over the angular coverage in a way that is impossible with a static array system. A novel strategy is presented to achieve this, which allows the rotating array system to better support the realistic situation of a high concentration of radar tasks in a narrow angular sector.

It is shown that the use of broadened transmit beams coupled with simultaneous multiple narrow receive beams can eliminate the compromise on radar beamwidth between the surveillance and tracking functions that is associated with multi-function radars. This technique would allow construction of multi-function radar systems with narrow beamwidths, giving improved tracking performance, without extending search frame times excessively.

Efficient tracking strategies for both static array and rotating array multi-function radars are developed. They are applied through computer simulation to demonstrate tracking of highly manoeuvrable targets with a narrow beam multi-function radar. Track robustness is attained through the use of multiple beam track updating strategies at little cost in terms of radar time.

To my Mother and Father.

ACKNOWLEDGEMENTS

Firstly, my thanks must go to Professor H.D. Griffiths. His help and supervision throughout this research have been unending, and he has made my stay at UCL both pleasant and memorable. Thanks too must go to Dr A.R. Moore and Mr W.A. Levett from DERA Portsdown, who have aided and encouraged me since I first entered the field of radar. Without their active support, completion of this research would not have been possible. I would also like to express my gratitude to Professor K. Milne and Professor R. Benjamin for their expert advice and stimulating discussions during their visits to UCL.

Also at DERA Portsdown, thanks are due to G. Rhees, E. Brice, P. Donnely, and in particular to M. Deighton and P. Clements whose help has gone beyond that which could have been expected. At BAeDS my thanks go to W.Stafford and S.Noyes.

Finally, I would like to give thanks to the friends and colleagues who have contributed either directly or indirectly to this thesis, and have put up with me throughout it. Particularly thanks go to R. Bullock, G. Davidson, W. Lee, H. Read and L. Vinagre from the Antennas and Radar Group at UCL, C. Andrew, R. Maunder, A. Ridehalgh and F. Read, for their complete lack of interest in the field of radar and the healthy antidote which they provided, my ever patient family E. Butler, J. Butler, E. Cooper and D. Cooper, and last to V.A. Byram who has proof read this thesis, and has helped more and put up with more than all of the above.

TABLE OF CONTENTS

LIST OF FIGURES

LIST OF PRINCIPAL SYMBOLS AND ACRONYMS

Symbol	*Definition*	*Units*
A_{beam_ruv}	area of beam in rotating UV space	m^2
A_{beam_uv}	area of beam in UV space	m^2
A_{sector_ruv}	area of surveillance sector in rotating UV space	m^2
A_{sector_uv}	area of surveillance sector in UV space	m^2
az_{max}	maximum azimuth extent of surveillance sector	m^2
A_r	effective aperture area of the antenna on receive	m^2
az	azimuth	radians
az_{min}	minimum azimuth extent of surveillance sector	radians
B	bandwidth of receiver	Hz
bw	antenna 3dB beamwidth	radians
C_n	receiver correction factor	
DERA	Defence Evaluation and Research Agency	
dt	dwell time in each beam direction	s
$E(\theta)$	antenna gain in direction θ	dB
el	elevation	radians
el_{max}	maximum elevation extent of surveillance sector	radians
el_{min}	minimum elevation extent of surveillance sector	radians
E_n	weighting function for each element	
ERP	Effective Radiated Power	W
E_x	smoothed, normalised residual in the x coordinate, between the target predicted and measured position	
f_d	Doppler frequency	Hz
GaAs	Gallium Arsenide	
G_r	gain of the antenna on receive	dB
G_t	gain of the antenna on transmit	dB
H	measurement matrix relating target state to target measurements	
IMM	Interactive Multiple Model	
JPDA	Joint Probabalistic Data Association	
J_x	normalised distance between the target predicted and measured position	
J_y	normalised distance between the target predicted and measured position	
J_z	normalised distance between the target predicted and measured position	
k	Boltzmann's constant	JK^{-1}
K	Kalman filter gain matrix	
MESAR	Multi-function Electronically Scanned Adaptive Radar	
MHT	Multiple Hypothesis Tracker	
MoD	Ministry of Defence	

MTI	Moving Target Indication	
n	number of pulses integrated	
N	number of elements, or subarrays in the array	
n_beams	number of surveillance or tracking beams	
O	occupancy of the task or function	%
Occ_{search}	occupancy of the search function	%
P'	covariance of predicted target state	
$\hat{P}$	covariance of smoothed target state	
P_{av}	average power	W
P_r	received power	W
PRF	Pulse Repetition Frequency	Hz
PRI	Pulse Repetition Interval	s
P_t	transmitted power	W
Q	plant noise term	
R	covariance of measured target state	
r, R	slant range of the target	m
RADAR	RAdio Detection And Ranging	
RCS	Radar Cross Section	m^2
R_{max}	maximum detection range	m
Rx	receive	
S	received signal power at the radar	W
S_{min}	minimum detectable signal	W
SNR, snr	signal to noise ratio	dB
snr_0	signal to noise ratio on array broadside	dB
snr_φ	signal to noise ratio at a scan angle of φ	dB
t	time	s
T	receiver temperature	K
TAS	Track And Scan	
t_{fn}	function time of the task or function	s
t_{fr}	frame time of the task or function	s
T_r	time taken by the pulse to travel to the target and return	s
TWS	Track While Scan	
Tx	transmit	
u	coordinate of UV space antenna coordinate system	
$\mathbf{u_r}$	coordinate of rotating UV space antenna coordinate system	
v	coordinate of UV space antenna coordinate system	
V_n	signal from the n^{th} channel	V
$\mathbf{v_r}$	coordinate of rotating UV space antenna coordinate system	
W_n	complex weight applied to a subarray or element	
X'	forecast target state	

$\hat{X}$	smoothed estimate of target state	
X_{res}	residual between predicted target position and measured target position	m
Y_{res}	residual between predicted target position and measured target position	m
Z	measured target state	
Z_{res}	residual between predicted target position and measured target position	m
ω	antenna rotation rate	radians/s
Φ	target transition matrix	
Ω_{beam}	solid angle of beam	steradians
Ω_{sector}	solid angle of surveillance sector	steradians
σ_x	standard deviation of the tracker prediction error	radians
σ_z	standard deviation of the measurement error	radians
δ	element spacing	m
$\Delta\Phi$	phase difference	m
φ	scan angle away from array normal	radians
λ	radiated wavelength	m
λ	smoothing constant for tracker residual estimate	
θ_3	3dB beamwidth	radians
θ_φ	beamwidth at scan angle of φ	radians
σ	monopulse accuracy	radians
σ_φ	monopulse accuracy at scan angle φ	radians

1 INTRODUCTION

1.1 Historical background

A Radar (*Ra*dio *D*etection *A*nd *R*anging) transmits radiowaves and measures the returned energy scattered by distant targets. Radar technology was invented some time before the beginning of the second world war when the benefit of the wireless technology to the air defence of Great Britain became apparent to the Ministry of War. There ensued a rapid period of development throughout the war, in which radar played a vital part in detecting both air and sea borne targets for the Royal Air Force and Royal Navy, making a significant contribution to the war's outcome.

Throughout World War II, as radar systems were developed with increasing functionality and performance, so the enemy's ability to counter the technology increased. This situation has continued, resulting in the invention of new techniques such as jamming, chaff, decoys and stealth. Also, the requirements asked of the radar have increased, such as the number of targets that must be tracked, and the precision with which this task must be carried out. The result is highly sophisticated modern day radars, which remain a vital tool for both civil and defence applications.

Early systems, at the beginning of the war, could simply provide angle and range estimates for detections made. Later, after the invention of the first plan position indicator (PPI) displays, plot tables were used to enable skilled operators to maintain track on targets.

The 1960s saw the widespread development of phased arrays which allowed electronic (rather than mechanical) steering of the antenna beam; some nineteen phased array projects starting in that decade [Billam, 1985]. This technology, with the emergence of digital control, allowed the automatic operation and control of phased array radars, and the advent of the multi-function radar, in which the electronically scanned antenna is multiplexed between many different tasks.

Since then, both microwave and digital technology have advanced at an extremely rapid

pace. New radars are emerging which are capable of adapting many aspects of their operation to the scenario and environment in which they are operating, under computer control. The flexibility provided by a software controlled phased array antenna supported by adaptive waveforms, signal processing and beamforming allows the modern multi-function radar to modify almost any aspect of its radar performance on a task to task basis. Such flexibility permeates all aspects of multi-function radar design and gives the potential to optimise performance and efficiency to meet weapon system design needs.

Whilst the concept of phased array multi function radars has been around for many years, the realisation of their full potential has been constrained by the availability of technology at realistic prices. It is only relatively recently that technology has progressed to a point where the software and processing power, and the antenna components have both become readily available to provide multi-function radars with the full flexibility that electronically adaptable phased arrays can offer.

1.2 Objectives

The aim of this work is to develop and investigate novel techniques for the control and tracking of a multi-function radar, with the objective of improving the overall efficiency and performance of the sensor. The emphasis will be particularly on improving the performance of the tracking function.

With the capability of performing multiple functions with a single sensor come drawbacks. Firstly, the total radar time-budget from this single sensor must be shared between each of the functions. This means that radar time is at a premium and in many practical scenarios, less radar time is available than is ideally required. Techniques that are efficient in their use of radar time are thus crucial, and this forms a significant focus of the work.

Secondly, a single sensor performing all of the functions normally undertaken by several other sensors, each dedicated solely to a single function, must inherently contain compromises. The most significant of these in the multi-function radar is the beamwidth that is used for the search and tracking functions. This normally results in a broader beamwidth being used than is ideal for the tracking function to ensure the search is

performed adequately. This is also addressed within the study.

It is likely that multi-function radars will exploit rotation of the array antenna, to avoid the need for the three or more phased array faces that are required for full hemispherical coverage. This will give a significant advantage in terms of cost. The study aims to establish the system implications of this, both for the tracking and surveillance functions, and to determine efficient techniques for control of the rotating array multi-function radar. This should enable a valuable comparison of the efficiency and performance of static and rotating systems.

New multi-function radars offer a wide variety of adaptivity and flexibility that may be controlled in real time, possibly as a response to one or more previous radar detections. In order to track targets with a wide range of dynamic capability reliably and efficiently, the algorithms for tracking and control must be highly adaptive and rapidly responsive. Techniques developed aim to exploit the many degrees of freedom that future multi-function radars will bring, such as adaptable update rate, antenna beamwidth, transmitted energy and frequency. Findings will build upon the research undertaken for the MESAR (Multi-function Electronically Scanned Adaptive Radar) experimental multi-function radar, and it is hoped that this work will result in improved techniques and algorithms being implemented in that radar.

1.3 Thesis Layout

Chapter 2 gives an introduction to some of the background topics pertinent to Multi-function radar. This includes a short definition of a multi-function radar and the functions it may be expected to undertake, as well as a brief introduction to some of the underlying theory of radar, phased arrays and multi-function radar.

Chapter 3 then gives a detailed introduction to the MESAR experimental multi-function radar, to which much of this research will be applicable. MESAR is an advanced experimental active phased array radar which has been developed collaboratively between the Defence Evaluation and Research Agency and British Aerospace Defence Systems (formerly Siemens Plessey Systems) since the early 1980s. The fully functional radar was completed in early 1993, and has been used as a test-bed for experimentation and demonstration of techniques. This chapter indicates the performance and capability

of a current, state of the art multi-function radar system, and gives a background to what has been achieved already and what flexibility remains to be harnessed.

Chapter 4 investigates the impact of two digital beamforming techniques that will be available in the future version of the MESAR radar, MESAR II. These are the generation of variable beamwidth, and simultaneous multiple receive beam processing. Novel methods are developed to allow an accurate analysis of the search time- budget for a sectored surveillance volume, for both static and rotating array multi-function radars. Two important conclusions are drawn out from the analysis made. Firstly it is shown that the traditional view that 3 or 4 fixed array faces is the best antenna configuration for a multi-function radar is not correct, and that rotating array systems can perform the surveillance function a great deal more efficiently. Secondly, it is demonstrated that the inherent compromise in beamwidth normally associated with a multi-function radar does not necessarily hold with a simultaneous multiple receive beam system. The search and track beamwidth could be de- coupled and each be optimised to their task.

Chapter 5 addresses the topic of resource management and task scheduling of a multi-function radar. It covers the objectives of resource management and task scheduling in multi-function radar, and presents figures of merit by which a scheduling and resource management system may be judged. It also covers the complications that arise with rotation of the array antenna, and presents a novel algorithm that copes with these complications. Models are presented that have been developed for both static and rotating array multi-function radars based around a task scheduler centered architecture, which are used to evaluate both scheduler performance against the proposed objectives.

Chapter 6 presents a detailed investigation of a static and rotating array adaptive tracking of manoeuvring targets. The objective of the work presented is to develop an effective tracking strategy against manoeuvring targets that is efficient in its use of the multi-function radar's resources. Models of both static and rotating array adaptive trackers are developed, and then applied through Monte Carlo simulation to determine an efficient signal to noise ratio to aim for when updating tracks. It is shown that multiple beam track updates are necessary to enable efficient and robust tracking, and a strategy for multiple beam update tracking is suggested. The impact of tracking using a narrow beamwidth is assessed, and successfully demonstrated through simulation.

Chapter 7 gathers together the most significant conclusions of chapters 4, 5 and 6, and presents a short assessment of a narrow beamwidth, rotating array multi-function radar which utilises simultaneous multiple beam processing. Its radar time-budget resources and detection performance are compared to a static array system, similar to the current MESAR system. The viability of the multiple beam rotating array system is demonstrated, and it is shown to have to have very favourable characteristics.

Finally chapter 8 presents the conclusions of the work so far, and suggest further work that would be beneficial in the area of this study.

1.4 Novel Aspects

The novel aspects of this thesis are contained in chapters 4, 5, 6 and 7, and are summarised here. In chapter 4, a new analysis of multi-function radars with different array antenna configurations and of simultaneous multiple beam processing has been made, utilising a novel method for accurate estimation of the surveillance resource requirements. Chapter 5 proposes a set of objectives for the resource management of a rotating array radar, which may be used to judge the effectiveness of future strategies. The existing MESAR scheduling algorithms are validated against these objectives. A novel rotating array scheduler has been developed and assessed, which takes advantage of a previously unrecognised ability of rotating array multi-function radar systems.

In chapter 6 a novel multiple beam, rotating array adaptive tracker is developed. This, along with a static array tracker based on that used in the MESAR radar, are applied in a Monte Carlo simulation to determine the most efficient operating parameters. The result is a comparison of the tracking performance and efficiency of static and rotating array multi-function radars. The capability of such systems operating with narrower beamwidths than those currently used is demonstrated against the benchmark tracking problem developed by Blair and Watson [Blair et al, 1994].

Chapter 7 demonstrates the viability of a narrow beamwidth multi-function radar system, and the benefits such a system would give.

2 AN OVERVIEW OF MULTI-FUNCTION RADAR

2.1 Background

This chapter gives an introduction to some of the topics pertinent to Multi-function radar. The functions of a multi-function radar for naval air defence are described in section 2.2 to give a short background and a 'time-line' of a multi-function radar's operation from surveillance through to missile interception.

Section 2.3 then gives a brief introduction to some of the underlying theory of radar, phased arrays and multi-function radar, which is relevant to this thesis. Finally, in sections 2.4 and 2.5, the benefits and drawbacks of using a multi-function radar rather than several specialised radars are discussed.

The multi-function radar is equivalent to a suite of radars, employed for some application such as air defence. To fulfil its purpose it performs several different functions which previously would have been undertaken by many different, dedicated radars. The exact functions that are undertaken are obviously dependent upon the application, but at least, the multi-function radar will provide search coverage and concurrent tracking of multiple targets.

The multi-function radar utilises one or more phased array antennas to give one or more electronically steerable beams, in azimuth, elevation or both. These beams are multiplexed between the different tasks in different directions under automatic digital control, so that the total radar time is shared amongst the functions.

At its simplest level a multi-function radar consists of the following:

i. a phased array antenna, (including the associated beamforming and microwave transmitting and receiving hardware)

ii. signal processing

iii. radar control computer

iv. waveform generator

It is the coupling of an electronically steerable beam, adaptive waveform generation and signal processing, with real time automatic computer control that gives the multi-function radar such power.

Many different types of antennas are utilised in multi-function radars. The antenna normally consists of one or more planar phased arrays, although cylindrical or spherical arrays have been used. It may be mechanically rotated or use fixed or positioned arrays, relying solely on electronic scanning to give the volume coverage.

It is essential to realise at the outset the importance that time plays in a multi-function radar. The multi-function radar is trying to do the job of many radars, each of which could dedicate all of its radar time to its own task whether it be short range surveillance or tracking for example. For this reason it is imperative that the multi-function radar's time is not wasted but is distributed as efficiently as is possible. Barton, [Barton, (1988)] recognises this, and gives it as the second of two critical design factors in multi-function radar;

- Choice of radar frequency, high enough to provide the narrow tracking beam, and low enough to permit rejection of clutter during volume search modes.
- Budgeting of radar time, to provide the dwell times necessary for clutter rejection in both search and tracking modes.

Billam [Billam, 1997a] discusses the issue of radar time in multi-function radar specifically in a recent paper. It is one of the dominant factors in the system design of a multi-function radar, and thus any techniques that are efficient with radar time are of prime importance.

2.2 Multi-function radar functions

The functions that a multi-function radar must undertake are specific to its application. Multi-function radars are utilised in land, sea and air based platforms. To date they are primarily used for military applications due to the high costs. A ship-borne or land-based multi-function radar may take over the functions of surface search, short, medium, and long range search, multiple target tracking, weapon control and aircraft control. An airborne multi-function radar may also take over the functions of navigation or terrain

mapping/avoidance.

The primary application of this research study is naval air defence; thus this will be used as an example here, and often inherently assumed throughout the rest of the thesis. Nevertheless, research presented is often still pertinent to land and air based multi-function radar.

Figure 2-1 below shows the functions that a multi-function radar performing naval air defence may undertake. The main functions are surveillance, tracking and missile guidance. A summary of these functions is given in sections 2.2.1 to 2.2.4 below. Other functions may well be needed, such as target recognition with specific requirements such as the need for long radar waveforms or very precise scheduling.

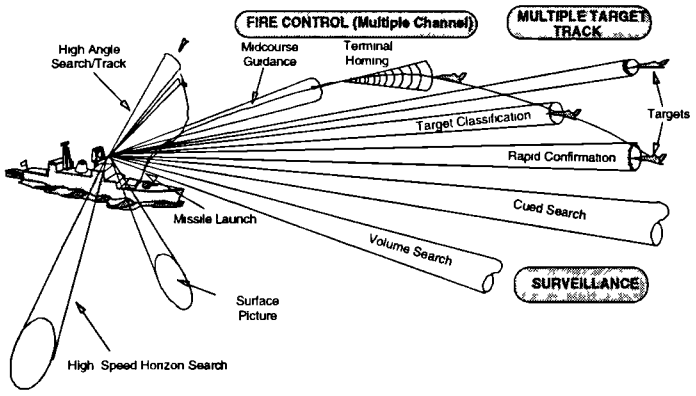

Figure 2-1 Functions of a multi-function radar for naval air defence

2.2.1 Search

The aim of the multi-function radar during search, is to survey a given volume of space within a given frame time and with a given detection performance, set by the operational requirement. It must do this with the lowest number of false alarms possible. Additionally, if the search function is being used for track while scan purposes, requirements in the positional accuracy of surveillance detections may be included.

In practice this requirement is often very difficult to achieve due to restrictions on the time-budget available to undertake the search function. Various strategies may be adopted with the aim of using the radar time optimally. This is discussed later in section 2.3.3.1. To minimise the radar time-budget for surveillance, the search volume will almost certainly be divided into several sectors, with the waveforms and frame times for each sector that are matched to the performance required.

2.2.2 Plot confirmation

A significant advantage of the multi-function radar is that it can rapidly confirm detections that are made during the search function, in order to distinguish them from false alarms due to thermal noise. This function is termed plot confirmation and is essential in minimising the reaction time of the multi-function radar.

Generally, a 'look back' is used with a waveform that has similar parameters to the original surveillance waveform that made the detection, to ensure that the target is detected again. The interval between the surveillance detection and the look back needs to be minimised to avoid the target decorrelating and hence not being detected. Typical look back times are between 10ms and 100ms.

Additionally the plot confirmation look back may be used to attempt to rapidly resolve an ambiguity in range or velocity by modifying the PRF of the waveform.

This technique is only used on detections that do not associate with existing tracks in the system. On each surveillance detection the radar must measure the position of the detection and compare this with the expected positions of targets that it is already holding in track (plot association). If the detection correlates with a predicted target position, then that information may be used as a plot to update that track. If not then a look back would be requested.

2.2.3 Track initiation

Upon a successful confirmed detection, track initiation is undertaken to establish a track of sufficient accuracy (in terms of position and velocity) that it may be handed to the track maintenance function. The aim of track initiation is to establish a track of a given accuracy in the shortest time possible.

The combination of the plot confirmation and track initiation functions provides the earliest reaction times and target threat assessment for weapon system needs. In comparison to a suite of dedicated radars the delay between initial detection can be significantly larger. In practice several detections are required from a dedicated surveillance radar (to fulfil an n out of m criterion) in order to obtain the low false alarm rates that are required before cueing the tracking radar. This requires several sweeps of the surveillance antenna, which is likely to take several seconds. The dedicated tracking radar must then perform a search to acquire the target, since the surveillance radar that

has cued it has a broader beam. This whole process may be achieved in the quickest time by a multi-function radar that may direct the beam at will.

2.2.4 Track maintenance

The multi-function radar is capable of undertaking two basic means of tracking; track-while-scan (TWS) and track-and-scan (TAS). Track-while-scan simply feeds plots from the surveillance function to the track extractor, so that the tracks are updated at the surveillance rate, as with conventional rotating surveillance radars (although the plots may not be updated at regular intervals with a multi-function radar, due to the random nature of the scan). Track-and-scan, sometimes referred to as de-coupled tracking, updates tracks independently, and at a rate higher than the surveillance rate. This therefore implies an additional load on the radar time-budget.

In general track-while-scan would only be used against low priority targets, or targets for which the surveillance update rate would give sufficient accuracy. The majority of targets of interest to a weapon system are likely to have the potential to manoeuvre or may be closing rapidly. It is most likely that they will have high update rate or accuracy requirements, and will therefore be tracked using track-and-scan. Thus it is track-and-scan that is the main consideration of this study.

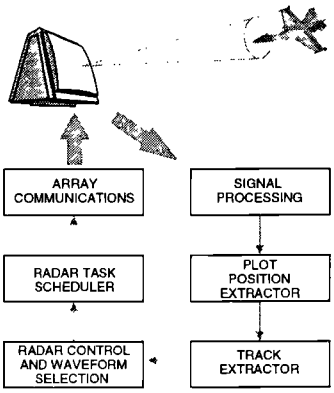

Figure 2-2 The closed loop multi-function radar tracker

The multi-function radar tracker is a closed loop, as shown in Figure 2-2. For successful multi-function radar target tracking the inter-related functions of plot to track association, track filtering and prediction, and radar assignment must all work seamlessly. If, for example, an incorrect waveform, or an update interval that is too long, is chosen on the basis of the tracker output, then the next update will be of poor quality, or may fail to illuminate the target.

2.2.5 Functional flexibility

The enormous flexibility of the multi-function radar system also allows it to be reconfigured for several different applications. For example a ship borne multi-function radar could be configured for medium range air defence as its main role. By changing the configuration of the search volume, the digital waveforms selected, the digital signal processing applied, and the control algorithms, the same radar could be applied to long range air defence, or to ballistic missile defence. This may be incorporated as a simple software, or menu driven option. Perhaps even more significantly, a major benefit of the multi-function radar is that it can in principle be rapidly reconfigured for unforeseen applications and eventualities.

2.3 Underlying theory of multi-function radar

A multi-function radar is a specific, and advanced type of radar. As such the well understood theory from radar and phased array systems is applicable, but also, as has been pointed out by Billam ([Billam, 1994]), new theory is developing pertinent purely to multi-function radar systems. This is exemplified by the two books published on this subject in recent years purely on multi-function radar system aspects ([Billeter, 1989], [Sabatini & Tarantino, 1994]). In some respects it could be said that the system level theory of multi-function radar - its application and control - is somewhat behind the capability that the various technologies involved in a multi-function radar suite can potentially offer. This may lead to a highly sophisticated and adaptable system being utilised in an essentially conventional way, simply by virtue that a well developed theory is not available at the radar design stage.

This section introduces the areas of radar theory and phased array theory relevant to this study, before giving a background to some of the system aspects of multi-function radars.

2.3.1 Radar systems

The subject area of radar is vast, and well covered in many texts. Notable introductions to the subject are given by Barton, Levanon and Skolnik ([Barton, 1988], [Levanon, 1988], [Skolnik, 1981]). The purpose of this section is to give only the broadest account of a complete radar system, and to present a brief introduction to the techniques and

equations that are applied within the scope of this study.

A highly simplified block diagram of a typical radar is shown in Figure 2-3 below.

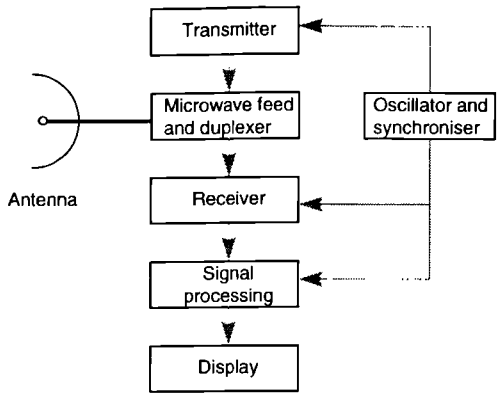

Figure 2-3 A simplified block diagram of a typical radar

A pulsed oscillator feeds a low power RF signal to a transmitter. This signal is amplified, and possibly modulated. The resultant signal is passed to the antenna for radiation into space. The antenna directs the transmit energy, in the desired direction. A target, illuminated by the energy radiated from the antenna, will scatter the energy in all directions. In general, only a very small amount of the energy will be re-radiated back in the direction of the antenna.

This small amount of energy, which competes with the energy reflected from other sources such as the land or sea, or external interference sources, re-enters the antenna. Received signals are amplified and generally mixed down to a lower frequency in the receiver before being fed to the signal processor.

The benefits of a highly directional antenna are clear. Firstly, both the energy that is transmitted, and that which is received, is maximised in the required direction. Secondly, the interference from other directions is minimised. Lastly, a narrow main beam formed by a highly directive antenna allows a high angular measurement and resolution capability.

The signal processor has the job of trying to recover the wanted information, if any, from the signal it is fed. It must determine, by varied means, whether a target is present or not in each radar resolution cell. It must extract information about that target, such as range, echo signal strength, angular position or Doppler velocity. If a target is detected, its range may be determined from the fundamental radar equation [2-1].

$$R = \frac{cT_r}{2} \qquad [2\text{-}1]$$

where R is the slant range of the target
c is the speed of propagation
T_r is the time taken by the pulse to travel to the target and return

Barton [Barton, 1988] gives a list of the major problem areas in radar, which, although recognised in the early days of radar, remain only partially solved today.

i. adequate signal to noise ratio in free space

ii. clutter reduction

iii. interference reduction

iv. signal selection

v. measurement accuracy

vi. size, weight, cost and reliability

It is useful to have these problems in mind when considering multi-function radar, since high performance must be attained in every one of these areas to ensure a good level of multi-function radar performance.

Often problems in one of these areas will affect the multi-function radar system in more complicated ways than a conventional radar. For example, poor clutter cancellation will lead to false detections, and subsequently to false track initiations. This, in turn, will lead to less radar time being devoted to other functions, such as surveillance, causing a drop in detection performance.

2.3.1.1 Radar range equation

The range equation is one of the most fundamental equations in radar theory. It allows the prediction of the range at which a target of given radar cross section may be detected, given basic information about the radar, the target, and the propagation path of the radiation through space. One form of this equation allows the determination of the signal strength given the range of a target:

$$S = (P_t G_t)\left(\frac{\sigma}{4\pi R^2}\right)\left(\frac{A_r}{4\pi R^2}\right) \qquad [2\text{-}2]$$

where S is the received signal power at the radar from a spherical target, of cross section σ
P_t is the power of the transmitter
G_t is the gain of the antenna on transmit
σ is the radar cross section
A_r is the effective aperture area of the antenna on receive
R is the slant range of the target

The first factor of the three in equation [2-2], is the effective radiated power in the direction of the target. The second is the fraction of this power that is intercepted by the spherical target. The final term is the fraction of the power, scattered by the spherical target, that is intercepted by the radar receiving antenna. This is more readily expressed as below.

$$S = \frac{P_t G_t G_r \lambda^2 \sigma}{(4\pi)^3 R^4} \qquad [2\text{-}3]$$

where G_r is the gain of the antenna on receive
λ is the wavelength of the transmitted signal

The physical relationship that the signal received varies with the inverse of R^4 means often tremendously high powers and highly directional antennas are required to detect targets that are far away. As air targets become faster and more stealthy it becomes increasingly difficult to detect them at sufficiently long ranges using radar.

Equation [2-3] may be rearranged to give the range at which a target may be detected, given the minimum signal strength that is sufficient for detection.

$$R_{\max} = \sqrt[4]{\frac{P_t G_t G_r \lambda^2 \sigma}{(4\pi)^3 S_{\min}}} \qquad [2\text{-}4]$$

where R_{max} is the maximum achievable detection range
S_{min} is the minimum detectable signal

In practice, the detection of a target depends not only on the signal strength returned from that target, but also on other signals with which the target signal is competing. Thus S_{min} is determined also by signals such as the noise generated in the receiver or noise from external sources such as jammers, or the residue of uncancelled clutter. This leads to advanced techniques for eliminating clutter and external interference.

2.3.1.2 Monopulse radar

For a simple radar system, that employed no angular processing techniques, the angular measurement accuracy that would be obtained is of the order of the beamwidth of the

radar. For target tracking this measurement accuracy is not sufficient, even when using a narrow pencil beam. To obtain a higher accuracy several methods exist. The most common of these is *monopulse.*

Monopulse extracts information about the angular location of a target within the radar main beam by comparing signals received in two or more simultaneous antenna beams. This technique may be used on just a single pulse, hence the name monopulse. Excellent accounts of monopulse are given in, amongst others, Skolnik ([Skolnik, 1981]), and further detail may be found in Rhodes ([Rhodes, 1959]).

Amplitude comparison monopulse employs two overlapping antenna patterns to obtain the angular error in one coordinate. These patterns may be generated either by two adjacent feeds with a reflector antenna, or in the case of a phased array, by correctly summing the outputs of each element. Figure 2-4, (reproduced from [Skolnik, 1981]), shows clearly the principle of monopulse.

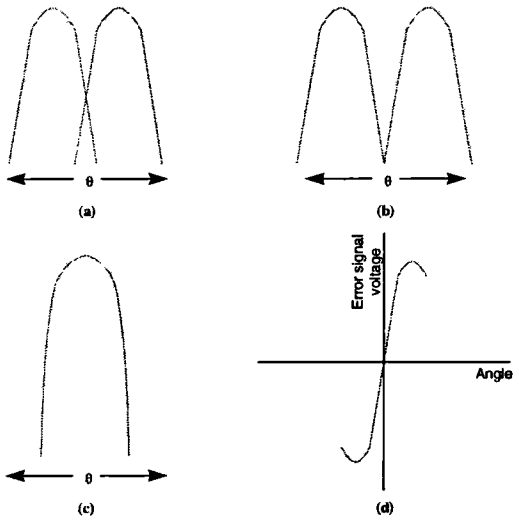

Figure 2-4 Monopulse antenna patterns and error signals. (a) overlapping antenna patterns, (b) difference antenna pattern, (c) sum antenna pattern, (d) error signal

The summation of these two overlapping patterns will generate the *sum beam,* Σ. This is the standard beam that would be used for transmission, and for detection and range measurement in receive. The difference of these two patterns will generate the *difference beam,* Δ. This beam contains the information upon reception which gives the angular position of the target. The signals received from the sum and difference patterns are combined in a phase sensitive detector to produce the error signal. If measurement of angle is required in both dimensions then, generally, two difference beams are formed as well as the sum beam, one for azimuth and one for elevation angle estimation.

The amplitude of the error is given by the ratio of the difference channel to the sum channel. The sign of the difference signal is measured by comparison of the phase between the sum and difference channels. Although the error signal is not linear, it can be accurately calibrated to estimate the target position.

In practice, with a phased array the elements are summed using different sets of weights to generate the beams. Barton [Barton, 1988], gives the optimum monopulse angle estimator for a noise only environment as that shown in Figure 2-5 below. These weighting functions are optimal in the sense that they give the maximum efficiency in the sum channel and maximum slope in the difference channel. The penalty associated with these weighting functions is the high sidelobes that are generated in the associated antenna patterns.

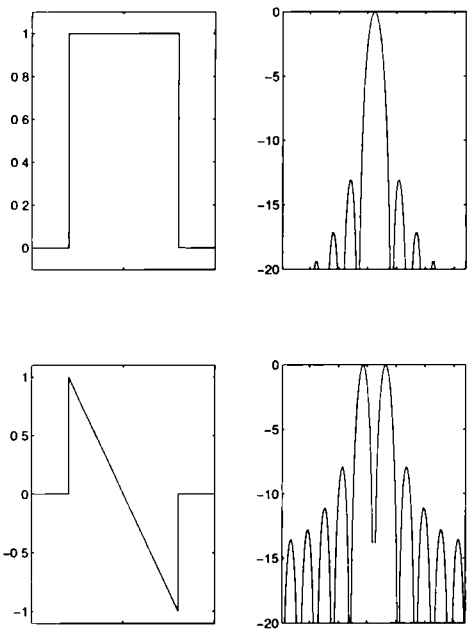

Figure 2-5 Weighting functions for minimum monopulse estimation error, and the associated beam patterns

Sidelobes as high as these can rarely be tolerated in any real application; therefore other weighting functions are employed, which always give a lower slope in the difference channel. The weighting function chosen depends upon the requirements for the sidelobe levels and the loss that can be accepted in main beam gain. An excellent paper by Harris [Harris, 1978], gives the main features and methods of calculation of many of the important weighting functions. Two of the most commonly used weighting functions used to generate a sum beam pattern are the Dolph-Chebyshev weighting function [Dolph, 1946] and the Taylor weighting function ([Taylor, 1955], [Villeneuve, 1984]).

These patterns give the minimum broadening of the main beam for a given sidelobe level. The Dolph-Chebyshev function gives an antenna pattern with all sidelobes of equal level. Taylor weighting function is an extension of this, to give an antenna pattern with only the first n sidelobes equal, thereafter decaying as sin(x)/x.

A two dimensional Taylor weighting function applied to a planar phased array is shown in Figure 2-6. The associated antenna pattern is also shown. The weighting function gives near in sidelobes of -40dB, broadening the main beam by a factor of 1.25.

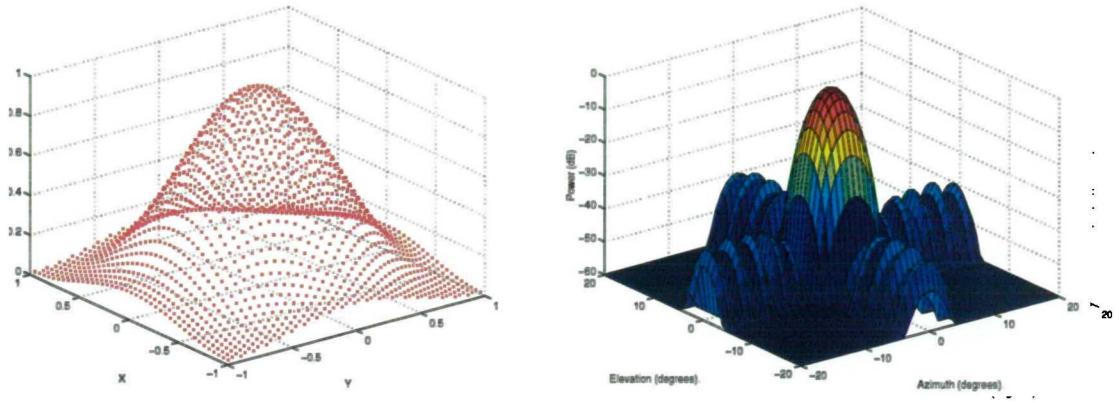

Figure 2-6(a,b) A 2 dimensional Taylor weighting function, and its associated antenna pattern

In the case of an active phased array, it is unlikely that the same weighting function will be used on transmit as in receive. Usually the transmit/receive modules require that a uniform weighting function is used when transmitting. Therefore, a heavier weighting function must be used in receive to ensure a low two-way sidelobe antenna pattern is obtained. This results in active phased arrays often operating with high antenna sidelobes in transmission, and a significantly broader beam on receive than in transmit.

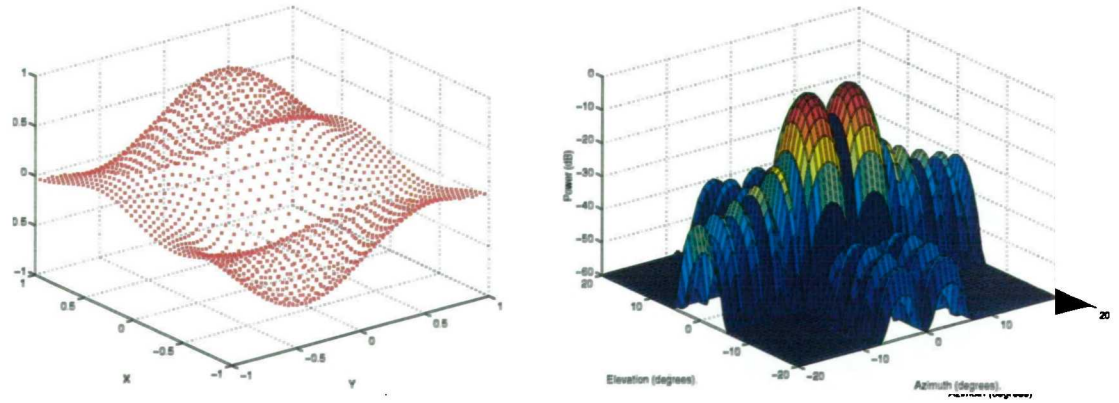

Figure 2-7 A Bayliss weighting function in one dimension and a Taylor weighting function in the other, and its associated antenna pattern

The equivalent, ideal, weighting to a Taylor pattern for generating a difference beam is the Bayliss [Bayliss, 1968] weighting function. This pattern generates the first

differential of the sum pattern that is obtained from the Taylor weighting function. A planar phased array illumination function of a Bayliss weighting function in one array dimension, coupled with a Taylor weighting function in the other dimension, and its associated antenna pattern are shown in Figure 2-7.

Monopulse was originally conceived as a technique for dedicated tracking radars, and as such was aimed at maintaining targets on the nose of the main beam, and null of the difference beam, termed beam boresight. However, when a target manoeuvres, a lag is created between the prediction that the track smoothing filter makes and the real position of the target. The magnitude of this difference is dependent upon the strength of the manoeuvre and the track update interval. As the lag increases and monopulse estimates are made away from beam boresight, so the estimates degrade in accuracy. For a multi-function radar, dividing its time between many targets, possibly with a strong manoeuvre capability, this lag, and the consequent degradation in estimate accuracy, can become significant.

Barton [Barton, 1988] gives the precision of a monopulse estimate close to beam boresight as;

$$\sigma \approx \left(\frac{\theta_3}{2\sqrt{(snr).(n)}} \right) \qquad [2\text{-}5]$$

where σ is the monopulse accuracy (rads)
θ_3 is the 3dB beamwidth
snr is the signal to noise ratio
n is the number of pulses integrated

2.3.2 Phased arrays

Skolnik (1981) defines a phased array radar as;

> ".. a directive antenna made up of individual radiating antennas, or elements, which generate a radiation pattern whose shape and direction is determined by the relative phases and amplitudes of the currents at the individual elements."

By properly varying the relative phases, it is possible to steer the direction of the radiation. The antenna elements themselves may be of any antenna type such as dipoles, or open ended waveguides. The array is made up of a number of these elements, suitably

spaced with respect to one another.

The two most common array geometries are the linear array and the planar array. The linear array consists of elements arranged in a straight line in one dimension. This will generate a fan beam, steerable in one dimension. The geometrical extension of this is the planar array, in which the elements are arranged to lie in a plane. This will generate a beam that may be steered in two dimensions. The beam may be either a fan shaped beam, or a pencil beam, depending on the shape of the array.

Less commonly, it is also possible to arrange the elements in a non planar fashion. Arrays with elements arranged on the surface of a cylinder or on the surface of a sphere have been made. An electronically scanned planar array with a narrow pencil beam that may be scanned in two dimensions is assumed in this study. Typically this type of array supports scanning to angles of up to 60° away from array broadside.

Phased arrays are split into *active* and *passive* arrays. In a passive array the power generated by a single, high power transmitter is divided by the array beamforming network. This network is also used in receive to recombine the received power. An active array utilises a transmitting/receiving module for every array element. This module usually contains the power amplification, the low noise receiver and the phase shifter.

The active array can give a high effective radiated power (ERP). The transmit and receive losses are often considerably less than those in a passive array. Also a high duty cycle can be sustained, typically up to 30% or so, compared to around 10% for a passive array. The cost of active arrays, to date, however is considerably greater than that of passive arrays. Also the transmit sidelobes are often higher than is desired.

2.3.2.1 Electronic beam steering

A beam is steered electronically through control of the signal radiated by the individual elements of an array to cause these signals to add coherently in phase in the desired beam direction [Kahrilas, 1976]. If all of the elements generate their normal pattern, with no relative phase shifts applied between each element, the composite phase front will propagate normal to the array face. This is shown below in Figure 2-8.

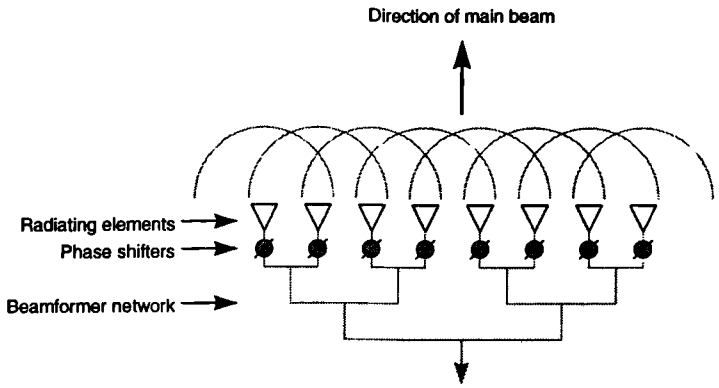

Figure 2-8 Generation of a phase front with no relative change in phase between each element

By introducing a constant, relative phase difference between adjacent elements, i.e. a phase gradient across the aperture, the beam may be steered away from the normal to the array face. This is shown in Figure 2-9.

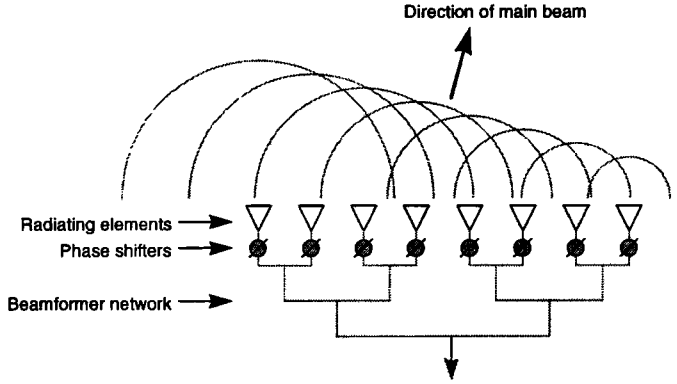

Figure 2-9 Generation of a phase front with a constant phase change between adjacent elements

The phase difference between adjacent elements must be such that the signals from each element add in phase in the desired direction. The phase difference required at each element along a linear array is shown in equation [2-6] below. It is dependent on the path length difference, $\delta.(n-1).\sin(\theta)$, that causes the signals from each element to add in phase in the desired direction.

$$\Delta\Phi = \frac{2\pi}{\lambda}\delta(n-1)\sin(\varphi) \qquad \text{for n = 1,2,..,N} \qquad [\,2\text{-}6]$$

where $\Delta\Phi$ is the phase difference (rads)
δ is the element spacing
φ is the scan angle away from array normal
λ is the wavelength
N is the number of elements in the linear array

For a planar array the phase shift in any given element is the sum of the phase shifts

required in each (orthogonal) dimension. The element spacing used within the array is usually somewhat less than half of the wavelength in order to avoid the generation of grating lobes.

The most common way to control the phase at each of the elements in a planar array is to introduce a phase shifter into the feed path to each element. These are of various types and technology. Very often digital phase shifters are employed which can control the phase among discrete values in the interval (0 , 2π). For very large arrays or when a large bandwidth signal is required a true time delay may need to be used instead of a phase shift that is limited to 2π.

The antenna pattern radiated from the array may be calculated by summing the signals radiated from each of the antenna elements;

$$E(\theta) = \sum_{n=0}^{N-1} E_n e^{j\left(\frac{2\pi}{\lambda}\right) n\delta \sin(\theta)} \qquad [2\text{-}7]$$

where $E(\theta)$ is the antenna gain in direction θ
E_n is the weighting function for each element
λ is the radiated wavelength
δ is the element spacing
N is the number of elements in the linear array

2.3.2.2 Properties of phased arrays

A fundamental property of the phased array is the change in effective aperture with scan angle. The effective aperture falls off with the cosine of the scan angle, (Figure 2-10).

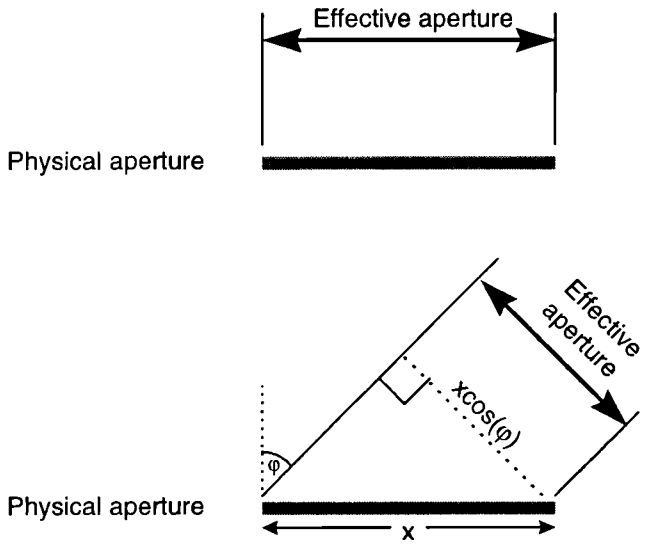

Figure 2-10 Change in effective aperture with scan angle

This causes an increase in the radar beamwidth, and a decrease in gain. The radar beamwidth broadens with the reciprocal of the cosine of the scan angle.

$$\theta_{\varphi} = \frac{\theta_3}{\cos(\varphi)} \qquad [2\text{-}8]$$

where θ_{φ} is the beamwidth at scan angle of φ
θ_3 is the 3dB beamwidth on array broadside

The reduction in antenna gain that is caused by the reduced effective aperture is proportional to the cosine of the scan angle. In a real system the antenna gain will fall off even faster due to the effects of the non-isotropic element pattern and mutual coupling. The total reduction in gain is generally closer to the cosine of the scan angle raised to the power of 1.5, although this depends on the exact elements and geometry used. Therefore the loss in the received signal power due to the two way reduction in gain, and thus the loss in the signal to thermal noise ratio, is proportional to the cosine cubed. This will be assumed throughout this study.

$$snr_{\varphi} = snr_0 \cos^3(\varphi) \qquad [2\text{-}9]$$

where snr_{φ} is the signal to noise ratio at a scan angle of φ
snr_0 is the signal to noise ratio for the same rcs target, on array broadside

The monopulse estimate accuracy when scanned away from broadside will be degraded twofold, since the beam is broader with respect to the broadside case, and the signal to noise ratio is lower with respect to the broadside case. The monopulse estimate accuracy stated in [2-5], now becomes [2-10] below.

$$\sigma_{\varphi} \approx \left(\frac{\theta_{\varphi}}{2\sqrt{(snr_{\varphi}).(n)}} \right) \approx \left(\frac{\theta_3}{2\sqrt{(snr).(n).\cos^5(\varphi)}} \right) \qquad [2\text{-}10]$$

where σ_{φ} is the monopulse accuracy at scan angle φ (rads)

From the above equations it is seen that if uniform performance, either in terms of detection capability or in terms of tracking accuracy, is required with varying scan angles, then the transmitted energy must be increased. This is discussed later in Chapter 5.

Figure 2-11 below, shows the variation in antenna beamwidth, signal to noise ratio and monopulse accuracy, as a function of scan angle.

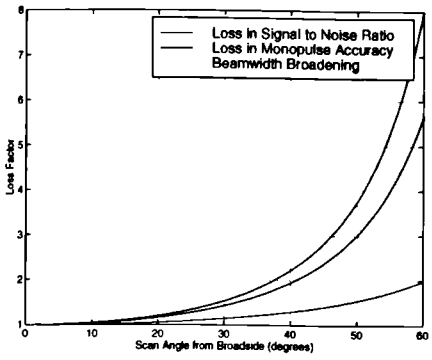

Figure 2-11(a,b) Beam broadening, loss in signal to noise ratio, and loss in monopulse accuracy as a function of scan angle

2.3.3 Multi-function radar system aspects

Here, some of the background pertinent to multi-function radars will be introduced. A detailed background to the subject may be found in one of the two texts that have been published which are dedicated to multi-function radar systems by Billeter, and Sabatini & Tarantino ([Billeter, 1989], [Sabatini & Tarantino, 1994]). There are also chapters in several texts ([Barton, 1998], [Kingsley & Quegan, 1992]). Firstly three important parameters are introduced; the *frame time, function time* and *occupancy.*

The multi-function radar's total radar time is shared between many tasks or functions. Two parameters are used to define a job such as search of a surveillance region, or the tracking of a target. The first parameter is the *frame time*, which, for surveillance, is the time over which the search of a region is made. In a tracking task, the frame time may be considered to be the track update rate.

The second parameter is the *function time*, which is the total radar time that is required to complete a job. For surveillance this would be the sum of all of the dwell times in each beam direction of a region. For a tracking job, this would be the dwell time of each update.

Thus with these two descriptors of a job, the distribution of the multi-function radar's load may be calculated. The percentage of radar time that is required to complete a task or function is called the *occupancy* of the task. This is defined below;

$$O = \frac{t_{fn}}{t_{fr}} \qquad [2\text{-}11]$$

where O is the occupancy of the task or function
t_{fn} is the function time of the task or function
t_{fr} is the frame time of the task or function

These parameters allow us to describe the distribution of the multi-function radar resources throughout the different functions and tasks.

2.3.3.1 Search

An advanced multi-function radar has the scope to modify many of its radar parameters on a beam by beam basis. Given this, it would be wrong to assume that the correct way to perform the search function with this type of radar is to replicate the operation of a conventional turning search radar. As Billeter [Billeter, 1989] states, the radar's data rate, sensitivity and type of processing need not, and usually should not, be uniform over the volume covered by the radar. The coverage volume to be surveyed by a multi-function radar is usually divided up into sectors, bounded by range and angle. Within these sectors the radar parameters may be adapted to suit the environment and the expected targets. An example of sectored coverage for a naval air defence radar is shown in Figure 2-12, below.

Regions are usually defined around an area in which the expected target characteristics and environmental characteristics are, very broadly speaking, homogeneous. The radar parameters within that region are matched to give a certain level of performance against these characteristics. For example, region 1 in the above diagram, may be characterised as searching for fast, pop-up targets in high levels of sea clutter. The radar parameters chosen to match these could utilise a short surveillance frame time, with excellent clutter processing. Another region may be characterised by searching for small cross section targets where there are high levels of barrage noise jamming. In this instance, waveforms giving a large transmitted energy and processing techniques to counter the jamming may be employed. These two examples assume highly threatening cases, of great interest to a weapons system. Equally, there may be benign regions where little radar time should be spent.

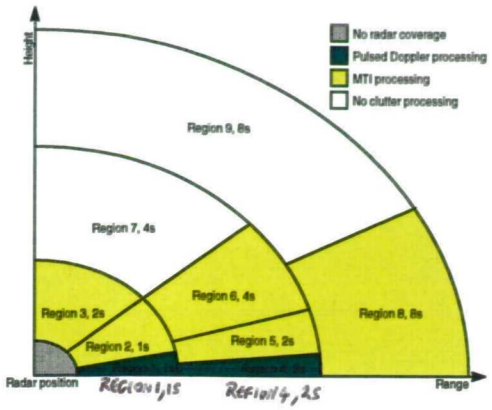

Figure 2-12 A cross section through a hemispherical search volume, showing sectored coverage with region number and frame time

The resultant search detection performance may vary with angle, and with time throughout the operational use of the radar. Figure 2-13 below shows an example of the angular and temporal variation in detection performance that may be provided by the multi-function radar. It is important for efficient utilisation of the multi-function radar, that the radar control computer allows this to occur. The radar beam scheduler must be flexible enough to cope with these variations. This is discussed in chapter 5.

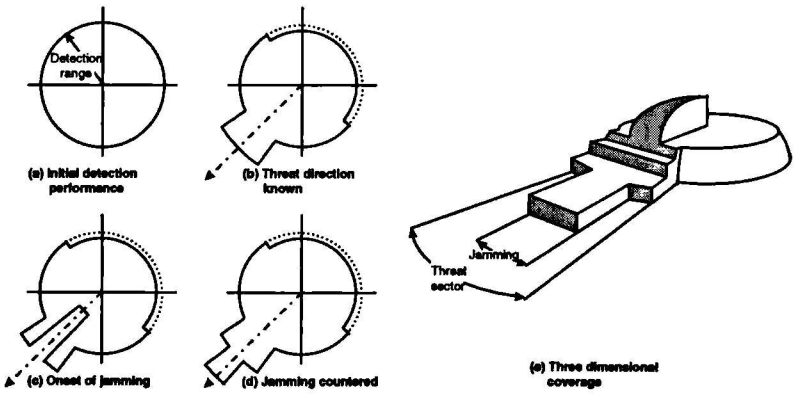

Figure 2-13(a-e) Angular and temporal variation in multi-function radar detection performance

The matching of the radar time budget, waveforms, signal processing and other radar parameters to these cases is a crucial part of the multi-function radar system design. A list of some of the parameters that may be adapted in the search function is given below.

i. Transmit power
ii. Transmit waveform (number of pulses and bursts, frequencies, pulse length)
iii. Doppler processing
iv. CFAR thresholds
v. Counter measure processing
vii. Beam spacing
viii. Transmit beamwidth
ix. Receive beamwidth(s)
x. Beam search pattern
xi. Plot confirmation delay
xii. Plot confirmation waveform and energy

vi. Frame time

Some parameters such as frame time or Doppler processing are likely to remain constant within a region, while others such as the total transmitted energy may vary for each beam position.

Optimisation of the multi-function radar parameters for the search function has been the subject of several published papers, notably those by Billam [Billam, 1982, 1986, 1989a, 1992, 1994].

2.3.3.2 Tracking

When discussing tracking radar, Skolnik [Skolnik, 1981] defines two distinct types; a *continuous tracking radar*, and a *track while scan radar.* The former supplies continuous tracking data on a particular target, while the track while scan radar supplies sampled data on one or more targets, derived from the surveillance function. The multi-function radar tracker lies somewhere between these two types of radar.

This is reflected in the tracking update rates that a multi-function radar might supply. Broadly speaking, a continuous tracking radar might supply update rates of the order of 100-10 Hz. A track while scan radar might use update rates of the order of 1 - 0.1Hz. A multi-function radar might use update rates in the order of 10 - 1Hz.

The beamwidth used for tracking in a multi-function radar is likely to be broader than desired. This is due to the necessity to perform the search with the same beamwidth. If a very narrow beam is used, the time taken to survey the volume will become too large. For a weapons system radar, with high track accuracy requirements, the multi-function radar is immediately at a disadvantage, having to use both a broader beam and lower track update rates than would be desired.

The tracker also needs to recognise that a variety of targets exist, some of greater interest than others. Billeter [Billeter, 1989] states;

"The radar needs to maintain a track, even if the user system does not want the information. The alternative is to continually re-detect the target. It is necessary to track a target to ignore it."

Re-detecting a target and forming another track on it is likely to be more expensive than maintaining track on it. Therefore, the multi-function radar must aim to track all targets within its coverage volume. There may be very many targets, with only few that are of genuine interest. The algorithms for tracker control must therefore attempt to minimise radar time and energy on targets that are not of interest, and maximise it on targets of interest. For this reason it is likely that both track while scan and track and scan will be used within the multi-function radar. Targets of little interest to the weapons system, referred to as *low priority targets* forthwith, may be tracked using track while scan, or track and scan with a low demanded accuracy. Targets of interest to the weapons system, termed *high priority targets,* for which accurate position and velocity information is desired, are likely to take the majority of the multi-function radar tracking resource allocation.

Optimising the performance of a multi-function radar tracker against rapid and manoeuvring targets is covered in Chapter 6.

2.3.3.3 Digital beamforming

In a digital beamformer the signal from each element or sub-array feeds a receiver, the output of which is digitised. The digital signals in each receiver channel are multiplied by a complex weight and then summed as shown in Figure 2-14 below.

The antenna pattern may now be adapted in several ways; the main beam and the antenna pattern nulls may be steered to any desired direction. The digital signal may be summed together in many different ways, or if the signal information is stored, it may be passed through the beamformer several times. This allows several antenna patterns to be generated for the same received signal information.

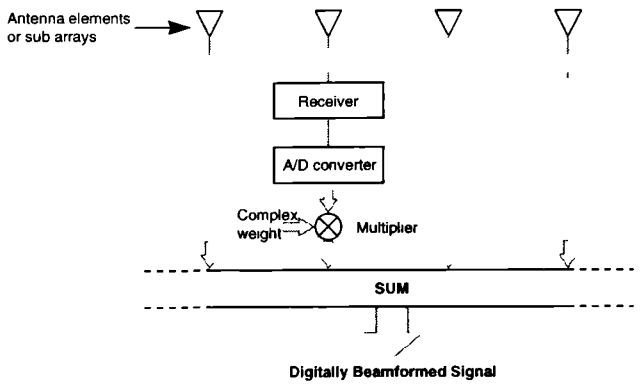

Figure 2-14 A digital beamformer

The array output is formed from the weighted sum of the element or sub-array outputs, as in equation [2-12] below.

$$Array\_output = \sum_{n=0}^{n=N-1} V_n W_n e^{-j2\pi n(d/\lambda)\sin(\theta)} C_n \qquad [2\text{-}12]$$

where N is the number of elements or sub-arrays
V_n is the signal from the nth channel
W_n is the complex weight applied
C_n is a receiver correction factor

This technique is used in several areas such as sonar and communications, as well as radar. The technique has several useful applications in radar. It may be used to place nulls in the antenna pattern in the directions of interference sources such as jammers. It may be used for superresolution processing in angle. Also, since the same information may be summed in different ways many times, it is possible to generate simultaneous multiple receive beams, and effectively search in several directions simultaneously (assuming these directions have been illuminated with the transmit beam).

Many aspects of digital beamforming have been demonstrated/researched using the MESAR radar. Within the scope of this study the two most important aspects of digital beamforming are the generation of a broadened antenna beam pattern to allow a 'variable beamwidth' mode of operation, and the processing of simultaneous multiple receive beams. These are discussed in further detail in Chapter 4.

2.4 Benefits of using a multi-function radar

The primary benefit of a multi-function radar is the ability to steer the beam at will, under automated computer control. From this capability, the multi-function radar may be tailored to its operating environment in a way that is impossible with a mechanically scanned antenna. As Billeter [Billeter, 1989] states,

> "Spatial allocation, temporal allocation, environmental adaptation, and situational adaptation are all related to the inherent flexibility of the beam-steering"

For the full flexibility of a multi-function radar to be realised, not only must the beam steering be flexible, but so must the waveform generation, pulse compression, digital signal processing, etc. Each may be required to perform a different operation at every

different pulse burst.

The process of hand-over from an initial surveillance detection to acquired track can be minimised in the multi-function radar. Once a surveillance detection is made, the multi-function radar can immediately confirm that this detection was from a real world object rather than noise, without having to wait for another sweep of the antenna as in a mechanically scanned system. A series of rapid updates may then be scheduled to enable a good positional and directional estimate of the target to be made. This process can require many sweeps of a mechanically scanned antenna, extending the track hand-over time. It is essential that this is minimised if a rapid weapons system reaction time is required.

The benefits may be summarised;

- Flexibility in resource allocation, spatially and temporally
- No collimation errors
- Minimisation of the search to track handover time
- Rapid dismissal of noise false alarms
- Non predictable operation for ECCM
- Variable track data rate
- Variable surveillance data rate

2.5 Penalties of using a multi-function radar

The multi-function radar by definition fulfils a combination of radar purposes. It replaces radars which are dedicated to a single purpose, each of which has its own optimised parameters for that purpose, such as beamwidth, frequency, energy and waveform. If the optimal parameters used by the individual, dedicated radar systems, are disparate from each other, then it is clear that the multi-function radar represents a compromise in those respects.

This is the case in practice. A typical naval tracking radar may operate with a frequency of around 10GHz, and a beamwidth of a fraction of a degree. This will give that tracking radar great angular plot accuracy with a relatively small antenna size. The surveillance radar that may be used to cue the tracking radar is likely to operate at a frequency of around 1GHz, with a beamwidth of several degrees in azimuth, and possibly tens of degrees in elevation. This gives the surveillance radar a smaller number of beams to

search the volume, thus allowing a greater dwell time per beam position for clutter cancellation and signal integration, with a penalty of decreased angular plot accuracy. If a multi-function radar is then adopted to perform both of the functions of search and track, there are immediately compromises that must be faced.

If the multi-function radar in this example were to adopt the parameters of the tracking radar, although its performance in that respect would be excellent, the time required to survey the sky for targets with such a narrow beam would be prohibitively long making it useless for the search function. Similarly, if the surveillance radar parameters were adopted, the tracking performance would not be adequate with such a broad beam. A compromise must be made on the parameters adopted for the multi-function radar that means it is sub-optimal for both functions.

Furthermore, the multi-function radar has to divide its time between the two functions. The tracking radar in the above example may dedicate all of its time to just one target, where as the multi-function radar not only has to share its time between many other targets, but also between the surveillance function. The multi-function radar therefore has significantly less time for this function than would ordinarily be desired. This is reflected in reality, by dedicated naval tracking radars providing update rates of tens of Hz, e.g. 50Hz, whereas a typical naval multi-function radar would only support update rates in the order of a few Hz for the tracking function.

The impact on the tracking function is thus twofold. Firstly the beamwidth is likely to be broader than would ideally be desired. Secondly the track update rate that may be supported is likely to be significantly lower than is desired. The outcome is that the plot accuracy from a multi-function radar may not be as good as that from a dedicated tracking radar, and that, due to the lower update rate, there is an increased probability that the target may manoeuvre and not be illuminated at the next update.

Both the compromise in beamwidth and the tracking issues discussed above are addressed within the scope of this study, in Chapters 4,6 and 7.

The penalties may be summarised;

- design compromises
- complex hardware, e.g. adaptive digital signal processing or beamforming
- complex software for control

- resource budget limitations
- limited spectrum
- vulnerability
- cost

Cost is a disadvantage both in terms of the research and development required for a multi-function radar system, but also in terms of hardware. Phased arrays, especially active phased arrays, are very expensive. Also, for each array face that is added, further hardware and signal processing are also required. Often systems use only one or two array faces to minimise cost, resulting in the multi-function radar having less than the full 360° instantaneous azimuth coverage. In this case the antenna must rely on mechanical rotation to give the full azimuth coverage.

2.6 Static versus rotating systems

The choice between the use of a static or a rotating antenna for an multi-function radar is most likely to be made on the basis of cost. In many cases, a system with enough faces to cover the required search volume with no mechanical rotation is too expensive, or unnecessary in terms of required performance. In these cases an antenna with one or two phased arrays may be employed, and mechanical rotation ensures that the whole volume may be covered over a certain time.

In a rotating multi-function radar there are some significant complications to the radar control problem that do not exist in the case of a static face multi-function radar, aside from the increased mechanical complexity. In light of this, it is worth pointing out that there are some benefits to be accrued by rotating the array antenna.

Surveillance is essentially a repetitive, periodic function. The search of beam directions may be synchronised with the rotation rate of a rotating array, so that the search function is performed on array azimuth broadside. This minimises the losses associated with scanning. Equally, in the tracking function, if updates on a particular target may be performed on array azimuth broadside, then the minimum beamwidth will be obtained, giving the maximum azimuth plot accuracy and resolution.

These factors can be very significant and are investigated further within Chapter 4, which makes a quantitative comparison of a variety of static and rotating array antenna

configurations, whilst also assessing the impact of multiple receive beam processing in those systems. A recent comparison of static and rotating multi-function radars has been made by Billam [Billam, 1997b], which concluded that a single faced rotating system was the most efficient option.

Another advantage of a rotating system is the possibility of distributing the radar time around the coverage volume in a way that is not possible with a static system. If a small sector exists with a higher than normal load of radar tasks, then in a static system, the one array face pointing in that direction will be more highly stressed than the other faces. In a rotating system it is possible to share the extra load amongst all of the faces to some extent. This is a technique that seems not to have been considered in the literature. It is discussed in further detail in Chapter 5.

3 MESAR: AN EXAMPLE MULTIFUNCTION RADAR SYSTEM

3.1 Introduction

This section gives an overview of the MESAR multi-function radar and the new capabilities that will come with the development of MESAR II, since the research from this study will be directly applied to that system. This chapter aims to give an indication of the performance and capability of a current, state of the art multi-function radar system, and to show what has been achieved and what flexibility remains to be harnessed in an optimal way. It pays particular attention to the tracking and control issues, describing the current MESAR tracker and the results that have been obtained through aircraft trials, and the advances in MESAR II that may be used within the tracker. A more detailed account of the system is given in many papers ([Moore, Levett & Butler, 1995], [Billam, 1986, 1987 & 1989b], [Salter, 1988], [Moore & Salter, 1995]), from which this overview is formed.

MESAR is an advanced experimental active phased array radar which has been developed collaboratively between the Defence Evaluation and Research Agency and British Aerospace Defence Systems (formerly Siemens Plessey Systems). It was developed through the late 1980s and early 1990s exploiting the recent advances in digital and solid state microwave technology then available. The complete fully functioning multi-function radar, Figure 3-1, was delivered to the DRA in early 1993, and is now used as a test-bed for experimentation and demonstration of techniques that will be applied to future multi-function radar systems.

The MESAR demonstrator radar was not intended to give the full radar performance that would be expected of an operational multi-function radar, but to be capable of demonstrating the system functionalities and control needed by such a radar. In fact, the MESAR demonstrator has surpassed this initial requirement and has been able to demonstrate several features with performance in excess of any conventional radar system. As such, it is one of the most advanced radars of its kind in existence. The

current MESAR experimental system incorporates the following features:

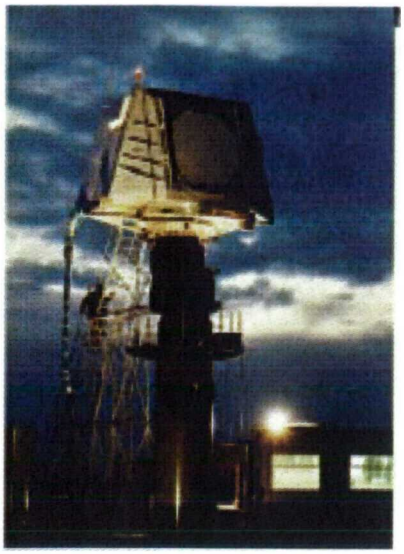

Figure 3-1 The MESAR multi-function radar

- A single solid state active phased array, with multiple sub-arrays. The array is thinned due to cost constraints on the research programme.
- A single agile surveillance beam.
- Simultaneously available pencil, circular difference and sidelobe blanking beam shapes.
- Wide-band frequency agility.
- Sectored surveillance for efficient use of energy.
- Variable surveillance data rate.
- Selectable choice of pulse repetition interval, expanded pulse length and compressed pulse length.
- Digital waveform generation giving a choice of pulse lengths and pulse compression laws.
- Digital pulse compression.
- Digital adaptive beamforming giving anti-jamming capability for the sum, difference and sidelobe blanking beams.
- Programmable, parallel signal processing.
- Variable track update rate.
- Computer control of all radar functions.
- Data recording for off-line analysis and processing

A simplified block diagram of the MESAR system showing the components is given in Figure 3-2. After combination of element outputs into sub-arrays, the entire system is digital, and therefore highly flexible.

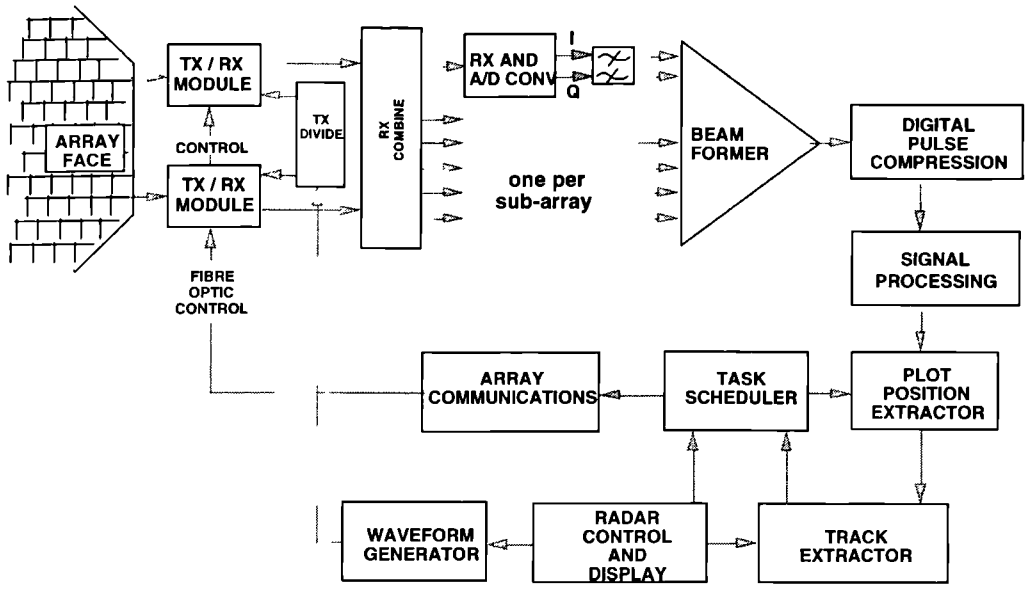

Figure 3-2 A simplified block diagram of the MESAR system

A new system is now under construction, creatively called MESAR II, which will include a new active array and signal processing. The tracking strategies that are developed from this study will be tested directly in experimental trials using the MESAR II radar.

3.2 Array face and transmit/receive modules

MESAR has a single, static, active array face. It consists of nearly one thousand radiating elements, although only one in six element positions is populated with an active transmit receive module due to cost limitations, see Figure 3-3. This results in the system having a lower output power, and higher antenna sidelobes than one using an equivalent fully filled array.

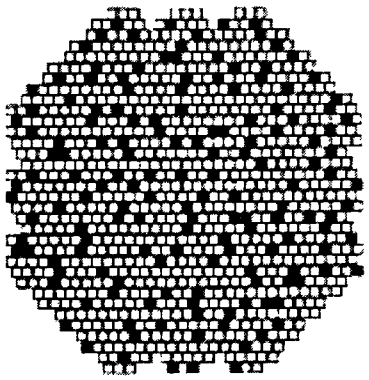

Figure 3-3 The thinned MESAR array

The array is just over 1.8m in diameter, with elements in a triangular lattice which radiate horizontally polarised waves. Operating at around 3GHz this gives the system a beamwidth of around 3^{o}.

The transmit/receive modules contain a transmit power amplifier and a low noise receive amplifier based on GaAs microwave integrated circuitry. The module also contains a 4 bit digital phase shifter and a phase computation and control processor, so that each module in the array can set its own phase shift. The phase computation requires only the position of the element in the array, which is stored in ROM, and the desired beam pointing direction and radio frequency, which are broadcast to all of the modules over a fibre optic link. This distributed phase computation avoids the need for a central phase computation engine and control system.

The new modules fabricated for MESAR II will allow several transmit and receive beam shape configurations. These may be used for generating variable transmit and receive beamwidths independently, thus allowing either broadened transmit/receive beams giving variable beamwidth operation, or broadened transmit with narrow receive beams to allow simultaneous multiple receive beam processing in the digital beamformer.

Each of the MESAR modules generates around a 2W output power, and can operate with a mean duty cycle of around 30%. This gives the MESAR system a very low mean output power of less than 100W. Therefore, in order to detect targets at any reasonable distance, the system requires a large amount of processing gain, which it achieves both through coherent and non coherent integration. The waveforms that are used in MESAR are thus unusually long in comparison to those which would be expected in an operational system.

3.3 MESAR adaptive beamforming

Digital adaptive beamforming in MESAR is used to provide an effective capability to cancel jammers both in the antenna sidelobes, and in the skirts of the main beam, termed *adaptive nulling*.

A block diagram of the MESAR digital beamformer is shown in Figure 3-4. The element signals for groups of elements are combined using analogue beamforming into a

number of subarrays. The signals from these subarrays are digitised, and the digital data from each subarray channel, corresponding to all the range cells in one or more pulse repetition intervals, is stored in a buffer. The weight computation unit now has the task of calculating, in real time, the required phase and amplitude weights needed by each subarray channel. The weights are chosen to allow the antenna gain characteristics in the required look direction to be maintained, whilst simultaneously generating nulls in the antenna pattern to adaptively cancel jamming and interference sources. These complex weights are then applied to the data stored in the buffer.

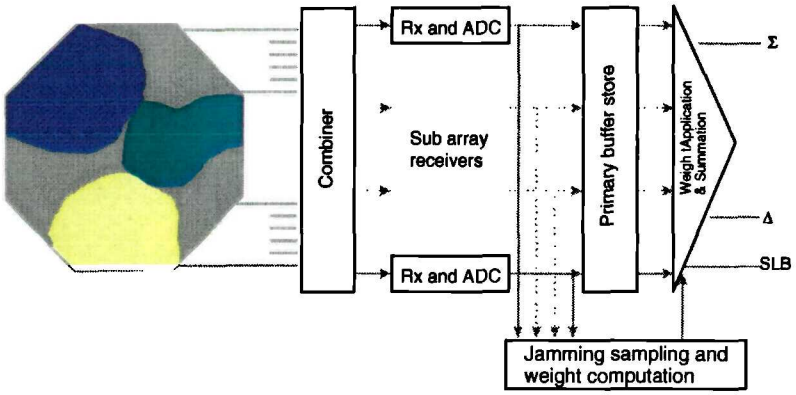

Figure 3-4 A simplified block diagram of the MESAR digital adaptive beamformer

Three sets of weights are calculated in MESAR in order that sum, difference and sidelobe blanking beams are generated. All three beams will then be protected from jamming and interference sources.

In MESAR II the digital adaptive processing is to be significantly enhanced to include processing for super resolution techniques and for generating multiple receive beams. Both of these functions may be used to aid the tracking function.

3.4 Radar control

Central to the success of MESAR is its radar control system. The radar control system is designed to allow the multi-function radar to achieve the required performance from each of its radar functions. The MESAR Radar Control process provides for the following [Stafford, 1990]:

- A priority structure for radar functions such that each function takes absolute priority over all other functions with lower priorities.
- An algorithm that determines in real time the sequence in which radar tasks must be

performed. It also permits the dynamic variation of data rates and dwell times.

- Adaptive waveform control according to environmental and ECM conditions.
- The ability to select in real time, waveforms for both surveillance and tracking which match the clutter and jamming conditions, and provide the required detection performance.
- Operating in real time the radar control process will be able to rapidly schedule 'look-back' tasks for plot confirmation and track initiation.
- To keep the antenna fully occupied for efficient use of transmitter energy.

MESAR's radar control is covered further within Chapter 5.

3.5 Adaptive signal processing and waveform generation

The flexibility asked of MESAR impacts upon the design of the entire multi-function radar system. Not only does it require a flexible control system, but also flexible waveform generation and adaptive signal processing.

MESAR uses a digital, programmable waveform generator. Digital samples of the pulse modulations for a variety of transmitted pulse lengths and frequency sweeps are stored in RAM. On transmission, the samples for the chosen waveform are passed through a D/A converter, filtered and frequency shifted. The transmit waveform may be changed on a pulse by pulse basis if required.

On receive, a purpose built digital pulse compressor convolves the returns with the sampled weighting function of the matched filter, which is suitably weighted to give low range sidelobes. The filter coefficients are programmable.

The remainder of the signal processing, Doppler filtering, constant false alarm rate processing, monopulse angle estimation and plot extraction, is performed on parallel distributed array processor containing 1024 processors. The processor has to be programmable so that the processing applied can be matched to the waveform transmitted; the signal processing algorithms are coded in parallel Fortran.

3.6 The plot processor and tracker

This section describes some of the adaptive aspects that are already an integral part of the current MESAR tracker.

3.6.1 Plot processing

The plot processor in MESAR [Noyes, 1990] uses a simple, nearest neighbour algorithm in most cases. However, unlike most other phased array systems using de-coupled tracking, it takes some account of the problems that may occur with closely spaced targets.

When the multi-function radar makes an update on a known track, the multi-function radar pencil beam will only illuminate the area of sky close to that track. This area of sky may include parts of the association gates of other targets. However, it is unlikely that the whole of the association gate for these other tracks will be included. The picture with which to make the correct association in this circumstance is not complete after a single update on a single track.

The effect of associating incorrect plots into a smoothed track is to degrade the track accuracy, and this should be avoided. Therefore, when a track update gives a conflict in association, the strategy adopted in the MESAR tracker is to avoid this by requesting an early update on the conflicting track. Then the tracker will await the output from this update, before making either association.

Data received from the surveillance function on a track is not fed into the track smoothing algorithms, since MESAR does not currently use monopulse during surveillance, thus the accuracy of the plots is significantly poorer.

3.6.2 Track filtering

The current version of the MESAR radar uses a single filter model for track smoothing. This is a constant velocity Kalman filter, with a manoeuvre detector strategy, which gives the filter an adaptive memory based upon the target manoeuvre conditions [Noyes, 1990]. This method allows a simple filter to be employed, with a relatively low plant noise, giving a higher track accuracy in phases of constant velocity flight. In the case of a manoeuvre the plant noise is increased somewhat to allow the filter to be more

adaptive to target manoeuvres.

Development of a simulation of the MESAR Kalman filter based tracker is covered in Chapter 6.

3.6.3 Adaptive track update rate

The look back interval of a track in MESAR is adapted on an update by update basis [Noyes, 1990]. The time of next update that is calculated is based on two factors;

i. *there is a high probability that the target falls within the 3dB beam on the next update.* This value will depend on the azimuth and elevation smoothed accuracy of the track, and on the amount that the track can possibly manoeuvre in azimuth and elevation.
ii. *there is a constant smoothed track accuracy in position or velocity.*

Choosing an update time that is too large will mean that one of the above is not fulfilled. Choosing and update time that is too small will mean the tracking function will increase the occupancy of the tracking function over its optimal value.

Thus in MESAR, there are two times that are used when requesting a track update;

a. *latest update time.* This is the earliest of the two possible outcomes of (*i*) above, depending on whether the azimuth or elevation manoeuvre capability is larger. It represents the time by which an update must be made before which there is a chance that the target will fall outside of the 3dB beamwidth, and not be detected.
b. *desired update time.* This is the time which is given from (*ii*) above. It must be less than the latest update time calculated in (a). If the update is not made on time, then it is unlikely that the track will be lost until (a) above is exceeded, but will mean the required track accuracy is not achieved.

Tracks will be scheduled using their desired update time. However, if the latest update time is exceeded, then the track task is elevated in priority to the *track maintenance* level, to ensure that it is scheduled at the earliest opportunity.

3.6.4 Adaptive transmit energy

Once a target is under track, unlike surveillance, we have some idea of the radar cross section of the target we are looking for. We may therefore tailor our transmit waveform to illuminate the target with only a sufficient amount of energy to give a desired detection performance.

A smoothed estimate of the signal to noise ratio is built up using a simple α smoothing filter with the measurements of signal to noise ratio from each update. This smoothed estimate is maintained between 26dB and 29dB by adapting the number of MTI bursts or pulses that are used in the transmit waveform [Stafford, 1991].

The objective of this is to ensure energy is not wasted on very large targets, or on targets that have got close in range to the radar, which would normally give signal to noise ratios in excess of useful levels.

3.6.5 MTI velocity response matching

During surveillance, no range rate information is available on the targets that are being searched for. Therefore several moving target indication (MTI) bursts must be transmitted in each beam direction to eliminate the blind velocities of each MTI filter.

In the tracking function however, an estimate of the target range rate is available. The MTI filter chosen may therefore utilise weights that ensure the estimated target range rate lies at the peak of the filter response [Stafford, 1991]. This gives two benefits;

- the target receives the maximum gain through the MTI filter
- the amount of radar time required for each target is kept to a minimum

3.7 Trials results

The first set of MESAR trials were undertaken in 1988 when a number of receive only tests were completed with the array in order to characterise the operation of the digital adaptive beamformer ([Salter, 1989], [Moore & Butler, 1994]). A typical result is shown in Figure 3-5, showing both adapted and unadapted beam patterns. This clearly demonstrates the adaption of the antenna pattern to generate nulls in the direction of jammers.

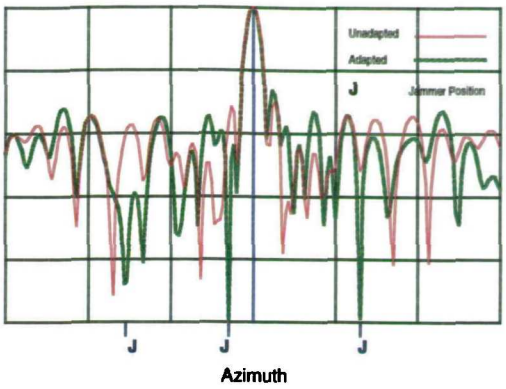

Figure 3-5 Adapted and unadapted beam patterns in the presence of jammers

An 18 month programme of trials commenced in early 1993. These were conducted at the DERA antenna test range, Funtington and the MoD Test and Evaluation range at West Freugh, Scotland, and were designed to test the radar performance in severe environmental and jamming conditions. These are reported fully in [Butler, 1995]. An overview of some of these results is given below.

3.7.1 Multi-function operation

Figure 3-6, below, is a photograph of the main radar display in the form of a Plan Position Indicator, showing surveillance and multi-target tracking results. The following information is displayed:

- Surveillance plots - the main detections from the surveillance functions. At this stage surveillance plots will include false alarms.
- Confirmed track update - those plots which are confirmed as true targets
- Missed track update - a track update which failed to detect
- Slow tracks - those tracks which fall below a specified velocity threshold

Whilst this display is only a snap-shot in time, it demonstrates the multi-function operation of MESAR.

3.7.2 Tracking

An established track is maintained by a series of updates, the rate of which can vary according to the target range and tracker confidence in plot prediction of the tracked object. Figure 3-7 shows the track plots obtained from two weaving aircraft. The spacing of the track plot updates shows the adaptive nature of the MESAR tracking function.

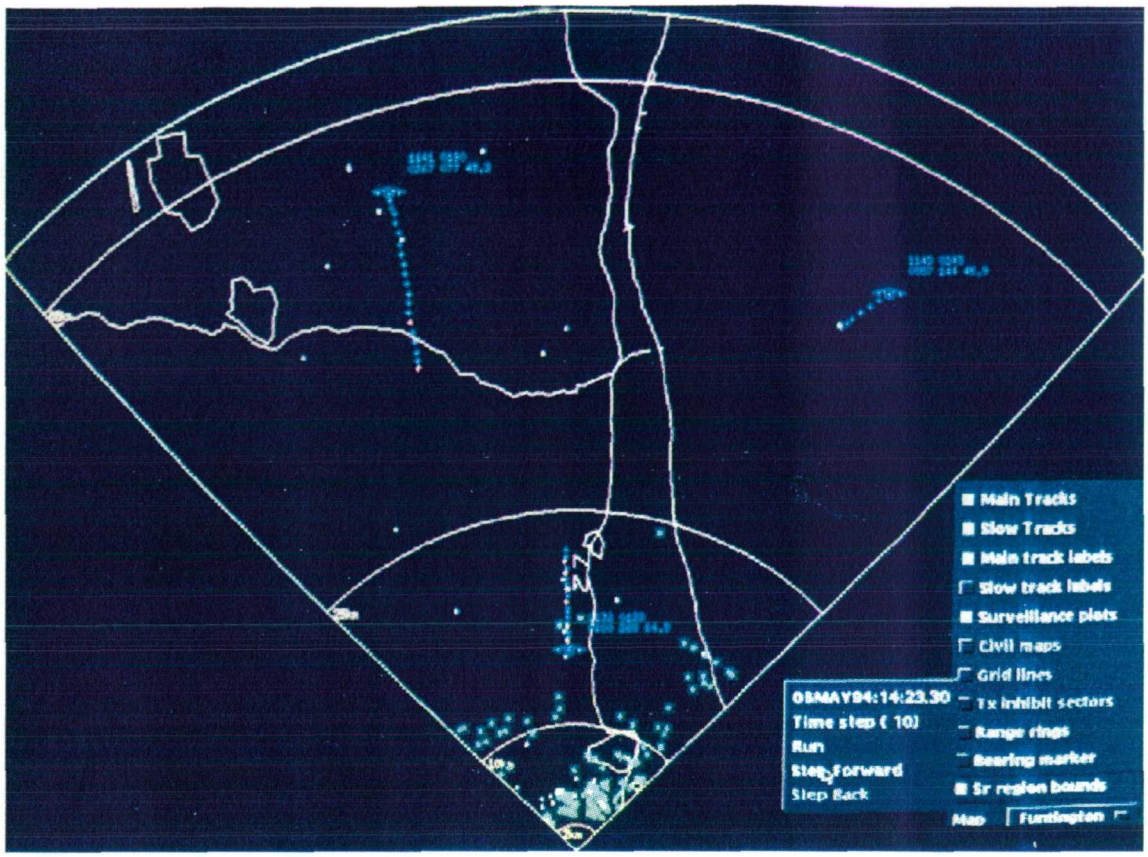

Figure 3-6 The MESAR PPI display, showing a recently initiated track

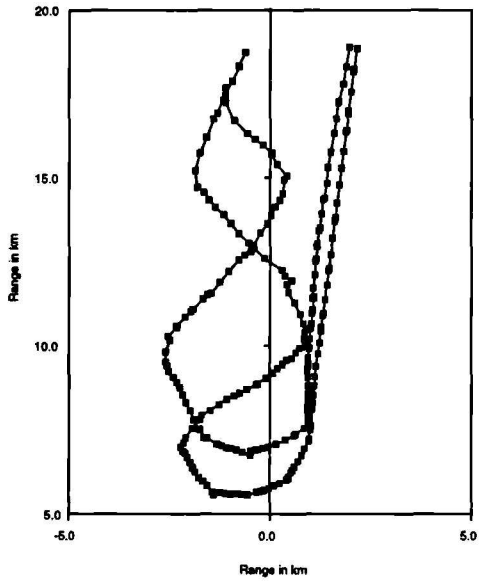

Figure 3-7 Adaptive update rate tracking

Of special interest is the situation where a track splits into two. The benefit of recognising split tracks is the early detection of multiple targets as they resolve and the ability to rapidly form tracks on the individual objects. Figure 3-8 shows a demonstration of this function through the separation of a 1000lb bomb from an aircraft

flying at 32,000ft.

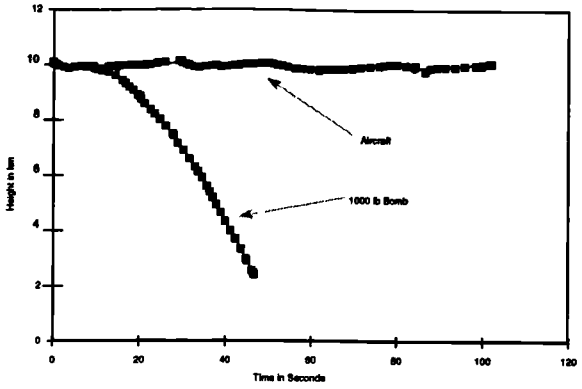

Figure 3-8 Track splitting function

3.8 Summary

MESAR is a fully functioning, active multi-function radar that already operates in real time using an adaptive tracker and control system. It consists of a single static array face, which is capable of generating only a single beam. Therefore it would be beneficial to consider the impact of a rotating array antenna and multiple beam techniques on the control and resource allocation of such a system.

Broadly speaking there are two main areas in which the tracker may be improved. The first is to use more advanced track filtering and plot association methods such as the Interactive Multiple Model (IMM) filtering methods, the various Joint Probabalistic Data Association (JPDA) methods, or Multiple Hypothesis Tracking (MHT) techniques. These issues are being addressed under the construction of MESAR II and the current MESAR research programme, and will not be covered within this study. The second area for improvement is that of utilising the new functionalities available such as variable beamwidths, simultaneous multiple receive beam processing and super-resolution techniques, as well as optimising the performance for a rotating system. This is the area that is followed in this study.

4 THE IMPACT OF VARIABLE BEAMWIDTH AND MULTIPLE BEAM PROCESSING ON MULTI-FUNCTION RADAR

4.1 Introduction

For a multi-function radar designed to operate in severe levels of clutter, a fundamental drawback is the compromise that must be made in the antenna beamwidth used for surveillance, tracking and other functions.

> For *tracking* a very narrow beam is required to give the maximum tracking accuracy and target resolution in a multiple target environment.
>
> For *surveillance* a broader beam is desired so that the time taken to perform the search is minimised, especially in regions of high clutter, where long Pulsed Doppler waveforms must be used to ensure adequate clutter cancellation.

The requirement for keeping the search occupancy within reasonable limits results in a beamwidth that is broader than is ideal for the tracking function. Significant benefits would be gained if a narrower beam could be supported without increasing the surveillance load excessively.

Future derivatives of multi-function radars such as MESAR will offer the capability to exploit digital control in shaping the transmit and receive antenna patterns. These will allow the beamwidth to be broadened through a suitable phase or amplitude weighting imposed at the array elements. Also multiple receive beams may be processed, either through provision of multiple receive channels, steered at the element level, or through the use of digital beamforming.

The inherent compromise with a multi-function radar on beamwidth does not necessarily hold with a variable beamwidth system. Search and track beamwidth could be de-coupled and each be optimised to their task. The impact of these variable antenna patterns on the multi-function radar is discussed here, working to the assumption that, in

general, the narrower the tracking beam is, the better the tracker performance will be, in terms of resolution and tracking of closely spaced targets, performance in multipath and jamming, and track accuracy. In particular, the impact of variable beamwidth and simultaneous multiple receive beam processing on the search time-budget is assessed.

Sections 4.2 and 4.3 discuss the generation of broadened beams and the use of simultaneous multiple receive beams. In section 4.4 novel methods of estimating the search time-budget for both a static and a rotating multi-function radar are developed. These are then applied in sections 4.5 and 4.6. In section 4.5 an accurate comparison of static and rotating multi-function radar systems performing the search function is made, which appears not to have been reported previously in the literature. Also in that section the impact of using broadened transmit and receive beams and simultaneous multiple beam processing is made in thermal noise only conditions. Section 4.6 then makes some account for the effects of clutter. Finally, section 4.7 presents some ways in which simultaneous multiple receive beams may be used for tracking in multi-function radar, and the conclusions of the work are contained in section 4.8.

4.2 Generating a broadened main lobe antenna pattern

It may be desirable to broaden the main lobe of the antenna pattern in some circumstances to enable a larger area of space to be illuminated than would occur with the uniformly illuminated antenna. This may be performed in either transmission or reception, and may be coupled with the use of simultaneous multiple receive beam processing, discussed in the next section.

The field of pattern synthesis has been the subject of a great deal of research, and much published literature exists on the subject. It is not an objective of this research to investigate or present techniques for pattern synthesis. However, it is important to demonstrate the feasibility of generating broadened main lobe antenna patterns since much of the work in the following chapters depends upon it.

An effective solution to the problem of radiation pattern synthesis for an array antenna has been given by Milne [Milne, 1987]. This method consists of selecting a 'scanning function', which is a physically realisable antenna pattern with desirable characteristics, such as low sidelobes. This antenna pattern may then be convolved with the ideal

pattern that is desired. This will yield a physically realisable antenna pattern that approximates the ideal pattern. The method is superior to methods based on the Woodward synthesis technique [Woodward, 1947], since it utilises both the amplitude and phase of the array illumination function. For an N element linear array, this gives 2N-1 rather than N degrees of freedom.

Figure 4-1 below shows the results of a convolution of a scanning function based upon the Dolph-Chebychev weighting function, used to obtain a uniform sidelobe level, with several ideal broadened main lobe antenna patterns. A 50 element linear array was considered, operating at a wavelength of 0.1m, and with a half wavelength element spacing. This resulted in a scanning function with a beamwidth of 2.76°, and a sidelobe level of 40dB below the main lobe peak (shown by the blue line in each figure).

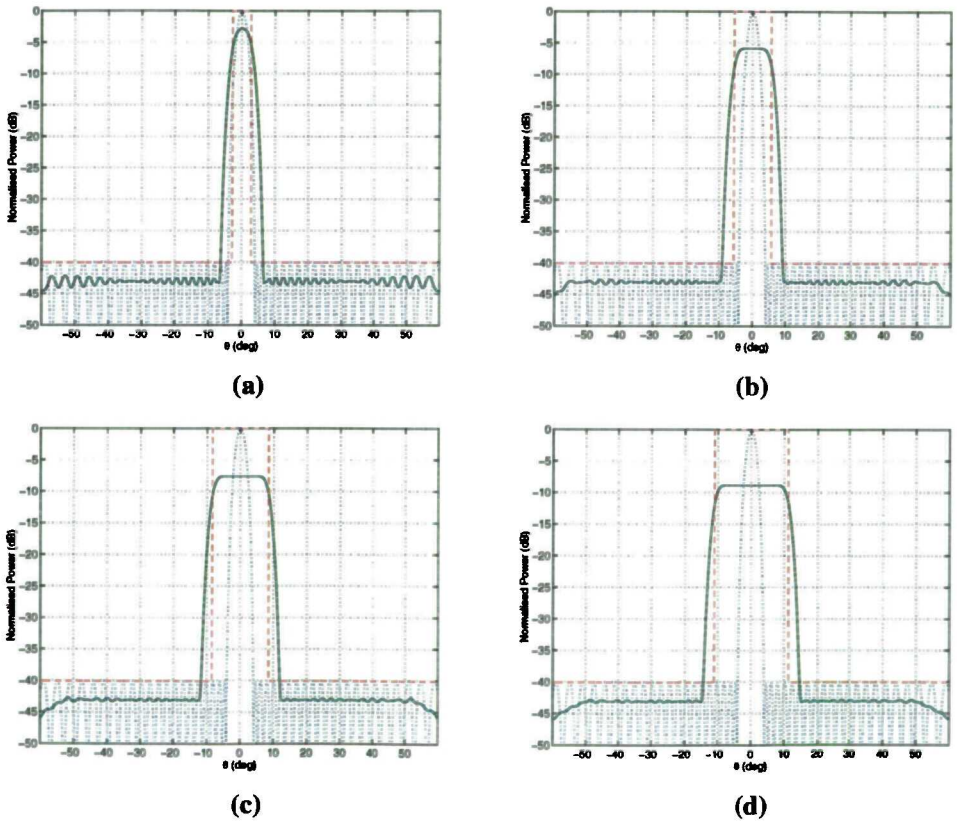

Figure 4-1(a,b,c,d) Synthesis of a broadened main lobe antenna pattern using Milne's method, showing broadening of the scan pattern main lobe by (a) a factor of 2, (b) a factor of 4, (c) a factor of 6, (d) a factor of 8. Blue line shows the scan pattern, red line shows the desired pattern, green line shows the realisable pattern.

Ideal patterns consisting of a rectangle function over the desired angular sector were chosen. The width of rectangle in the ideal pattern was related to the 3dB beamwidth of the scanning function. Broadening factors of 2, 4, 6 and 8 times the scanning function 3dB beamwidth were chosen (shown by the red line in each figure). The physically

realisable patterns, (shown by the green line in each figure), are seen to retain the low sidelobes whilst approximating the ideal pattern well.

This method is appropriate to both a passive array multi-function radar and also an active array multi-function radar when in reception. However, in transmission the amplitude of the active array must remain uniform, and the formation of the desired pattern must be made using only a variation in the element relative phases. In this instance, the broadened main lobe antenna pattern will suffer from the high sidelobes associated with the uniformly illuminated active array antenna.

4.3 Processing of simultaneous multiple receive beams

A radar may observe multiple directions simultaneously, by illuminating a large area with a broadened transmit beam, and generating multiple narrow receive beams to cover that area, as shown in Figure 4-2, below. This is most commonly performed in 'stacked beam' rotating surveillance radars, where all elevation angles of interest are surveyed in one observation. The cost of the technology required to achieve this has prevented the technique from becoming widespread in multi-function radars thus far.

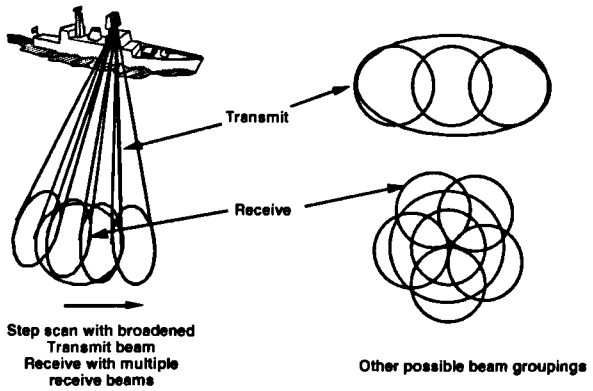

Figure 4-2 Example tx and rx beam formations using simultaneous multiple beam processing

Currently, real time digital beamforming at element level for arrays operating at the desired radar frequencies are not practicable. Therefore, digital beamforming is usually performed at subarray level, where the analogue output of many elements is combined before analogue to digital conversion. Formation of multiple receive beams may either take place at subarray level, through digital beamforming, or at the element level, as one or more separate receiver channels.

The advantage of forming the beams at subarray level is the adaptive control over the beam pattern clusters that are generated. Beams may be separated by different offsets, and in different patterns if required. However, there are some constraints laid in forming the beams at this stage in the receiver chain. Firstly, the receive beams formed must be within the sub-array beam width to avoid degradation in gain. Secondly, beamforming at sub-array level introduces a quantisation in the phase taper across the array, which can degrade the sidelobe levels of the receive beam. These disadvantages are eliminated if the beamforming is performed at element level, but at the expense of providing a separate receive channel for each beam.

MESAR II will initially provide multiple receive beams at the element level. This will be achieved through using the difference channel, thus only two simultaneous receive beams may be generated. It is anticipated that multiple beamforming at sub-array level will be added at a later date.

4.4 Calculation of the search function time

The search function time is the total radar time needed to perform a search of a given region of space. It is determined by two factors; the number of beam directions that are needed to fully cover the region of space, and the dwell time required in each beam direction. From this parameter the search occupancy may be obtained by including the frame time over which the search is to be completed. For a single face, equation [4-1] gives the search occupancy.

$$Occ_{search} = \frac{search\_function\_time}{search\_frame\_time} \qquad [4\text{-}1]$$

It is usual (see section 2.3.3.1) for the search volume to be divided into sectors, each sector having a uniform detection performance with angle (in most conditions). This section presents novel methods for estimating the search function time for a given sector, for both a static and a rotating multi-function radar system. These methods are compared to exact calculation of the beam lattice for every sector. The methodology is then applied in the following sections 4.5 and 4.6.

4.4.1 Static phased array multi-function radar system

If the antenna characteristics were invariant with scan angle, the calculation of search function time would be a simple matter. This is the case for a spherical array, where the beamwidth and gain do remain invariant with scan. The search function time is given simply by

$$function\_time = \sum_{i=1}^{i=n\_beams} dt_i = n\_beams.dt \qquad [4\text{-}2]$$

where dt is the dwell time in each beam direction
n_beams is the number of beams

since for all directions the same dwell time will give the same detection performance at any angle. It is possible to avoid calculating each beam direction explicitly to derive the number of beams. If it is assumed that the beams are arranged in a triangular, close packed lattice, with their 3dB beamwidth contours overlapping, the number of beams may be approximated by the ratio of the solid angle of the sector to be searched to the solid angle of the beam (at its 3dB contours). Then a good approximation of the search function time is given by equation [4-3] below.

$$function\_time \approx \frac{\Omega_{sector}}{\Omega_{beam}} dt \qquad [4\text{-}3]$$

where Ω_{sector} is the solid angle of the search sector
Ω_{beam} is the solid angle of the beam

With a planar array, however, the calculation is complicated by the change in effective aperture with scan angle, varying both the beamwidth and detection performance. The calculation is further complicated by the tilt of the array with respect to vertical. These issues make determining the surveillance function using simply the real world coordinate system difficult.

Fortunately, the calculation is made simpler if we apply a strategy often adopted by antenna engineers for this problem, which is to use direction cosines in the antenna coordinate system, often called UV space [Best, 1962].

This coordinate system has the useful property that the antenna beam pattern remains invariant with the scan off angle from broadside. The coordinate system and equations are shown below. (It is important to note the angles θ and φ do not correspond to

azimuth or elevation in this case). The unit vectors **u** and **v** lie in the plane of the array. The angle θ, measured from the normal to the array plane, represents the scan angle.

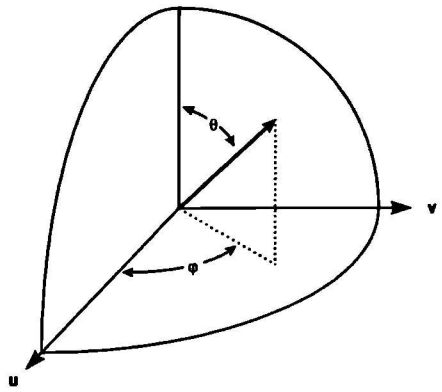

$$u = \sin(\theta)\cos(\varphi) \qquad [4\text{-}4]$$

$$v = \sin(\theta)\sin(\varphi)$$

Figure 4-3 The UV space coordinate system and equations

A useful visualisation of the UV space transform has been described by Von Aulock [Von Aulock, 1960]. This is shown below in Figure 4-4(a). Beams projected from the plane below the unit sphere (the UV plane) onto the surface of the unit sphere broaden exactly as does the antenna beam, scanned from array broadside. Once the beamshape is known in UV space it is relatively simple to calculate a square or triangular lattice of beam directions since the beam may be linearly translated in UV space without regard to the scan angle of the beam, as shown in Figure 4-4(b). This projection is equivalent to the orthographic projection [Chamberlin, 1947], used in the field of cartography for projecting lines of latitude and longitude onto a sheet of paper.

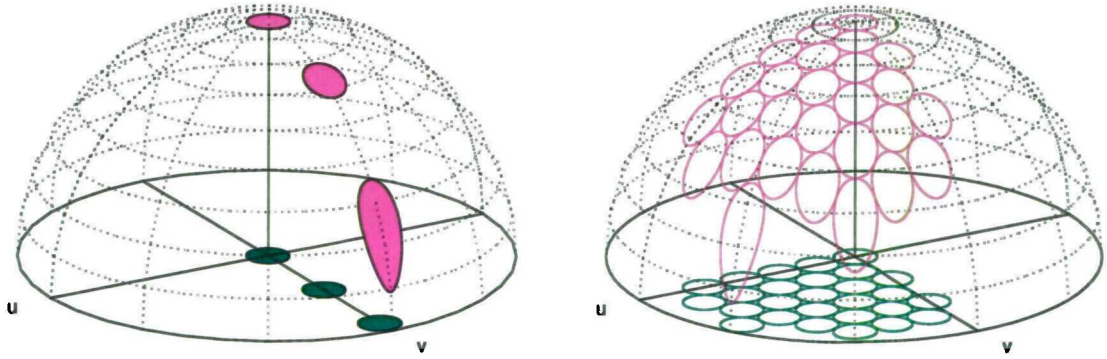

Figure 4-4 (a) A visualisation of UV space, showing beam broadening, (b) the same visualisation showing a triangular lattice of beams

To relate the UV coordinates of a beam to real space coordinates we must include a rotation between the two coordinate systems to account for the tilt of the array from vertical.

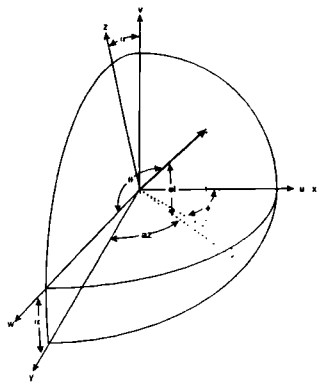

$$u = x$$
$$v = z\cos(\alpha) - y\sin(\alpha) \qquad [4\text{-}5]$$
$$w = y\cos(\alpha) + z\sin(\alpha)$$

Figure 4-5 The relationship between the uv and real world coordinate systems, and the associated equations

Figure 4-5, above, shows the relation between UV space and real space for an array tilted back α° from vertical. The unit vector **w** is assigned to the array normal direction. The transformations from UV space coordinates **u**, **v**, **w** to real world coordinates **x**, **y**, **z**, are those in equations [4-5].

Therefore we may derive **u** and **v** from azimuth and elevation, and vice versa, using equations [4-6] and [4-7].

$$u = \cos(el)\sin(az)$$
$$v = \sin(el)\cos(\alpha) - \cos(el)\sin(az)\sin(\alpha) \qquad [4\text{-}6]$$
$$w = \cos(el)\sin(az)\cos(\alpha) + \sin(el)\sin(\alpha) = \sqrt{1-\left(u^2+v^2\right)}$$

$$az = \tan^{-1}\left(\frac{u}{\sqrt{1-\left(u^2+v^2\right)}\cos(\alpha) - v\sin(\alpha)}\right)$$
$$el = \sin^{-1}\left(v\cos(\alpha) + \sqrt{1-\left(u^2+v^2\right)}\sin(\alpha)\right) \qquad [4\text{-}7]$$

Figure 4-6, below compares lines of constant azimuth and elevation for an array which is vertical, and an array which is inclined 15° back from vertical. We see that in the tilted array case, lines of constant elevation are not horizontal as they are in the vertical case, implying that to trace a line of constant elevation, the array scan angle is constantly changing.

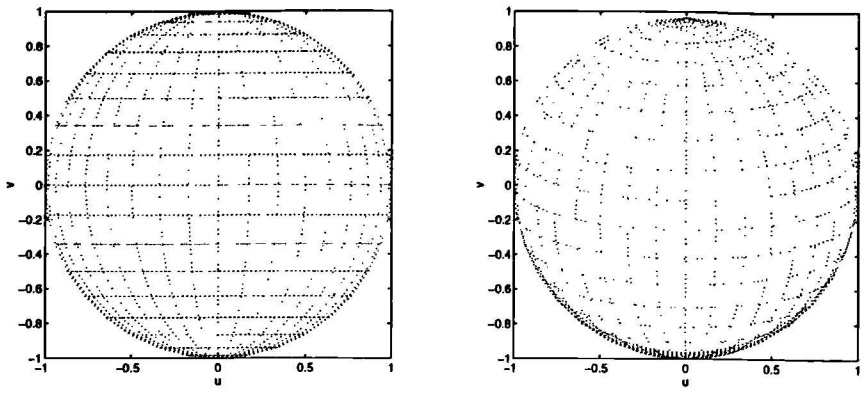

Figure 4-6(a,b) A comparison of lines of constant azimuth and elevation for (a) a vertical array, and (b) an array inclined 15° back from vertical

It is now a relatively simple matter to calculate the exact beam directions for a given search volume using UV space. Figure 4-7 shows the calculated beam directions using one of the MESAR search configurations as an example. The limits of this configuration are ±45° in azimuth and 1.18° - 52.5° in elevation. An array broadside 3dB beamwidth of 3.1° is assumed, with beams overlapped at 0.85 beamwidths. The exact number of beams that are used for this search sector in MESAR is 595.

Since we now have a spatial system in which the beam remains invariant, we can apply the same method as used for the spherical array above in equation [4-2], to estimate the number of beams in the search volume, without explicitly calculating each beam direction. This estimate is given by the ratio of the search sector in UV space to the area of the beam in UV space. The area of the beam in UV space, A_{beam_uv}, is given simply by equation [4-8].

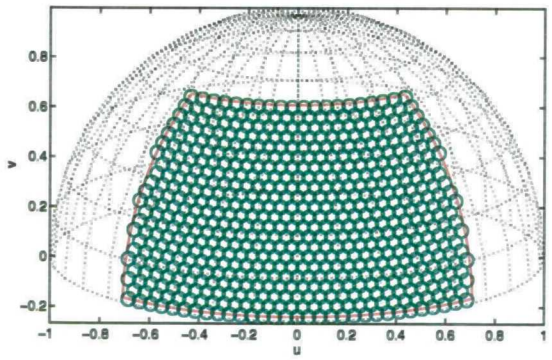

Figure 4-7 Beam directions in UV space, using MESAR as an example

$$A_{beam\_uv} = \pi \sin^2(\theta_3) \qquad [4\text{-}8]$$

The area of the sector to be searched, A_{sector_uv}, may be found by integration between the

curves which define the sector in UV space, shown in Figure 4-8(a) below. The area is given by [4-9], here expressed as the sum of three integrals of the three curves bounding the sector in UV space.

$$A_{sector\_uv} = 2\left[\begin{array}{l}\left[\int_{el\_min}^{el\_max} u\frac{\delta v}{\delta el}\delta el\right]_{az=az\_max} \\ +\left(u_{az\_max,el\_min}v_{az\_max,el\_min} - \left[\int_{0}^{az\_max} v\frac{\delta u}{\delta az}\delta az\right]_{el=el\_min}\right) \\ -\left(u_{az\_max,el\_max}v_{az\_max,el\_max} - \left[\int_{0}^{az\_max} v\frac{\delta u}{\delta az}\delta az\right]_{el=el\_max}\right)\end{array}\right] \qquad [4\text{-}9]$$

This integral may either be calculated numerically, or in this case it has an analytical solution which may be evaluated. This gives a result within 8% of calculating the number of beams exactly. This is sufficient to perform an initial analysis of the search function time.

To obtain the search function time, we also need to include the dwell times. The dwell time of each beam is given by the broadside dwell time, $dt_{broadside}$, divided by $\cos^3(\theta)$. If this is plotted as a surface above the beam directions in UV space, where the height of the surface represents the dwell time at that angle, then the volume under this surface represents the total radar time for search. This is shown in Figure 4-8(b).

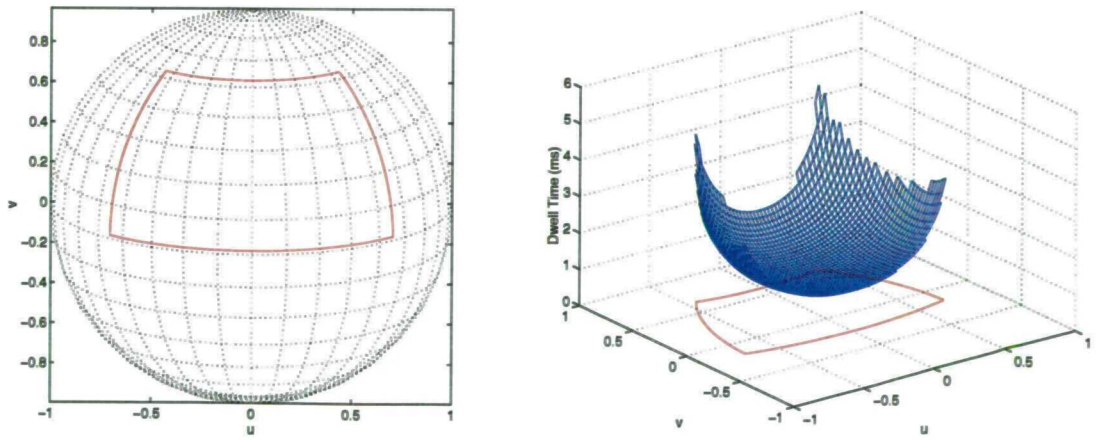

Figure 4-8 (a) MESAR coverage limits in UV space, (b) Beam dwell time plotted as height above the UV plane

We may calculate an average dwell time, dt_{av}, from this surface, which when multiplied

by the number of beams, gives us the search function time.

$$dt_{av} = \frac{1}{A_{sector\_uv}} \int_{el\_min}^{el\_max} \int_{az\_min}^{az\_max} \frac{dt_{broad\_side}}{\cos^3(\theta)} \qquad [4\text{-}10]$$

This integral has no analytical solution, so it must be solved numerically.

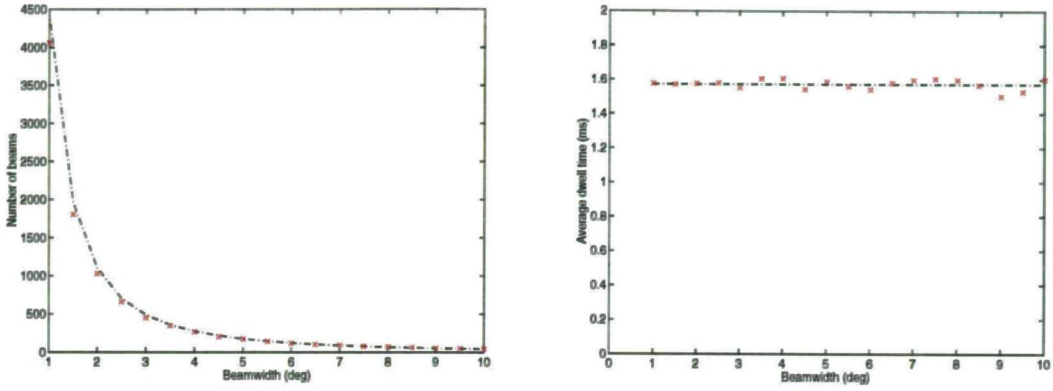

Figure 4-9 (a) Number of beams, and (b) average beam dwell times as a function of beamwidth. Crosses represent answer from exact calculation of all beam directions and dwell times, the line represents the estimate from the UV method outlined above

Thus we can determine the area of the coverage sector and volume under the dwell time surface by simply integrating the expressions for u, v and dt_{av}, over the desired azimuth and elevation limits. This then allows the calculation of the number of beams and beam dwell times as a function of the beamwidth. Figure 4-9 compares the estimates given by this method to those from calculating every search beam direction and dwell time exactly, using the same MESAR search sector as an example. The method gives excellent correlation to within a few percent. The search function time is simply the product of the number of beams and the average dwell time down each beam.

4.4.2 Rotating phased array multi-function radar system

In this section a new spatial system is derived to allow the same methodology that is used to determine the search function time for the static phased array system, described above in section 4.4.1, to be applied to the rotating phased array system.

Assuming that the surveillance function is to be carried out on array azimuth broadside, then scanning only occurs in the elevation plane. UV space is not an appropriate way to represent the search sector in these circumstances, since it depends on the beam broadening in both planes. An equivalent spatial representation may be derived in which

the beam areas remain constant for an elevation only scanning system.

A visualisation of this spatial system is shown in Figure 4-10 below, with the associated equations relating $\mathbf{u_r}$ and $\mathbf{v_r}$ to azimuth and elevation.

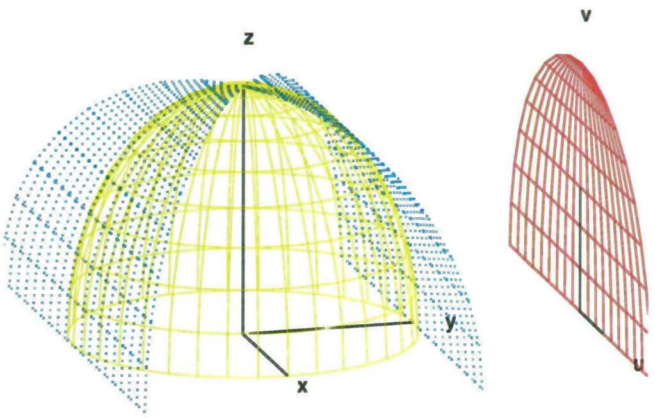

$$u_r = az.\cos(el) \qquad [4\text{-}11]$$
$$v_r = \sin(el - \alpha)$$

$$az = \frac{u_r}{\left(\sin^{-1}(v) + \alpha\right)} \qquad [4\text{-}12]$$
$$el = \sin^{-1}(v) + \alpha$$

Figure 4-10 A visualisation of the rotating UV space, and the associated equations

A unit hemisphere with lines of constant azimuth and lines of constant elevation plotted on its surface is shown. The lines of constant elevation are 'unwrapped' onto the surface of a cylinder. Since they are unwrapped, no distortion of the azimuth occurs. The lines on the cylinder are then projected onto a flat surface in the x-z plane. Comparing this to the UV space projection above, where the surface of a sphere is projected onto a plane - thus distorting space in 2 dimensions, in this case the surface of a cylinder is projected onto a plane - causing a distortion in just one dimension - the elevation dimension.

This projection will be referred to as rotating UV space, and the earlier static projection simply as UV space. This projection gives the desired result, that the beam area remains invariant with scan angle. It is interesting to compare the projection of lines of constant azimuth and elevation with a vertical rotating array, shown in Figure 4-11 below, to the static vertical array, shown in Figure 4-6(a). It is clear that the lines of constant azimuth do not become compressed at the extremes of the figure as they do in the UV space projection, although the lines of constant elevation remain the same in both figures.

Although the image in Figure 4-11 looks rather like the orthographic projection above and does look somewhat familiar, it has not been found in the cartography literature; the most similar projections found being the Sanson-Flamsteed sinusoidal and Mollweid [Adams, 1914], which are both equal area projections. Usually the desire in cartography is to conserve either the area or the distance when projecting from the surface of a globe onto a flat plane (it is impossible to conserve both). This projection conserves neither,

so is presumably of little interest in that field.

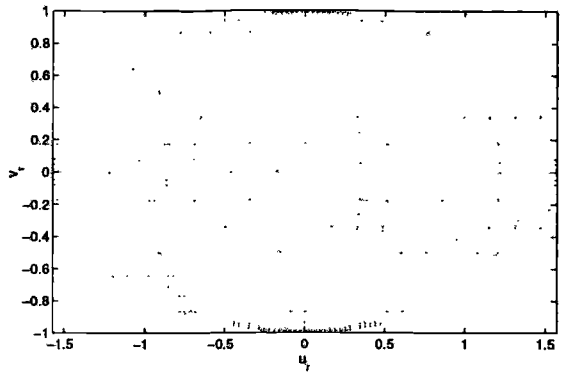

Figure 4-11 Lines of constant azimuth and elevation in the rotating UV space, for a vertical array

Figure 4-12 shows the variation in the projection as a function of array tilt angle from vertical.

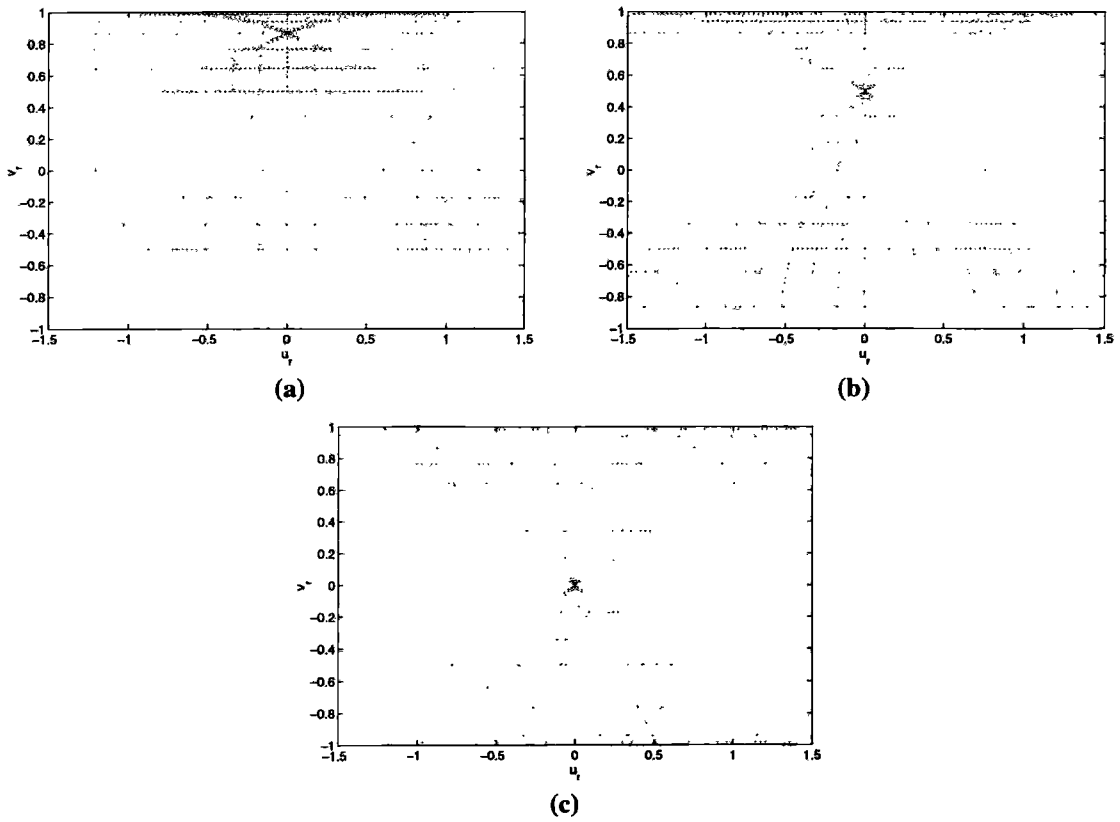

Figure 4-12 (a,b,c) Lines of constant azimuth and elevation in the rotating UV space, for arrays inclined back from vertical (a)30°, (b)60°, (d)90°

As in the static array case, we may use this spatial system to derive the exact beam directions for a rotating radar, given the azimuth and elevation limits of the sector. For a rotating system, it is likely that sectors will cover all azimuth directions. However to enable comparison to section 4.4.1 above, we will consider the same MESAR search

configuration as before, with limits of ±45° in azimuth and 1.18° - 52.5° in elevation, and a 3dB beamwidth of 3.1°, with beams overlapped at 0.85 beamwidths. Figure 4-13 shows the calculated beam directions in the rotating UV space. The exact number of beams that are used for this search sector in MESAR is 657. As we would expect, the rotating system requires a greater number of beams to search a given sector because the beam area is smaller than in the static case, due to the absence of azimuth scanning.

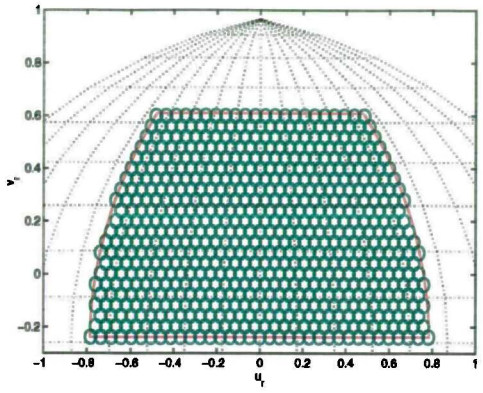

Figure 4-13 Beam directions in rotating UV space, using a MESAR search configuration as an example

Similarly, we may also estimate the number of beams in the search volume, without explicitly calculating each beam direction. The estimate is now given by the ratio of the search sector in rotating UV space to the area of the beam in rotating UV space. The area of the beam in rotating UV space, A_{beam_ruv}, is the same as that in the static form of UV space;

$$A_{beam\_ruv} = \pi \sin^2(\theta_3) \qquad [4\text{-}13]$$

The area of the sector to be searched, A_{sector_ruv}, may again be found by integration.

$$A_{sector\_ruv} = 2\left[\int_{el\_min}^{el\_max} u_r \frac{\delta v_r}{\delta el}\delta el\right]_{az=az\_max}$$

$$= az\_\max\left[\frac{1}{2}\sin(2el-\alpha)+el.\cos(\alpha)\right]_{el\_min}^{el\_max} \qquad [4\text{-}14]$$

The result is simpler in the rotating case, having a simple analytical solution, since the lines of constant elevation remain horizontal in rotating UV space, even when the array is tilted. The area given by equation [4-14], is shown in Figure 4-14(a). As in the static case, this approximation gives a result within 8% of calculating the number of beams

exactly.

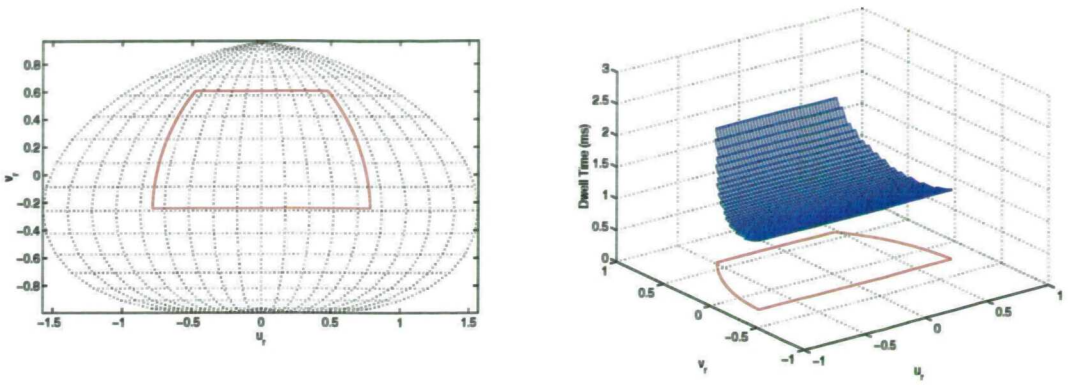

Figure 4-14 (a) MESAR coverage limits in rotating UV space, (b) Beam dwell time plotted as height above the rotating UV plane

Figure 4-14(b) shows the dwell time in each beam direction plotted as a surface above the beam directions in rotating UV space. As in the static case, the dwell time of each beam is given by the broadside dwell time, $dt_{broadside}$, divided by $\cos^3(\theta)$, but now, θ depends simply on the elevation. Thus, the average dwell time, dt_{av}, is given simply by equation [4-15], below.

$$dt_{av} = \frac{\left(\int_{el\_min}^{el\_max} \frac{dt_{broad\_side}}{\cos^3(el-\alpha)} \partial v \right)}{\sin(el\_max-\alpha) - \sin(el\_min-\alpha)}$$

$$= \frac{dt_{broad\_side}}{\sin(el\_max-\alpha) - \sin(el\_min-\alpha)} \left(\int_{el\_min}^{el\_max} \frac{1}{\cos^2(el-\alpha)} \partial el \right)$$

$$\therefore dt_{av} = \frac{\tan(el\_max-\alpha) - \tan(el\_min-\alpha)}{\sin(el\_max-\alpha) - \sin(el\_min-\alpha)} . dt_{broad\_side} \qquad [4\text{-}15]$$

Thus we can simply estimate the number of beams and beam dwell times as a function of the beamwidth for a rotating array system. The estimates this method gives are compared to calculating every search beam direction and dwell time exactly in Figure 4-15 below, using the same MESAR search sector as an example. Again, the method gives excellent correlation.

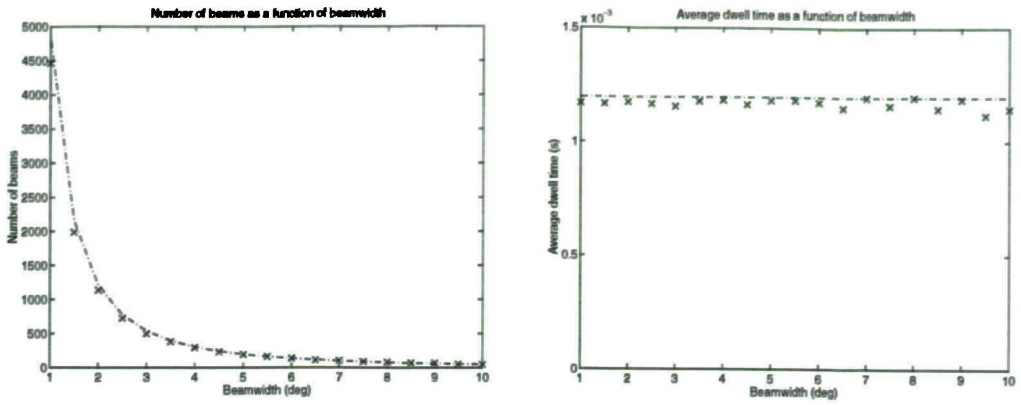

Figure 4-15 (a) Number of beams, and (b) average beam dwell times as a function of beamwidth, for a rotating array multi-function radar. Crosses represent answer from exact calculation of all beam directions and dwell times, the line represents the estimate from the rotating UV method outlined above

4.5 Search time in a noise limited environment

The methods derived in sections 4.4.1 and 4.4.2 are now applied to a comparison of different static and rotating multi-function radar antenna configurations. In this section only targets whose detection is limited by thermal noise are considered. Clutter is considered in the following section. From this an understanding of the effects of using broadened beams and simultaneous beam processing will be obtained, as well as a system level comparison of the multi-function radars.

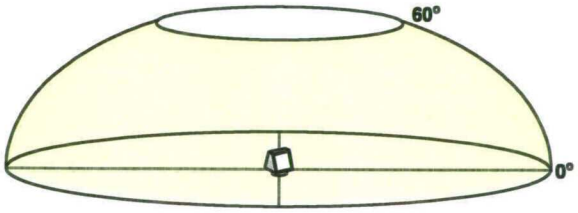

Figure 4-16 The example surveillance coverage volume for comparison of different multi-function radar antenna configurations

The configuration we will consider will be of a search of 0-360° azimuth and 0-60° in elevation, with a multi-function radar tilted 20° back from vertical, shown in Figure 4-16, above. Nominally, a 1ms dwell time is assumed on array broadside, which is increased (assuming coherent integration of pulses) to offset a two way loss in gain of the array that varies with the cube of the cosine of the scan angle (see section 2.3.2.2 above). Two static array antenna configurations will be considered; a 4 faced system, requiring scanning in azimuth to ±45° , shown in Figure 4-17(a), and a 3 faced system, requiring scanning in azimuth to ±60°, shown in Figure 4-17(b).

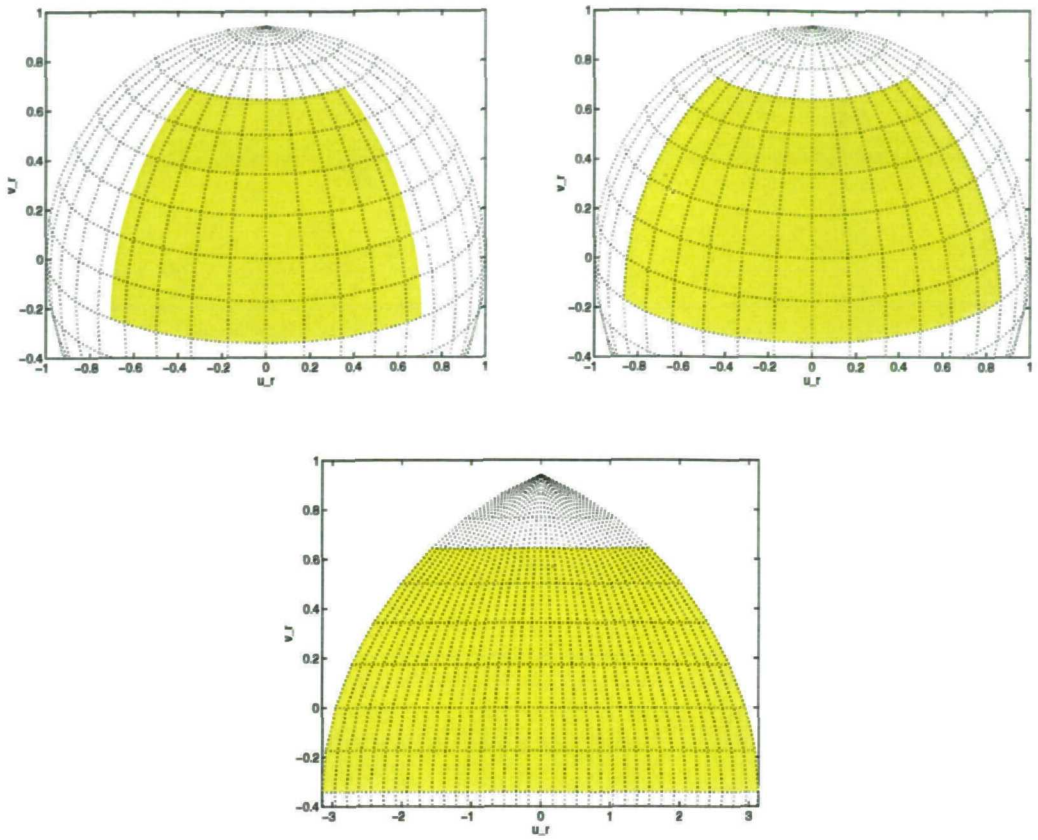

Figure 4-17 (a,b,c) 0°-60° elevation search sector plotted in (a) UV space for a 4 faced multi-function radar scanning to ±45°, (b) UV space for a 3 faced multi-function radar ±45°, (c) Rotating UV space, applicable to a 1,2,3 or 4 faced multi-function radar

Rotating systems with 1 - 4 faces will be considered. In the rotating case, the number of beams and the dwell time required for each beam is independent of how many array faces the multi-function radar has, since there is no azimuth scanning for the search function. Thus one representation of the search sector in rotating UV space is all that is required for all of the rotating multi-function radar systems, shown in Figure 4-17(c).

Figure 4-18, below, compares the number of beams in the total search volume as a function of beamwidth, for the 3 and 4 faced static multi-function radar systems and the rotating multi-function radar systems. Figure 4-18(b) shows the ratio of the number of beams required in the static systems to the rotating systems. It is seen that the rotating systems require a greater number of beams than the static systems to cover the example search volume. Around 8% fewer beams are required by the 4 faced static system, and 15% less are required by the 3 faced static system. This is due to the extra beam-broadening that occurs with azimuth scanning.

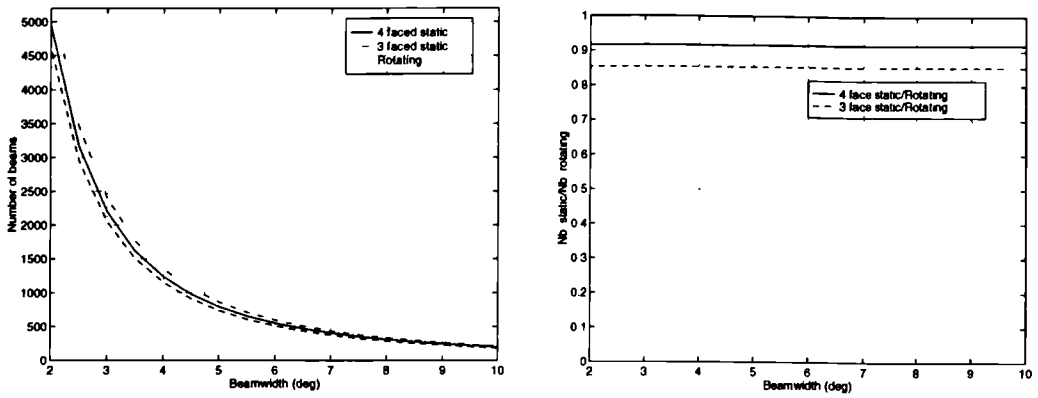

Figure 4-18 (a,b) Number of beams required to search the specified volume as a function of beamwidth, and the comparison of the static and rotating systems

Figure 4-19 compares the average dwell time required to search the volume, assuming a nominal 1ms dwell time in the array broadside direction. At this stage no compensation in transmit energy is made for the loss in gain in broadening either the transmit or receive beams; thus the average dwell time remains constant with beamwidth. The ratio of the average dwell times required by the static systems to those of the rotating systems, shown in Figure 4-19(b), shows a dwell time over 25% greater is required by the 4 faced static system, and over 70% greater than the 4 faced static system, to achieve the same detection performance.

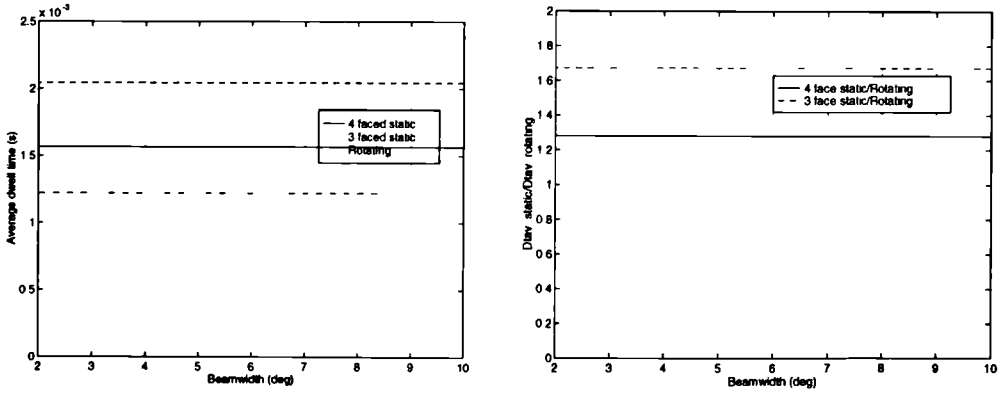

Figure 4-19 (a,b) Average dwell times and comparison

The increase in average dwell time required by the static systems greatly outweighs the fewer beams necessary for search. This is reflected in the total search function times for the systems, shown in Figure 4-20(a) as a function of beamwidth. The comparison in Figure 4-20(b) shows that the 3 and 4 faced static systems require 18% and 44%, respectively, more radar time to perform the same search as the rotating system.

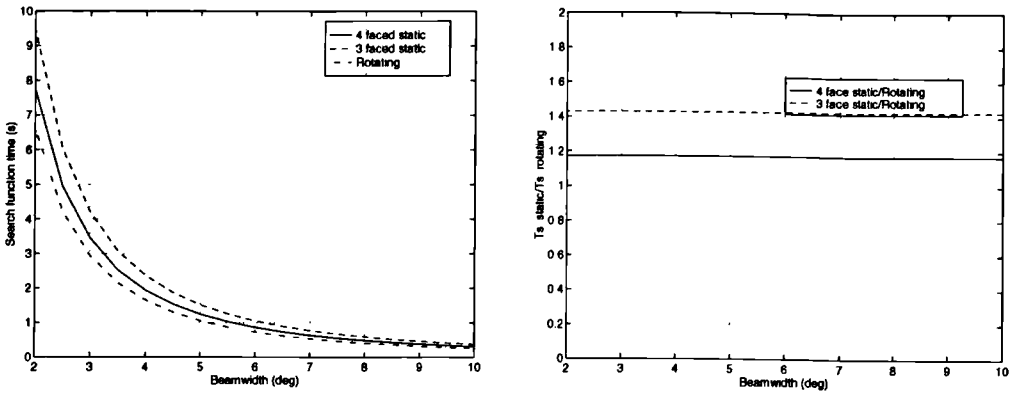

Figure 4-20 (a,b) Search function time and comparison

Table 4-1 below summarizes the results from this comparison, using a 2.5° beamwidth as an example.

Antenna Configuration	No of beams (per face)	Average beam dwell time	Search function time (per face)	Search function time (total)
1 face rotating	3380	1.17ms	4.0s	4.0s
2 face rotating	1690	1.17ms	2.0s	4.0s
3 face rotating	1127	1.17ms	1.3s	4.0s
4 face rotating	845	1.17ms	1.0s	4.0s
3 face static	963	2.03ms	1.9s	5.7s
4 face static	774	1.55ms	1.2s	4.8s

Table 4-1 Summary of static and rotating multi-function radar search comparison for a 2.5° beamwidth

Table 4-1 presents two interesting results. Firstly, when comparing the 4 faced and 3 faced static systems with their rotating equivalents, it is found that the static systems require 20% (4 faced) and nearly 50% (3 faced) more radar time to execute the search. More significantly, when comparing the 3 faced static system with a 2 faced rotating system, nearly the same amount of radar time must be dedicated from each of the 3 faces as is required from just 2 faces in the rotating case. Thus this comparison suggests one of the 3 faces could be eliminated if rotation was employed with very little detriment to the search. The savings are thus significant, although they do vary depending on the search volume and the array tilt angle. Interestingly these findings are in agreement with a recent paper by Billam [Billam, 1997b], in which different static and rotating multi-function radar's performance is compared.

4.5.1 Dwell time compensation

Compensation for the loss of gain associated with broadening the antenna patterns is now considered, through coherent integration of pulses. First the case of broadening both the transmit and receive beams is considered.

Figure 4-21(a) below shows the decrease in search function time that occurs for the multi-function radar systems as the beamwidth is broadened, with a nominal broadside waveform of 1ms dwell time. Clearly since the broadside waveform is not being increased to offset the loss in both transmit and receive gain, the signal to noise ratio and probability of detection drop rapidly, Figure 4-21(b,c).

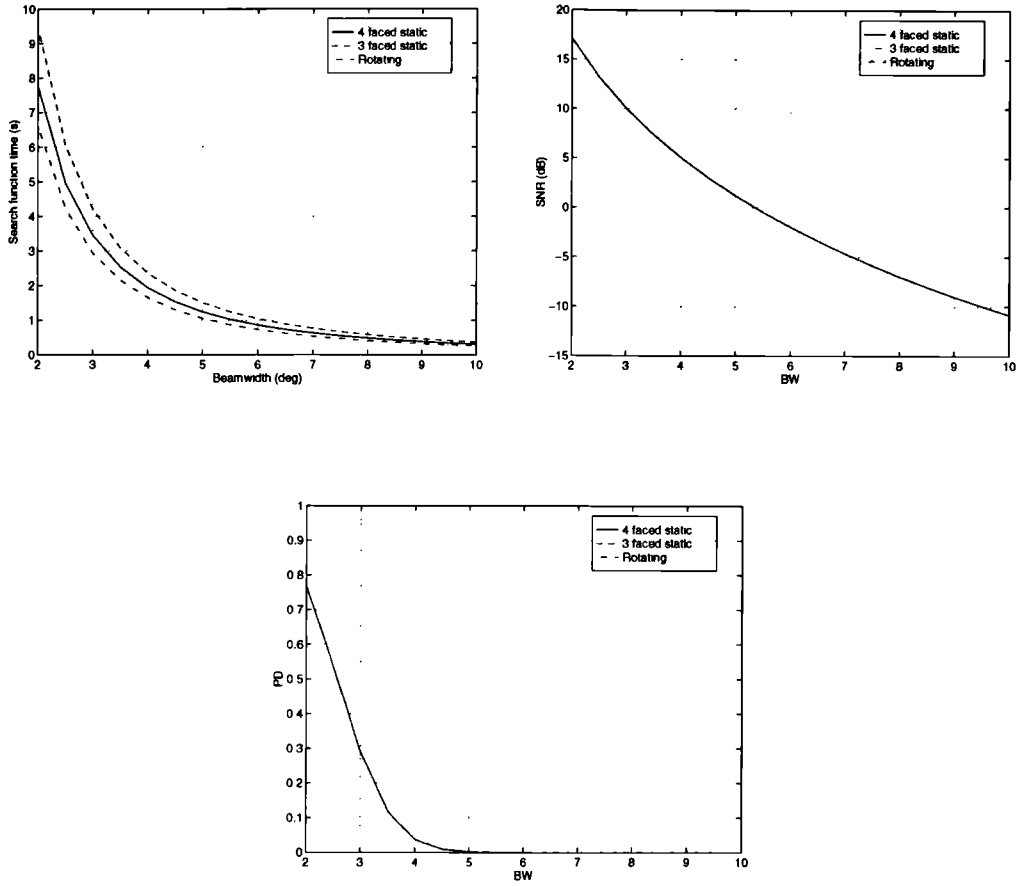

Figure 4-21 (a,b,c) Signal to noise ratio and Probability of detection as a function of beamwidth, with broadening of both the transmit and receive beams, using the nominal 1ms waveform above - ie not compensating for the loss in two way gain

If it is now assumed that the broadside waveform is increased in length, to allow extra pulses to be coherently integrated, then the impact on the search function time can be seen. Figure 4-22 shows that in order to maintain uniform detection performance as the transmit and receive beams are broadened, the search function time increases very rapidly. It is obvious that using both broad transmit and receive beams would be an extremely inefficient way to perform the search.

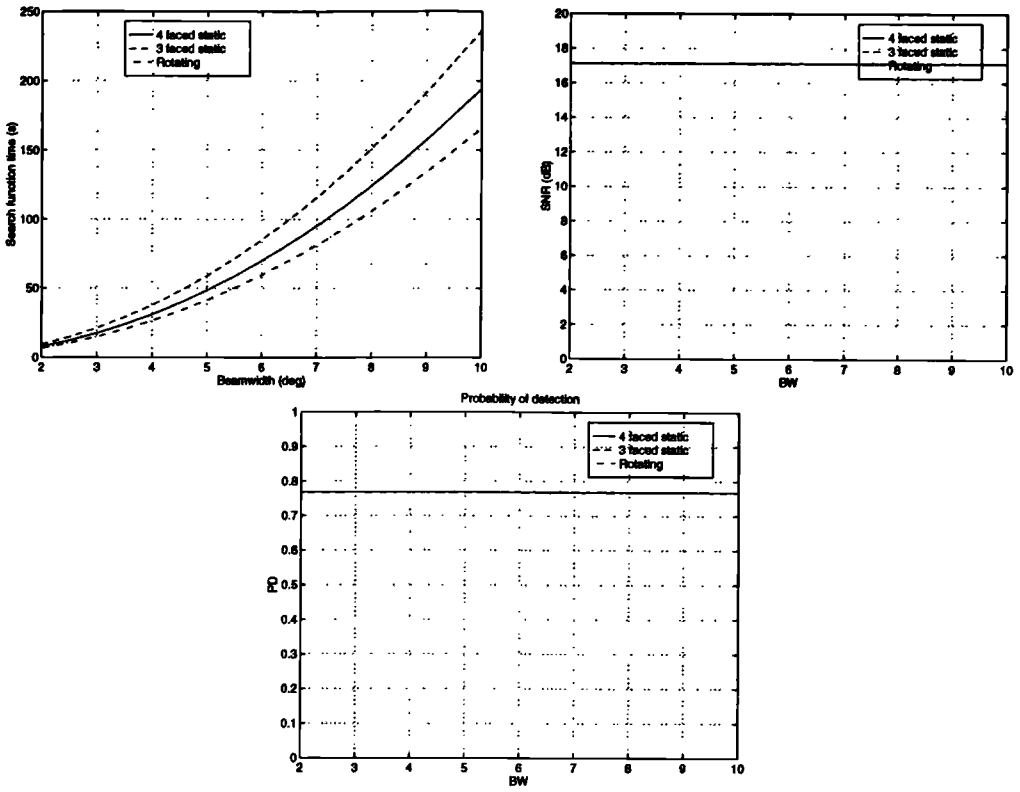

Figure 4-22 (a,b,c) Search function time required to maintain a uniform detection performance with broadened transmit and receive beams

Figure 4-23 and Figure 4-24, below, now consider search function time when using simultaneous multiple narrow receive beams coupled with a broad transmit beam.

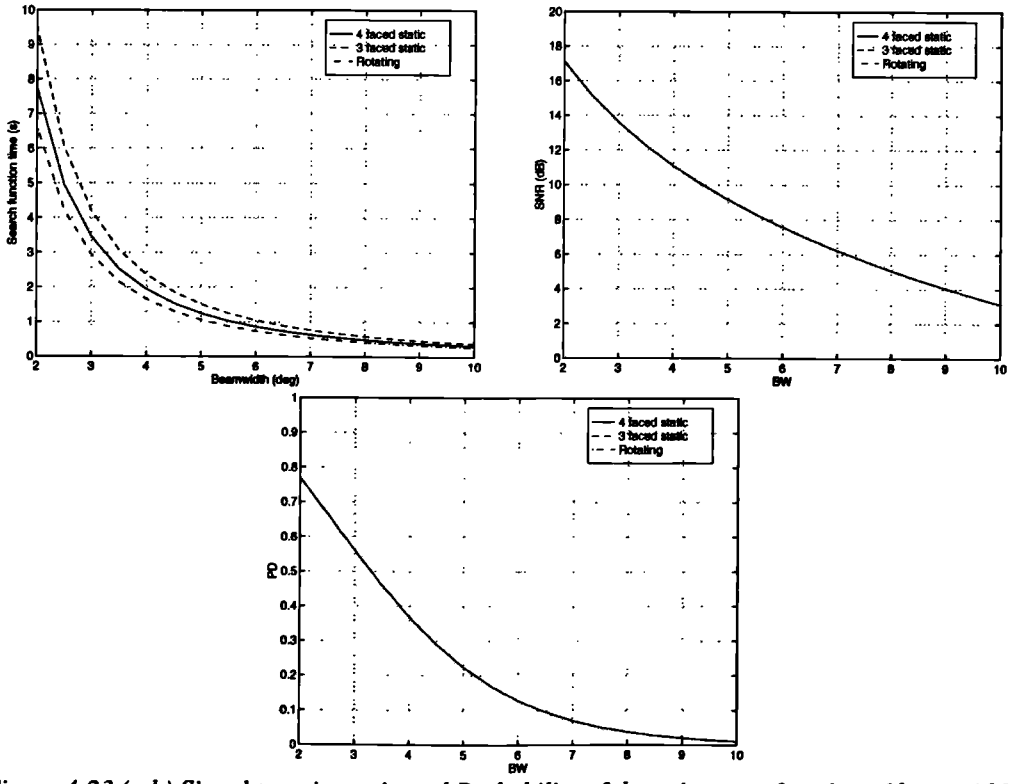

Figure 4-23 (a,b) Signal to noise ratio and Probability of detection as a function of beamwidth, with broadening of only the transmit beam, using the nominal 1ms waveform above - i.e. not compensating for the loss in one way gain

Figure 4-23 shows the decrease in search function time, signal to noise ratio and pd that occur as the transmit beamwidth is broadened, with a nominal broadside waveform of 1ms dwell time.

When the broadside waveform is increased to compensate for the loss in transmit gain, the search function time is found to be invariant with transmit beamwidth, in order to provide uniform detection performance. This is the familiar result given by the search radar equation, and is shown in Figure 4-24.

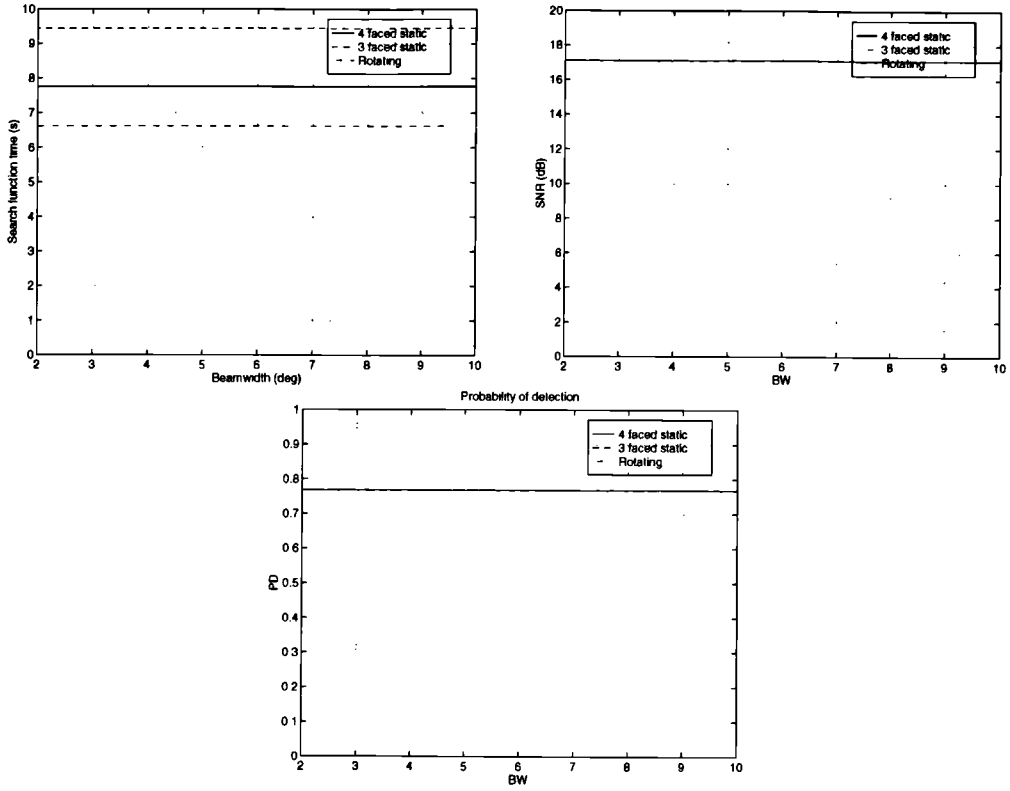

Figure 4-24 Search function time required to maintain a uniform detection performance using a broadened transmit beam and simultaneous multiple narrow receive beams

4.6 Search time in a clutter limited environment

Clutter is a notoriously difficult factor to predict through either mathematical modelling, or through statistical calculations. Clutter, and the methods of separating it from targets of interest, is one of the largest areas of theoretical and experimental research in the radar field. Not only are the clutter statistics highly dependent on what is being illuminated, and how it is being illuminated by the radar (in the sense of resolution and PRF), but also on the filtering and processing that occur upon reception within the radar.

For this reason, it is only sensible in a system level analysis such as this to incorporate the effects of clutter in their broadest terms. Here, the effects of variable beamwidth operation and simultaneous multiple beam processing on a multi-function radar with MTI and Pulsed Doppler processing are shown using only relevant elements of the radar equation.

Table 4-2 compares the relevant parts of the radar equation for the three different types of system under consideration; a single narrow pencil beam system, a variable beamwidth system in which both the transmit and receive beamwidths have been doubled, and a simultaneous multiple beam system in which the transmit beamwidth is doubled, but narrow receive beams are used. No clutter is assumed in this case; the target competes with thermal noise only. Nominally a 1° beamwidth is assumed for the narrow beamwidth system, which is assigned a nominal gain of 1. Thus the broadened beam system has a two way gain of $1/16^{th}$ of the narrow beam system, and the multiple beam system has a two way gain of ¼, for a doubling of beamwidth. It is assumed in this case that the search function time available is 1s. Therefore, the dwell time available in each beam direction is simply 1/number of beams.

System	Narrow Beam	Broadened Beam	Multiple Rx Beams
Beamwidth	1° Tx / 1° Rx	2° Tx / 2° Rx	2° Tx / 1° Rx
Transmit Gain, G_{tx}	1	¼	¼
Receive Gain, G_{rx}	1	¼	1
Number of Search Beams	4000	1000	1000
Dwell Time per Beam, t_d	1/4000 s	1/1000 s	1/1000 s
Search Time	1 s	1 s	1 s
SNR $\propto G_{tx}G_{rx}t_d$	1/4000	1/16000	1/4000
Relative SNR	4	1	4

Table 4-2 Radar equation comparison of narrow beam, broadened beam, and multiple beam systems, assuming noise limited detection

The result is that for the same search function time, the broadened beam system has a quarter of the signal to noise ratio of the narrow beam system, whilst the multiple beam system maintains the same signal to noise ratio.

If clutter is now considered, the story is somewhat different. Resolution in the Doppler domain is governed by the dwell time, t_d. It is this that will define the detection performance in the presence of strong clutter. This is shown in Figure 4-25(a) below, reproduced from Barton [Barton, 1988]. He gives the contamination of the velocity spectrum as per equation [4-16] below.

Figure 4-25(b), below, plots the percentage of filters contaminated by sea clutter as a function of the number of pulses for a 3GHz system. Here an unambiguous range of 30km is assumed, and a clutter spectral width of 1.4m/s, corresponding to sea state 5 according to the DERA Naval Environment Clutter, Attenuation and Propagation Specification [Money, 1995].

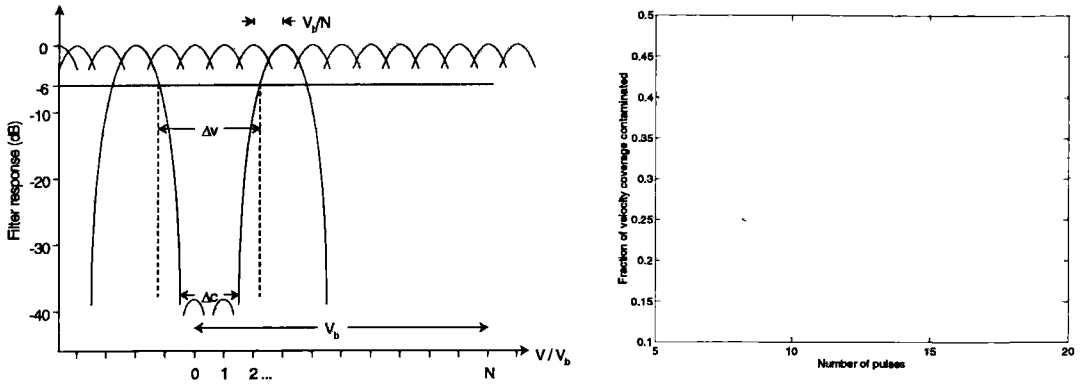

Figure 4-25(a,b) Contamination of Doppler filters by clutter

$$\Delta v = \Delta c + \frac{2V_b}{N} \qquad [4\text{-}16]$$

where Δv is the velocity spectrum that is contaminated
Δc is the clutter spectral width
V_b is the unambiguous velocity
N is the number of pulses per Doppler burst

The case of clutter limited target detection is shown in Table 4-3 below. In this instance t_d remains fixed in all three systems, at a nominal value of 1ms. For the narrow beam system this results in an increase in search time from 1s to 4s, but with what may be regarded as an excess of signal to noise ratio; it exceeds the signal to noise ratio required for detection by a factor of 4 compared to the noise limited case. The system with broadened transmit and receive beams can complete the search in the same 1s frame time with the 1ms dwell time, but has a relative signal to noise ratio of just 1, as in the noise limited case.

The multiple receive beam system has the same 1s search time as in the earlier case of noise limited detection. It also retains the same relative signal to noise ratio of 4, as in the earlier case. Thus there is no penalty in using the simultaneous multiple receive beams in the clutter limited case. The same signal to noise ratio is achieved as was in the noise limited case. However, the longer dwell time coupled with multiple beams, allows the clutter cancellation requirement to be met with a search time of 1s, compared to 4s

for the narrow beam system. Hence multiple beam processing may be regarded as an extra degree of freedom for the multi-function radar, trading off energy transmitted in a given direction for time, and therefore allowing longer waveforms to be transmitted without increasing the function time.

System	Narrow Beam	Broadened Beam	Multiple Rx Beams
Beamwidth	1° Tx / 1° Rx	2° Tx / 2° Rx	2° Tx / 1° Rx
Transmit Gain, G_{tx}	1	¼	¼
Receive Gain, G_{rx}	1	¼	1
Number of Search Beams	4000	1000	1000
Dwell Time per Beam, t_d	1/1000 s	1/1000 s	1/1000 s
Search Time	4 s	1 s	1 s
SNR $\propto G_{tx}G_{rx}t_d$	1/1000	1/16000	1/4000
Relative SNR	16	1	4

Table 4-3 Radar equation comparison of narrow beam, broadened beam, and multiple beam systems, assuming clutter limited detection

4.7 Impact on the tracking functions

Generally, higher performance may be obtained for the tracking function by using a narrower beam. This is particularly the case for current multi-function radars which use relatively broad beams in the region of 2° to 3°. It has been shown in the previous section that the surveillance function time, theoretically, does not increase with narrower beams, if multiple receive beam processing is possible; the compromise in beamwidth that is normally associated with an air defence multi-function radar ([Barton, 1988], [Moore & Salter, 1995]), is no longer valid. Thus multi-function radars may benefit from the narrower beamwidths normally associated with dedicated tracking radars, giving benefit in terms of resolution, plot accuracy and performance in jamming and multipath.

However, the narrower beamwidth, coupled with the low track update rates associated with multi-function radars generates a problem in tracking manoeuvring and rapidly crossing targets. It is possible that the target will not be illuminated at the next track update if the target manoeuvres or if azimuth/elevation crossing rate certainty is low. Multiple beam updates should therefore be considered for the tracking function. Figure 4-26 below shows how the use of multiple beams could be envisaged for tracking and surveillance.

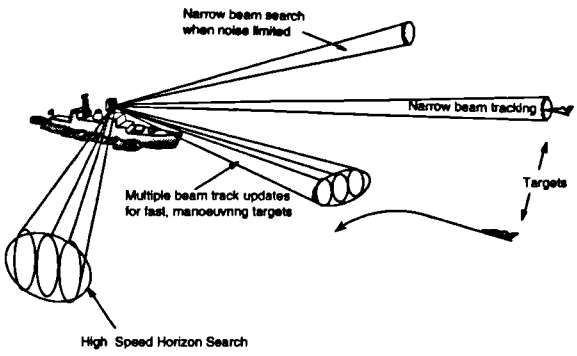

Figure 4-26 An example of the use of single beam and multiple beam updates in the surveillance and tracking functions

The results of sections 4.5 and 4.6 suggest that, assuming perfect coherent integration of pulses, in principle, we may use simultaneous multiple beams for tracking wherever we wish, without detriment to the detection performance. In a noise limited situation the increase in dwell time required as the transmit beam is broadened, will be exactly offset by the loss in gain. In a clutter limited situation, there may be an advantage to using multiple beam track updates, since the waveform length may be determined by the Doppler resolution required to separate the clutter from the target, rather than the target from noise.

4.8 Conclusions

A novel method of calculating the search function time for a static radar has been developed. This gives analytical expressions which may be quickly evaluated for a range of beamwidths and search sectors, without explicitly calculating each beam direction and dwell time. This will allow surveillance configurations of a multi-function radar to be evaluated rapidly using simple equations. The method is based on estimating the number of beams and the dwell times required in each beam direction in UV space, in which the beam area remains invariant.

By creating a similar projection to the UV space projection, involving a transformation onto the surface of a 3D cylinder, another spatial system may be produced in which the beam area of a rotating multi-function radar system remain invariant. This projection is somewhat akin to the Sanson-Flamsteed sinusoidal and Mollweid projections used in the field of cartography. The above methodology for estimating the beam directions and dwell times, and thus the search function time, may be applied in this spatial system for

the rotating system.

The above methods for static and rotating multi-function radars have been compared with the process of calculating beam directions and dwell times exactly, and have found answers to within a few percent. The accuracy decreased somewhat as the beamwidth increased (to around 8% for a 10° beamwidth), due to the exact number of beams required to cover the edges of a given region.

A comparison of the search function for different configurations of static and rotating array multi-function radars has been made. It was found that the static systems require 20% (4 faced) and nearly 50% (3 faced) more radar time to execute a complete search of the same volume. When comparing the 3 faced static system with a 2 faced rotating system, it was found that nearly the same amount of radar time must be dedicated from each of the 3 faces as is required from just 2 faces in the rotating case. Thus this comparison suggests one of the 3 faces could be eliminated if rotation was employed with very little detriment to the search. These figures will vary to some degree, depending upon the exact volume that is to be surveyed, and the tilt angle of the arrays.

The impact of using a broadened beam both in transmit and receive on the multi-function radar system has been evaluated. For any significant broadening of the beam there is a heavy penalty to be paid both in the tracking and surveillance functions.

The variation of surveillance search time has been determined as a function of transmit beamwidth for target detection limited both by thermal noise and by clutter, assuming multiple narrow receive beams. When detection is limited by thermal noise the result is as predicted by the familiar search radar equation; the search time is invariant with transmit beamwidth, since a wider beam requires a longer dwell time to regain the signal to noise ratio.

When target detection is limited by clutter, the search time may be decreased by broadening of the transmit beam. This is because the dwell time in that instance is determined by the resolution required in the Doppler domain, governed by the length of the transmit waveform.

Although the study has been aimed at investigating the effects of using broadened beams, it is not implied that systems should necessarily use broader beams than they currently do. Quite the reverse. The implication from these arguments is that systems

may be built with narrower receive beamwidths than those in use currently, whilst still retaining the clutter cancellation levels required. This can be achieved within the time-budget constraints of the multi-function radar, through using broadened transmit beams and multiple receive beams. This would allow the benefits of a dedicated tracking radar to be realised, such as excellent monopulse accuracy, resolution of closely spaced targets, and resistance to main beam jamming.

5 RESOURCE MANAGEMENT IN STATIC AND ROTATING ARRAY MULTIFUNCTION RADAR

5.1 Introduction

To provide the functions of volume surveillance, horizon surveillance, track maintenance, missile uplink, etc., the multi-function radar must rapidly switch the beam between many tasks. It is the job of the multi-function radar resource manager to ensure that the most appropriate radar tasks are chosen as time progresses and to allocate the multi-function radar resources in a sensible manner. This chapter covers the resource management and task scheduling of a multi-function radar.

There are two objectives. Firstly, to investigate resource management and task scheduling in multi-function radar, and particularly the complications that arise with rotation of the array antenna. Secondly, to develop models of static and rotating array multi-function radars based around a task scheduler centred architecture, which may be used to evaluate both the scheduler performance and tracker algorithms.

A background to the areas of resource management and task scheduling is given below. Section 5.2 presents a set of objectives that are proposed here to be used for multi-function radar resource management and scheduling systems. Section 5.3 then covers task scheduling in a static multi-function radar. Here a model of a multi-function radar centred on the task scheduling algorithm used in the MESAR radar is developed, and the validation and results from that model are presented. In section 5.4 task scheduling in a rotating multi-function radar is covered. In this case, no suitable algorithms or strategies were at hand for implementation into a computer model. Therefore a novel algorithm was created. An analysis of the complications due to rotating the array antenna is presented, along with an algorithm which successfully copes with those complications. Results from the development of a second model of a multi-function radar, centred on the rotating scheduler algorithm, are presented. Section 5.5 discusses ways in which the performance of both the static and rotating scheduler algorithms may be improved by using penalty functions or fuzzy logic, and section 5.6 contains the

conclusions of the work.

The distinction between the functions of resource management and task scheduling is somewhat blurred and to some extent varies from system to system, so a definition that will be adhered to in this chapter is given below.

In order for efficient multi-function radar resource management to be achieved two distinct processes must be completed;

i. *All tasks must be ranked in a priority order.* Note that the priorities of tasks may change throughout an engagement.
ii. *Tasks must be formed into a timeline for the multi-function radar to perform.* This is the specific job of the task scheduler.

The first of these processes, ranking the functions in priority order, is usually determined a priori using the expert knowledge of an engineer; however the priorities of tasks may be elevated or lowered if necessary under automatic control algorithms. This, together with the calculation of desired time for tasks to be scheduled and the amount of radar time required, may be defined as the job of resource management. The resource manager may also include macroscopic rules for the radar's management and allocation; for example, the manner in which surveillance is degraded in the case of an overload of tasks. These rules may take information from several areas of the sensor, and also from outside of the sensor. The resource management algorithms must allow robust multi-function radar operation in all scenarios that may be encountered, and allow a tactically sensible degradation of performance if the multi-function radar becomes overloaded with tasks.

The task scheduler is a subsystem of the multi-function radar resource manager. It is fed tasks, with their desired times for scheduling, their relative priority, and possibly other constraint information. At any time the task scheduler will have a large list of tasks, each of which has a different priority and timing constraints pertaining to it. The task scheduler should try to maximise the use of radar time, whilst ensuring that the radar time is also given to the most important of these tasks throughout the duration of a scenario.

The formation of the timeline may be done in advance over a small time interval, as

suggested by Sabatini & Tarantino [Sabatini & Tarantino, 1994], or it may be decided in real time, task by task, as in MESAR ([Stafford, 1990], [Wray, 1992]). A drawback of using the former approach is that, although it may be simpler from the computation and processing aspect, it is difficult to accommodate jobs which rapidly appear, such as plot confirmation jobs, without throwing away or delaying others. In practice all scheduler algorithms must accommodate a small queue of the order of microseconds to allow for hardware setup times, for example in the phase shifters.

The scheduler's task in constructing this timeline is complicated due to the constraints which apply to each task;

i. *tasks vary in the criticality of the time period in which they must be scheduled.* Some may have a small window of opportunity which must be met for the task to be successful, while others may have much looser time constraints.
ii. *tasks differ significantly in length.*
iii. *tasks may become suddenly necessary or urgent, or may become unnecessary.*
iv. *tasks may have to adhere to some constraint such as close to array broadside operation in a rotating system.*

5.2 Resource management and task scheduling objectives

The resource manager is central to the effective control of the multi-function radar. If it does not perform its job correctly, every aspect of multi-function radar performance may be sub-optimal. In this section a set of objectives for a resource manager are presented, against which its performance may be measured.

The following broad objectives are suggested for resource management and task scheduling.

i. *schedule each task as near to the requested time as possible.*
ii. *schedule each task as close to array broadside as possible.*
iii. *schedule each task to minimise the radar idle time.*
iv. *schedule each task to maximise the tactical benefit of the multi-function radar.*

It is important to note that these are conflicting objectives and it is highly unlikely that all can be met for any sustained period of time. For example, it may be much more important to schedule a particular task at exactly the right time, than to constrain it to array azimuth broadside. Therefore these objectives must be reflected in the constraints with which a task is specified by the resource manager.

The first three may be viewed as primarily the responsibility of the task scheduler. The fourth objective then is the responsibility of the resource manager. It does not lend itself to use as a figure of merit, but it may be broken down into measurable objectives if we are to use it as figure of merit. These objectives will depend on the mission of the multi-function radar system and also the stage through the mission. A set of objectives for a naval air defence system are proposed below;

i. achieving a surveillance detection performance
ii. achieving a surveillance data rate, for track while scan
iii. achieving rapid track initiation
iv. achieving a tracking accuracy
v. maintaining missile communications

The relative importance of these at a given time will vary. For example, achieving the required detection performance for surveillance is imperative at the early stages of an engagement scenario. However, if the channels of fire of the weapon system are saturated, then the emphasis is less on detecting new targets, and more on retaining those already detected.

5.3 Task scheduling in a static array multi-function radar

5.3.1 Background

In a static multi-function radar, the constraint of scheduling tasks such as surveillance close to array broadside that must be adhered to in the rotating case does not apply. This significantly simplifies the task scheduling problem, and hence this is the case that was addressed first.

Two scheduler algorithms were considered; firstly the original MESAR scheduler

algorithms ([Chestnutt, 1984], [Birch, 1989], [Stafford, 1990]). These are the algorithms currently implemented in the MESAR system, although in the system itself they are now in a modified form. Subsequently a modified version of these algorithms was generated involving primarily a change to the time balance strategy.

It should be noted that since MESAR design note 242 [Birch, 1989] was written the algorithms implemented in MESAR have been further developed and thus the design note is somewhat out of date. Therefore an explanation of the current algorithm implemented in MESAR is given below in section 5.3.2.

5.3.2 The MESAR algorithm

The MESAR static task scheduling architecture centres around a prioritised list of all of the radar jobs. The following priority levels exist;

7. track maintenance	(highest priority)
6. plot confirmation	
5. track initiation	
4. track update	
3. surveillance	
2. slow track map/surface picture	
1. receiver calibration	(lowest priority)

A description of what constitutes a job, a task, and a look in MESAR is given below for clarification. A job may be surveillance of a sector or region, maintaining track on a specific target, or track initiation of a target. It will typically consist of several tasks, for example, searching a single surveillance beam position, performing one track update, or performing one track initiation update. Each task will typically consist of several activities which are non coherently integrated to give a detection. A look is one or more activities from a task that are transmitted coherently by the radar.

These looks are scheduled one at a time, and may be interleaved with looks from other tasks. Only when all of the looks that make up a task have been completed is the whole task said to have been scheduled. The only advantage in breaking tasks into smaller looks is that the scheduling delay of other tasks may be minimised. Thus if tasks are already small enough, this is unnecessary.

A timebalance scheme controls the scheduling of tasks on the job table [Birch, 1989].

Every job has a timebalance associated with it, which tells the scheduler how much radar time is owing to that job at that time. Only radar time that will actually be available to a job will be credited to its account. A positive timebalance indicates that the job is in need of radar time in order to complete a task. A zero timebalance means this job has had exactly the right amount of radar time, thus far. Finally, a negative timebalance means that this job does not need any radar time at this time.

When a look is scheduled from a task, the look time that has just been used is shared out amongst all the other jobs on the radar job table. The time balances of all other tasks are incremented by a fraction of the look-time in proportion with their own desired occupancy. The highest priority levels receive their shares of the look time first, and then each lower level receives its share. Lower levels only receive increments if the look time has not been shared out completely to the higher levels. Therefore, if the radar is overloaded, i.e. the desired occupancy of all the jobs in the job table is greater than 100%, then lower level timebalances will not be incremented, and thus the tasks from these levels will be delayed.

When all the looks that make up a task have been scheduled and the task is complete, the job's timebalance is decremented by the total dwell time of the task.

A new job may be inserted onto the job table with a negative timebalance, in order that it is not scheduled for some time. In this case all other job time balances must be incremented by a proportion to ensure the timebalances always have a sum of zero. This guarantees that timebalances are incremented relative to the radar resources available.

A flow diagram of the MESAR algorithm is shown in Figure 5-1, and a description is given below.

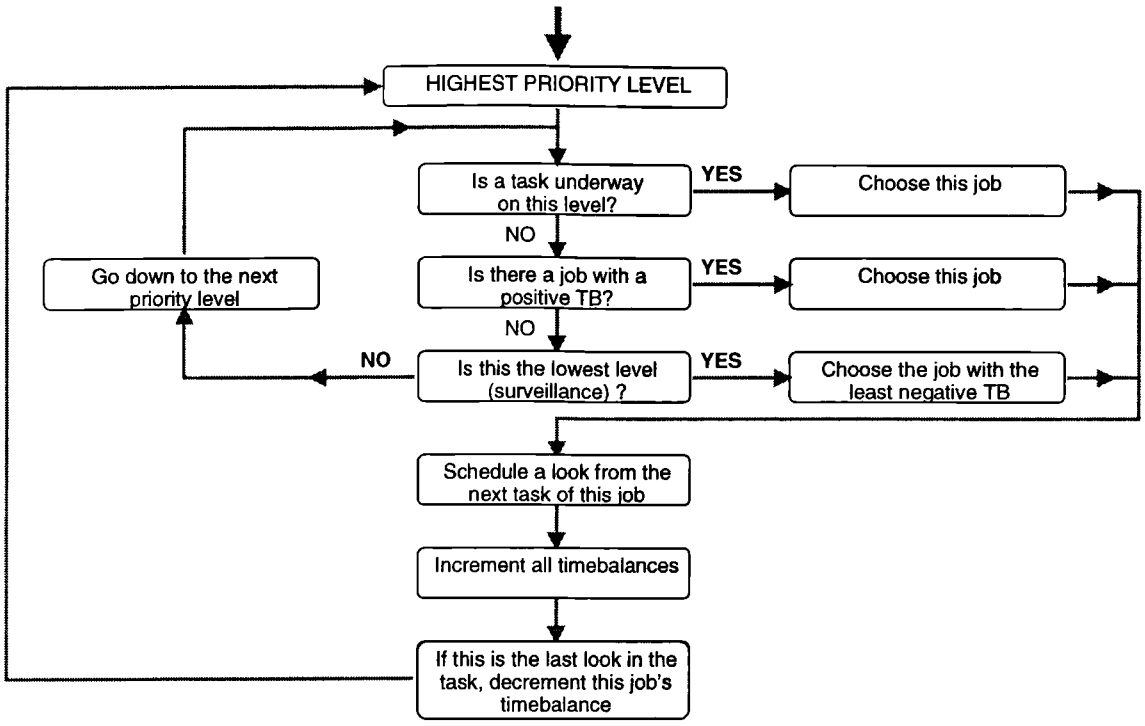

Figure 5-1 Flow diagram of the MESAR scheduler algorithm

Starting from the highest priority level;

i. If a job is already underway on that level, then that job is chosen for scheduling of looks. This means that tasks from each level will be completed sequentially, rather than many tasks from the same level being interleaved, and thus drawn out in time.

ii. If no task is underway then the task is chosen with the most positive time balance.

iii. If no task has a positive time balance then move down to the next level and repeat (i)-(iii)

iv. If no task has a positive time balance on the job table, then choose the surveillance task with the least negative time balance.

v. Schedule one look from the chosen task, and increment all other time balances by a fraction of this task.

vi. If that was the last look of a task decrement this job's time balance by the task dwell time.

In this way, looks are scheduled from a task one by one. Scheduling of looks from a task may only be interrupted by jobs at a higher level on the priority table. The timebalances are in effect simply used to measure when a task is ready for scheduling. Once looks from a task on a particular level have begun being scheduled, that task is always chosen, regardless of its own and other tasks' timebalances, unless it is interrupted by higher priority jobs.

The algorithm only allocates radar time to the lower priority levels if it is available, i.e. unrequired by higher priority levels. Since surveillance is the lowest priority level in MESAR, the occupancy of the surveillance function, and thus the surveillance frame times, increase and decrease as the tracking load changes. This is shown in Figure 5-2, below. The multi-function radar may be specified to meet its surveillance detection performance when say, surveillance has an 80% occupancy. If there are no tracking tasks, surveillance will thus exceed its detection performance. Conversely, if the system has more tracking tasks than the 20% headroom allowed, surveillance will fail to meet its detection performance requirement.

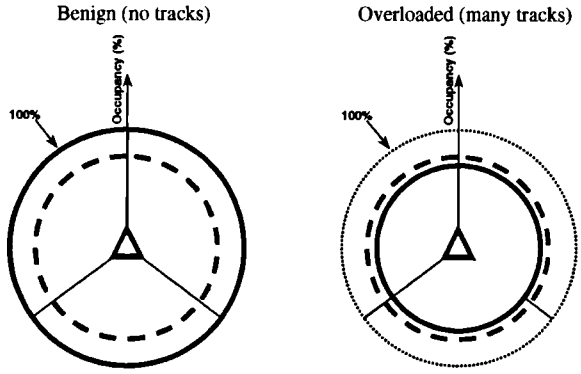

Figure 5-2 Degradation of surveillance detection performance

Timebalances appear, in practice, to be used in a simpler way than their rather complicated calculation warrants. This is reflected in the recent modifications to the MESAR scheduler which simply schedule tracking tasks on their desired update time, disregarding the timebalance completely. This should have no effect on the scheduling of tracking tasks, but is simpler.

The radar job controller, maintains the radar job table and acts as an interface with the rest of the radar control processing such as the tracker. It inserts and deletes jobs as is necessary, for example a plot confirmation job request as a result of a successful surveillance detection. In this way the task scheduling algorithms themselves can be

kept simple, since much of the complexity specific to each function's operation resides in the radar control processing.

5.3.3 The modified MESAR algorithm

The modified algorithm involves primarily a change to the timebalance scheme. In MESAR the timebalances are a 'bank account' of radar time for each job. They represent how much radar time is owed to a job at any instant, and in overload situations, how much radar time can be given to that job by the radar. In practice, however, the timebalances are only used to determine whether a task is ready for scheduling - i.e. if the job has a timebalance greater than or equal to 0 then this job is ready.

In the modified version of the algorithm the timebalances simply represent how early or late tasks from a job are. The timebalance units are now seconds, which makes the values themselves meaningful; if a task does not need to be scheduled for 1s, its timebalance is -1s. This simple change will not affect the performance in any way. It merely allows for easy understanding of the scheduler operation.

Two versions of the algorithm have been coded. The first follows the MESAR algorithm closely, allowing tasks to be broken down into smaller looks, and following the MESAR algorithm rules for their scheduling. The second is a simplification which schedules tasks as whole units. The simplified version operates more quickly, and may be applicable if the simulation is going to be of a high power radar representative of an operational radar. The waveforms in this case are likely to be considerably shorter than in MESAR and therefore will not delay tasks significantly.

The scheduler now uses simply the task look back interval (the time between successive tasks - e.g. the track update interval, or the surveillance beam revisit time), and the task time (the dwell time of the task) to control the scheduling of tasks.

A zero timebalance indicates this is the exact time for the job to be scheduled. A positive timebalance indicates the job is now late, and a negative indicates the job is not ready to be scheduled yet. As time passes the timebalances are continually incremented. The job's timebalance is now only decremented or reset when that job has been scheduled.

Jobs may be inserted with a negative timebalance, so that they are not first scheduled for

some time. This would happen immediately after a surveillance task for example, when a plot confirmation task would be inserted onto the job table with a timebalance of -0.1s.

Once a task has been scheduled one of two things may happen to the job timebalance which are subtly different in their result;

i. *the timebalance is decremented by the task look back interval.*
ii. *the timebalance is reset to minus the task look back interval, so that the next task will not occur until the desired time has elapsed.*

In the first case, if the task was late then it is possible that the timebalance of that job would still be positive after it was decremented. Therefore more tasks may be scheduled for that job straight away. This is useful in the context of surveillance for example, where if the search of a region is running late due to overload, the search may catch up by searching several beams very rapidly.

This is not a useful property for all functions however. When updating a track for example, there is little benefit accrued from scheduling two or more track updates in rapid succession. In this instance the timebalance should be reset to minus the task interval, so that all track updates are spaced with the look interval. (Note that the look interval used could be modified to be shorter or longer if required).

Currently the algorithm resets the timebalance of tracking jobs. Surveillance and track initiation job timebalances are decremented by the task look back interval, so that if they are running late, they may catch up by scheduling several looks. Neither situation applies to plot confirmation jobs since they only exist for the period of one task.

5.3.4 Simulation architecture

The task scheduling simulation architecture is shown in Figure 5-3 below. It has been made intentionally very similar to the architecture used in MESAR where a job controller looks after every job on the radar job table, from its initial request until completion. It is the job controller's responsibility to ensure such tasks as the selection of beam direction, and selection of waveform parameters such as PRF, frequency, number of bursts etc. are calculated. If the job is successful, the job controller may need to trigger a new job request, or delete a job from the radar job table.

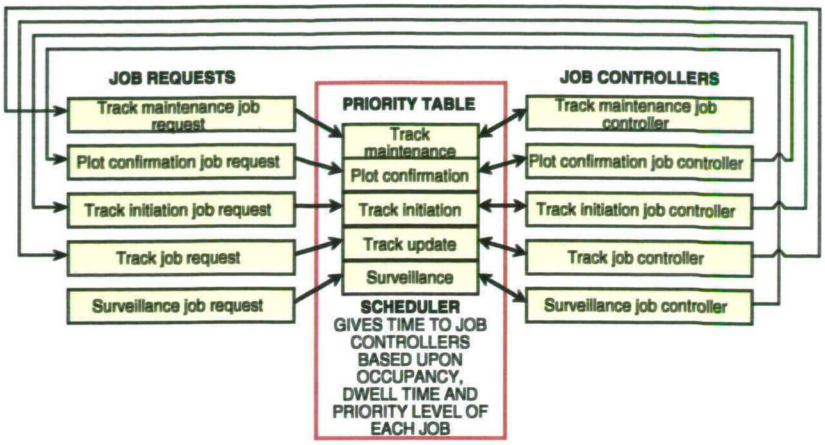

Figure 5-3 Static multi-function radar task scheduling simulation architecture

5.3.5 Scheduling using a simple two sector surveillance system

Initially investigation was limited to a simple two sector surveillance system for both validation of the algorithms and ease analysis of results.

The following surveillance volume was constructed, consisting of 2 regions, both of which spanned a 90° azimuth sector. Region 1 spanned 0°-20° in elevation, and region 2 spanned 20°-50° in elevation. The parameters of the regions specific to the scheduler are shown in Table 5-1 below. Figure 5-4 shows the beam directions and dwell times.

Region	Broadside Dwell time	Occupancy	No of beams	Frame time	Function time	Look Interval
1	1ms	20%	283	1.415s	0.283s	5ms
2	2ms	80%	343	0.8575s	0.686s	2.5ms

Table 5-1 Scheduler specific parameters of the 2 region surveillance volume

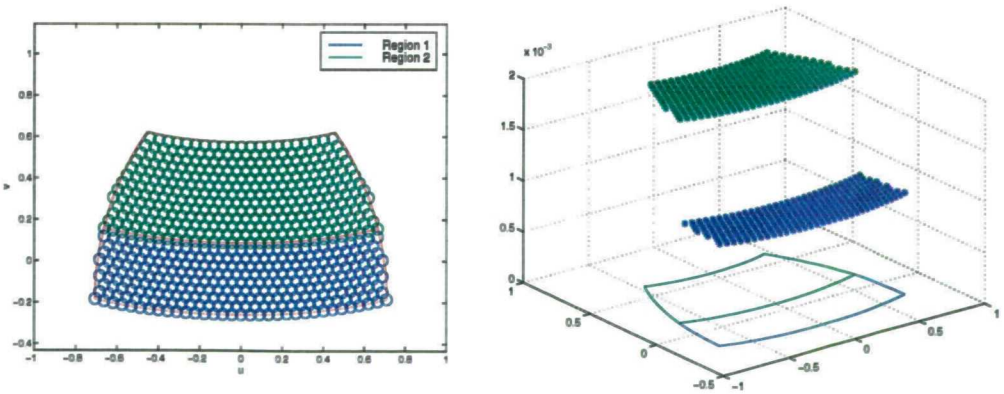

Figure 5-4(a,b) Beam directions plotted in UV space, and beam dwell times plotted above the UV plane

Initially no compensation in the dwell time was made for the loss of gain due to scanning. Thus the broadside dwell times quoted for each region apply to every beam direction within the region. The beam directions are plotted in UV space in Figure 5-

4(a) and the flat dwell time surface is plotted above the UV plane in Figure 5-4(b).

The simulation allows targets to enter the surveillance volume with a set probability of detection. Initially this was set to 0 so that no detections were made, and only surveillance of the 2 regions took place. Surveillance tasks were not broken down into looks in this case. The results of the simulation are shown in Figure 5-5 and Figure 5-6, below.

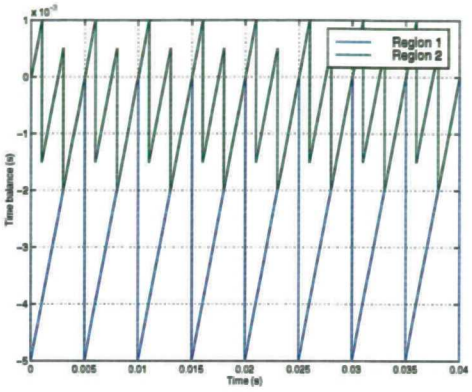

Figure 5-5 Surveillance time balances as a function of time, with no target detections

Figure 5-5 shows the timebalances of each region for a few milliseconds at the beginning of the simulation. The time balances of both regions start at 0. Each time a task is scheduled that region's timebalance is decremented by the look interval. With these simplistic dwell times the timebalances are clearly periodic, region 1's timebalance being decremented every 5ms and region 2's timebalance being decremented every 2.5ms.

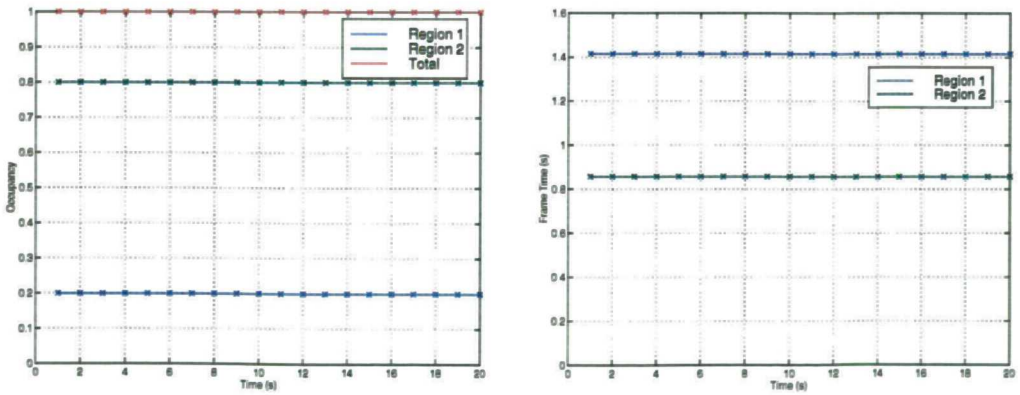

Figure 5-6(a,b) Achieved averaged occupancies and frame times over the simulation period

Figure 5-6 above shows the achieved occupancies and frame times of the surveillance regions over a 20s period. These are calculated as an average over an interval of time, in this case, 1s. The solid lines show the desired values, and the crosses plot the achieved

values. In this simple case the occupancies and frame times are achieved with great precision, as would be expected.

A more realistic surveillance volume was constructed by allowing the surveillance dwell times to increase with scan angle, to compensate for the loss in gain with coherent integration of pulses. As elsewhere, the two way gain is assumed to fall with $\cos^3(\varphi)$. The same two regions were used, covering 0°-20° and 20°-50° in elevation. Table 5-2 shows the scheduler parameters of the new regions. The function time of each region is increased over that shown in Table 5-1, since the dwell times in each beam direction are all greater than the broadside dwell time. Correspondingly this increases both the frame time and the look interval, since the desired occupancies of the two regions has remained fixed.

Region	Broadside Dwell time	Occupancy	No of beams	Frame time	Function time	Look Interval
1	1ms	20%	283	2.0386s	0.4077s	7.204ms
2	2ms	80%	343	1.3882s	1.1106s	4.047ms

Table 5-2 Scheduler specific parameters of the 2 region surveillance volume

The dwell time surface, shown in Figure 5-7, now shows two distinct bowls as the beam dwell times increase towards the limits of the two regions.

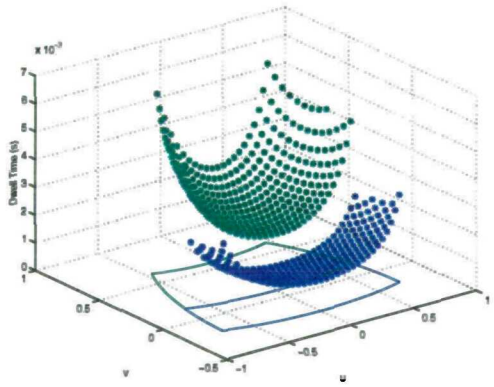

Figure 5-7 Beam dwell times plotted above the UV plane for the 2 region surveillance volume

Again the probability of detection was set to 0, so that no targets were detected during the simulation. Neither were surveillance tasks broken down into smaller looks. The surveillance regions were searched in a pseudo-random order. The results of the simulation are shown in Figure 5-8 and Figure 5-9 below.

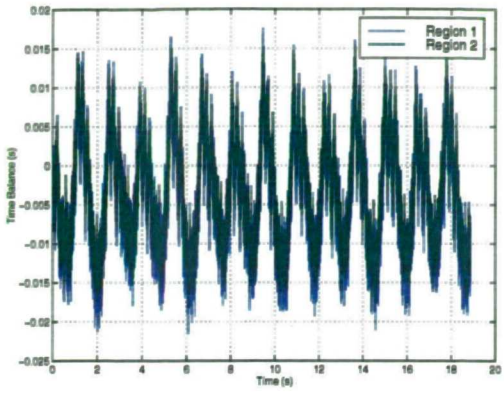

Figure 5-8 Surveillance time balances as a function of time, with no target detections

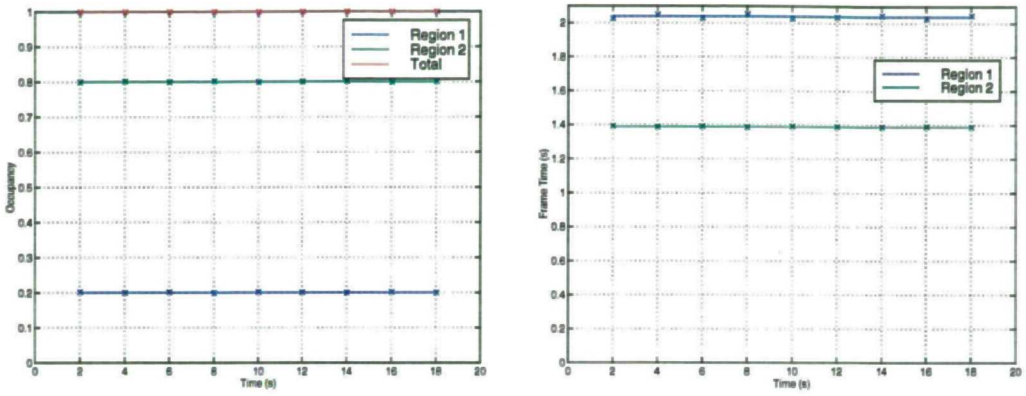

Figure 5-9 Achieved averaged occupancies and frame times over the simulation period

Figure 5-8 shows the timebalances over the simulation interval. Again they can be seen to be periodic, related to the frame times; however even for this simple two region system they show a more variable nature due to the variation in dwell time for each beam surveyed. The achieved occupancies and frame times, shown in Figure 5-9, also meet their targets very accurately. At all times a 100% total system occupancy is achieved.

The impact of introducing tracks into the system was then analysed. At time t=2s, a target was introduced into the simulation. This target was given a probability of detection 1; thus it was detected in surveillance and confirmed by plot confirmation. A track was then initiated, and subsequently track updates were scheduled every 1s. The waveform used for plot confirmation, track initiation and track maintenance was that of the surveillance waveform which detected the target. At time t=4s, another track was introduced, and so on, a new track being introduced every 2s for the 120s duration of the simulation. The results are shown in Figure 5-10 to Figure 5-12 below.

Figure 5-10, below, shows some of the timebalances for the first few seconds of the simulation. The process of scheduling plot confirmation, track initiation and track tasks

can be clearly seen here. At time t=2, the first plot confirmation job request is made, and a task inserted into the radar job table with a time balance of -0.1s. As surveillance carries on, this task's timebalance increases until it becomes positive, at which point it is scheduled. Subsequently 10 track initiations can be seen, the track initiation time balance being decremented by the look interval (0.1s) each time a task is scheduled. Finally at time t=3.1 a track job request is made, and track updates commence at time t=4.1s.

From time t=2 onwards, the surveillance timebalances oscillate around an increasingly positive value, rather than zero. This is indicative of the surveillance jobs becoming later and later as far as the scheduler is concerned. This occurs because the surveillance regions were specified to use 100% of the multi-function radar system occupancy. Thus as tracking tasks are introduced and require occupancy, the total surveillance occupancy decreases. The value around which the surveillance timebalances oscillate indicates how far behind schedule surveillance is in seconds.

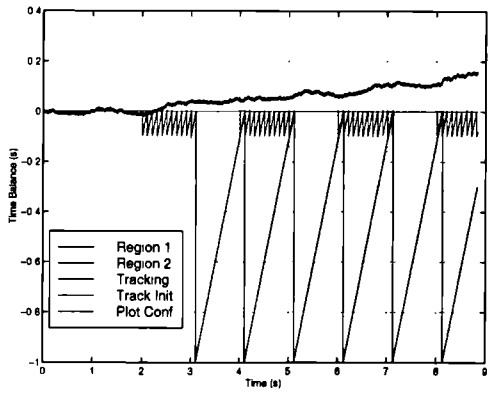

Figure 5-10 Surveillance, plot confirmation, track initiation and tracking timebalances with new target detections every 2s

Figure 5-11(a), below, shows the total achieved occupancy of each function. As more tracks are introduced into the system, the track occupancy increases and thus the lower priority surveillance occupancy decreases correspondingly. Again it is important to note that a 100% total system occupancy is achieved at all times. Figure 5-11(b) shows the decrease in surveillance region timebalances as the tracking occupancy increases. It shows the two regions occupancies decrease in proportion with their desired occupancies - i.e. the occupancy of region 2 decreases four times faster than region 1. The frame time of the regions is plotted in Figure 5-12.

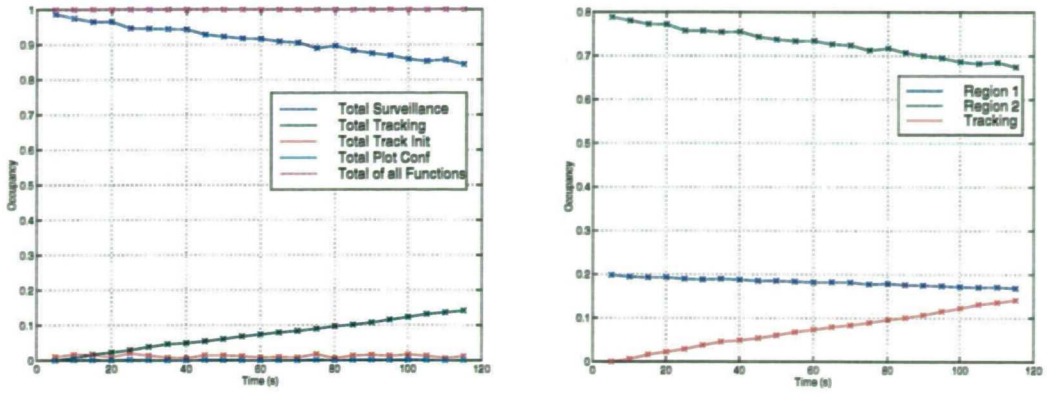

Figure 5-11(a,b) Total achieved occupancies of each function vs time, and achieved surveillance region occupancies with track occupancy vs time

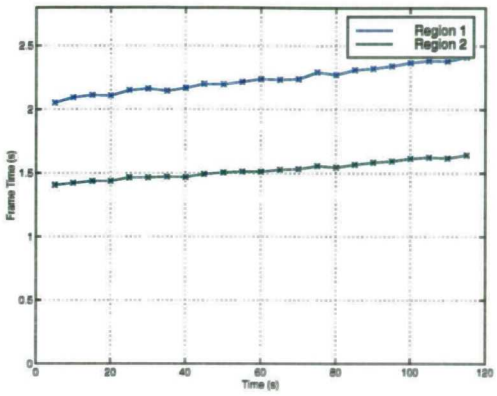

Figure 5-12 Achieved surveillance frame times vs time

5.3.6 Scheduling using the MESAR surveillance volume

MESAR in its standard surveillance configuration has a total of 9 surveillance regions. The region spatial limits are given in Table 5-3, below, and are shown in Figure 5-13. The scheduler specific parameters of the MESAR regions are given in Table 5-4.

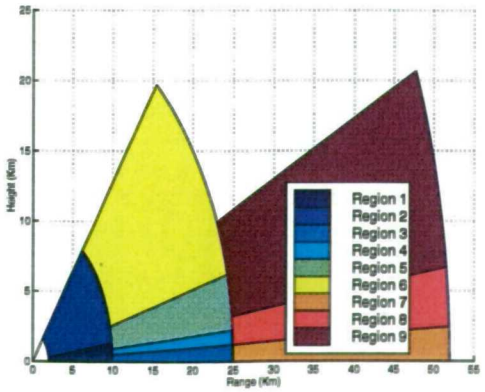

Figure 5-13 MESAR search regions in standard configuration

Region	Min Range (Km)	Max Range (Km)	Min Elevation (degrees)	Max Elevation (degrees)
1	2.0	10.0	0	7.4
2	2.0	10.0	7.4	52.0
3	10.0	25.0	0	2.7
4	10.0	25.0	2.7	5.1
5	10.0	25.0	5.1	14.3
6	10.0	25.0	14.3	52.0
7	25.0	52.0	0	2.7
8	25.0	52.0	2.7	7.4
9	25.0	52.0	7.4	23.4

Table 5-3 MESAR search region parameters

Region	Broadside Dwell time	Occupancy	No of beams	Frame time	Function time	Look Interval
1	0.83ms	1.4383%	92	9.38s	0.1349s	0.1013s
2	0.62ms	6.2080%	503	9.52s	0.5910s	0.0189s
3	15.65ms	3.2724%	31	23.78s	0.7781s	0.7671s
4	11.32ms	2.1511%	30	24.05s	0.5173s	0.8017s
5	10.92ms	8.1835%	122	24.32s	0.1990s	0.1993s
6	7.54%	21.6652%	412	24.62s	0.5334s	0.0024s
7	8.08%	15.9922%	31	24.80s	3.9661s	0.8000s
8	3.51%	12.0177%	61	26.75s	3.2147s	0.4385s
9	5.84%	6.2691%	207	27.69s	1.7359s	0.1338s
Total Occupancy		77.197%				

Table 5-4 Scheduler specific parameters of the 2 region surveillance volume

Again, initially, the probability of detection was set to 0, so that no targets were detected during the simulation. A maximum look time of 5ms was specified. Thus every task that was scheduled, was scheduled in looks of no more than 5ms. This was necessary since the MESAR dwell times can be extremely long as it uses integration of pulses in order to overcome its very low power. Many beams have dwell times in excess of 100ms, the longest beam dwell time being over 200ms. The surveillance regions were searched in a pseudo-random order, as in MESAR.

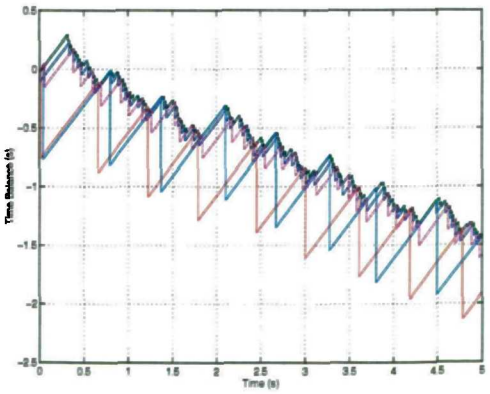

Figure 5-14 Surveillance timebalances for the 9 regions of MESAR, with no detections

Figure 5-14 shows the timebalances of the 9 surveillance regions from the first 5s of the

simulation.

In this instance, the timebalances oscillate around an increasingly negative value. This is due to the total surveillance occupancy being just 77%, thus surveillance tasks are being scheduled earlier and earlier. The frame times achieved are therefore shorter than the desired frame times.

Figure 5-15(a) shows the achieved occupancies of each of the 9 regions. In this case, the solid lines representing the desired occupancy of each region, have been scaled up to account for the fact that the total surveillance desired occupancy is less than 100%, although the achieved occupancy with no tracking tasks will equal 100%. A great deal more oscillation around the desired values is seen in this instance. This is primarily due to the averaging interval (5s) being small with respect to the frame times of the regions. Over a complete frame time, the desired occupancies are achieved, but since the scheduler works on a fixed look interval basis, the achieved occupancy fluctuates throughout the frame time period.

Figure 5-15(b) shows the achieved frame times. Again, there is considerable fluctuation around the desired values over the short averaging period chosen, although the frame times are met over a complete scan of a region.

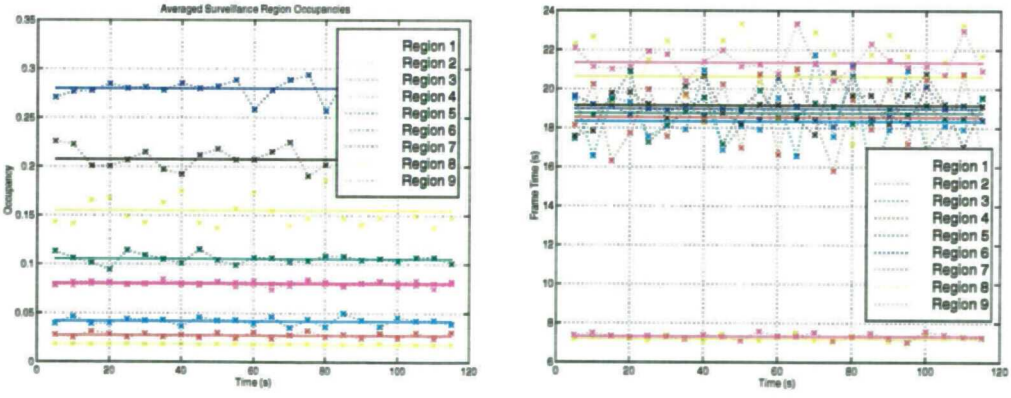

Figure 5-15(a,b) Achieved averaged occupancies and frame times over the simulation period. Solid lines show desired values scaled to account for a desired surveillance occupancy of less that 100%

Figure 5-16 shows the total occupancies of each function. Obviously the occupancies of all tracking related functions are zero. The plot only serves to show that surveillance has expanded to use 100% of the multi-function radar system occupancy, and that 100% utilisation of the multi-function radar is again achieved.

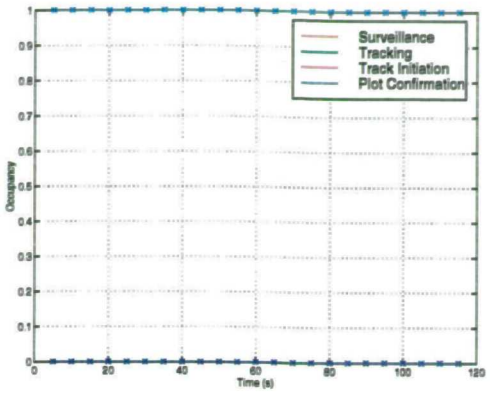

Figure 5-16 Total achieved occupancies of each function vs time

Tracks were then introduced as in section 5.3.5. Tracks were introduced every 2s for the duration of the simulation, and the same waveform was used for plot confirmation, track initiation and track maintenance as that of the surveillance waveform which detected the target. The results are shown in Figure 5-17 to Figure 5-19 below.

Figure 5-17 shows the timebalances for the first seconds of the simulation. Initially the surveillance time balances become increasingly negative, since surveillance expands to use the full 100% system occupancy. Then at t=2s, quite the reverse occurs, and surveillance becomes completely shut out, its occupancy decreasing to zero briefly, whilst plot confirmation and track initiation are carried out on the detection. Interestingly the waveform which detected the target had a dwell time in excess of the look back interval requested for plot confirmation and track initiation.

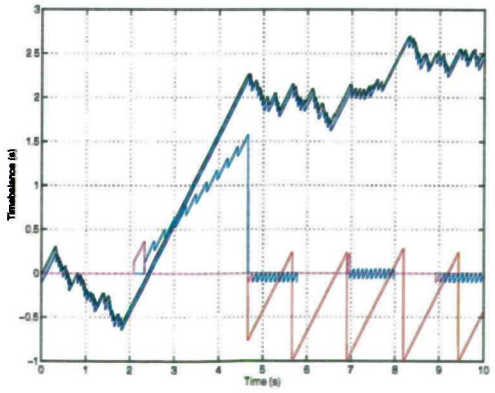

Figure 5-17 Surveillance, plot confirmation, track initiation and tracking timebalances with new target detections every 2s. GREEN & BLUE = SURVEILLANCE, MAGENTA = PLOT CONFIRMATION, CYAN = TRACK INITIATION

Thus even though the job was scheduled immediately after the surveillance waveform which detected the target, it was still late. This can be seen in the plot confirmation timebalance. The plot confirmation job was inserted into the radar job table with a positive timebalance, indicative that the job was already late. Also the track initiation

timebalances become more and more positive, (unlike those for subsequent track detections), showing that the desired update rate cannot be achieved.

Figure 5-18(a) shows the achieved occupancies of each function. The surveillance occupancy falls away as time goes on, to meet the tracking occupancy demands, which, by t=85 fully occupy the radar, squeezing out surveillance completely. At time t=45s there is a particularly high track initiation load which is met by lowering the occupancy of both tracking and surveillance since they are both lower priority tasks. Figure 5-18(b) shows the surveillance region occupancies decreasing in proportion with their desired occupancies, such that they all reach 0% occupancy at the same time.

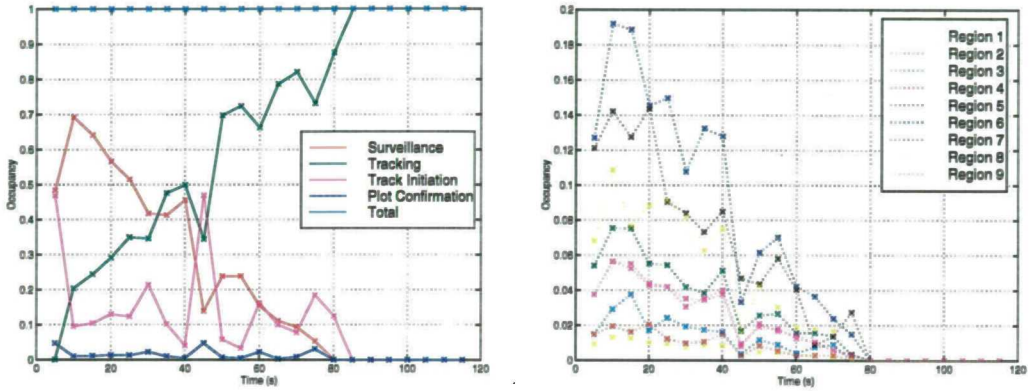

Figure 5-18(a,b) Total achieved occupancies of each function vs time, and achieved surveillance region occupancies vs time

Correspondingly, Figure 5-19 below shows the surveillance frame times increasing throughout the simulation, until they become infinite when the surveillance occupancy reaches 0%.

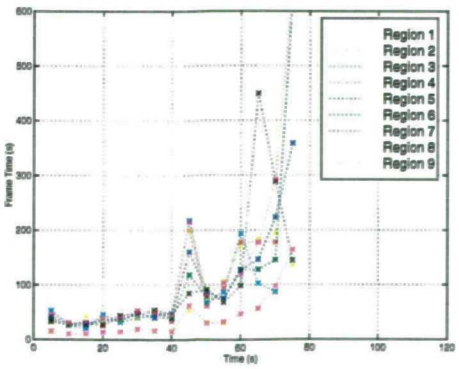

Figure 5-19 Surveillance region frame times for MESAR, with track detections every 2s

5.3.7 Plot confirmation latency using the MESAR scheduler

The MESAR scheduling algorithm is not sophisticated in its method of trying to schedule jobs very close to their desired schedule time. Many algorithms are more complex, and attempt to shuffle jobs around to formulate an efficient time schedule in advance [Orman & Potts, 1997], [Orman et al, 1996]. Although this strategy can result in most of the jobs being scheduled very close to their desired times, there is a risk that there will be empty periods in the schedule, such that the multi-function radar is not utilised 100% of the time. To avoid this, MESAR selects the most appropriate job that is ready at the instant the last job scheduled has finished. This means that the selected jobs are always scheduled late by some amount- the maximum delay being the dwell time of the previous task scheduled. This however, ensures that the multi-function radar is 100% utilised at all times.

The delay caused by the scheduler cannot be tolerated for functions such as plot confirmation or track initiation in instances where long radar waveforms are used. To get around this problem, large tasks are broken down and scheduled in smaller units. The scheduling of one task may be interrupted by the scheduling of a higher priority task. This is of particular significance to fast, crossing or low signal to noise ratio targets, where rapid look back can be essential in maintaining the target in track, without resorting to searching multiple beams.

Figure 5-20 plots the look number of each task scheduled as a function of time. Some tasks are made up of in excess of 45 looks. It is difficult to see any interleaving of tasks on Figure 5-20(a); however when the time axis is expanded, as in Figure 5-20(b), the interleaving of plot confirmations with surveillance becomes clear.

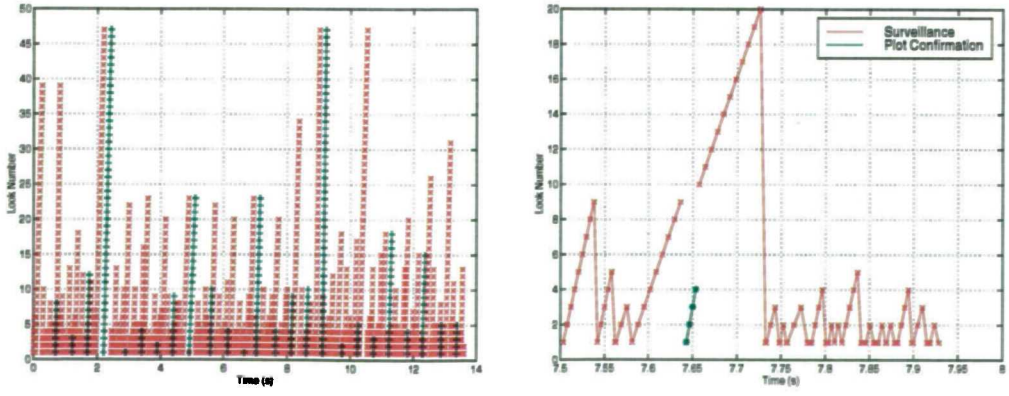

Figure 5-20 Look number scheduled as a function of time for plot confirmation tasks (green x) and surveillance tasks (red +)

By performing a simulation over a large period of time, and inserting many targets, it is possible to show the delay in scheduling of plot confirmation tasks. Figure 5-21 compares the delay in scheduling of plot confirmation tasks with the MESAR scheduling algorithm (a), to the delay if the MESAR algorithm scheduled tasks as single un-interruptible units (b). By scheduling tasks in smaller looks the delay in scheduling of plot confirmation tasks is minimised; 97% of plot confirmations were scheduled within 10ms of their desired time. Conversely just 55% of plot confirmations were scheduled within that period when tasks were not broken down, and more than 5% were scheduled over 0.1s late.

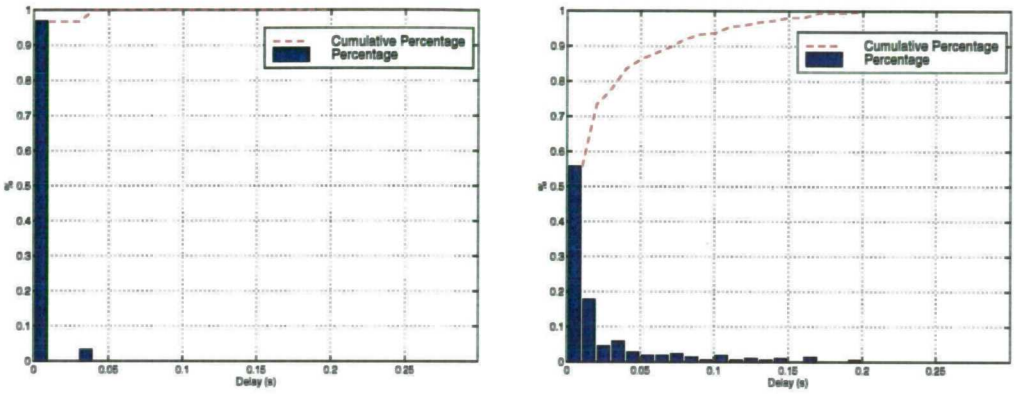

Figure 5-21(a,b) Histogram of the delay in scheduling plot confirmation tasks. (a) the MESAR algorithm scheduling looks, (b) the MESAR algorithm scheduling un-interruptible tasks

5.4 Task scheduling in a rotating array multi-function radar

5.4.1 Background

In a rotating multi-function radar there are three significant complications to the task scheduling problem.

i. blind arcs in the antenna coverage

ii. tasks must be scheduled close to array azimuth broadside where possible

iii. radar occupancy may be distributed non-uniformly with azimuth

Each of these is discussed in further detail below.

5.4.1.1 Blind arcs in the antenna coverage

Firstly, if full 360° illumination is not available from the multi-function radar's array

antenna, then the scheduler must deal with rotating blind arcs, where no tasks may be scheduled. This also has the effect of limiting the maximum sustainable track update, depending on the azimuth scan capability of the multi-function radar's phased array faces and the rotation rate of the arrays.

5.4.1.2 Scheduling tasks close to broadside

Secondly, as discussed in Chapter 2, a heavy penalty may be paid for scheduling tasks away from array azimuth broadside unnecessarily. Scheduling of tasks scanned away from array azimuth broadside will result in broadening of the beam in azimuth and a loss in signal to noise ratio. These in turn result in a degraded monopulse estimate accuracy.

Using Barton's expression for estimating the monopulse accuracy that is achieved for a dwell of n pulses [Barton, 1988];

$$\sigma \approx \left(\frac{\theta_3}{2\sqrt{(snr).(n)}} \right) \qquad [5\text{-}1]$$

where σ is the monopulse accuracy (rads)
θ_3 is the 3dB beamwidth (rads)
snr is the signal to noise ratio

we estimate the factor by which the monopulse estimate of a beam degrades as the beam is scanned from broadside to be;

$$\text{degradation factor} \equiv \frac{\sigma_\varphi}{\sigma_{bs}} \approx \left(\frac{1}{\cos^{5/2}(\varphi)} \right) \qquad [5\text{-}2]$$

where φ is the scan angle off broadside(rads)
σ_{bs} is the monopulse acc. at array broadside
σ_j is the monopulse accuracy at scan angle φ

This is clearly of significance for both surveillance and tracking radar tasks, giving a degradation of a factor of around 5.6 for a scan angle of 60°. Broadly speaking there are three potential courses of action that may be taken as a result of the degradation described above;

i. accept the degradation in both detection performance and angular plot accuracy

ii. try to regain the original broadside detection performance, but accept a

degradation in angular plot accuracy due to a broader beam

iii. *try to regain the detection performance, and moreover, try to regain the same angular plot accuracy achieved on broadside (in radians/degrees)*

Option (i) above obviously does not require any increase in radar dwell time, but will result in poorer radar performance for tasks off array broadside.

Option (ii), assuming coherent integration, will require an increase in dwell time equal to the loss caused by scanning; i.e. if a 3dB loss is experienced due to scanning the beam, the dwell time must be doubled to recover the original signal to noise ratio. The 9dB loss caused by scanning at the extreme scan angle of 60° requires 8 times the dwell time to compensate.

To regain the original broadside performance in both detection capability and angle estimation, option (iii), requires a very large increase in the dwell time. From the equations above we may go on to derive the factor by which the dwell time must be increased to recover the broadside angular plot accuracy (assuming coherent integration of pulses);

$$\text{factor by which to increase dwell time} \approx \left(\frac{1}{\cos^5(\varphi)} \right)$$

This suggests a dwell time of a factor of 32 times longer than the broadside dwell time is required to give the same monopulse accuracy when scanned to 60°.

In terms of surveillance, which may already take 80% of the multi-function radar's time-budget when on broadside, options (ii) and (iii) may not be feasible without increasing the surveillance frame times. Some degradation in signal to noise ratio or azimuth plot accuracy may have to be accepted. It should be noted however, that, although the dwell times increase, this is offset by the number of beams required to perform the search decreasing, due to beam broadening. This means the total search function time increases as $1/\cos^4(\varphi)$ to recover monopulse accuracy and $1/\cos^2(\varphi)$ if only signal to noise ratio is to be recovered.

Thus it is clear that the penalties for unnecessarily performing tasks away from array broadside are large, manifesting themselves either in the form of degraded detection performance and plot accuracy, or in terms of increased dwell times for a task, and that

the exact timing of track updates is crucial in maximising the efficiency of the tracker.

5.4.1.3 Distributing radar occupancy with a non uniform angular loading

The final complication in a rotating system is that, if we wish, radar-time may be concentrated from all of the available array faces in a given direction. This can be extremely useful if the multi-function radar loading is not uniform with azimuth, which it is highly unlikely to be in an operational scenario. Nothing has been found in the literature which addresses this topic, suggesting that current systems do not employ this additional flexibility in their task schedulers.

Figure 5-22 below shows the difference between a static multi-function radar and a rotating multi-function radar if the radar loading is not uniform with azimuth angle. In both cases, the surveillance detection performances may be met if, for example, 80% radar occupancy is dedicated to search. In this example, this leaves 20% for any other functions such as tracking tasks or missile uplink. If any less than 20% is required for these functions the surveillance detection performance will be in excess of the requirement. Any more than 20% will cause a shortfall in surveillance detection performance.

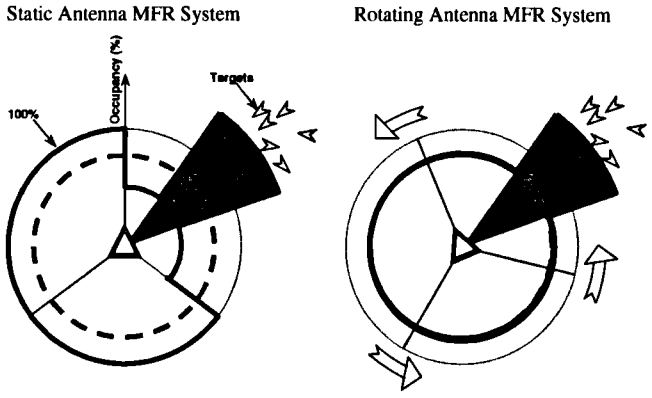

Figure 5-22 A comparison of static and rotating multi-function radars in the presence of a non-uniform loading with azimuth

If a distinct azimuth angular sector exists with a higher radar loading than throughout the rest of the coverage, then the static multi-function radar will have a non uniform loading between its faces. Two or three of the faces (depending on whether it is a three or four faced multi-function radar) will not be facing in the direction of the high load angular sector. These faces will have less than the example 20% loading for functions other than search, and will thus have a surveillance detection performance in excess of the requirement. The one face that is pointing in the direction of the high load angular

sector will have more than the 20% loading allowed for other functions, and thus the surveillance detection performance for this antenna face will be degraded below the requirement. Unfortunately, this is likely to be just the direction where a good search performance is desired.

In the rotating multi-function radar the unequal loading with azimuth angle does not necessarily translate to an unequal loading between the multi-function radar array faces as it does in the static case. Forward and back-scanning of the surveillance beams may be used to dedicate higher amounts of radar time from each antenna face in a particular direction.

In the directions where there is less than the example of a 20% tracking load above, surveillance may expand to use this extra occupancy and search more beams. In these directions the surveillance azimuth direction will move ahead of the antenna direction as beams are being searched at a higher rate. This is termed forward scanning.

Similarly, in directions where more than the example 20% loading is present, surveillance beams will be searched at a slower rate, and the surveillance direction will fall behind the antenna broadside direction. This is termed back-scanning.

A rotating scheduler algorithm should be able to utilise forward and back-scanning when necessary in order to cope with directions of higher than average radar loading. However, forward and back-scanning should be avoided whereever possible due to the penalties associated with performing tasks away from broadside. This suggests that the rotating scheduler algorithm is likely to be required to monitor the multi-function radar time loading and act appropriately for efficient task scheduling to be possible.

5.4.2 An algorithm for task scheduling in a rotating multi-function radar system

A scheduler algorithm for a single array faced rotating MFR has been described, based upon the use of a queue to store delayed volumetric search tasks which cannot be performed in a scan due to an overload of tracking tasks [Barbato & Giustiniani, 1992]. Here an algorithm which aims to avoid the occurrence of this situation is developed. A rotating scheduler algorithm is proposed below which is designed to cope with the complications of;

i. rotating blind arcs

ii. constraining tasks to array broadside where possible

iii. forward and back-scanning of surveillance when overloaded

The algorithm works using the same timebalance scheme to control the scheduling of tasks as in the Modified MESAR static algorithm described above in section 5.3.3. The timebalances are again calculated using the task look back interval (the time between successive tasks - e.g. the track update interval, or the surveillance beam revisit time), and the task time (the dwell time of the task).

Additionally, the rotating scheduler algorithm uses the concept of windows of opportunity. These are angular limits, relative to array azimuth broadside, within which the task must be inside, in order for it to be scheduled.

A surveillance window of opportunity is shown in Figure 5-23 below. In the example shown, the window has a limit of ~10° ahead of array broadside and a limit behind array broadside set to the extreme of antenna coverage. To understand the effect of the window of opportunity consider a multi-function radar which starts its surveillance on array azimuth broadside. As the multi-function radar rotates, it searches surveillance beams at a rate which keeps the beam directions on array broadside, as long as surveillance is receiving its desired occupancy. In areas where the multi-function radar is under-loaded, surveillance beams will be searched at a higher rate and will move ahead of array broadside. This will occur until the forward limit of the window of opportunity is reached at 10°, beyond which surveillance is not allowed. In regions where the multi-function radar is overloaded with tasks, surveillance beams will be searched at lower data rates, freeing up occupancy for higher priority tasks. Surveillance will start lagging behind array azimuth broadside until the overloaded region is passed. In this way, forward and back scanning are used to take antenna time from angular sectors which are under-loaded and given it to those which are overloaded.

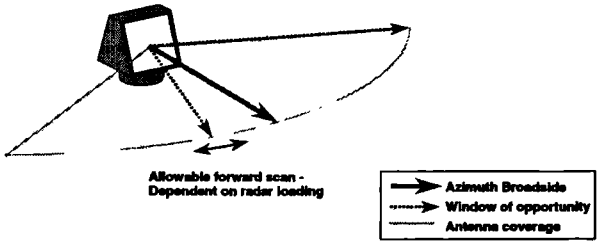

Figure 5-23 A surveillance window of opportunity

The forward limit of the window of opportunity in the above example was set to 10° ahead of array azimuth broadside. In practice this would be varied depending upon the loading of the multi-function radar expected over successive scans. If the multi-function radar was under-loaded then there would be no reason that the window of opportunity should extend ahead of array azimuth broadside, since this would incur off broadside losses with no reason. If the multi-function radar was very heavily overloaded the forward limit of the window should extend to the forward extreme of antenna coverage to allow maximum forward scanning.

The backward limit of the window of opportunity need not be adaptive in the same way. The surveillance beam directions will only lag behind array azimuth broadside if the multi-function radar is overloaded.

This strategy allows the control of scheduling of tasks when surveillance is within its window of opportunity. However, what happens when surveillance reaches the forward or backward limits of the window? Currently, if the radar is under-loaded and surveillance reaches the forward limit of the window, the simulation injects null tasks for a duration of 1ms. i.e. the antenna is not used for 1ms. If the radar is overloaded, and surveillance reaches the backward limit of the window, then surveillance beams will be dropped. Clearly both these actions are not ideal and would not be desirable in a real system. Possible ways to avoid these situations are taken up in section 5.4.5 below.

A flow diagram for the rotating scheduler algorithm proposed is shown in Figure 5-24. The algorithm schedules in units of tasks rather than looks at this stage. A description is given below.

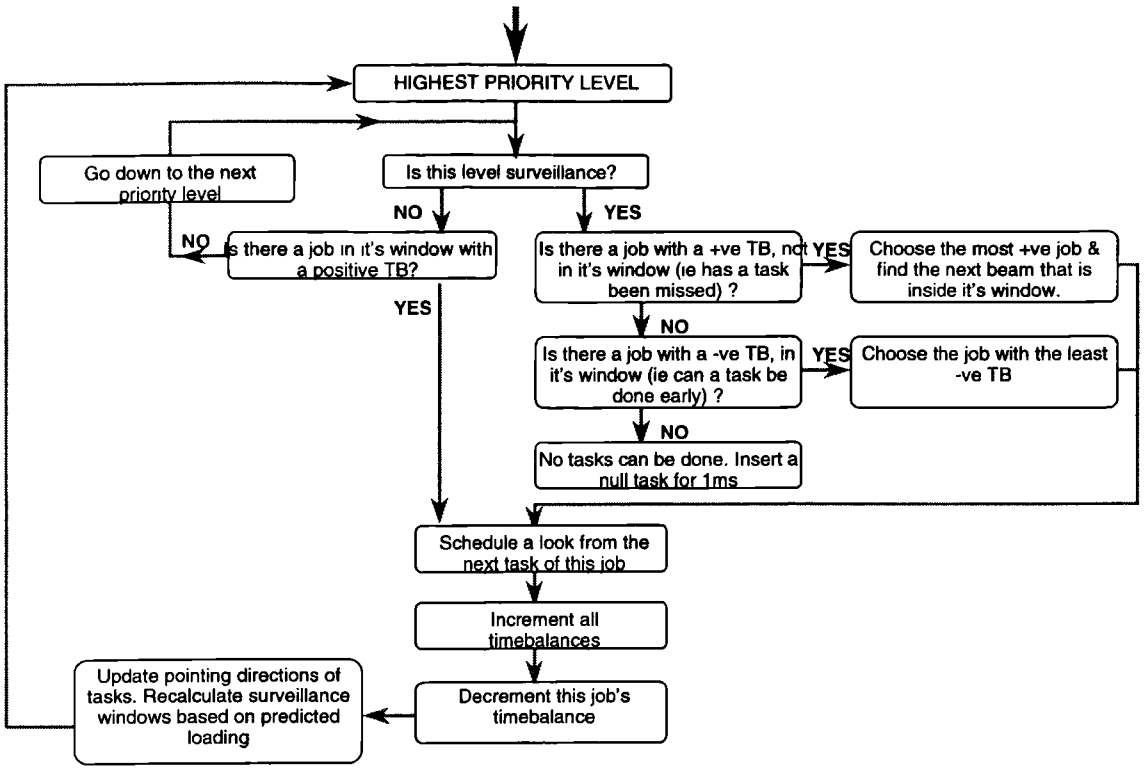

Figure 5-24 Flow diagram of the rotating scheduler algorithm

Starting from the highest priority level;

i. If this level is surveillance determine whether a surveillance region is behind its window of opportunity - if so then drop this beam and find the next beam inside the window. Choose this job.

ii. If this level is surveillance and a job has a positive timebalance then this indicates a surveillance job can be done, which may be early. Choose this job.

iii. If this is surveillance and no jobs can be done from (i) or (ii) above, then the forward limit of the window has been reached; insert a null task for 1ms.

iv. If the level is not surveillance (i.e. a higher level), and if there is a job with a positive time balance, in its window of opportunity, then choose this job. Otherwise, go down to the next level, and repeat from (i)

v. Schedule the chosen task or a null job.

vi. Increment all timebalances

vii. Decrement the chosen job's timebalance

viii. Update the pointing directions of tasks, such as tracking tasks, to take account of target movement.

ix. Recalculate surveillance window of opportunity based upon predicted radar loading.

5.4.3 Beam search patterns with a rotating multi-function radar

Figure 5-25 shows how the beam directions are represented in space. (Note that the circles on the figure are nominal, and in the simulation broadening of the beams in elevation is taken account of). As the elevation increases, the number of beams required in each row decreases, until as we approach 90° elevation only a single beam is necessary.

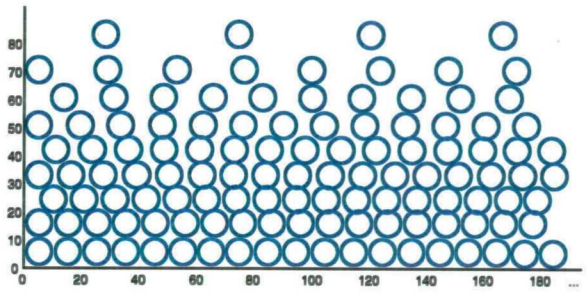

Figure 5-25 Surveillance beam directions plotted in real space coordinates

Figure 5-26 shows the method used to number the beams in order to generate a search sequence for each surveillance region.

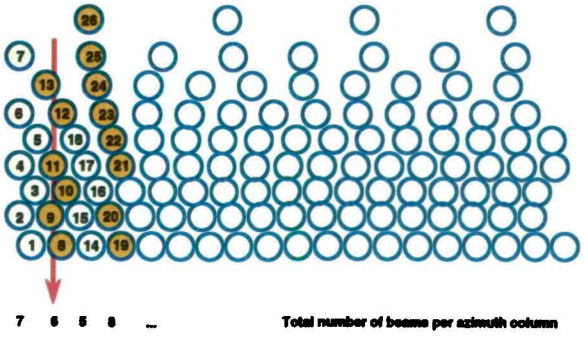

Figure 5-26 Search order of surveillance beam directions for a rotating system

The beams are numbered consecutively with increasing elevation in order that an elevation column of beams is searched at each azimuth angle, from the bottom beam up. Due to the irregular distribution of beams in space there will not be a uniform number of beams per elevation column. In the figure the beams are numbered as belonging to one large surveillance region from 0° elevation to 80° elevation. In practice, an elevation

sector this large would be split into several regions, or perhaps even 1 region per elevation row, reducing this non-uniformity.

The beam ordering scheme shown in Figure 5-26 will generate a uniform search pattern of each region, in regular columns, from the bottom elevation of the region to the top elevation of the region. If there is only one elevation row in a region, the scheme produces simply a raster scan search pattern.

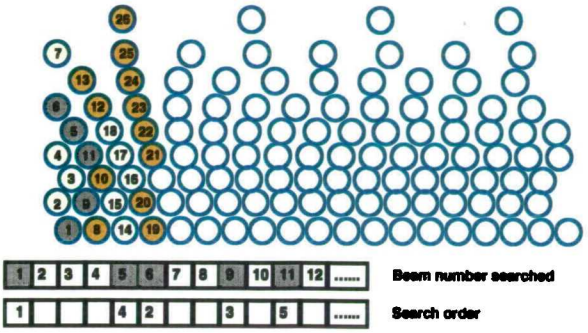

Figure 5-27 Generating a pseudo-random search pattern with a rotating system

Figure 5-27, on the other hand, shows the simple method that is used within the simulation to allow a pseudo random scan pattern to occur, for some preset angle away from array broadside (or the forward or back-scan angle that the surveillance region is currently at). The beams are still numbered in the same way as before. However, in this case, the order in which they are searched is randomised over a small number of beams ahead. The beam chosen for search is no longer the next beam in the sequence. The next beam will instead be the next beam number plus some random integer. This random integer should be chosen to represent one or more columns of beams. In the example shown in the figure, if 18 were chosen to be the random integer, and no beams had been searched (i.e. current beam number was 1) then the next beam to be searched may be anywhere within the first three columns of beams. By keeping track of the beams that have been searched a pseudo random scan around the array broadside direction is made.

5.4.4 Results with the rotating multi-function radar task scheduler algorithm

In principle surveillance may be scanned forward to the full azimuth scan limit of the array in regions where the total occupancy is less than 100%. This would then mean that the full angular coverage of the array may be dedicated down a single highly loaded sector through forward and back scanning, if required, without reducing the surveillance load. For an array with a scan capability of 60°, this would allow distribution of 1/3 of

its resources (2*60°/360°) in any given direction. Thus an occupancy of much more than 100% may be demanded from the multi-function radar *within a small angular sector*, as long as a total occupancy of less than 100% is demanded in other regions. In the case of scanning to the array limit of 60°, with a highly loaded sector of 30° in extent, an occupancy within that sector equivalent to 400% can be sustained.

However, forward and back scanning of surveillance tasks to allow the multi-function radar to distribute its load will degrade the performance of those tasks due to the decreased gain, and increased beamwidth. Clearly, to obtain this maximum value of forward and back scanning, the surveillance performance would be significantly degraded. At 60° the surveillance beamwidth has doubled, and detection performance reduced by 9dB.

In practice, as discussed in section 5.4.1.2, if we wish to maintain a uniform surveillance detection performance, then as we scan forward or back from array azimuth broadside, then we must increase the dwell time down each surveillance beam. Thus, even though we are only achieving the same detection performance, the surveillance occupancy rises; no further forward scanning will occur when the surveillance occupancy that reaches 100%. Therefore there is a limit on the angle of forward and back-scanning that can be achieved, that is dependent on the array azimuth broadside surveillance occupancy chosen [Butler et al, 1997]. This theoretical limit of forward or back scanning of surveillance is shown in Figure 5-28, below, as a function of the surveillance occupancy on array azimuth broadside.

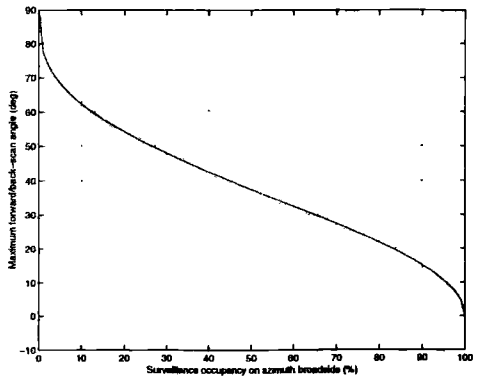

Figure 5-28 Limit of forward/backward scanning, assuming a two-way gain loss with $cos^3(\varphi)$

For a system which is compensating surveillance waveforms with a factor of $\cos^3(\varphi)$, the maximum radar time that may be dedicated towards tracking functions in an

overloaded angular sector through the use of forward and back scanning of surveillance, t_{max}, *before the onset of any surveillance degradation*, is given by;

$$t_{max} = \frac{2.\cos^{-1}\left(\sqrt[3]{occ_{surveillance\_bs}}\right)}{\omega} \qquad [5\text{-}3]$$

where ω is the antenna rotation rate
$occ_{surveillance\_bs}$ is the surveillance occupancy on array azimuth broadside

For a multi-function radar which has a broadside surveillance occupancy of 80%, a maximum scan limit of 21.8° is imposed. Thus the multi-function radar may dedicate double this amount in a given direction, *with no detriment to the surveillance detection performance*; equivalent to more than 12% of the total time-budget of each array face.

This theoretical value cannot be achieved in practice. It is limited by the need for surveillance to 'catch up' within a rotation; after servicing a highly loaded sector, surveillance must be able to go from fully back scanned, to fully forward scanned, within one rotation period. This is scenario dependent - it depends on the angular distribution of the tracking load. To determine the exact performance that may be obtained through forward and back scanning, a simulation of the scenario is necessary.

Figure 5-29 and Figure 5-30 present the results of a simulation of a rotating multi-function radar in the presence of a highly loaded sector. In this experiment a high loading of tracking tasks were injected in an angular sector of 30° in azimuth. A surveillance volume was constructed, consisting of a single region, which spanned 0°-20.5° in elevation, covering all azimuth angles. The parameters of the regions specific to the scheduler are shown in Table 5-5 below. An array leaning back at an angle of 20° from vertical, and generating a 2.6° beamwidth was assumed.

Region	Broadside Dwell time	Occupancy	No of beams	Frame time	Function time	Look Interval
1	0.589ms	80%	1359	1s	0.8s	0.736ms

Table 5-5 Scheduler specific parameters of the surveillance volume

Figure 5-29 demonstrates forward and back scanning of surveillance tasks during the simulation. In the interval 0-1s, no tracking tasks were present. Forward scanning from 0°, at the simulation start, to the limit of around 22° occurred in the first third of a second . In the interval 1-2s, a large number of long tracking tasks were introduced over a 30° sector, causing a desired occupancy from the multi-function radar in that sector in

excess of 100%. Surveillance was temporarily suspended in this case, due to the extremely high tracking load, and was reinstated some 18° behind array azimuth broadside. It is also important to note that the tracking tasks were performed as close as possible to azimuth array broadside with this method.

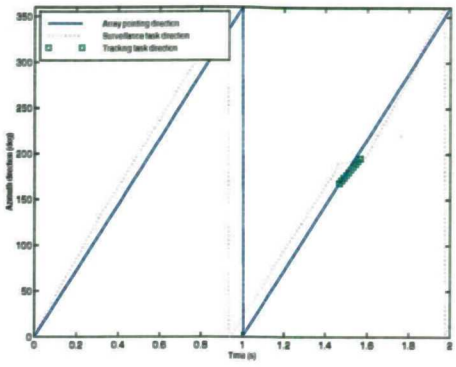

Figure 5-29 A comparison of the array pointing direction with the azimuth direction of surveillance and tracking tasks

Figure 5-30(a) shows the desired occupancy from the multi-function radar, needed to service the surveillance and tracking tasks as a function of azimuth. Since the tracking tasks lay within a 30° sector, the desired occupancy over most of the coverage was simply that required by surveillance (80%). In the 30° sector, however, the total occupancy of tasks consisted of 80% for surveillance and 135% for tracking.

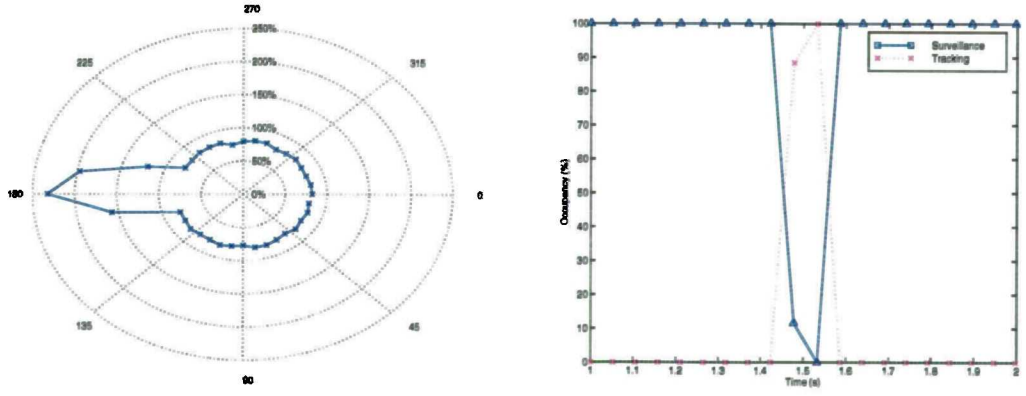

Figure 5-30 (a) Total desired occupancy of surveillance and tracking tasks as a function of azimuth angle, (b) Surveillance and tracking occupancies used to service the desired occupancies shown in (a)

Figure 5-30(b), shows the actual occupancies of surveillance and tracking that were needed to service the desired occupancies of Figure 5-30(a). In regions where only an 80% occupancy was desired, 100% of the occupancy was devoted to surveillance to allow forward scanning to occur.

Thus, this experiment showed a desired tracking occupancy of around 94% of the theoretical value, could be serviced by the multi-function radar using forward and back scanning. This experiment was repeated for several other values of sector size and surveillance broadside occupancy. The results are presented in Table 5-6.

Surveillance occupancy on broadside (%)	Sector Width (deg)	Simulated maximum track occupancy (%)	Theoretical maximum track occupancy (%)	Percentage of theoretical value achievable (%)
80	10	410	437	93.93
80	20	205	218	93.93
80	30	135	146	92.78
80	40	100	109	91.63
70	10	535	548	97.67
70	20	265	274	96.75
70	30	175	183	95.84

Table 5-6 Theoretical and Practical (through simulation) maximum achievable track occupancies

5.4.5 Other resource management issues for a rotating multi-function radar

Currently the algorithm performs forward scanning of surveillance in azimuth angular sectors where the radar loading is less than 100%. It may be desirable to forward scan the antenna even when the loading in an angular sector is 100% or more. Also, when surveillance reaches the boundaries of its window of opportunity either null tasks must be inserted (if the forward boundary is reached), or surveillance beams must be dropped (if the backward boundary is reached). Neither of these are desirable for the multi-function radar system.

The following are examples of action that may be taken in the radar control in the case of under-loading or overloading of the radar;

i. increase or decrease surveillance frame times in some regions

This must be done in multiples of the rotation period of the antenna.

ii. increase or decrease the surveillance dwell times

Two methods exist for achieving this; firstly, the number of pulses in a given direction may be increased or decreased to modify the dwell time. The disadvantage of this is that the number of pulses added or subtracted may have to be in units of bursts of pulses. Another method is to modify the PRFs of the surveillance waveforms adaptively, extending or decreasing the unambiguous range.

iii. increase or decrease the surveillance beam spacing

This is an effective alternative to changing the surveillance frame time significantly, which will modify the surveillance detection performance. A disadvantage is that if the beam spacing is increased too much, then there may be regions in the surveillance coverage with large dips in detection performance. This may be alleviated by utilising scan interlacing as suggested by Billam.

iv. increase tracking data rate or dwell times

This applies only in the case of under-loading, since our main aim is to avoid decreasing higher priority functions in the case of overload.

These mechanisms may then be included in the resource management of the rotating system allowing radar time to be freed from areas where it is not required and spent in other areas.

5.5 Penalty functions and fuzzy logic for efficient scheduling

The approach of the rotating task scheduling algorithm implemented above is closely related to the MESAR static task scheduler algorithm of section 5.3.2. All tasks are scheduled at, or slightly after their desired time, depending upon the radar load, and their relative priorities. It is not an optimal method of scheduling the tasks. What is not reflected in this scheduling strategy is what the penalties of scheduling these tasks early or late are. Different functions will be affected in different ways when their tasks are scheduled early or late, or ahead of or behind azimuth array broadside. Surveillance tasks for example may suffer no penalty if delayed by only a small amount of time relative to the search frame time. However the same delay may cause a track to be lost, or a plot confirmation to fail.

An improvement would be to reflect these penalties in the task constraints that are passed from the resource manager to the scheduler. This is being considered in the airborne case by Harvey, although no work has been published at this stage. In the static case, the penalty functions need only reflect the temporal variation of the task usefulness. In the rotating case, the penalty functions need also to include the effect of the azimuth scan angle on the task.

This is proposed as an area for further work; however it is considered outside the scope of this study.

5.5.1 The use of fuzzy logic

In the rotating case, the window of opportunity concept for regulating the scheduling of tasks may be extended using fuzzy logic to represent the windows. Rather than the forward and backward limits of the window representing hard and fast boundaries, beyond which no tasks may be scheduled, but inside of which they may, fuzzy logic may neatly represent the penalties of scheduling beyond, or just inside of, a window boundary.

Figure 5-31 and Figure 5-32 show example windows of opportunity for surveillance and for a tracking update. The figures show how fuzzy windows may be used to cope with the fact that in reality there is no sharp cut-off, beyond which a surveillance update or a track update should not be scheduled.

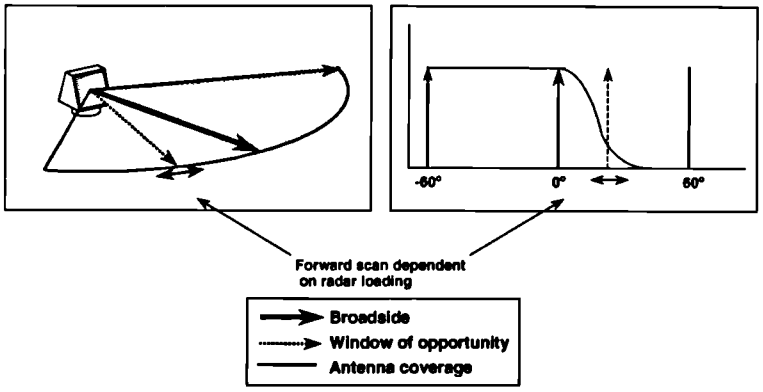

Figure 5-31 Fuzzy windows of opportunity for a surveillance task

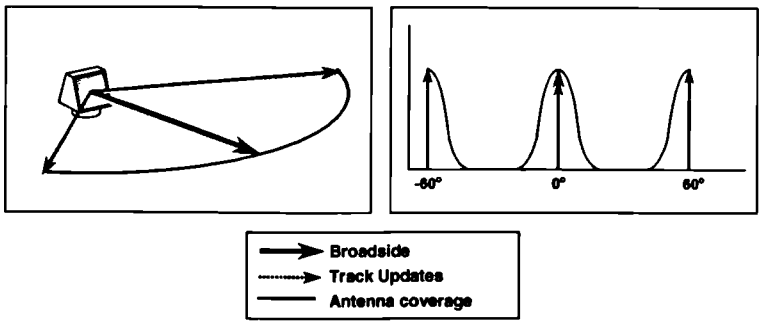

Figure 5-32 Fuzzy windows of opportunity for a tracking task

Simple membership functions, for example 'in_window', may be generated which represent how appropriate it may be to schedule this task, at this time. The shape of the membership function should be based on relevant penalty functions such as scheduling

away from the exact update time and scheduling away from array azimuth broadside.

Fuzzy logic has been successfully applied to the control of an airborne intercept radar by Popoli [Popoli & Blackman, 1987]. A fuzzy logic control strategy has not been attempted thus far, but it may provide a simple, effective and flexible solution to the rotating scheduling problem.

5.6 Conclusions

A set of objectives which a scheduling algorithm should attempt to meet have been proposed. It is immediately clear that not all objectives can be perfectly met in a practical situation, thus the importance of each objective to the multi-function radar system must be reflected in the scheduling algorithm.

A simulation model of a static multi-function radar, centered upon the task scheduler has been implemented. This allows design of multi-function radar search coverage volumes and analysis of the performance at a macroscopic and a microscopic level. Three static task scheduler algorithms have been incorporated into the simulation and tested. The first is a simulation of the MESAR look based scheduler. The other two work on the same principle, but are modified to calculate and reset time balances in a different way. Of these, one is a look based scheduler as per MESAR, the other is a simplified version which assumes that tasks are not broken down into looks, having some execution time advantage.

The simulation has been tested and validated using the MESAR search region parameters as a test case. A detailed assessment of the MESAR scheduler has been made. This was important since there was some question over whether this algorithm was performing as expected in the MESAR radar [Godbehere, 1996].

The results show that the scheduler algorithms achieve 100% utilisation of the multi-function radar antenna in all circumstances. This was the second of the three objectives which applied to a static multi-function radar, and reflects the importance attached to full utilisation of the multi-function radar antenna. This objective is achieved at the expense of scheduling tasks as close as is possible to their desired time (the first objective). Tasks are always scheduled after their desired update time to some extent.

This is minimised in the scheduling architecture, by splitting waveforms up into smaller looks so that the scheduling of a long waveform may be interrupted by a higher priority function. This entails, however, some extra complication in the signal processing since data from the interrupted waveform must be buffered to allow the interruption.

The MESAR algorithm is not optimal, in that better algorithms could be devised which give 100% radar utilisation and schedule tasks closer to their desired time by allowing tasks to be scheduled early. However, according to the requirements set out for timely scheduling, the MESAR algorithm is sufficient, and need not be more complicated.

The scheduler algorithms used in MESAR themselves are simple and flexible. This is because MESAR uses what may be called a distributed resource management architecture. Many of the computations which result in allocation of the multi-function radar resources are made in other separate areas of the radar control software.

An analysis of the differences between static and rotating multi-function radars has drawn out the complications that the scheduling algorithms must overcome for efficient operation of the multi-function radar. These are summarised;

i. blind arcs in the antenna coverage
ii. tasks must be scheduled close to array azimuth broadside where possible
iii. radar occupancy may be distributed non-uniformly with azimuth

It is concluded that a rotating scheduler algorithm should include some form of prediction of the radar load over one or more successive scans in order to allocate resources efficiently in situations of high radar loading. For resources to be allocated correctly in this situation a rotating multi-function radar scheduler must allow the use of forward and backward scanning of tasks to enable distribution of resources with angle. The theoretical extent to which this can be achieved has been determined for a multi-function radar which does not compensate the transmitted energy in surveillance with scan angle, and for a multi-function radar which does.

The cost of unnecessarily scheduling tasks away from array broadside in rotating multi-function radar systems has been determined in terms of the decrease in detection performance and in terms of the decrease in angular estimation accuracy when using monopulse. (and resolution capability). It was found that dwell times must be increased

by $1/\cos^3(\varphi)$ in order to maintain detection performance, but by $1/\cos^5(\varphi)$ in order to maintain plot accuracy. In surveillance the increased dwell times are offset somewhat by the increase in beamwidth (so a reduced number of search beams), and therefore the search function time needs only be increased by a factor of $1/\cos^2(\varphi)$ in order to maintain detection performance, and by $1/\cos^4(\varphi)$ in order to maintain plot accuracy.

An algorithm has been presented for the scheduling of tasks in a rotating radar that copes with the problems outlined in (i) to (iii) above. It is highly efficient in distributing the radar occupancy to the angular sectors which require it most. It will automatically adjust from a situation in which tasks are uniformly distributed throughout the MFR coverage to a situation in which the threat may come from a particular angular sector, so that many of the MFR tasks are concentrated in a small azimuthal sector.

A simulation of a rotating multi-function radar centered upon the above algorithm has been implemented. Results from this have validated that the algorithm performs well in both under-loaded and overloaded situations. Simulation has shown that around 94% of the theoretical maximum loading can be serviced through the use of forward and backward scanning. This smaller value arises due to the time taken for surveillance to 'catch up', from scanned to the maximum angle behind broadside, to the maximum angle ahead of broadside, in one rotation of the array antenna.

6 ADAPTIVE TRACKING IN MULTIFUNCTION RADAR

6.1 Introduction

This chapter looks at the problem of tracking highly manoeuvrable targets efficiently with a multi-function radar. It investigates strategies to prevent the loss of manoeuvring targets or targets with high angular crossing rates. Importantly the case of a rotating array multi-function radar is considered, for which little published literature has been found.

The following section describes the problem of tracking manoeuvring targets with a multi-function radar in more detail, and poses some of the significant questions that arise. Section 6.3 then compares the approach of the MESAR tracking system with some pertinent published work that was developed for the ELRA bistatic multi-function radar built by FFM, Germany, on parameter optimisation for a static array multi-function radar. It is shown that there are some important differences between the two, and that it would be beneficial to apply the parameter optimisation method that has been used in the ELRA system to a model of the MESAR tracking system.

Section 6.4 then presents the development and validation of a model of a MESAR like multi-function radar tracker system. This section contains the development of algorithms for the multiple beam updating of targets and for performing track updates with a rotating array antenna. These models are then applied to perform a similar parameter optimisation to that used for the ELRA system, using the benchmark tracking problem scenarios, developed by Blair and Watson [Blair et al, 1994]. An extensive analysis of the performance and radar time-budget requirements of using systems with a narrow radar beamwidth and systems using a rotating array antenna system is made. These results are given in section 6.5. Finally, the conclusions of the chapter are contained in section 6.6.

6.2 Tracking of manoeuvring targets with a narrow beam adaptive tracker

Chapter 4 showed that construction of a multi-function radar with a narrow beam is possible without increasing the search time-budget and search frame times to excessive lengths, through the use of simultaneous multiple beam processing. This would give good tracking performance compared to multi-function radars that are forced to use a broad beam from the inherent compromise between beamwidth requirements for the search and tracking functions. In Chapter 5 it was seen that multi-function radar resources are limited, and that radar time saved from one function may be used by another within the scheduler if it is correctly designed. Thus there is a strong drive to keep track update rates low where ever possible, to minimise the radar time-budget used for tracking each target, and allow this radar time to be used elsewhere. Also in Chapter 5, it was seen that rotating arrays that do not provide instantaneous coverage of the azimuthal volume (i.e. systems which utilise just one or two array faces), limit the maximum track update that can be supported.

Thus, although the inclusion of simultaneous multiple beam processing will allow multi-function radars to utilise a narrower beamwidth for the tracking function, the same, relatively low track update rates that are associated with a multi-function radar will still be enforced. These low update rates, coupled with a narrow beam will increase the probability that a manoeuvring target, or a target with high angular crossing rate, will not be illuminated by the multi-function radar pencil beam at the next track update. This will either result in an increased probability of losing the track, or in the necessity to widen the search around the expected target position for track updates.

Several papers have been published looking at adaptive update rate target tracking with a phased array radar ([Cohen, 1986], [Gardner & Mullen, 1988], [Wilkin et al, 1991], [Munu et al, 1992]). These papers however have not quantified the efficiency of such algorithms in terms of their use of multi-function radar resources. This has been performed more recently by Shin et al. [Shin et al., 1995], who propose an adaptive update rate IMM tracker for efficient use of multi-function radar resources. None of the above mentioned papers, however, consider the additional question of what energy should be transmitted on the target with a given update strategy. Neither do they consider the effects of rotating array systems, or the use of multiple beams for track

updating.

Some significant questions that arise when considering these problems are given below.

i. *Is there an optimal signal to noise ratio at which to perform tracking?*
ii. *Is it possible to track the required range of manoeuvring targets with a given beamwidth?*
iii. *Is this possible in the rotating array case when blind arcs limit the track update rate?*
iv. *How much radar time is used in a rotating system compared to a static system?*
v. *How much radar time is used in a narrow beamwidth system?*
vi. *To what extent do we require the use of multiple beams for track updates against manoeuvring targets?*

These questions are addressed throughout the remainder of this chapter.

6.2.1 Simplified analysis of tracking manoeuvring target with a narrow beamwidth

As a precursor to the detail simulation results that follow later in this chapter, a simplified analysis of the problem of maintaining track on manoeuvring targets is given. The case of a linear predictor with no smoothing filter and noiseless measurements is considered.

The antenna configurations that are studied as part of this investigation are shown in Table 6-1 below, along with the angular width of the blind sector that the antenna configurations suffer, and also the period, T_{blind} , that this leads to. This is the period for which no updates may be made in a given direction due to the blind sector, and therefore defines the minimum update interval which may be sustained. It is defined by the interval between two updates in the target direction, the first of which is made at the maximum back-scanned angle (60° behind of azimuth array broadside), and the next possible update in the target direction, which must be made at the maximum forward scanned angle (60° ahead of azimuth array broadside). It is this interval which is one of the limiting factors in maintaining track on manoeuvring targets.

Antenna Configuration				
Static/Rotating	**Number of Faces**	**Rotation Period**	**Blind Sector Width**	**T_{blind}**
Static	-	-	-	0.1 s
Rotating	1	1 s	240°	0.67 s
Rotating	1	2 s	240°	1.33 s
Rotating	2	1 s	60°	0.17 s
Rotating	2	2 s	60°	0.33 s

Table 6-1 Multi-function radar antenna configurations considered

In the case of the static array multi-function radar, there is no blind sector (given 3 or more faces), and thus T_{blind} should actually be zero. However, in Table 6-1 T_{blind} is represented by the minimum track update interval which can be achieved, which for this investigation has been taken to be 0.1s. The benefit for the tracking of manoeuvring targets of having a second array face in a rotating system is apparent. The blind sector width is reduced by a factor of 4 giving smaller values of T_{blind}. (Obviously in the case of a third array face, T_{blind} would have no significance as in the static case).

A target trajectory was created, consisting of a period of constant velocity flight before execution of a constant acceleration 180° turn in azimuth. Both the range at which the manoeuvre occurred, and the strength of the manoeuvre were varied. The predictor used simple linear extrapolation between the last two measurements to predict target position at the time of next update. The maximum error between the predicted target position and true target position is then the value plotted for the following figures.

Figure 6-1 shows the results for each of the values of T_{blind} considered in the study. It should be noted that these results are highly optimistic. The introduction of any smoothing will introduce a lag which will worsen the maximum prediction error. Also, the introduction of noise into the measurements and of a probability of detection of less than 1 will increase the maximum prediction error. Thus it is difficult to relate these graphs to the absolute tracking prediction errors that may be expected in a realistic situation. Figure 6-1 does however given an indication of the relative performance that may be expected of the different antenna configurations.

The results show that an increase in T_{blind} implies a shift of the surface up the z axis. Figure 6-1 (a) and (b) show indiscernible results for the minimum update rates of 0.1s and 0.17s, suggesting that the tracking performance against manoeuvring target for the two faced array system, rotating at 1s should give nearly identical performance to that of a static system.

This is not however the case for the remainder of the results in Figure 6-1. Each shows a significant increase in the maximum prediction errors that occur. In the last case of a single array, rotating with a period of 2s, strongly manoeuvring targets at close range give maximum prediction errors of several degrees. Given that the maximum prediction error must be kept within the radar beamwidth, and that these results are likely to be very optimistic, this would imply that tracking using multiple beam updates would be essential to maintain track on close, manoeuvring targets with such a system.

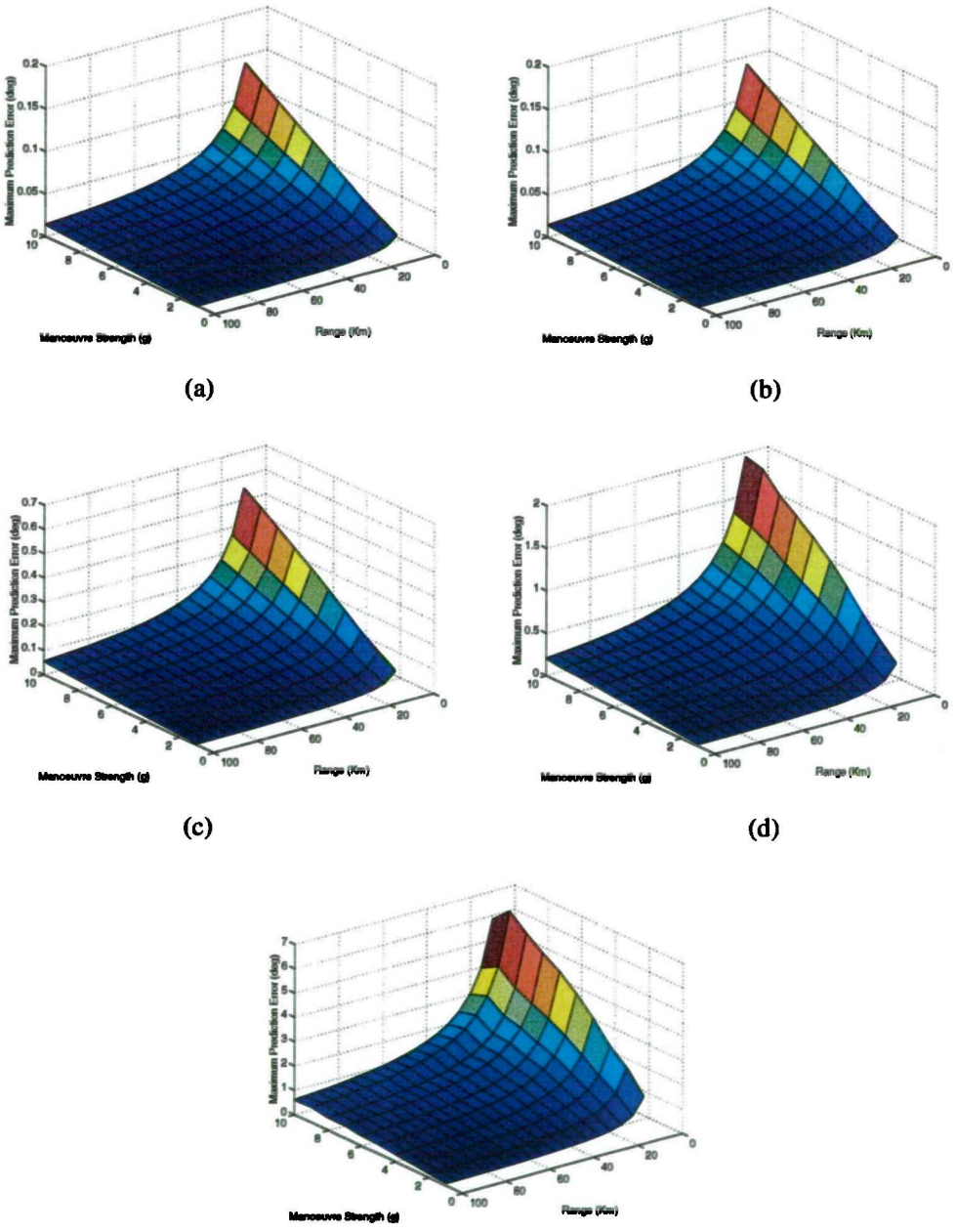

(a) (b) (c) (d) (e)

Figure 6-1(a,b,c,d,e) Maximum prediction error between a constant velocity prediction and a manoeuvring target, with varying manoeuvre strength and range of manoeuvre start. (a) T_{blind}=0.1s, (b) T_{blind}=0.17s, (c) T_{blind}=0.33s, (d) T_{blind}=0.67s, (e) T_{blind}=1.33s

Figure 6-2 extracts the special case of a 7g manoeuvre at a range of 40km from the above results. This corresponds to the situation that occurs in benchmark trajectory 6.

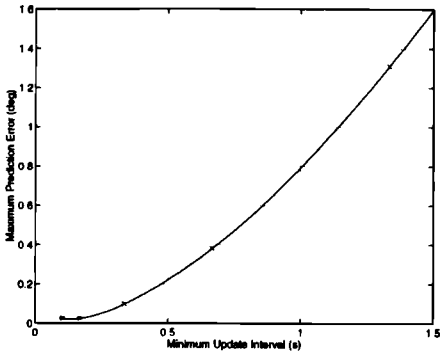

Figure 6-2 Maximum prediction error between a constant velocity prediction and a target manoeuvring with a lateral acceleration of 7g at a range of 40km

A cubic spline (green line) has been fitted through the extracted data points (red crosses). This gives an indication of the relative performance that the different systems will give. The difference between the two rotating systems with the smallest values of T_{blind} (the twin faced systems) and the static system is minimal. However the two single faced systems experience significantly increased maximum prediction errors, and we may therefore expect a decreased track robustness from these systems against benchmark trajectory 6.

These results have given a relative indication of the performance we may expect to obtain from the different antenna configurations. However it is impossible to relate these graphs to the absolute tracking performance of a given tracker due to the complexity involved. This may only be obtained through a detailed simulation of the track smoothing filters, plot measurement errors, track update strategy and use of multiple beam updates.

6.3 Allocation of resources in tracking for a static array system

Little has been found in the open literature on tracking and resource management for a rotating array system, thus we start by looking at the static case. The first two important questions that must be addressed for an adaptive tracking system are;

i. when should track updates be scheduled?

ii. what energy should be used for these updates?

Two different strategies to address these points have been adopted in the MESAR multi-function radar system and in the ELRA multi-function radar system, developed at FFM, Germany. These two strategies are compared below, and the impact of using significantly narrower beamwidths than those that are implemented in the MESAR and ELRA systems are considered.

6.3.1 Allocation of resources for tracking in MESAR

As discussed in section 3.6.3, MESAR calculates the time of next update for a track based on two criterion [Noyes, 1990];

i. there is a high probability that the target falls within the 3dB beam on the next update. This value will depend on the azimuth and elevation smoothed accuracy of the track, and on the amount that the track can possibly manoeuvre in azimuth and elevation.

ii. there is a constant smoothed track accuracy in position or velocity.

Choosing an update interval, ΔT, that is too large will mean that one of the above is not fulfilled. Choosing an update interval that is too small will mean the tracking function will have a track occupancy greater than its necessary value. Thus in MESAR, there are two times that are used when requesting a track update;

a. latest update time. This is the earliest of the two possible outcomes of (*i*) above, depending on whether the azimuth or elevation manoeuvre capability is larger, and the track uncertainty in each coordinate. It represents the time by which an update must be made before which there is a chance that the target will fall outside of the 3dB beamwidth, and not be detected.

b. desired update time. This is the time which is given from (*ii*) above. It may be greater or smaller than the latest update time.

The track updates will be scheduled using the minimum of these two intervals. The track update interval is constrained to a maximum of 5s and a minimum of 0.1s.

MESAR attempts to maintain the target signal to noise ratio between 26dB and 29dB

[Stafford, 1991]. A smoothed estimate of the integrated signal to noise ratio is maintained, and the number of waveforms integrated for each track update is modified in an attempt to keep this smoothed estimate constant. The figures of 26dB and 29dB are thought to be chosen rather arbitrarily in MESAR, to give good plot accuracy from the monopulse estimate. It is possible that there is room for improving the efficiency of the tracker in this respect.

6.3.2 Parameter optimisation for allocation of resources in the ELRA adaptive tracking system

The problem of efficient allocation of multi-function radar resources for the tracking function has also been investigated by Van Keuk [Van Keuk & Blackman, 1991]. He attempted to obtain an optimal strategy for tracking by looking at the update interval, energy used for the updates, and the accuracy requirements as a coupled system.

As Van Keuk states, if ΔT is chosen to be small, then the probability density function of the extrapolated target position is highly concentrated in angle space, which will lead to a good signal to noise ratio at the next update. This has the consequence of a higher detection probability and a higher plot accuracy. Also, since the beamwidth is significantly larger than the variance in the probability density function of the target, there is no need to search in adjacent beam directions to ensure detection. On the other hand, a very small value of ΔT is expensive in terms of radar time.

Conversely, a large value of ΔT leads to a large variance of the probability density function of the extrapolated target position, which in turn leads to a reduced signal to noise ratio, and plot accuracy. Also, a large value of ΔT increases the probability that the extrapolated target position will exceed the area illuminated by the multi-function radar pencil beam, and will thus necessitate a search of more than one pencil beam.

There is clearly an optimal choice of ΔT which will minimise the radar time expended on the target, and this ΔT will have a corresponding track accuracy.

Equally, a similar optimisation may be applied to the signal to noise ratio, SNR_o, used for each track update. Assuming coherent integration, the track update dwell time will be proportional to the signal to noise ratio. Using a long dwell time will lead to good signal to noise ratio and plot accuracy, but can lead to wasted resources. Conversely,

although a shorter dwell time saves resources, a lower signal to noise ratio and plot accuracy is achieved, and the probability of wasting energy due to missed detections is increased.

By making a considerable number of simplistic assumptions, an analytical solution may be found that gives an optimal tracking strategy in terms of radar time. Assumptions are made about beam positioning losses, target detection criterion, target dynamics, and the search strategy employed which allow formulation of analytical expressions relating track update rate, signal to noise ratio, accuracy requirement and radar time on target.

Van Keuk introduces a track sharpness parameter, V_o. This may be understood as the point in time at which a track update must be scheduled to maintain a fixed angular accuracy. Let the major axis of the target position error ellipsoid, defined by the positional elements of the predicted target covariance matrix, be denoted by G. This parameter will increase as a function of time. A threshold is defined as $V_o.(bw/2)$, as the acceptable track inaccuracy. Thus ΔT, the period after which another track update must be scheduled, may be calculated from the point at which G is greater than $V_o.(bw/2)$, shown in equation [6-1] below.

$$G\langle t_{N+1} | N \rangle \cong V_o \left(\frac{bw}{2} \right) \qquad [6\text{-}1]$$

A useful approximation to ΔT, valid when the tracking filter converges, given by Van Keuk [Van Keuk, 1978] is shown in equation [6-2], below. Thus, given the parameters of a Singer target manoeuvre model, we may calculate an update interval for a track as a function of the tracking accuracy required.

$$\Delta T \cong 0.4 \left(\frac{r\sigma\sqrt{\Theta}}{\Sigma} \right)^{0.4} \frac{U^{2.4}}{1+\frac{1}{2}U^2} \qquad [6\text{-}2]$$

where r is the target range
σ is the measurement accuracy
Θ is the Singer model acceleration correlation time
Σ is the Singer model acceleration
$U = (\frac{1}{2}bw.V_o)/\sigma$

Also, given a search strategy for a track update of one or more pencil beams, an approximation to the number of beams that must be searched in order to detect a target

may be made. Van Keuk uses the expression given in equation [6-3], below.

$$N_{beams} \equiv \frac{1}{PD_o}\left[1+(\alpha V_o^2)^2\right]^{1/2} \qquad [\,6\text{-}3\,]$$

where $\alpha \approx 1+14(\,|\ln P_f| / SNR_o\,)^{1/2}$

$PD_o = P_f^{1/(1+SNRo)}$

The track update interval and number of beams required are plotted in Figure 6-3, below, for a range of values of V_o and SNR_o. The target parameters chosen were r=60km, Σ=10m/s^2, Θ=60s, P_f=10^{-5}, and bw=1°.

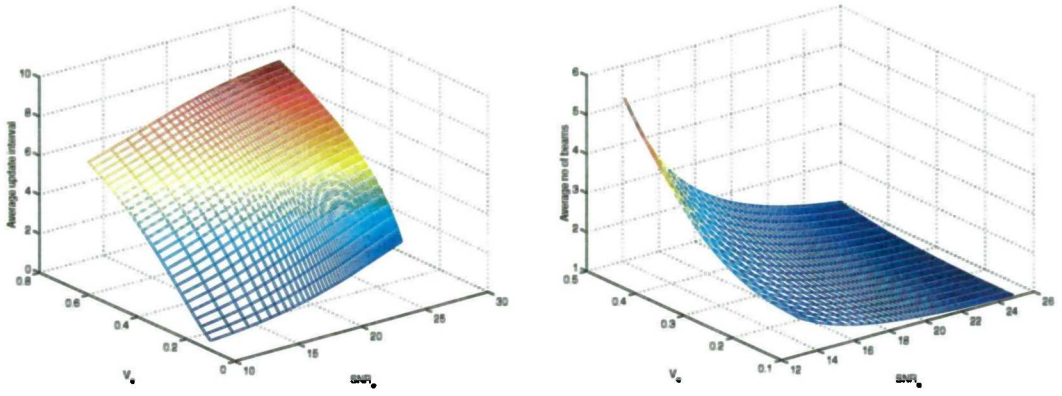

Figure 6-3(a,b) Track update interval, and number of beams required for each track update as a function of track accuracy requirement (V_o) and signal to noise ratio (SNR_o)

From these parameters we may now make an estimate of the radar load. The average number of track update beam directions required per unit time, Nb_{av}, is given by the average number of beams for each track update, divided by the average track update interval used. Then the radar load of the track is Nb_{av} multiplied by the dwell time of each track update. Since the dwell time is proportional to the required signal to noise ratio for tracking, SNR_o, the radar load can be approximated by equation [6-4].

$$L_r \propto \left(\frac{\Sigma}{(bw/2)r\sqrt{\Theta}}\right)^{0.4} \frac{1}{PD_o} f(V_o, SNR_o, P_f) \qquad [\,6\text{-}4\,]$$

The form of equation [6-4] shows that L_r may be optimised in terms of V_o and SNR_o, independently of target range and dynamics. Figure 6-4 shows L_r as a function of V_o and SNR_o, for the same set of target parameters as used in Figure 6-3 above.

The analytical simplification of the problem results in a minimised value of radar load for values of SNR_o=15dB, and V_o=0.3. Thus the optimal accuracy requirement in terms of minimising the radar load for tracking is 0.15 beamwidths, independent of the

beamwidth used.

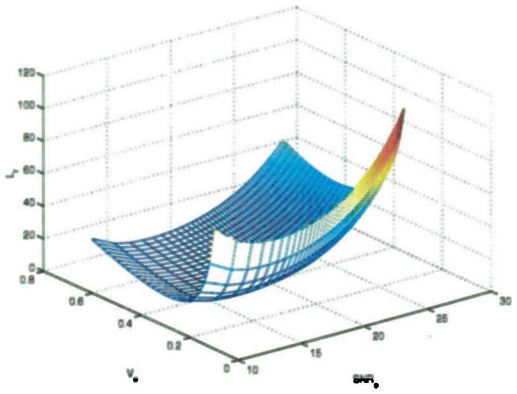

Figure 6-4 Radar load as a function of track accuracy requirement (V_o) and signal to noise ratio (SNR_o)

A more accurate estimation of the optimal values of SNR_o and V_o can only be obtained through a Monte Carlo simulation. By performing this, Van Keuk concluded that the estimate for V_o was accurate. However the analytical estimate of the optimal signal to noise ratio was an underestimate; a value of 18dB for SNR_o was indicated from the simulation.

6.3.3 Comparison of the two strategies

Both the MESAR and Van Keuk strategies arrive at similar values for the track update intervals that must be used. A difference between the two strategies comes from the difference in the tracking accuracy requirement that is demanded. The Van Keuk strategy is to allow the accuracy demanded to be a parameter which may be optimised, resulting in a value of 0.15 beamwidths. In the MESAR system, this is a user specified value; an assumption that is in keeping with an air defence tracking system.

Neither strategies reflect different priorities of target, in the requirements used. A weapons system radar is likely to have to track a large number of targets, only a few of which are of genuine interest to the weapons system. Thus different requirements need to be specified for these different target types. Low priority targets such as airliners and other commercial traffic need only be tracked with an accuracy that allows track maintenance to occur with a low probability of track loss, meanwhile high priority targets, such as incoming missiles, need to be tracked with fixed accuracy requirements, specified by the weapons system demands.

The difference in the values of signal to noise ratio chosen for tracking is considerable (up to 11dB). Therefore, it will be beneficial to apply the same optimisation as has been used by Van Keuk on the ELRA system, to the MESAR system.

This will be achieved through development of a Monte Carlo simulation of the MESAR tracker, described in the following sections of the chapter. Rather than investigate the performance of this system with a random model, such as the Singer model, it is thought to be more useful to use a range of realistic target trajectories, representative of those that a multi-function radar may encounter in its operation. Therefore, the model has been developed and validated using the target trajectories proposed in the Benchmark Tracking Problem. This was first published in 1994 [Blair et al, 1994] to cope with the lack of a common means of comparing different tracker systems. The benchmark problem addressed beam pointing control of a phased array radar against highly manoeuvring targets, and has been widely applied in the U.S. ([Rhatigan et al, 1994], [Sastry et al, 1994], [Sworder & Boyd, 1994], [Daeipour et al, 1994], [Tsaknakis & Athans, 1994], [Blair & Watson, 1994], [Kirubarajan et al, 1998]). It was considered useful to utilise these trajectories since they are representative of a number of different air targets, and will ultimately allow results to be more widely comparable. The benchmark tracking problem and trajectories are described in Appendix A.

6.4 Development of an adaptive tracking system simulation model

A model has been developed that is based on the MESAR adaptive tracker. The development of the model is described here. The validation and testing of the model, and subsequent modifications that were necessary, are described in the following section. Before the tracker itself, and the validation of it, are presented, the modelling of the target measurement process is presented.

6.4.1 Modelling of the target measurement process

The beamwidth is assumed to broaden with the reciprocal of the cosine of the scan angle, and is assumed to be separable in azimuth and elevation, as in equation [2-8]. The gain is assumed to decrease with the cube of the cosine of the scan angle, as in equation [2-9]. The scan angle of the beam from array broadside is calculated using equations [4-6], where the array is assumed to lean back from vertical at an angle of

20°.

The target is modelled as having a signal to noise ratio, with a one way loss which varies with the angle from boresight as in equation [6-5], [Skolnik, 1982]. Here φ is the angle of the target from beam boresight, and θ is the radar 3dB beamwidth at the current scan angle.

$$snr = snr_0 e^{2.78\frac{\varphi^2}{\theta^2}} \qquad [\,6\text{-}5\,]$$

This gives rise to a probability of detection, P_D, given by equation [6-6], where P_F is the probability of false alarm, taken to be 10^{-6}.

$$P_D = P_F^{1/(1+SNR)} \qquad [\,6\text{-}6\,]$$

The accuracy of the monopulse estimate of the target's position within the beam is given by equation [2-5]. Figure 6-5 shows the monopulse accuracy of the estimate as a function of the signal to noise ratio. The standard deviation of the range measurements used was 15m.

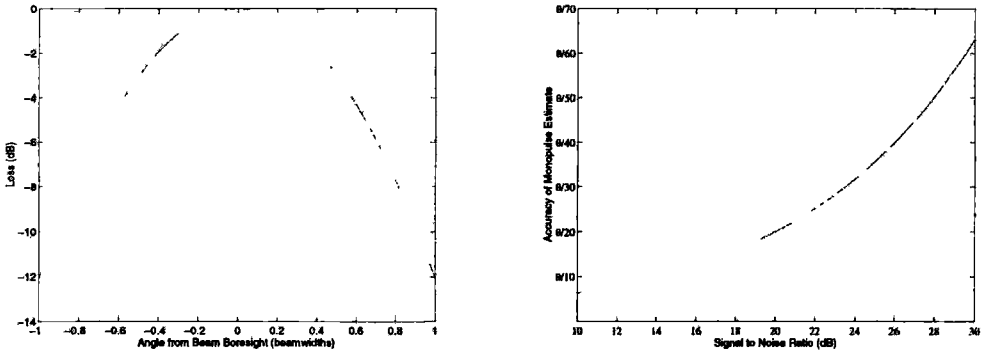

Figure 6-5(a) Signal to noise ratio as a function of target angle from beam boresight, (b) Accuracy of monopulse estimate as a function of the target signal to noise ratio

6.4.2 Kalman filtering

In order that a Monte Carlo analysis/optimisation may be performed to find the most efficient method of tracking targets, a Kalman filter model must be developed. For this the same strategy has been used as has been adopted in the MESAR radar. A rotated line of sight coordinate system is used ([Blackman, 1986], [Daum & Fitzgerald, 1983]). This has the advantage that the filter may be de-coupled, since the positional and velocity errors are maintained in the diagonal of the covariance matrix. Also, the Cartesian filter

terms may be simply related to the polar measurements.

A simple 2 state, constant velocity Kalman filter was adopted for the study. The stages of the Kalman filter are shown below [Tunnicliff, 1980].

1. Find forecast position and velocity

$$X'_{K+1} = \Phi_K \hat{X}_K \qquad [6\text{-}7]$$

2. Find the uncertainty in the forecast

$$P'_{K+1} = \Phi_K \hat{P}_K \Phi_k^T \qquad [6\text{-}8]$$

3. Use the uncertainty in the forecast and measurement to calculate the filter gain

$$K_{K+1} = P'_{K+1} H_{k+1}^T \left[H_{k+1} P'_{K+1} H_{k+1}^T + R_{k+1} \right]^{-1} \qquad [6\text{-}9]$$

4. Find the smoothed position and velocity

$$\hat{X}_{k+1} = X'_{k+1} - K_{k+1} (H_{k+1} X'_{k+1} - Z_{k+1}) \qquad [6\text{-}10]$$

5. Find the uncertainty in the smoothed position and velocity

$$\hat{P}_{k+1} = P'_{k+1} - K_{k+1} H_{k+1} P'_{k+1} \qquad [6\text{-}11]$$

This type of filter is optimal only for constant velocity target motion. In the instance of a manoeuvring target, this type of filter must be augmented with some form of manoeuvre detection and adjustment of the filter to avoid very poor performance. This is seen clearly in Figure 6-7 - Figure 6-13 below, which show the output of such a Kalman filter model using the benchmark trajectories 1 and 3. Figure 6-6 shows both a 3 dimensional and a 2 dimensional view of the first trajectory, the modelled noisy measurements, and the smoothed filter estimate of position. Figure 6-7 - Figure 6-9 then show the errors between the smoothed position and velocity and the true position and velocity, and compares those to the errors between the measurements of radar plots. Figure 6-10 - Figure 6-13 then show this for benchmark trajectory 3. Tracks were updated with a constant update rate of 1Hz for this example. A target which gave a 20dB signal to noise ratio on beam boresight and at array broadside was used in this case.

The filter showed good performance in periods of constant velocity flight, however, very poor performance during a manoeuvre; smoothed estimates of position were considerably poorer than the raw measurements. After a manoeuvre, the error in the smoothed estimate decayed slowly. Although the amount of smoothing that was applied

was limited to prevent an ever increasing confidence in the filter's estimate, the filter, unsurprisingly, still reacted poorly to a target manoeuvre.

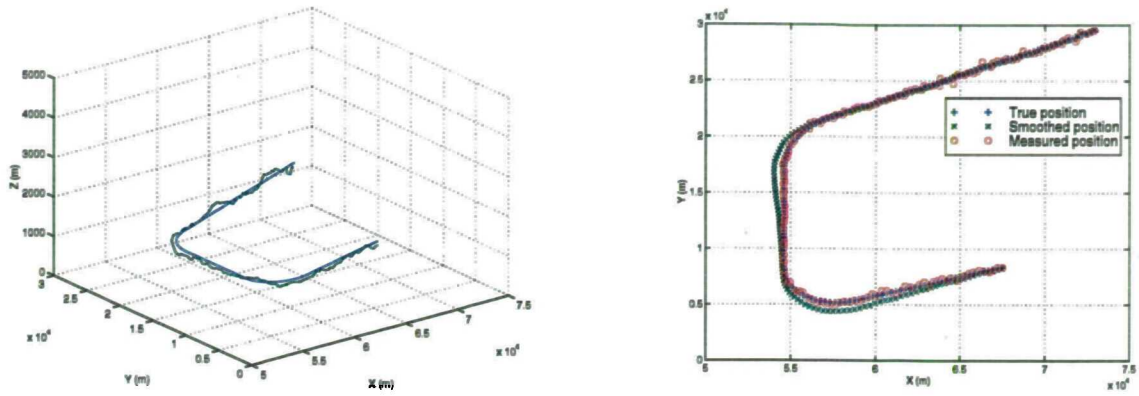

Figure 6-6(a,b) 3 dimensional and 2 dimensional plot of Benchmark Trajectory 1, showing position truth, position measured, and smoothed filter output

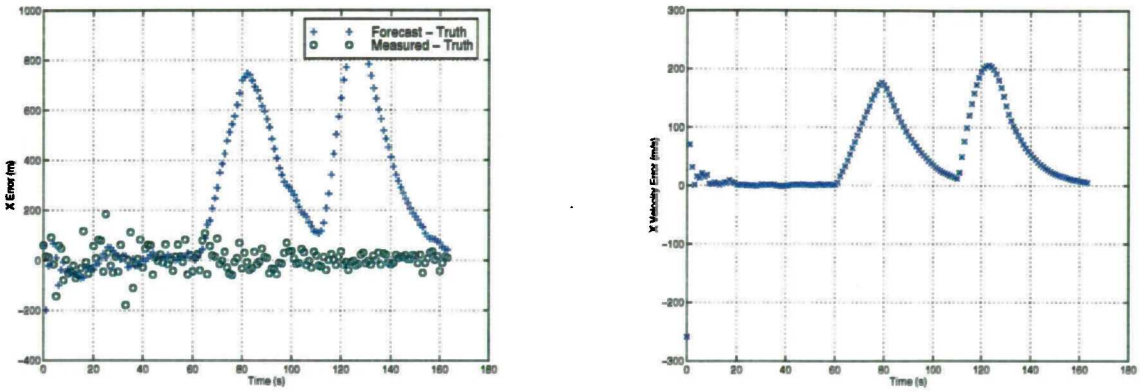

Figure 6-7(a,b) X-coordinate position and velocity errors for Benchmark Trajectory 1

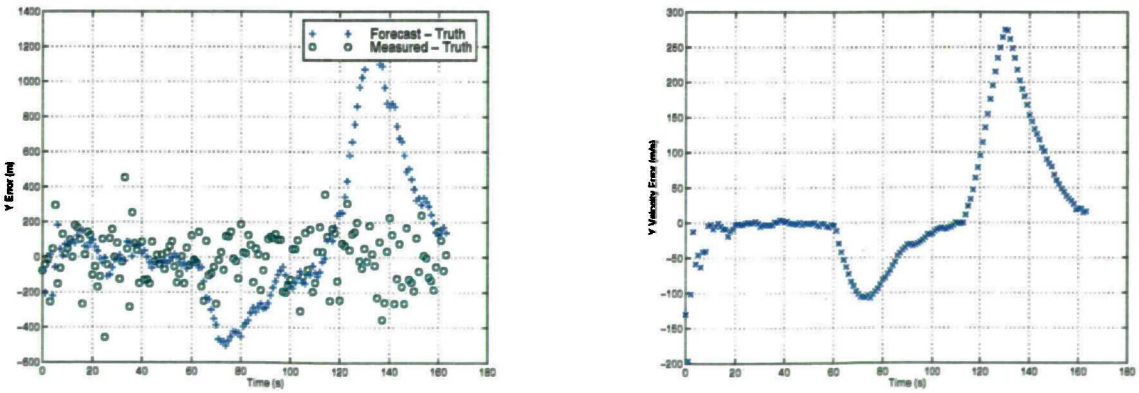

Figure 6-8(a,b) Y-coordinate position and velocity errors for Benchmark Trajectory 1

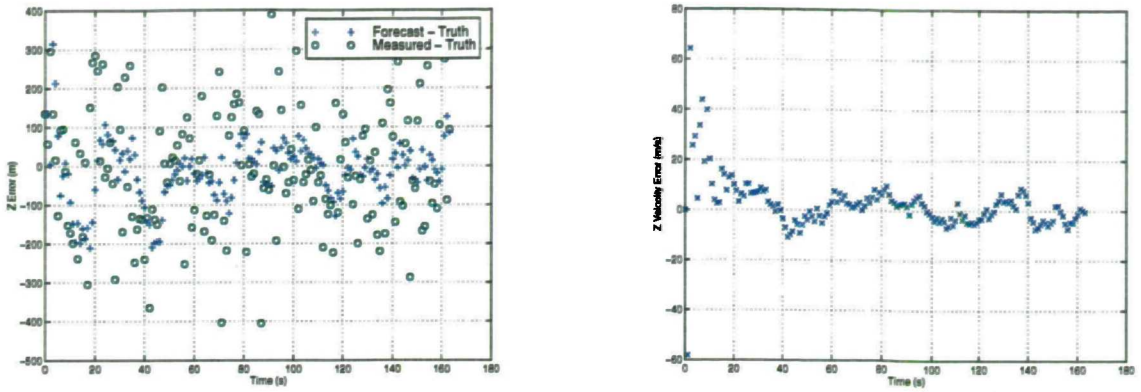

Figure 6-9(a,b) Z-coordinate position and velocity errors for Benchmark Trajectory 1

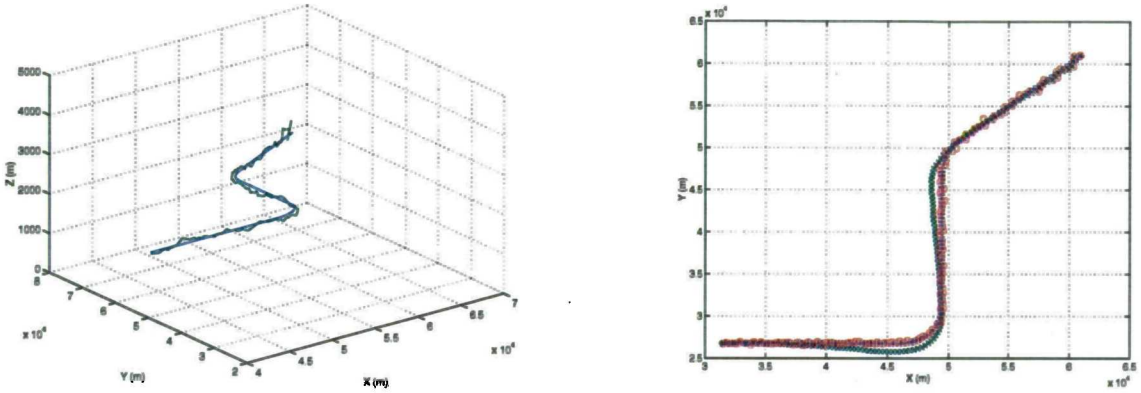

Figure 6-10(a,b) 3 dimensional and 2 dimensional plot of Benchmark Trajectory 3, showing position truth, position measured, and smoothed filter output

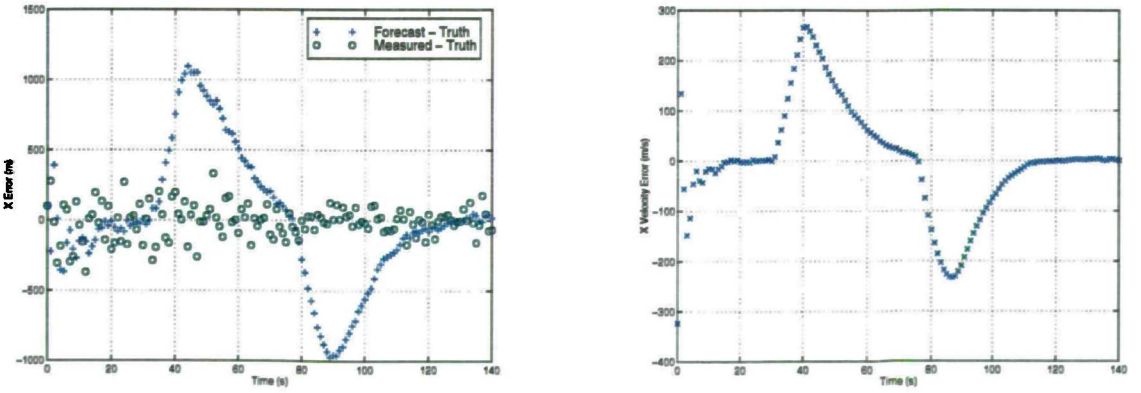

Figure 6-11(a,b) X-coordinate position and velocity errors for Benchmark Trajectory 3

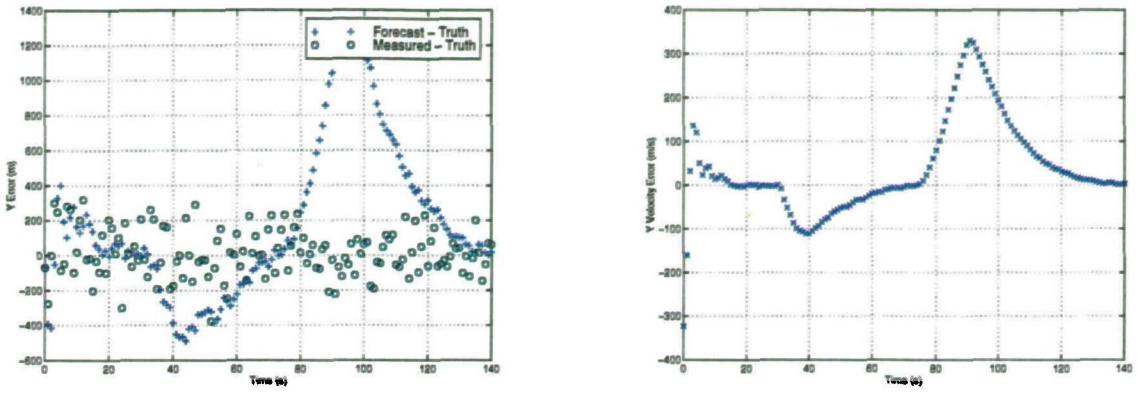

Figure 6-12(a,b) Y-coordinate position and velocity errors for Benchmark Trajectory 3

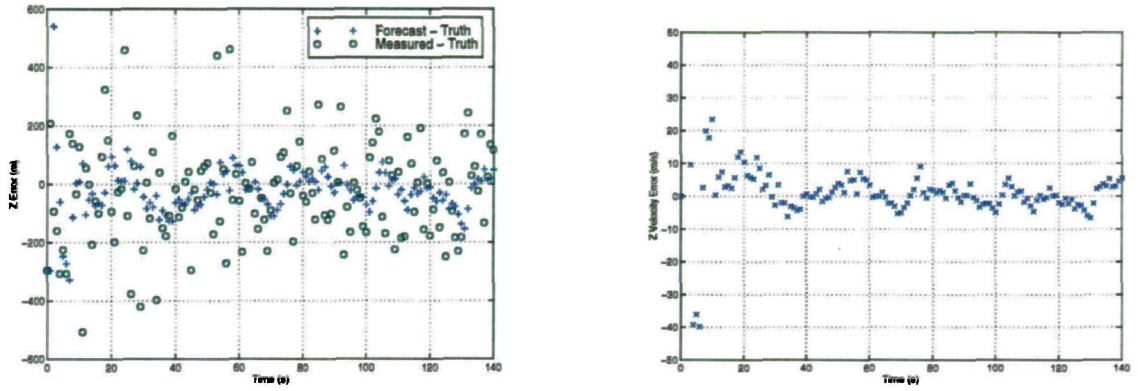

Figure 6-13(a,b) Z-coordinate position and velocity errors for Benchmark Trajectory 3

6.4.3 Augmenting the constant velocity Kalman filter for manoeuvring targets

The performance of the standard, constant velocity Kalman filter described above is too poor to be used in this study. The errors indicated in the figures above are such that the target would have manoeuvred out of the beam and been lost, purely due to the lag in the filter response. A manoeuvre detection and response scheme was thus implemented to reduce this problem. The strategy adopted was that first suggested by Quigley [Quigley, 1975].

6.4.3.1 Manoeuvre detection

The onset of a target manoeuvre may be indicated by the normalised distance (i.e. the number of variances or standard deviations) between the predicted target position and the measured target position. This quantity, let us call it J, may be broken down into its three components in X, Y and Z. J_x, J_y and J_z are simply the residuals (X_{res}, Y_{res} and Z_{res}) between the target expected position and measured position, divided by the standard deviation expected of the residual.

$$J_x = \frac{X_{res}}{\left(\sigma_{x'}^2 + \sigma_z^2\right)^{1/2}} \qquad [6\text{-}12]$$

Here, $\sigma_{x'}$ is the standard deviation of the prediction error, and σ_z, is the standard deviation of the measurement error. These residuals are then smoothed from one update to the next, so that the manoeuvre detection decision is based on more than one update.

$$E_{\lambda_{n+1}} = (1-\lambda)E_{\lambda_n} + (\lambda)J_{x_n} \qquad [6\text{-}13]$$

Where E_x is the smoothed, normalised residual in the x coordinate, and λ is the smoothing constant. Once this smoothed residual exceeds a certain threshold, in any of the three coordinates, a manoeuvre may be indicated.

If the manoeuvre threshold is exceeded in any one of the three coordinates, a confirmation update is requested 0.1s later. Only upon confirmation of the threshold crossing is a manoeuvre flagged. The state covariance matrix would then be adjusted to reduce the smoothing applied through the filter. This strategy was adopted to reduce the number of false alarms due to manoeuvre.

6.4.3.2 Manoeuvre response

The manoeuvre response is achieved by adding a plant noise term, Q, to equation [6-8] above. This results in a smaller confidence in the filter prediction, and thus more weight is given to the radar measurements.

$$P'_{K+1} = \Phi_K \hat{P}_K \Phi_K^T + Q \qquad [6\text{-}14]$$

The Q matrix is derived for a single dimension as, per equation [6-15] below [Castella, 1980]. The value of q that is used is proportional to the smoothed residual, so that a larger manoeuvre will result in a higher manoeuvre response.

$$Q = qT\begin{bmatrix} T^2/3 & T/2 \\ T/2 & 1 \end{bmatrix} \qquad [6\text{-}15]$$

The manoeuvre detection strategy has the effect of increasing the Kalman filter performance in the instance of a manoeuvre, but with some reduction in the performance against constant velocity targets due to declaration of false manoeuvres. This is seen in the results shown in Figure 6-14 - Figure 6-23 below. The simulations

above were repeated for benchmark trajectories 1 and 3, with manoeuvre detection implemented. A constant track update rate of 1Hz was again used, however updates were scheduled after 0.1s when a manoeuvre was flagged.

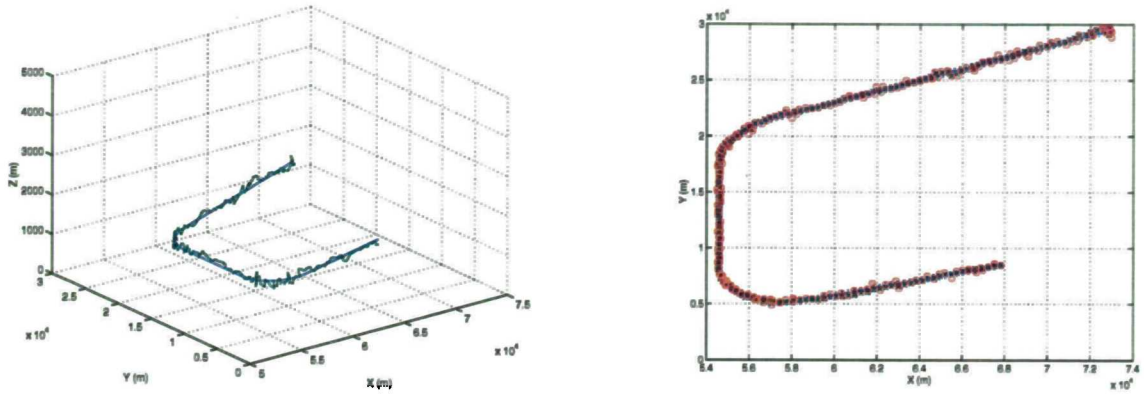

Figure 6-14(a,b) 3 dimensional and 2 dimensional plot of Benchmark Trajectory 1, showing position truth, position measured, and smoothed filter output

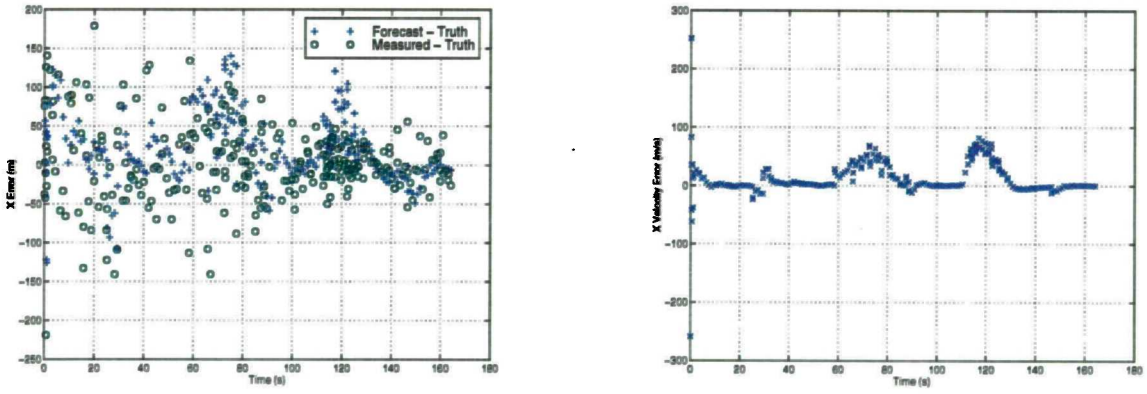

Figure 6-15(a,b) X-coordinate position and velocity errors for Benchmark Trajectory 1

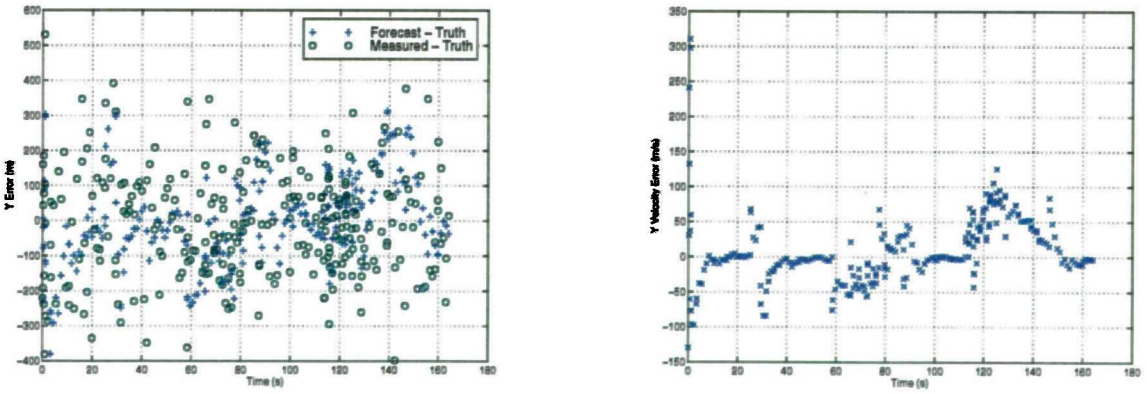

Figure 6-16(a,b) Y-coordinate position and velocity errors for Benchmark Trajectory 1

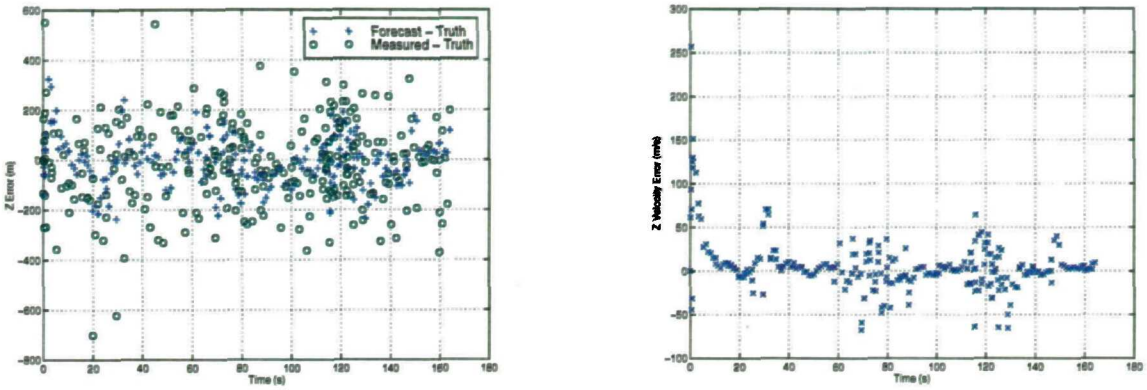

Figure 6-17(a,b) Z-coordinate position and velocity errors for Benchmark Trajectory 1

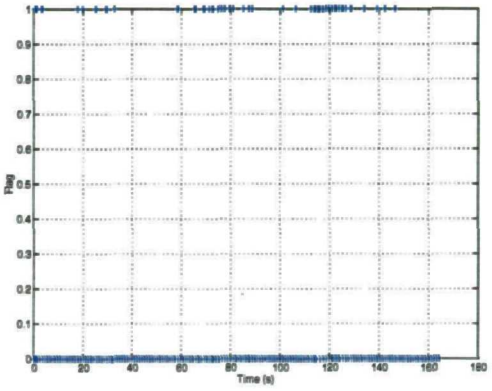

Figure 6-18(a,b) Manoeuvre detection flag for Benchmark Trajectory 1

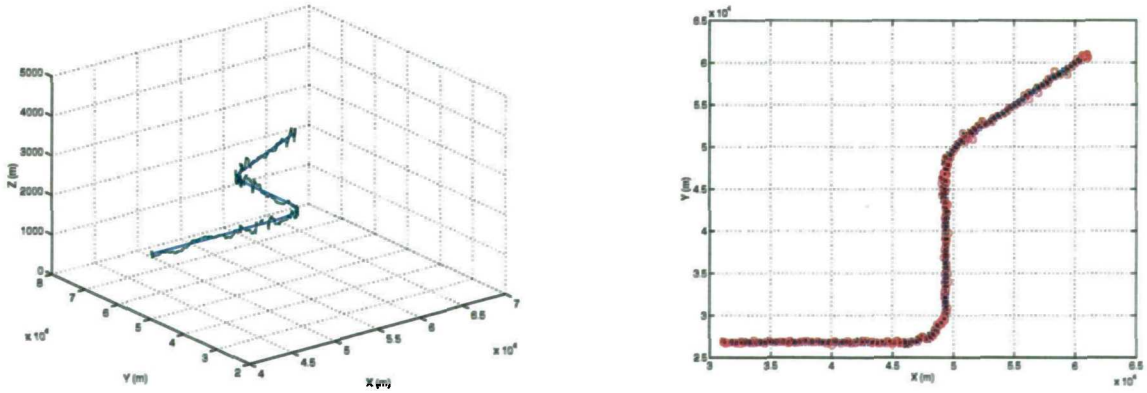

Figure 6-19(a,b) 3 dimensional and 2 dimensional plot of Benchmark Trajectory 3, showing position truth, position measured, and smoothed filter output

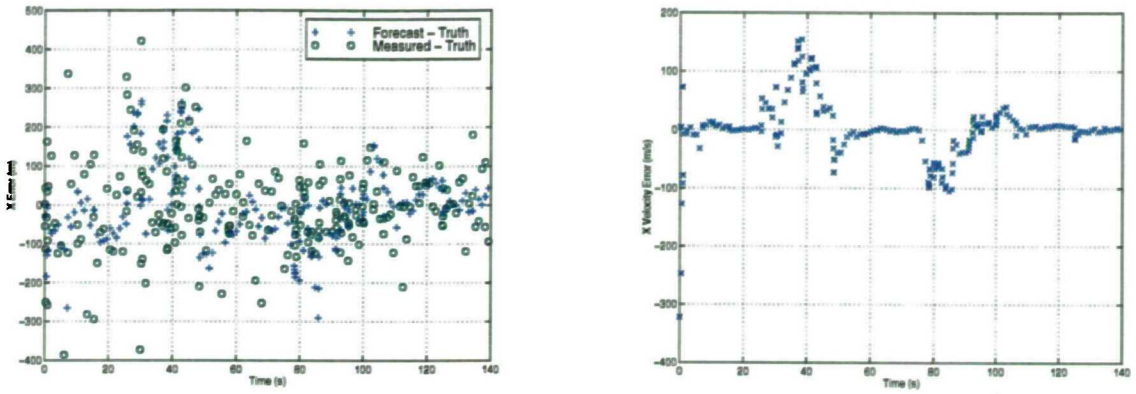

Figure 6-20(a,b) X-coordinate position and velocity errors for Benchmark Trajectory 3

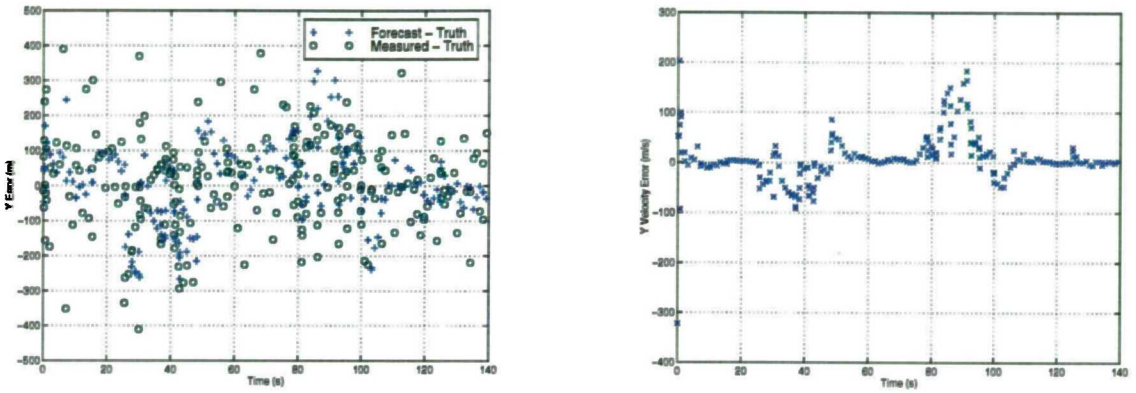

Figure 6-21(a,b) Y-coordinate position and velocity errors for Benchmark Trajectory 3

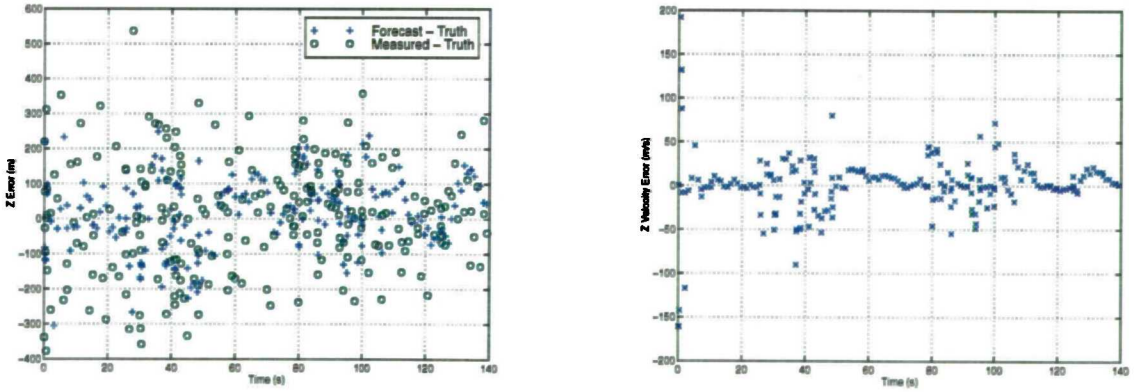

Figure 6-22(a,b) Z-coordinate position and velocity errors for Benchmark Trajectory 3

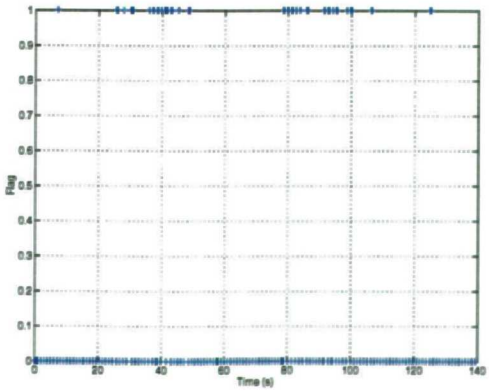

Figure 6-23(a,b) Manoeuvre detection flag for Benchmark Trajectory 3

The results show a considerable improvement in performance during target manoeuvre, with only a small impact on the constant velocity filter performance.

As stated by Watson [Watson & Blair, 1993], tracking of manoeuvring targets with single model track filters supplemented by manoeuvre detection in this way, gives poor performance in comparison to multiple model techniques. The common method of increasing the filter state estimate error variances suffers from two problems. Firstly, the filter response is delayed because the error variances are not increased until after a manoeuvre is declared. Secondly, after a manoeuvre has finished, the filter has large error variances, making a bias difficult to detect, and thus resulting in a delay in the decision to reduce the covariance matrix errors. Watson proposes the use of the Interacting Multiple Model (IMM) to improve performance in these circumstances.

However, the objective of this study is to determine an efficient method of multi-function radar resource allocation for target tracking. Absolute tracking accuracy is not the most important issue. Therefore, the approach taken here will be to develop an efficient tracking strategy for static, rotating and simultaneous multiple beam multi-function radars using a simple single model filter, supplemented with manoeuvre detection. This may then be extended to use multiple model methods such as IMM, for implementation into a real system, when high accuracy tracking is crucial.

Thus the aim of the optimisation will therefore be to determine the most efficient tracking strategy that will give the desired track accuracy, neglecting that during target manoeuvre. It is accepted that using a constant velocity predictor during phases of manoeuvre will give a poor smoothed tracking accuracy, and that this may be improved upon in several ways.

6.4.4 Adaptive update rate strategy

The model uses the MESAR adaptive update strategy described in section 6.3.1 above. The time of next update is bounded between 0.1s and 5s. An example of this is shown in Figure 6-24 - Figure 6-26, which show results from tracking benchmark target 1. Figure 6-24 shows the three dimensional and plan views of the simulation output. The adaptive update rate is clearly visible; during the early phase of the track, the update rate is high, before becoming lower as the confidence in position and velocity grow. At the points of manoeuvre, the update rate can be seen to increase again, reflecting the increased

uncertainties in the covariance matrix, causing a decreased desired update interval. This is more clearly visible in Figure 6-25, which plots the latest, desired and chosen update times over the course of the simulation. The results presented are those for a target which gives a 20dB signal to noise ratio on beam boresight and array broadside, and for a radar beamwidth of 2.5°.

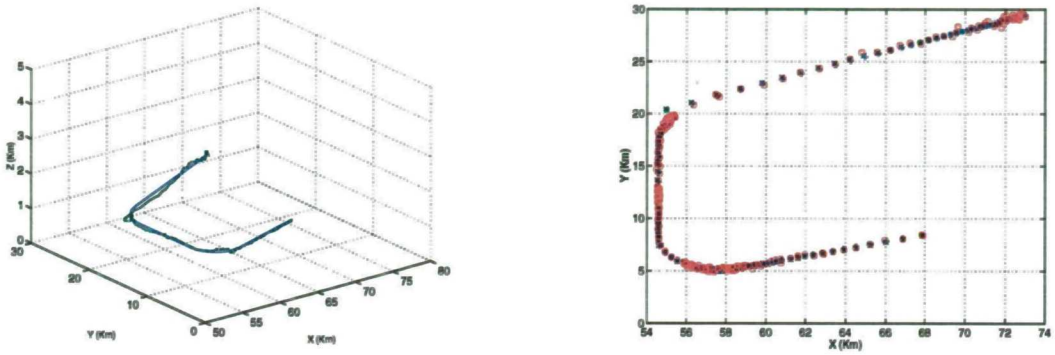

Figure 6-24(a,b) 3 dimensional and 2 dimensional plot of Benchmark Trajectory 1, showing position truth (blue crosses), position measured (red circles), and smoothed filter output (green plus signs)

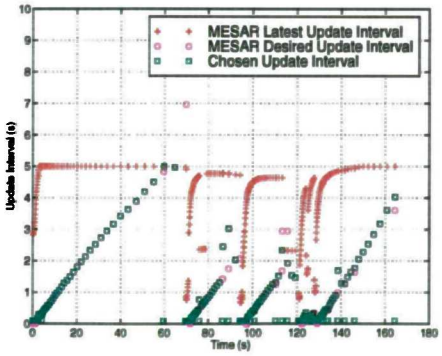

Figure 6-25(a,b) Track update interval used for tracking of Benchmark Trajectory 1

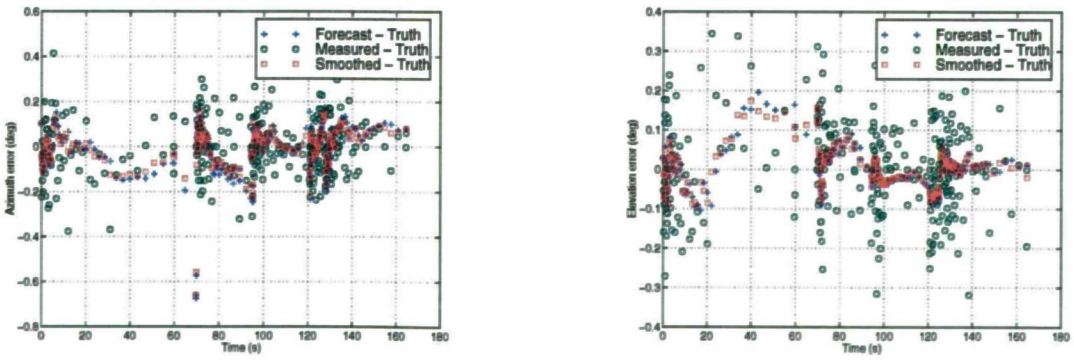

Figure 6-26(a,b) X and Z coordinate (azimuth and elevation) position and velocity errors for Benchmark Trajectory 3

6.4.5 Adaptive transmitted waveform energy

The modelling of MESAR's adaptive transmitted waveform energy is performed in a simplistic fashion. A nominal waveform of 1ms is assumed to give a signal to noise ratio of 18dB. This waveform length is then increased or decreased in proportion, assuming perfect coherent integration, to achieve the desired signal to noise ratio. Each time a track update is made, this waveform length is added to the total radar time that has been used to track the target. The waveform length is adjusted on a continuous scale, and takes no account of the actual PRF of the waveform, or whether it was some kind of Doppler burst which would inevitably quantise the units in which the waveform may be adjusted.

6.4.6 Missed detections and declaration of lost track

If a track update failed to detect the target, updates are scheduled at the minimum update interval, 0.1s, until the target is re-detected. The same energy is used in the transmitted waveform as for the previous update.

If the target is not re-detected within 20 updates then the target is declared lost. No data from such a target will be included in the Monte Carlo results, except the fact that the target was lost.

6.4.7 Development of a multiple beam track update strategy

A strategy devised for multiple beam track updates, to allow robust tracking of manoeuvring targets, is described below.

In the instance that the target has not been detected for a set interval of time, multiple sequential beams are searched at each track update rather than a single beam. The period of time after which this occurs is based upon the latest update interval calculated within the MESAR tracker, described in section 6.3.1.

The latest update time gives the period after which a target which *starts* executing a manoeuvre of the maximum assumed strength will be outside of the radar 3dB beamwidth. In the event that multiple missed detections occur, it is assumed that the start of the manoeuvre is not detected, and thus the target could manoeuvre out of the radar beamwidth in a smaller interval than the latest update interval. Thus, if the target has not been detected for more than half of the latest update interval, a multiple beam

update is triggered.

The use of multiple beam track updates is shown in Figure 6-27. Initially, a four beam cluster is searched around the predicted target position. Each of the beams is searched in turn, until either the target has been detected, or all of the four beams have been searched. The four beam cluster is continually used until the target is re-detected. Also, the latest update interval is recalculated using an *effective beamwidth* of double the radar beamwidth originally used in the calculation. If the target remains undetected for longer than this second latest update interval, then the use of a seven beam cluster is initiated. . Similarly the latest update time is again recalculated using an effective beamwidth of three times the original value, and if the target remains undetected still, then the tracker activates the use of a 19 beam cluster for track updates.

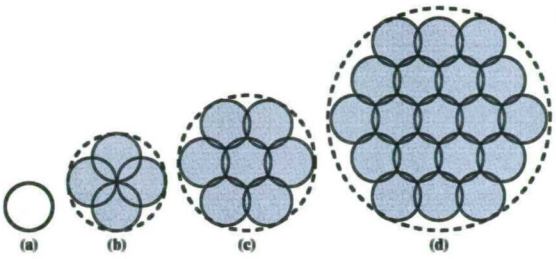

UPDATE TYPE	WHEN USED
Single Beam	$t < \frac{1}{2} t_{latest}$; $bw_{effective} = bw_{3dB}$
4 Beam	$t > \frac{1}{2} t_{latest}$; $bw_{effective} = bw_{3dB}$
7 Beam	$t > \frac{1}{2} t_{latest}$; $bw_{effective} = 2\ bw_{3dB}$
19 Beam	$t > \frac{1}{2} t_{latest}$; $bw_{effective} = 3\ bw_{3dB}$

Figure 6-27(a,b,c,d) Beam update strategies, and their periods of use

Figure 6-28 and Figure 6-29, below, show results from using the multiple beam update tracking strategy.

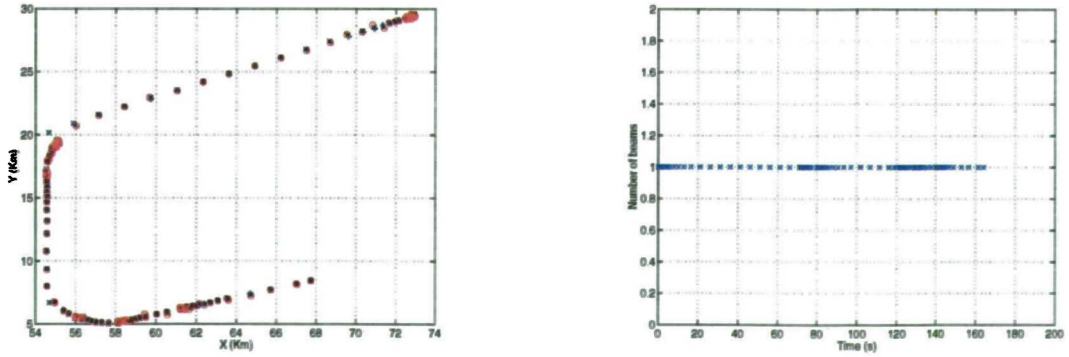

Figure 6-28(a,b) Multiple beam update tracking of Benchmark target trajectory 1 using a signal to noise ratio of 25dB and a desired accuracy of 1/40th of a beamwidth. (a) Plan view of track showing position truth (blue crosses), position measured (red circles), and smoothed filter output (green plus signs), (b) Number of beams as a function of time

Figure 6-28 shows the situation for a signal to noise ratio of 25dB, and a desired track accuracy of $1/40^{th}$ of a beamwidth. In this instance, with the 2.5° beamwidth used, multiple beam updates were at no point requested. However, in Figure 6-29, where the

signal to noise ratio has been reduced to just 12dB, and the desired accuracy reduced to $1/20^{th}$ of a beamwidth their use is clear. (Note that the target would certainly have been lost in this instance if multiple beam updates had not been used).

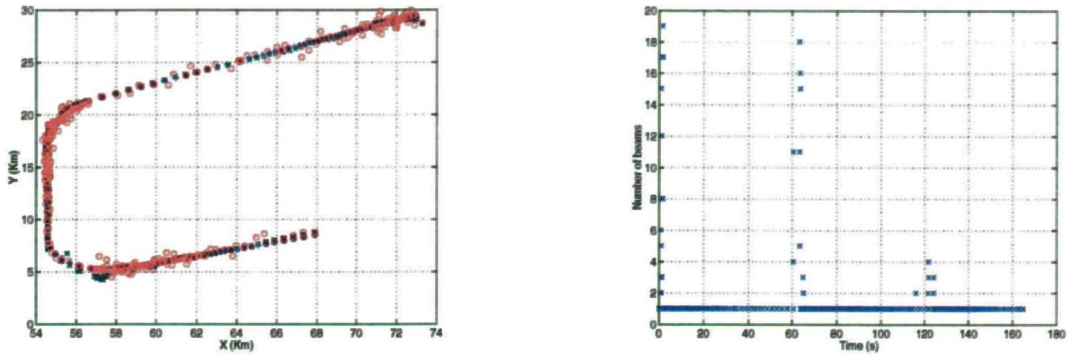

Figure 6-29(a,b) Multiple beam update tracking of Benchmark target trajectory 1 using a signal to noise ratio of 12dB and a desired accuracy of $1/20^{th}$ of a beamwidth. (a) Plan view of track showing position truth (blue crosses), position measured (red circles), and smoothed filter output (green plus signs), (b) Number of beams as a function of time

6.4.8 Development of a rotating array track update strategy

No literature has been found on adaptive update rate tracking for a rotating array multi-function radar. It is thought that the majority of current systems simply use a fixed update interval, related to the rotation period of the array.

This strategy could have been adopted here, however such a system suffers a poor efficiency in terms of radar time. Therefore, the adaptive track update strategy used in the MESAR static array system has been adapted for use with a rotating array. This also enables a comparison to be made between the performance and efficiency of a static array and rotating array system, based upon similar tracking strategies.

The desired and latest update intervals are calculated in the same manner, and are then adjusted to cope with the additional constraints imposed by the rotating array/s. The strategy adopted updates tracks on array azimuth broadside wherever possible to ensure that maximum efficiency and accuracy is attained in the majority of track updates. Track update intervals are shortened in most cases to ensure the desired update and latest update intervals are always met. This results in a slightly higher average update rate in the rotating array tracker to that in the static array. This in turn may result in a higher total radar time required for target tracking, although this is offset by the lower average track waveform dwell times that are required, since the majority of updates are made on array azimuth broadside and do not require extra integration gain.

Once in a situation of a stable track, update intervals will extend over one or more sweeps of the array faces past the target direction. In this situation the update interval may be shortened so that it occurs at the closest passing of array azimuth broadside. This is shown in Figure 6-30, which plots the track update directions relative to the array coverage.

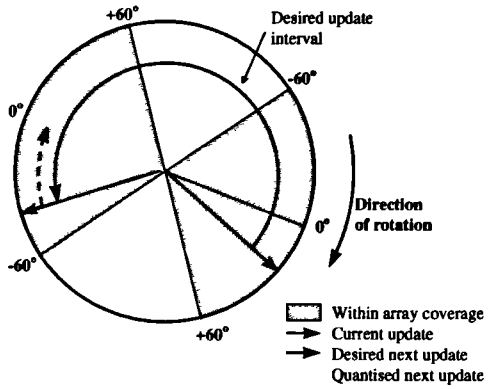

Figure 6-30 Quantisation of track update directions to array azimuth broadside, shown for a twin faced array multi-function radar

Figure 6-31 shows the different conditions of track update interval which require different action to be taken. An explanation of these different conditions and the actions arising from them is given below.

If the current track update has been made ahead of array azimuth broadside, then there are just two conditions for the calculation of the next update interval. These are shown in Figure 6-31(a).

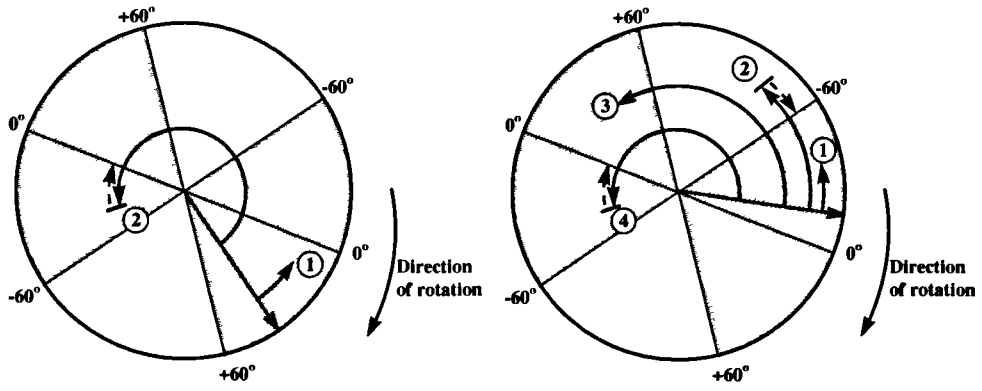

Figure 6-31(a,b) Different conditions for the quantisation of track updates, shown for a twin faced array multi-function radar. (a) Conditions for a current track update ahead of array azimuth broadside, (b) Conditions for a current track update behind of array azimuth broadside

In the first condition, the interval to the next track update is less than the time before the track direction crosses array azimuth broadside. In this instance, the desired update

interval remains unchanged to ensure the track accuracy is met, or to ensure the target remains within the radar beam. In the second condition, the desired update interval is long enough for the track direction to pass in front of the array azimuth broadside direction. In this case the update interval is shortened by the smallest amount that ensures the track update occurs on array azimuth broadside. Both conditions ensure that the next track update will occur within the array coverage limits.

Figure 6-31(b) shows the different conditions that arise if the current track update was made behind of array azimuth broadside. In this case there are four different conditions requiring different forms of action. If the next update is within the same array coverage as the current update, condition 1, then the update interval remains unchanged. If however the next track update falls outside of this array coverage, as in condition 2, then the update interval is shortened so that the next update is made 60° behind azimuth array broadside. This shortening gives rise to the possibility that the resultant track update interval will be less than the minimum allowed, assumed to be 0.1s here. Then, the next track update interval has to be extended to allow the blind arc to pass, and the update will be made at 60° ahead of array azimuth broadside. If this occurs then the desired track update interval is not met.

Condition 3 shows an update interval that is long enough to have exceeded the period of time in which the track direction falls within the blind arc, but still not long enough for the track to have passed in front of array azimuth broadside. In this instance, the track update interval again remains unchanged.

Finally, condition 4 shows the case of update intervals long enough for the track direction to have passed in front of array azimuth broadside. Again, in this instance, the track update interval is quantised down to allow the update to be made on azimuth array broadside.

The results from the rotating array adaptive update strategy are shown in Figure 6-32 - Figure 6-34 below. These are for a $1/40^{th}$ of a beamwidth desired track accuracy with a beamwidth of 2.5°, and for a signal to noise ratio of 20dB. The case of a multi-function radar with a twin faced array rotating with a period of 2s has been chosen.

Figure 6-32(b) shows the desired, latest and chosen update intervals for the rotating array update strategy. The quantisation of the update interval is clear. In periods of

constant velocity flight the update rate can be seen to be quantised to the interval between array azimuth broadside crossing the track direction (1s). This is clearer still in Figure 6-33, which shows the azimuth angle of the track updates away from array broadside. In periods of constant velocity flight the track updates are almost always made very close to 0°, resulting in the maximum azimuth plot accuracy and minimum possible scanning losses.

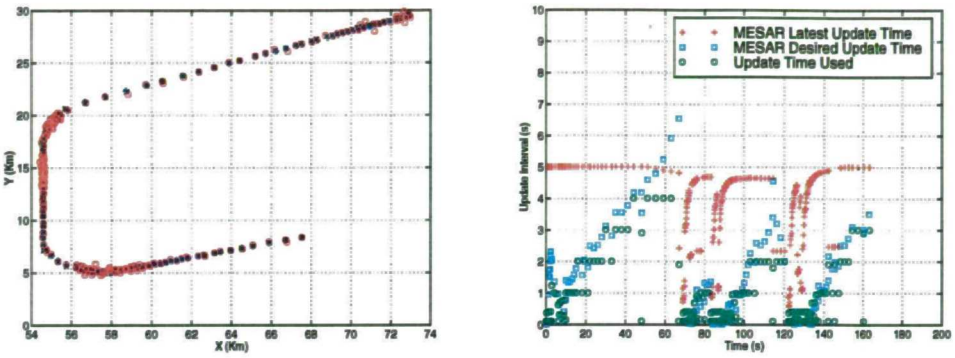

Figure 6-32(a,b) Rotating array update strategy tracking of Benchmark target trajectory 1 using a signal to noise ratio of 25dB and a desired accuracy of 1/40th of a beamwidth. (a) Plan view of track showing position truth (blue crosses), position measured (red circles), and smoothed filter output (green plus signs), (b) Track update interval as a function of time

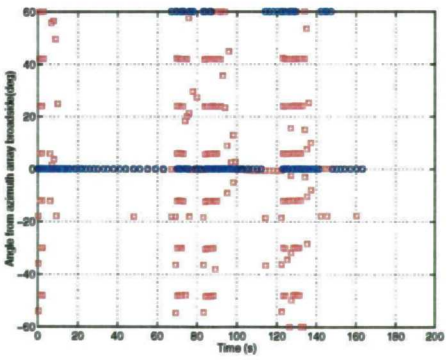

Figure 6-33 Angle of track updates away from array azimuth broadside for the rotating array update strategy (red squares). Overlaid is the manoeuvre flag (blue circles), showing where the tracker perceived a manoeuvre

Also shown on Figure 6-33 is the manoeuvre flag of the tracker. In periods of manoeuvre when the desired update interval becomes small, track updates are forced to be made away from azimuth broadside. This is also visible during track initiation for the first few seconds of the track life.

Figure 6-34 shows the track accuracy that was achieved against benchmark target trajectory 1. The adaptive update rate rotating tracker was successful in achieving an accuracy in excess of that desired, excluding periods of manoeuvre.

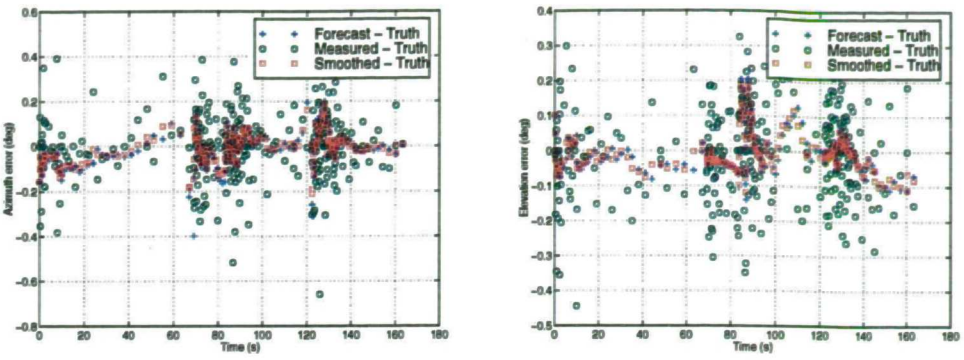

Figure 6-34(a,b) X and Z coordinate (azimuth and elevation) position and velocity errors for Benchmark Trajectory 1 using the rotating array track update strategy

6.4.9 Validation and testing of the adaptive tracking system simulation model

For the purposes of parameter optimisation the models were to be used over a very wide range of parameters. It was essential to ensure that the tracker performed sufficiently well over the parameter range for successful conclusions to be drawn. In practice, this became an iterative process, and improvements to the tracking algorithms were made when inconsistencies arose. These are outlined below.

The modifications that were made to the initial model are listed below;

i. *Manoeuvre response;* it was found that the response to a manoeuvre was often not large enough; i.e. the uncertainty terms in the covariance matrix terms were not increased enough to ensure the filter gave much greater weight to the target position measurements. This was due to a very short update interval being used at the point of manoeuvre detection. In some circumstances, particularly when using a narrow beam, this was significant enough to cause track loss. The solution was to use the maximum of either the last update interval, or the average of all of the update intervals in the track life, in the manoeuvre response calculation.

ii. *Termination of a manoeuvre declaration;* it was found that the flagging of manoeuvres was often turned off prematurely. The solution was to enforce a strategy for termination of manoeuvre similar to that of declaration. Two consecutive updates were required with residuals below a threshold for the manoeuvre declaration to be terminated.

iii. *Calculation of the latest update time;* it was found that at very high signal to noise ratios, and with narrow beamwidths, targets were lost unexpectedly

during a manoeuvre. This was due to the fact that in these circumstances, the target would be tracked throughout the manoeuvre using the latest update time, instead of the desired update time (because the tracking accuracy requirements were met purely by the plot accuracy). However, the latest update time is calculated assuming a manoeuvre has only just begun, and was too long to retain the target in the beam if the manoeuvre had been underway for some time.

iv. *Calculation of the desired update time;* it was found that at very low signal to noise ratios, the desired track accuracy was not being successfully met. This was due to several missed detections in a row causing the desired update time to be exceeded. The solution was to scale down the desired update interval by a factor proportional to the target probability of detection.

This process was considered valuable, and ultimately, resulted in a robust tracker capable of performing over a wide range of signal to noise ratios, desired accuracies and radar beamwidths. It is thought a worthwhile process for any such system, since it is generally unknown in advance what parameter range the system will be operating in, and how that will change. For example, at the point of target detection, the tracker may be operating with a very low signal to noise ratio. Conversely there may be times where the signal to noise ratio is high, for example if the target approaches close in range. Also, the desired accuracy on the target may change, depending on whether it is a target of genuine interest or not.

6.5 Results

6.5.1 A summary of the results collected

Since the tracking systems proved to have a complicated performance with the variation of the parameters, it was decided to perform the Monte Carlo simulations over all of the parameters, rather than a select few. This would ensure that any anomalies in the tracker performance against each of the bench mark targets with a given parameter set were observed. Also, it would allow any deviation in the optimal signal to noise ratio or desired track accuracy to be observed.

Table 6-2 shows the variation in the parameters that were performed. A total of 10 different signal to noise ratios and 20 different desired smoothed track accuracies were calculated for each data set; averaged results from tracking 25 targets were used at each data point. This was performed for each of 7 target trajectories (the 6 benchmark trajectories, and 1 constant velocity test target), and for each of the 4 different radar beamwidths. Since this was repeated for each of the final total of 10 different static and rotating adaptive tracker configurations the total number of targets tracked in the data set was 1.4 million.

Parameter	Minimum	Maximum	Step
Signal to Noise Ratio	12 dB	30 dB	2 dB
Desired Smoothed Track Accuracy (Fraction of a beamwidth - 1/N BW)	N = 2	N = 40	N = 2
Radar Beamwidth	0.5°	3.5°	1°
Target Trajectory Number	1	7	1

Table 6-2 Variation in parameters for the Monte Carlo simulations

A total of 10 different tracker configurations were examined, shown in Table 6-3. The majority of these were for the different configurations of arrays for a rotating multi-function radar system. The most likely candidates for a system performing air defence were considered, namely either a single or double faced system with a rotation period of either 1 or 2 seconds.

Antenna Configuration			
Static/Rotating	**Number of Faces**	**Rotation Period**	**Single/ Multiple Beam Updates**
Static	-	-	Single
Static	-	-	Multiple
Rotating	1	1 s	Single
Rotating	1	1 s	Multiple
Rotating	1	2 s	Single
Rotating	1	2 s	Multiple
Rotating	2	1 s	Single
Rotating	2	1 s	Multiple
Rotating	2	2 s	Single
Rotating	2	2 s	Multiple

Table 6-3 Antenna configurations considered for the Monte Carlo simulations

Clearly, it is not possible, or worthwhile, to display all of the results of such an analysis in this thesis. Therefore it has been decided to present the results for benchmark target 6 only here. This proved to be one of the most stressful cases, containing strong angular manoeuvres in both azimuth and elevation (up to 7g), and also longitudinal manoeuvres (up to 1g). The track filtering performance against other targets was generally superior to the results obtained against this target, unless otherwise stated.

A complete set of results against all 7 target trajectories is given for the cases of the static array multiple beam update system, and the rotating array multiple beam update system. These are contained in Appendices B and C respectively. Results for the other rotating array configurations considered are given for benchmark target trajectory 6 only, for comparison. These are also contained in Appendix C.

6.5.2 Single beam static array multi-function radar tracker

The first results obtained were for a static array multi-function radar using a single beam for each update. This tracker is equivalent to that currently implemented in the MESAR system. A relatively broad radar beamwidth of 2.5° was used, representative of that used or envisaged for current multi-function radar systems. The track update rate was limited to between 0.1s and 5s. The target signal to noise ratio was varied from 12dB up to a maximum 30dB, and the desired smoothed tracking accuracy was varied from ½ a beamwidth to $1/40^{th}$ of a beamwidth.

Figure 6-35 - Figure 6-37 show the variation of the significant outputs of the Monte Carlo analysis; the total radar time required to maintain the track, the percentage of successful tracks, the average track update interval used, and the smoothed tracking accuracy that was achieved. Each data point on the graphs, here as throughout this chapter, has been calculated by taking an average of the results of tracking 25 successive targets.

Figure 6-35 shows clearly that there are large savings to be made by reducing the signal to noise ratio at which tracking is performed from that used in MESAR (26dB-29dB). However, this may only be safely undertaken if the robustness of the tracker is not decreased (i.e. the chance of losing a track), and the smoothed track accuracy requirements are met.

These two parameters are shown in Figure 6-35(b) and Figure 6-36(b). Although the smoothed tracking accuracy is met at low signal to noise ratios (the most stressing case of $1/40^{th}$ of a beamwidth is met above a signal to noise ratio of around 15dB), the track robustness decreases at low signal to noise ratios. This reflects the difficulty in tracking highly manoeuvrable targets with a single pencil beam.

Figure 6-35 also shows that there are savings to be made from using a low desired track accuracy wherever possible, though the savings made are less pronounced. In an air

defence application this parameter is likely to be set by the requirements of the weapons system for high priority targets, and thus will not be a variable parameter. However for low priority targets, that must be tracked, but are not of genuine interest to the system, it shows the savings that may be made.

These results show that not only is the inclusion of multiple beam track updating important from the aspect of maintaining track on highly manoeuvrable targets, but it is essential to enable target tracking to be efficient in its use of the multi-function radar time resources. If multiple beam track updates were utilised to increase the track robustness, it would be safe to use a considerably lower signal to noise ratio than that used currently in the MESAR system. A conservative reduction is suggested, down to a figure of 20dB. This is considerably higher than the minimum signal to noise ratio required to meet even the most stringent tracking accuracy requirement, but is low enough that the majority of the saving in radar time-budget is met.

Figure 6-37 shows the potential savings in radar time that could be made for this track trajectory as a function of the desired smoothed track accuracy. It shows the percentage of the radar time required if tracking were performed at 20dB instead of the upper value of the MESAR tracker of 29dB. If only a poor desired tracking accuracy is required, (the case for the majority of low priority targets), then less than 20% of the radar time is needed. This would effectively allow the multi-function radar to track as many as 5 times the number of such targets as it currently does. The saving that is made decreases with increasing tracking accuracy requirement, to a value of around 40% of that when tracking with a 29dB signal to noise ratio, for the most accurate tracking accuracy requirement of $1/40^{th}$ of a beamwidth.

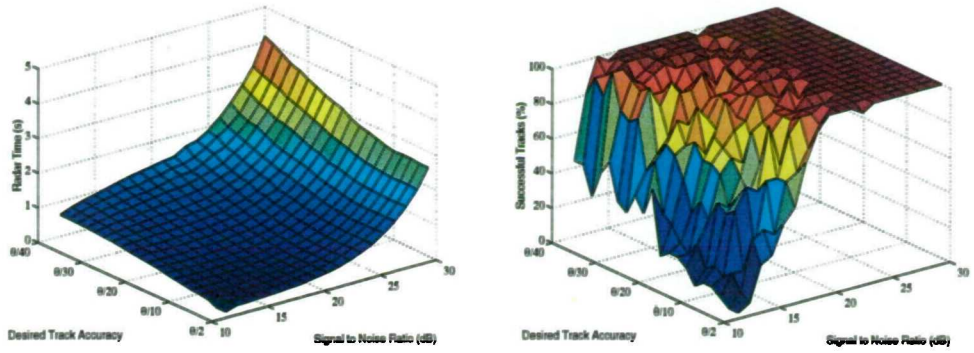

Figure 6-35(a,b) Total radar time required to maintain track on Benchmark target trajectory 6, and (b) the percentage of successful tracks, with a beamwidth of 2.5°

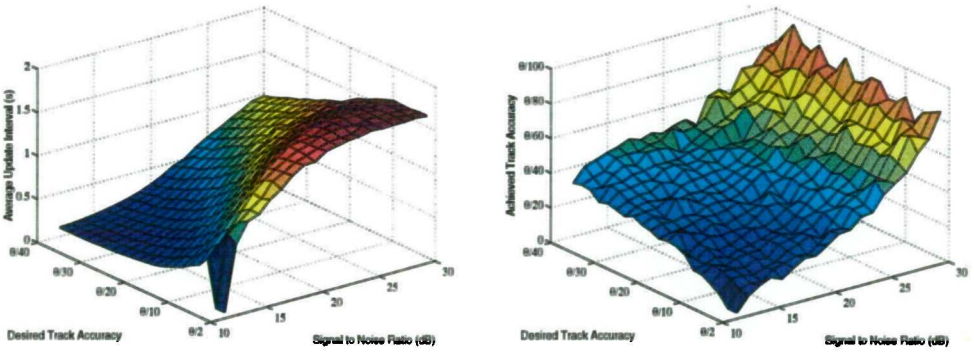

Figure 6-36(a,b) Average track update interval required to maintain track on Benchmark target trajectory 6, (b) Achieved smoothed track accuracy for Benchmark target trajectory 6, excluding periods of manoeuvre, with a beamwidth of 2.5°

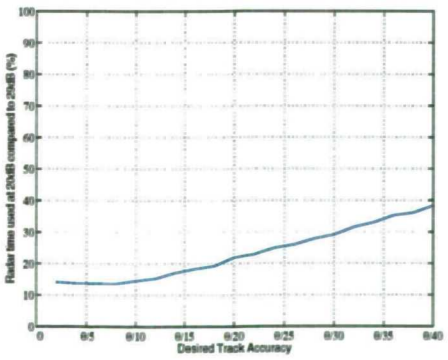

Figure 6-37 Percentage of radar time required for tracking Benchmark target trajectory 6 using only a 20dB signal to noise ratio instead of a 29dB signal to noise ratio, with a beamwidth of 2.5°

Figure 6-38 - Figure 6-40 show the results from the same situation as above with the exception that a radar beamwidth of 0.5° instead of 2.5° has been used. The results show the increased difficulty in maintaining track on a manoeuvring target with a narrower beamwidth. Only at the very highest signal to noise ratios considered here is robust target tracking achieved, i.e. successful tracking throughout the target trajectory life of close to 100% of the targets. This effectively limits this single beam tracking strategy to these high signal to noise ratio values, and thus high uses of the multi-function radar time resources.

The variation of radar time with signal to noise ratio and desired track accuracy is similar to that of the 2.5° case, the decrease in beamwidth increasing the radar time required for maintaining track. Thus these results show even more vividly the need for multiple beam updating for the purposes of robust and efficient tracking. The potential savings from tracking at a signal to noise ratio of 20dB instead of 29dB, shown in Figure 6-40, are seen to be slightly greater than for the 2.5° system. A value of around 30% of that when tracking with a 29dB signal to noise ratio, for the most accurate tracking accuracy requirement of $1/40^{th}$ of a beamwidth is seen.

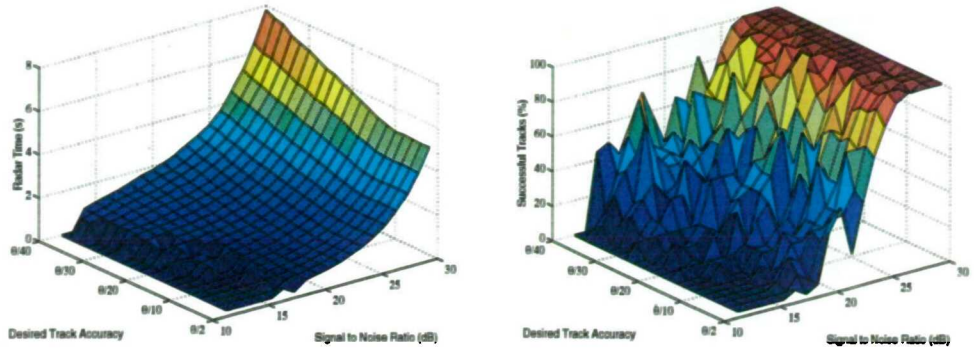

Figure 6-38(a,b) Total radar time required to maintain track on Benchmark target trajectory 6, and (b) the percentage of successful tracks, with a beamwidth of 0.5°

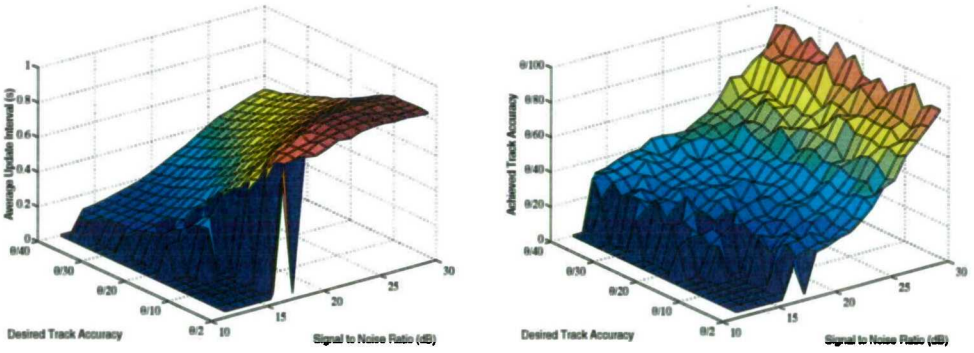

Figure 6-39(a,b) Average track update interval required to maintain track on Benchmark target trajectory 6, (b) Achieved smoothed track accuracy for Benchmark target trajectory 6, excluding periods of manoeuvre, with a beamwidth of 0.5°

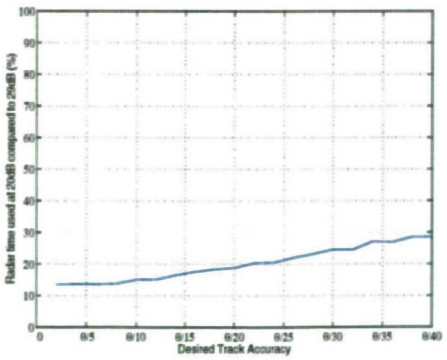

Figure 6-40 Percentage of radar time required for tracking Benchmark target trajectory 6 using only a 20dB signal to noise ratio instead of a 29dB signal to noise ratio, with a beamwidth of 0.5°

Figure 6-41, below, compares the radar time required to maintain track on benchmark

target trajectory 6 for the 2.5° and 0.5° single beam track update cases. The increase in radar time that is needed to maintain track on the manoeuvring target varies with both signal to noise ratio and desired accuracy, and at worst it is seen that the radar time required to track with the narrower beamwidth doubles.

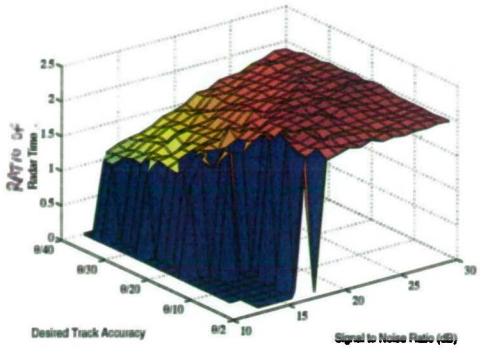

Figure 6-41 Ratio of radar time required to track Benchmark trajectory 6 with a 0.5° beamwidth to that with a 2.5° beamwidth, for a system employing single beam track updates

Figure 6-42 then takes the case of a target tracking signal to noise ratio of 20dB and a desired tracking accuracy of 1/40th of a beamwidth. These values are chosen because they represent a case of both efficient and accurate tracking of a target. They show the variation in the radar time required to track benchmark target 6 and the percentage of successful tracks as a function of radar beamwidth. Although the increase in radar time required to track the target at a lower beamwidth does not increase dramatically over the ranges considered, (comparing a 2.5° beamwidth to a 0.5° beamwidth system gives roughly a 40% increase in radar time), the track robustness does decrease. This would prohibit considering narrower beamwidths for weapons system applications where track robustness is required to be close to 100%.

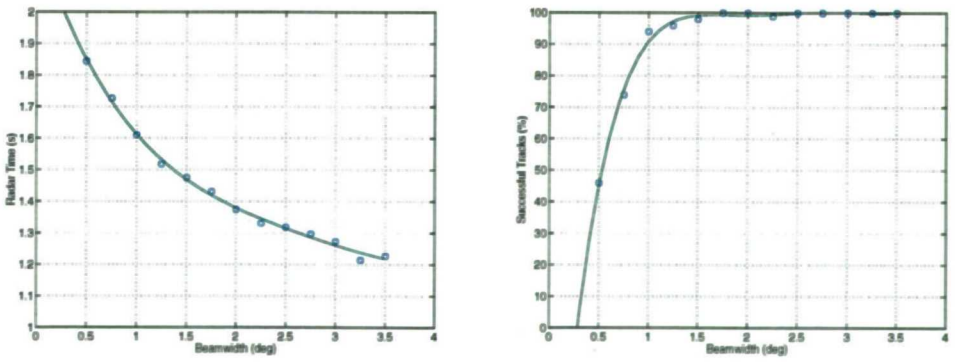

Figure 6-42(a,b) Total radar time required to track Benchmark target trajectory 6, and (b) Percentage of successful tracks, as a function of radar beamwidth

6.5.3 Multiple beam static array multi-function radar tracker

The results from the previous section show that to enable efficient as well as robust target tracking of a manoeuvring target, multiple beam updates must be employed. Results from the same example cases as in the previous section of a 2.5° and 0.5° beamwidth system are presented below.

Figure 6-43 - Figure 6-48 show the results for the 2.5° and 0.5° multiple beam update systems (adhering to the multiple beam update strategy developed in section 6.4.7). The format of the Monte Carlo results presented is the same as in the previous section, although in this case the average number beams that were required over the track life is also presented (Figure 6-44(b) and Figure 6-47(b)).

Again we see a similar variation in the total radar time required to maintain track on benchmark target trajectory 6 as in the single beam cases of section 6.5.2. However we see a considerable increase in the track robustness, illustrated by the increase in the percentage of targets tracked (particularly in the 0.5° case). The use of multiple beam updates allows a lower signal to noise ratio to be used for tracking whilst still retaining the desired track robustness and tracking accuracy requirement.

The average number of beams required for each track update is seen to be very close to one over large ranges of signal to noise ratios and desired track accuracies. This shows that it was only very occasionally necessary to employ multiple beam updates in most cases. The exception to this occurs when the desired track accuracy approaches the half beamwidth limit, and the signal to noise ratio used for tracking is low. In the worst case over three beams were required on average per update, causing a threefold increase in radar time.

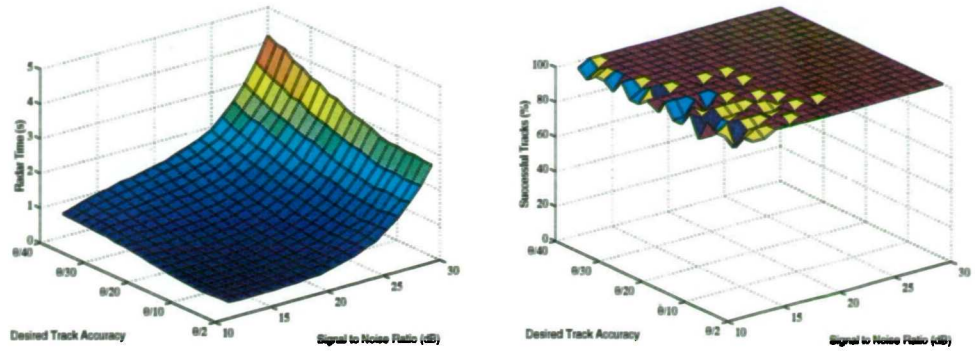

Figure 6-43(a,b) Total radar time required to maintain track on Benchmark target trajectory 6, and (b) the percentage of successful tracks, with a beamwidth of 2.5°

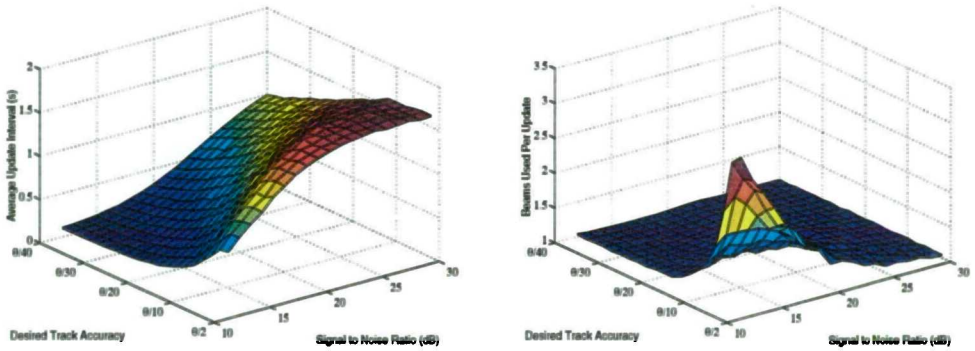

Figure 6-44(a,b) Average track update interval required to maintain track on Benchmark target trajectory 6, (b) Average number of beams required for each track update, with a beamwidth of 2.5°

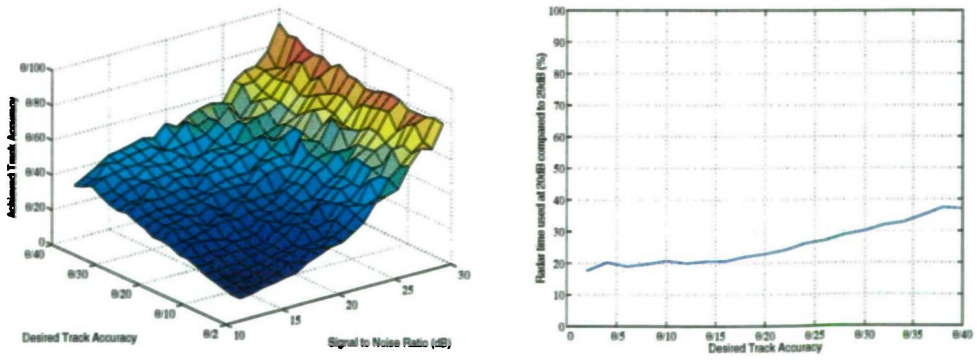

Figure 6-45(a,b) Achieved smoothed track accuracy for Benchmark target trajectory 6, excluding periods of manoeuvre, and (b) Percentage of radar time required for tracking Benchmark target trajectory 6 using only a 20dB signal to noise ratio instead of a 29dB signal to noise ratio, with a beamwidth of 2.5°

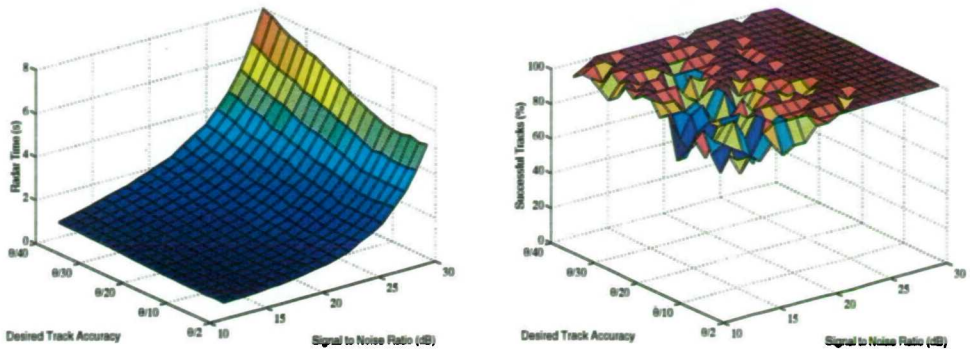

Figure 6-46(a,b) Total radar time required to maintain track on Benchmark target trajectory 6, and (b) the percentage of successful tracks, with a beamwidth of 0.5°

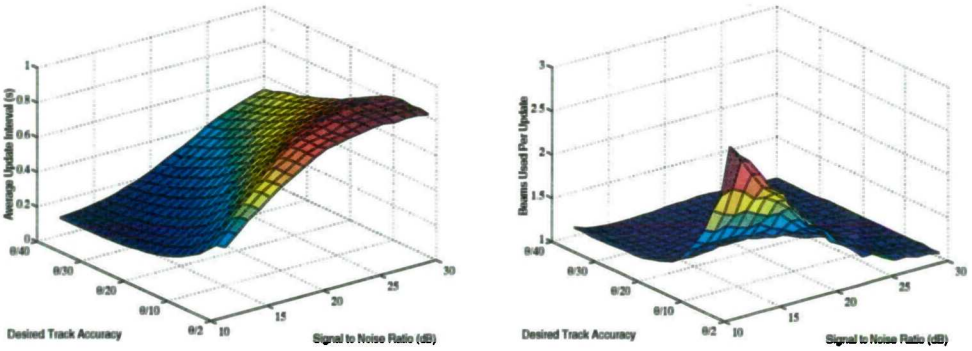

Figure 6-47(a,b) Average track update interval required to maintain track on Benchmark target trajectory 6, (b) Average number of beams required for each track update, with a beamwidth of 0.5°

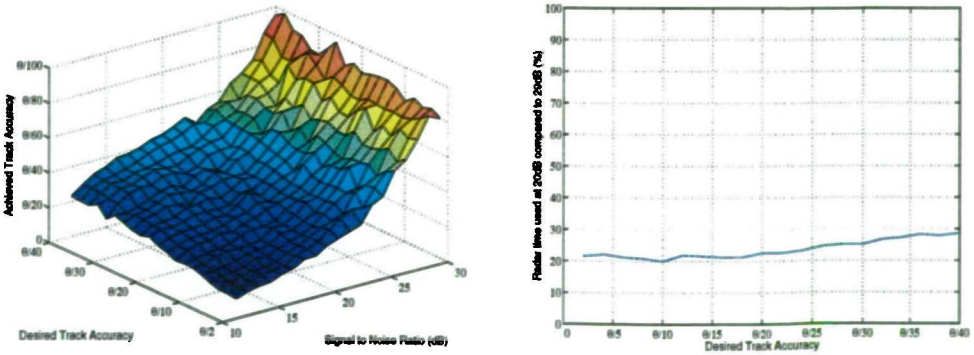

Figure 6-48(a,b) Achieved smoothed track accuracy for Benchmark target trajectory 6, excluding periods of manoeuvre, and (b) Percentage of radar time required for tracking Benchmark target trajectory 6 using only a 20dB signal to noise ratio instead of a 29dB signal to noise ratio, with a beamwidth of 0.5°

Figure 6-49, below, shows the ratio of radar time required for multiple beam update tracking at 0.5° to that at 2.5°. It shows an extremely similar result to that in Figure 6-41, showing roughly a doubling of radar time is required to track the same target with the narrower beamwidth. Figure 6-50 then takes the case of a 20dB signal to noise ratio and 1/40th of a beamwidth desired tracking accuracy, and shows the variation in radar time and successful tracks as a function of radar beamwidth.

Figure 6-51 compares the radar time required for tracking benchmark target trajectory 6 using the multiple beam system to that required for the single beam system, for the same values of signal to noise ratio and desired track accuracy as above. A very small difference is seen between using multiple beam track updates and single beam track updates. In the case of the smallest beamwidth considered, a difference of less than 10% was observed.

These results show that accurate tracking of manoeuvring targets is most efficiently performed at a lower signal to noise ratio than that used in the MESAR system currently. The use of multiple beam updates in the tracker provides track robustness at a small cost in terms of radar time. For a 2.5° beamwidth, the multiple beam tracker operating at a signal to noise ratio of 20dB and a desired accuracy of 1/40th of a beamwidth requires just 38.9% of the radar time of the single beam tracker operating at a 29dB signal to noise ratio, representative of the MESAR system. It suffers no degradation in track robustness. For the 0.5° system the saving in radar time increases, the multiple beam system requiring just 29.5% of the radar time of the higher signal to noise ratio, single beam system.

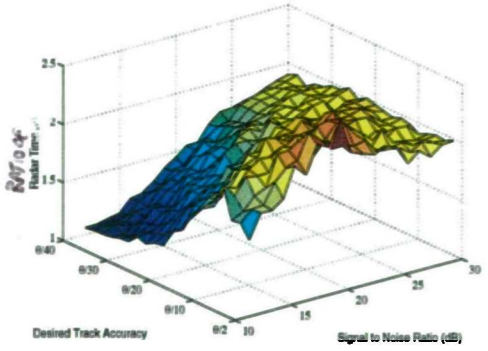

Figure 6-49 Ratio of radar time required to track Benchmark trajectory 6 with a 0.5° beamwidth to that with a 2.5° beamwidth, for a system employing multiple beam track updates

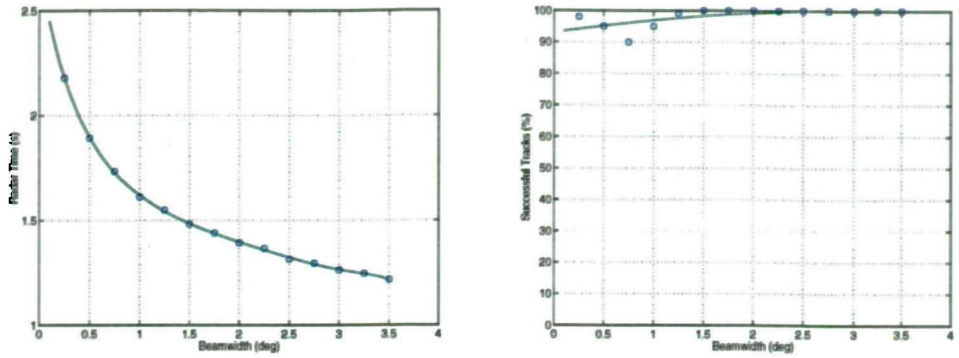

Figure 6-50(a,b) Total radar time required to track Benchmark target trajectory 6, and (b) Percentage of successful tracks, as a function of radar beamwidth, using multiple beam track updates

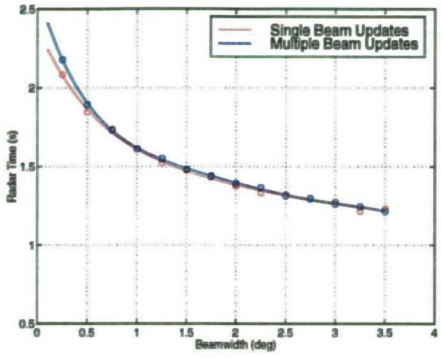

Figure 6-51 A comparison of the total radar time required to track Benchmark trajectory 6 with the static and multiple beam track update systems

6.5.4 Single beam rotating array multi-function radar tracker

The results for the two rotating array antenna configurations considered (single array system rotating with a period of 1s, and a twin faced array system rotating with a period of 2s), are presented in the current and the following section. The results for the two other antenna configurations discussed in section 6.5.1 (single array system rotating with a period of 2s, and a twin faced array system rotating with a period of 1s), are contained in Appendix C.

Figure 6-52 - Figure 6-57 show the results for the antenna with a single array, rotating with a period of 1s, using single beam track updates. The radar time surfaces, shown in Figure 6-52 and Figure 6-55, show similar trends to the static array case, although the surface is not exactly the same shape, reflecting the difference in the track update intervals used. Importantly they still suggest that using a lower signal to noise ratio would be beneficial in terms of radar time.

The desired accuracy, shown in Figure 6-53(b) and Figure 6-56(b), in the most strenuous case of $1/40^{th}$ of a beamwidth, is not achieved at a signal to noise ratios as low as that in the static case. This is due to the limit in update rate imposed by the blind sectors in antenna coverage. The desired accuracy is met in all cases above a value of around 19dB. Therefore the value of around 20dB for tracking of targets suggested from the static array results would remain appropriate in this case, since the desired accuracy could still be met. Comparing the radar time that could be saved by reducing the signal to noise ratio from 29dB to 20dB, shown in Figure 6-54 and Figure 6-57, we see that the rotating system gives similar reductions to the static array system, of between around 15% to 30% (depending on the desired accuracy).

Although the results again confirm the need for multiple beam track updates, the track robustness, is in fact slightly increased above that in the static array case. This is due to the necessity to make track updates at large scan angles away from azimuth array broadside to support the desired update rate. This results in a broadening of the azimuth beamwidth during periods of manoeuvre, reducing the chance of failing to illuminate the target at the next update. At 60° from azimuth array broadside, the azimuth beamwidth has doubled in size.

It is important to note that the necessity to reduce the update interval, and hence increase the number of track updates that are made off of array azimuth broadside during periods of manoeuvre, has a significant effect on the total radar time required to track the target. The updates made away from array azimuth broadside not only have a broadened beamwidth, but also require a large increase in dwell time to recover the loss in gain. Thus, the total radar time required to track the target in the case of the rotating array tracker system is highly dependent on whether the target manoeuvres, and period of this manoeuvre.

Figure 6-58 - Figure 6-63 show the results for the twin faced system, rotating with a period of 2s. The results show only modest differences to the single array case. The track robustness is increased at very low signal to noise ratios, and the signal to noise ratio at which the most strenuous desired track accuracy of $1/40^{th}$ of a beamwidth is met is decreased to 16dB. This reflects the reduction in the value of T_{blind} between the two systems. Broadly, however, the performance is essentially the same as the static array system rotating twice as fast.

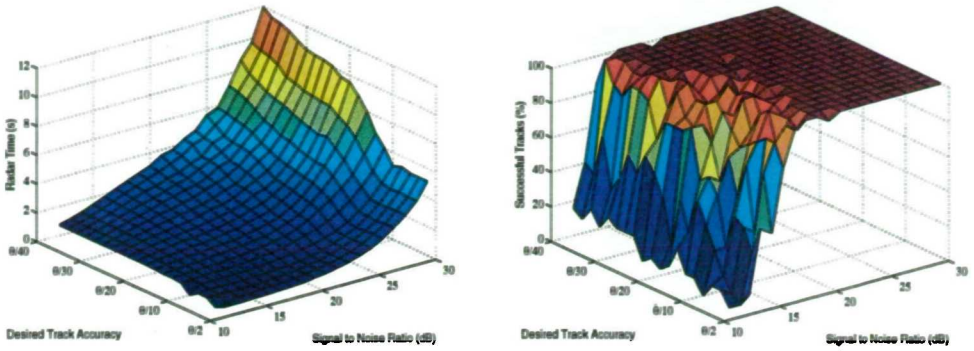

Figure 6-52(a,b) Total radar time required to maintain track on Benchmark target trajectory 6, and (b) the percentage of successful tracks. Single faced rotating system with a beamwidth of 2.5°

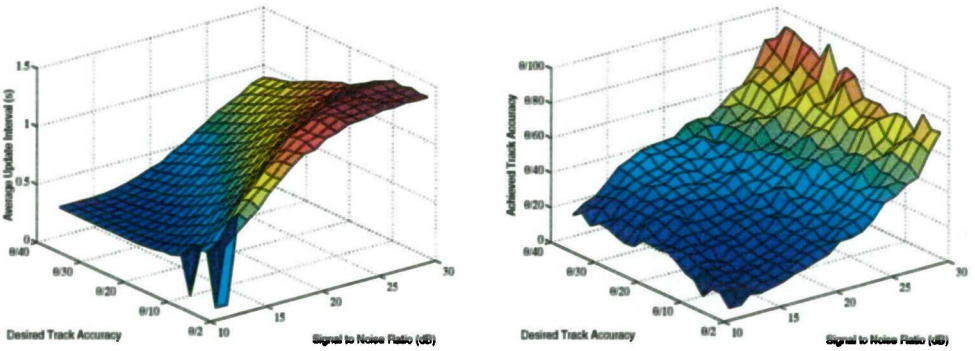

Figure 6-53(a,b) Average track update interval required to maintain track on Benchmark target trajectory 6, (b) Achieved smoothed track accuracy for Benchmark target trajectory 6, excluding periods of manoeuvre. Single faced rotating system with a beamwidth of 2.5°

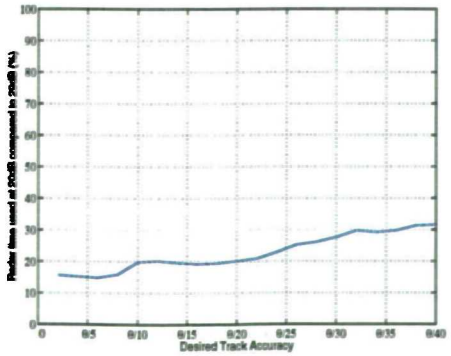

Figure 6-54 Percentage of radar time required for tracking Benchmark target trajectory 6 using only a 20dB signal to noise ratio instead of a 29dB signal to noise ratio. Single faced rotating system with a beamwidth of 2.5°

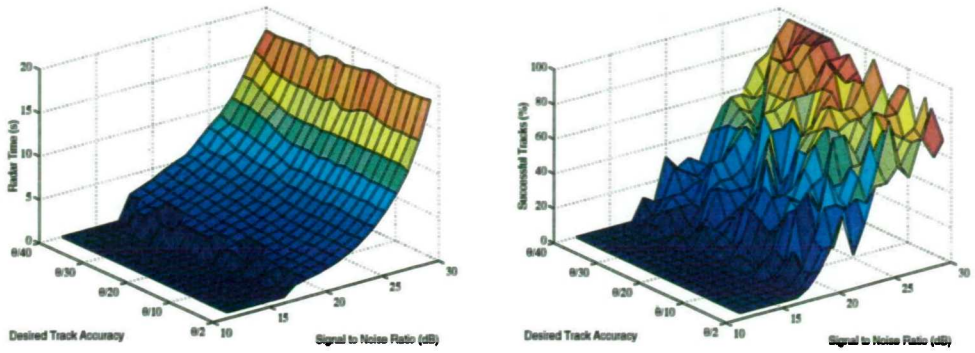

Figure 6-55(a,b) Total radar time required to maintain track on Benchmark target trajectory 6, and (b) the percentage of successful tracks. Single faced rotating system with a beamwidth of 0.5°

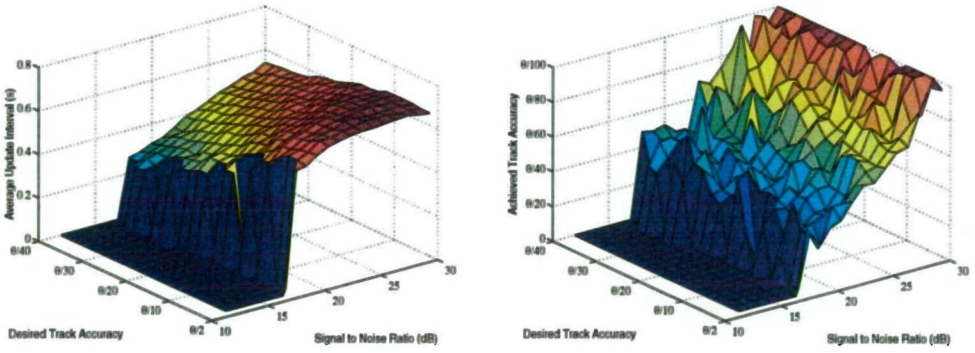

Figure 6-56(a,b) Average track update interval required to maintain track on Benchmark target trajectory 6, (b) Achieved smoothed track accuracy for Benchmark target trajectory 6, excluding periods of manoeuvre. Single faced rotating system with a beamwidth of 0.5°

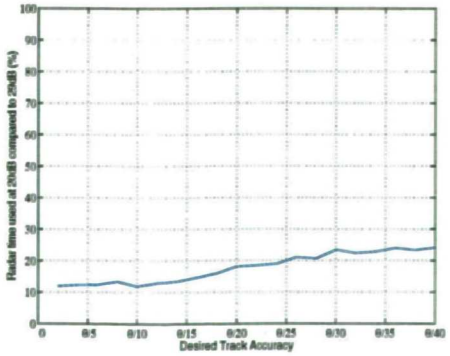

Figure 6-57 Percentage of radar time required for tracking Benchmark target trajectory 6 using only a 20dB signal to noise ratio instead of a 29dB signal to noise ratio. Single faced rotating system with a beamwidth of 0.5°

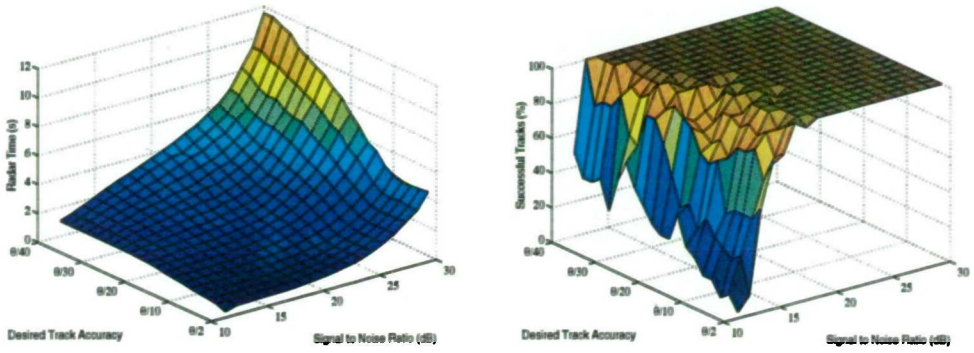

Figure 6-58(a,b) Total radar time required to maintain track on Benchmark target trajectory 6, and (b) the percentage of successful tracks. Twin faced rotating system with a beamwidth of 2.5°

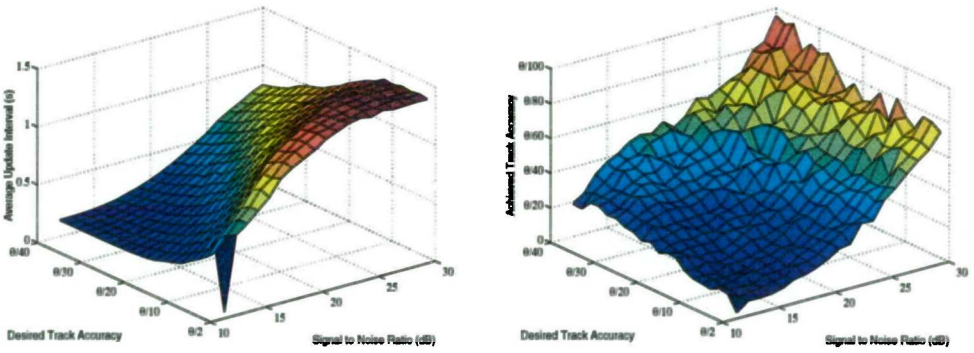

Figure 6-59(a,b) Average track update interval required to maintain track on Benchmark target trajectory 6, (b) Achieved smoothed track accuracy for Benchmark target trajectory 6, excluding periods of manoeuvre. Twin faced rotating system with a beamwidth of 2.5°

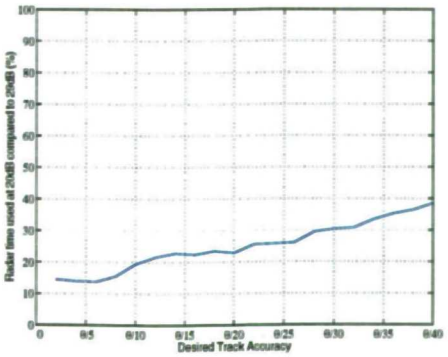

Figure 6-60 Percentage of radar time required for tracking Benchmark target trajectory 6 using only a 20dB signal to noise ratio instead of a 29dB signal to noise ratio. Twin faced rotating system with a beamwidth of 2.5°

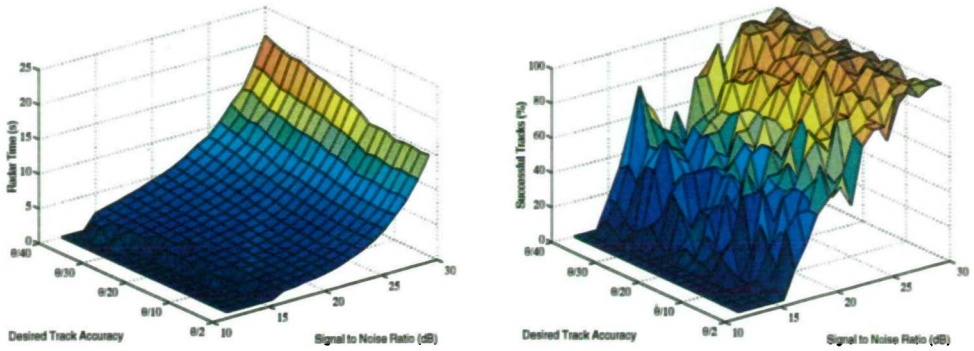

Figure 6-61(a,b) Total radar time required to maintain track on Benchmark target trajectory 6, and (b) the percentage of successful tracks. Twin faced rotating system with a beamwidth of 0.5°

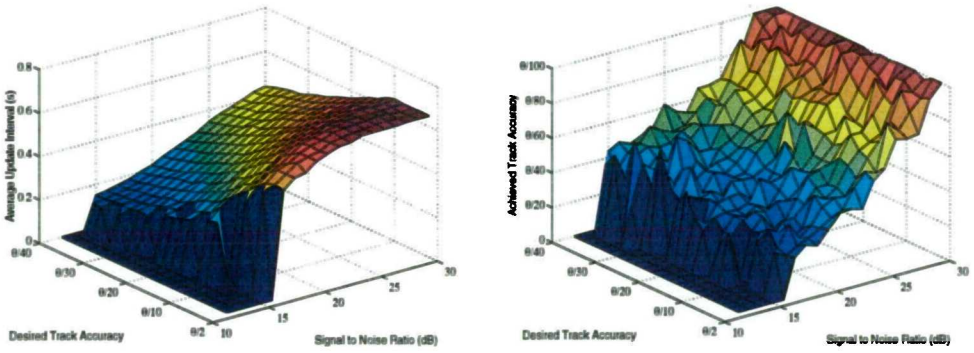

Figure 6-62(a,b) Average track update interval required to maintain track on Benchmark target trajectory 6, (b) Achieved smoothed track accuracy for Benchmark target trajectory 6, excluding periods of manoeuvre. Twin faced rotating system with a beamwidth of 0.5°

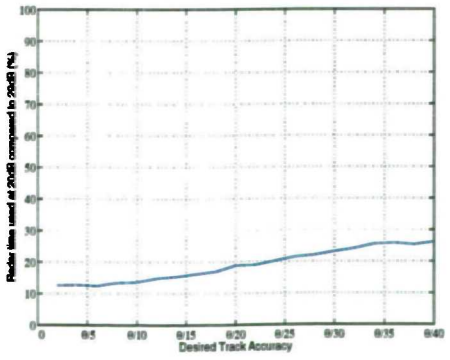

Figure 6-63 Percentage of radar time required for tracking Benchmark target trajectory 6 using only a 20dB signal to noise ratio instead of a 29dB signal to noise ratio. Twin faced rotating system with a beamwidth of 0.5°

6.5.5 Multiple beam rotating array multi-function radar tracker

Finally, Figure 6-64 -Figure 6-73, show the results for the two rotating systems using multiple beam track updates.

The results show the track robustness to be greatly improved, as would be expected. They show that very satisfactory tracking performance in terms of achieved accuracy, track robustness and efficiency can be achieved with the rotating systems as was achieved with the static array system.

The value of 20dB chosen in the static case for efficient, accurate and robust tracking at $1/40^{th}$ of a beamwidth remains appropriate in this instance.

The final figure, Figure 6-76, compares the radar time required for the different single beam and multiple beam rotating systems. As in the static case, the difference in radar time required for the multiple beam updating of tracks was less than 10% in all cases. In fact, in all but one case (the single faced array with a 0.5° beamwidth), the difference was less than 5%.

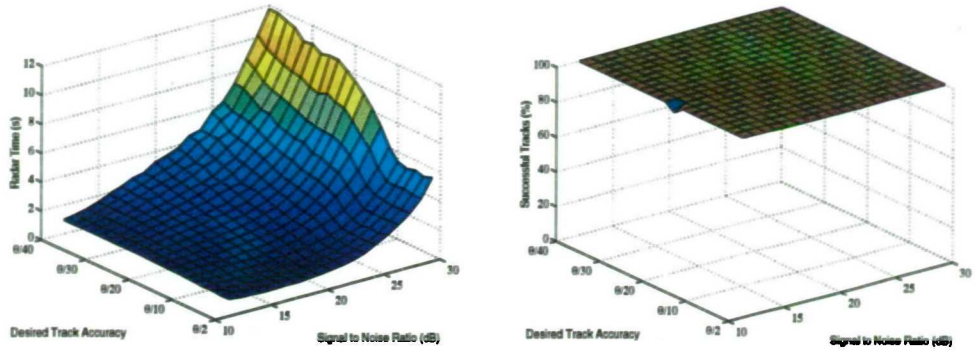

Figure 6-64(a,b) Total radar time required to maintain track on Benchmark target trajectory 6, and (b) the percentage of successful tracks. Single faced rotating system with a beamwidth of 2.5°

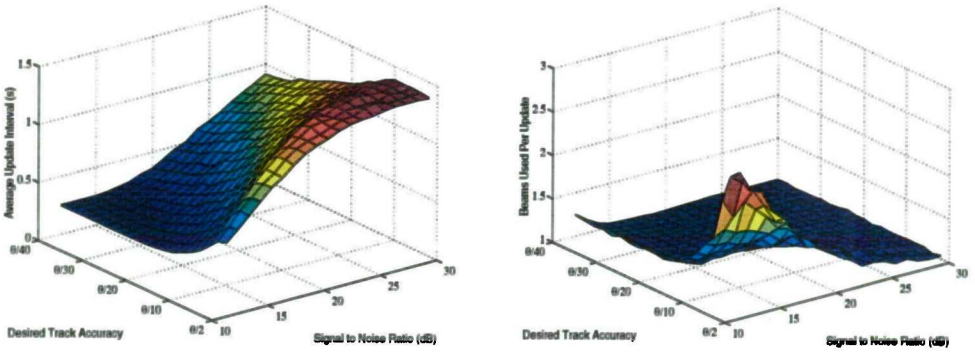

Figure 6-65(a,b) Average track update interval required to maintain track on Benchmark target trajectory 6, (b) Average number of beams required for each track update. Single faced rotating system with a beamwidth of 2.5°

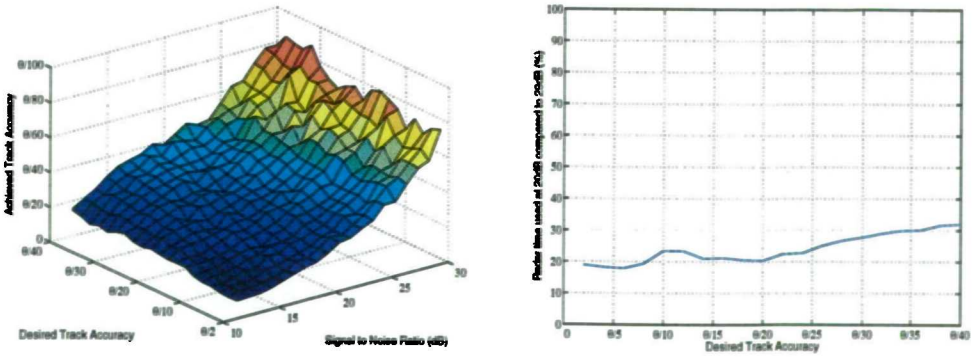

Figure 6-66(a,b) Achieved smoothed track accuracy for Benchmark target trajectory 6, excluding periods of manoeuvre, and (b) Percentage of radar time required for tracking Benchmark target trajectory 6 using only a 20dB signal to noise ratio instead of a 29dB signal to noise ratio. Single faced rotating system with a beamwidth of 2.5°

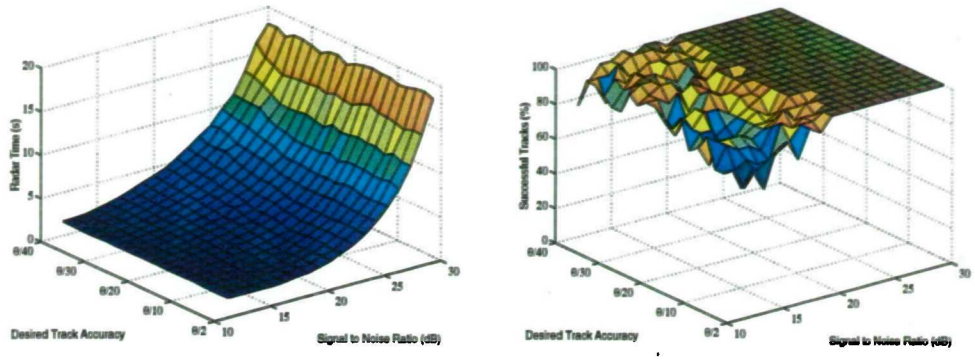

Figure 6-67(a,b) Total radar time required to maintain track on Benchmark target trajectory 6, and (b) the percentage of successful tracks. Single faced rotating system with a beamwidth of 0.5°

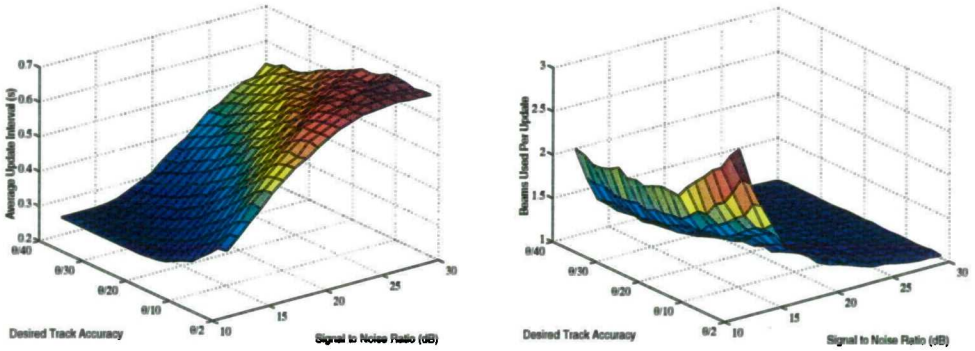

Figure 6-68(a,b) Average track update interval required to maintain track on Benchmark target trajectory 6, (b) Average number of beams required for each track update. Single faced rotating system with a beamwidth of 0.5°

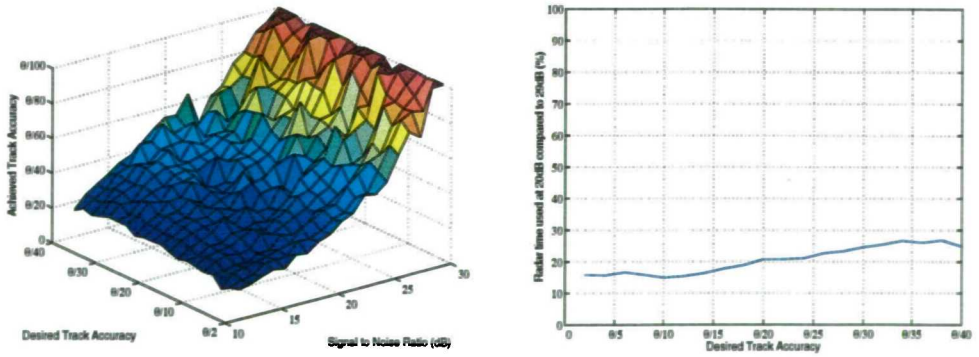

Figure 6-69(a,b) Achieved smoothed track accuracy for Benchmark target trajectory 6, excluding periods of manoeuvre, and (b) Percentage of radar time required for tracking Benchmark target trajectory 6 using only a 20dB signal to noise ratio instead of a 29dB signal to noise ratio. Single faced rotating system with a beamwidth of 0.5°

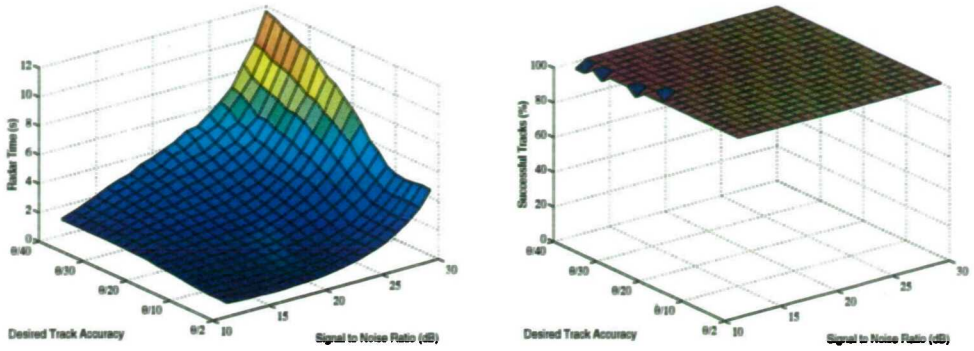

Figure 6-70(a,b) Total radar time required to maintain track on Benchmark target trajectory 6, and (b) the percentage of successful tracks. Twin faced system with a beamwidth of 2.5°

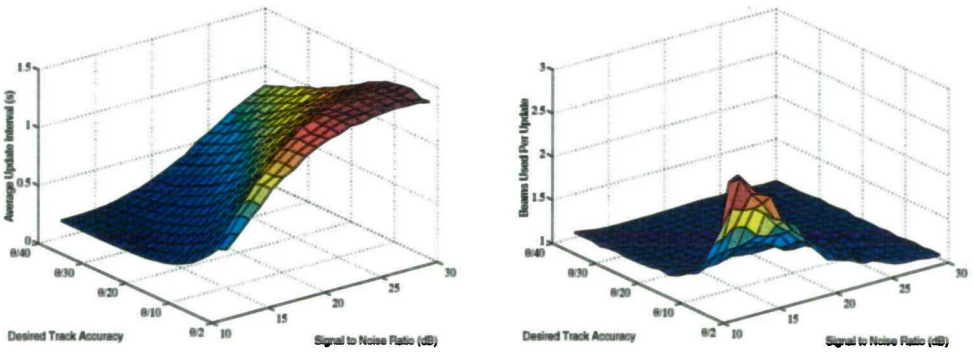

Figure 6-71(a,b) Average track update interval required to maintain track on Benchmark target trajectory 6, (b) Average number of beams required for each track update. Twin faced system with a beamwidth of 2.5°

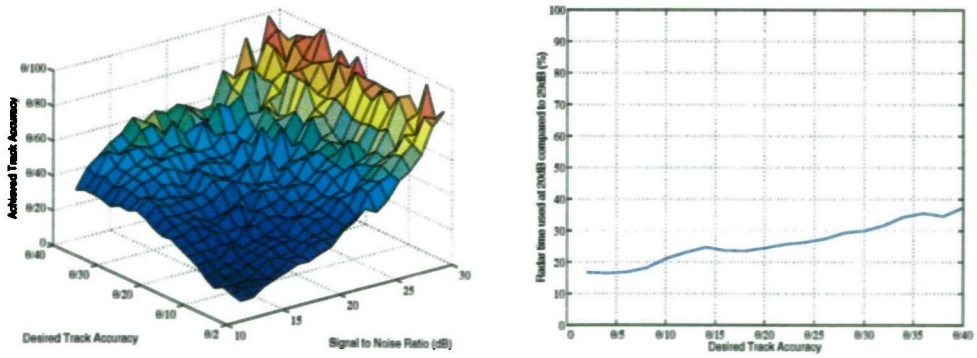

Figure 6-72(a,b) Achieved smoothed track accuracy for Benchmark target trajectory 6, excluding periods of manoeuvre, and (b) Percentage of radar time required for tracking Benchmark target trajectory 6 using only a 20dB signal to noise ratio instead of a 29dB signal to noise ratio. Twin faced system with a beamwidth of 2.5°

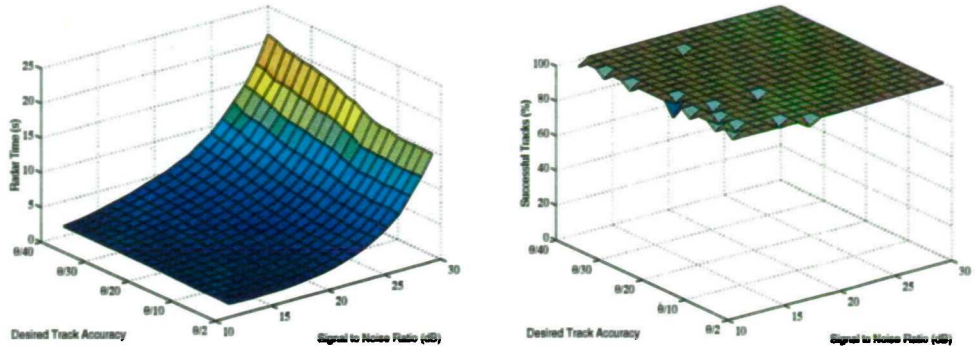

Figure 6-73 Total radar time required to maintain track on Benchmark target trajectory 6, and (b) the percentage of successful tracks. Twin faced system with a beamwidth of 0.5°

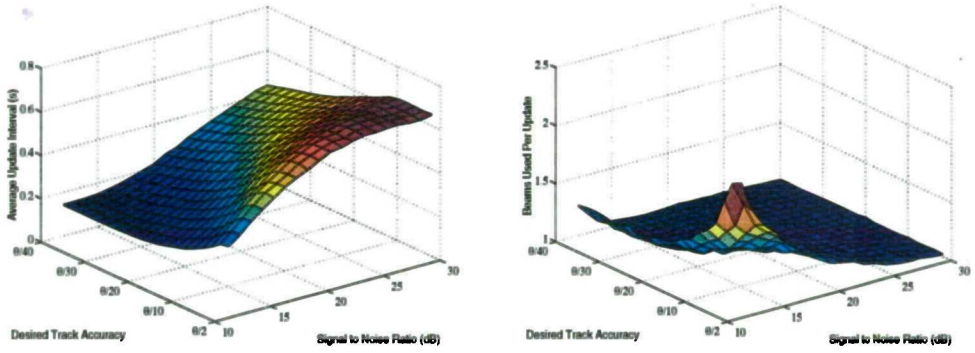

Figure 6-74(a,b) Average track update interval required to maintain track on Benchmark target trajectory 6, (b) Average number of beams required for each track update. Twin faced system with a beamwidth of 0.5°

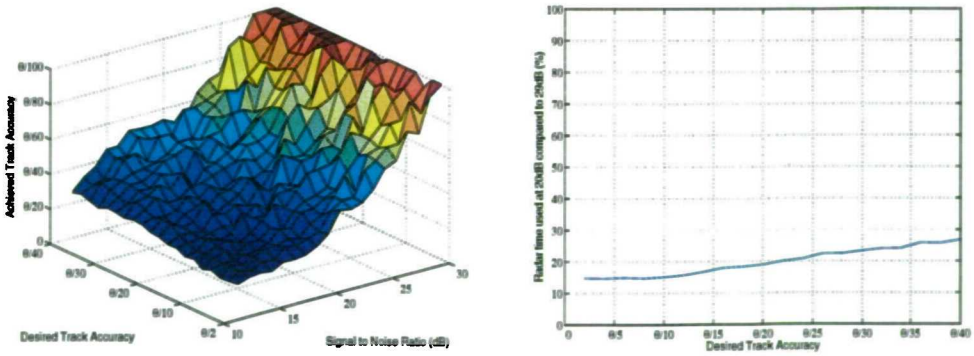

Figure 6-75(a,b) Achieved smoothed track accuracy for Benchmark target trajectory 6, excluding periods of manoeuvre, and (b) Percentage of radar time required for tracking Benchmark target trajectory 6 using only a 20dB signal to noise ratio instead of a 29dB signal to noise ratio. Twin faced system with a beamwidth of 0.5°

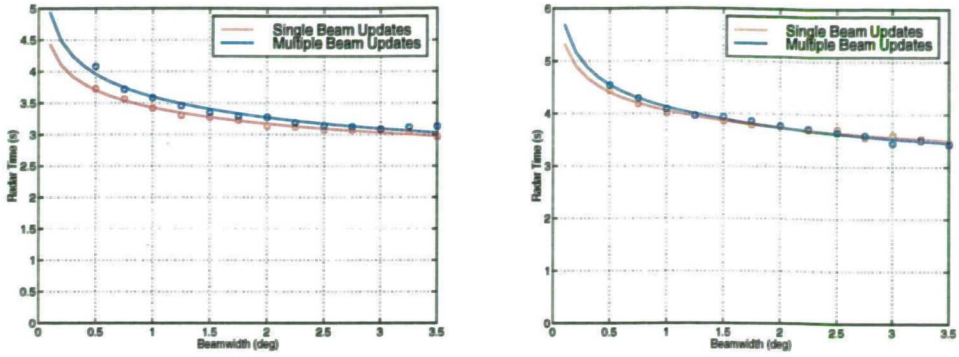

Figure 6-76(a,b) Comparison of the radar time required to track Benchmark target trajectory 6. (a) Single faced array system, (b) Twin faced array system

6.5.6 Comparison of static and rotating array tracker performance

The results presented in sections 6.5.2 to 6.5.5 have shown that very satisfactory performance can be obtained from both the static and rotating systems operating at a low signal to noise ratio, coupled with the efficient use of multiple beam track updates. Both systems can achieve a track robustness close to 100%, even in the case of the narrowest beamwidth considered of 0.5°. Finally, a comparison of the radar time the different rotating and static systems required to perform tracking of benchmark target trajectory 6 is presented.

It is important to note however in this comparison, that the radar time required by both the static and rotating systems is dependent on the trajectory characteristics. In the static case, a target trajectory which is close to the edges of the array coverage when compared to a similar trajectory close to array azimuth broadside will require a considerably greater amount of radar time. Conversely in the rotating case, although the general azimuthal direction of the trajectory does not affect the total radar time requirements, a target which is manoeuvring for much of its trajectory will require a greater amount of radar time than one which follows mostly a constant velocity trajectory.

An important difference however, is that the rotating array tracker can overcome this problem to some extent, where the static array tracker cannot. By inclusion of another smoothing filter model of the target manoeuvre, track updates may continue to be made close to array azimuth broadside as in the case of level flight. It is likely that updates away from array azimuth broadside would be required only at a point close to switching between the two models. This would allow the rotating array tracker to benefit from the minimum azimuth beamwidth for much of the track life, and give the potential for

superior accuracy to the static array system.

Figure 6-77 and Figure 6-78 compare the radar time required to track benchmark target trajectory 6 for the static and rotating array systems using a 20dB signal to noise ratio and a desired accuracy of $1/40^{th}$ of a beamwidth. The single array rotating system requires between 2.1 and 2.5 times radar time of the static array system to track benchmark trajectory 6, depending upon the beamwidth being used. This figure increases slightly for the twin faced rotating system.

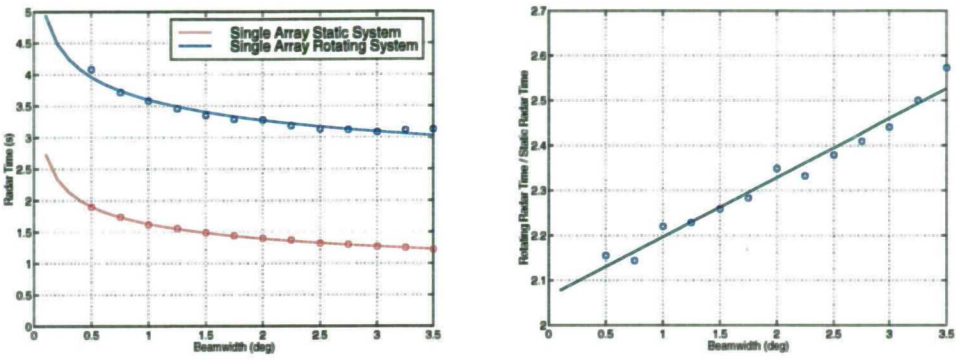

Figure 6-77(a,b) Comparison of the radar time required to track Benchmark target trajectory 6 with a single faced rotating array multiple beam system and a single faced static array multiple beam system (a) Absolute radar time required by each system, (b) ratio of the radar time used by rotating system to the static system

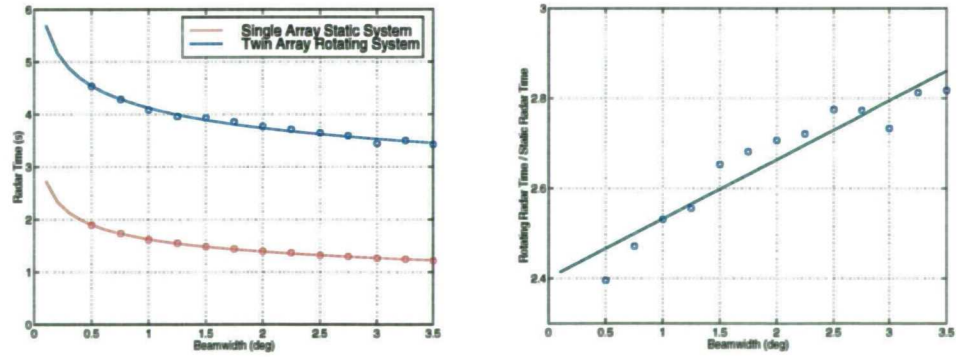

Figure 6-78(a,b) Comparison of the radar time required to track Benchmark target trajectory 6 with a twin faced rotating array multiple beam system and a single faced static array multiple beam system (a) Absolute radar time required by each system, (b) ratio of the radar time used by to rotating system to the static system

This situation may be contrasted to the case of the constant velocity target, approaching at an azimuth angle of 0° (array azimuth broadside for the static system). This can be seen from the constant velocity results shown in Appendices B and C. In this the static system requires roughly the same amount of radar time as the single faced rotating system. If this trajectory was rotated such that it lay 60° away from azimuth array broadside of the static array system, then the static system would require a greater

amount of radar time than the rotating array system.

6.6 Conclusions

Most importantly these results have shown the viability of a narrow beam multi-function radar tracker for the tracking of manoeuvring targets, for both static and rotating array systems. They have indicated the most efficient values of signal to noise ratio to aim for in the updating of tracks, and have shown that the robustness of track can be maintained through the use of multiple beam track updates. The extra radar time for such updates is not prohibitive, requiring less than a 10% increase in radar time in most cases.

The study has quantified the variation in both radar time and track robustness when the radar beamwidth is varied. At narrow beamwidths the use of multiple beam track updates is imperative to allow robust tracking. An efficient strategy for the use of multiple beam track updates has been proposed, and the increase in track robustness made using this update strategy has been quantified.

The results have shown that accurate tracking of manoeuvring targets is most efficiently performed at a lower signal to noise ratio than that used in the MESAR system currently. The signal to noise ratio may be reduced considerably (by at least 6dB), without decreasing the track robustness below a reasonable level, or the tracking accuracy below that desired. In the case of a 2.5° beamwidth, and a $1/40^{th}$ of a beamwidth desired tracking accuracy, the results indicate that the savings in radar time from utilising a multiple beam tracker operating at 20dB, rather than 29dB as in MESAR, would allow more than double the number of targets to be tracked. In the case of a 0.5° radar beamwidth, the savings in radar time would allow around three times the number of targets to be tracked using this system.

A rotating array adaptive tracker has been constructed based upon the same track updating strategy used in the MESAR static array tracker. The rotating array tracker uses roughly the same amount of radar time as the static array tracker for constant velocity targets. However, it requires considerably more radar time than the static array system during periods when the target executes a strong manoeuvre. This is due to the necessity for track updates to be made at large scan angles from array azimuth broadside. In the case of the most stressful target trajectory considered, benchmark

target trajectory 6, the rotating array system required roughly 2½ times the radar time of the static array system.

However, the increase in radar time is heavily dependent on the exact target trajectory; on the period of the manoeuvres, and on the azimuth angle of the target. This is due to the amount of track updates which must be made at large scan angles from array azimuth broadside, necessitating long dwell times to offset the loss in antenna gain. For example, in the case of a manoeuvring target trajectory which was mainly close to array azimuth broadside of the static array, the radar time required for tracking in the rotating array case would almost certainly be more than the static case, due to the relative number of track updates that must be made at large scan angles between the two systems. Conversely, if the same target trajectory was now rotated such that it was close to 60° away from azimuth broadside of the static array, the situation is likely to be reversed; the rotating array tracker would require less radar time than the static array tracker.

It is thought that the implementation of a multiple model tracker which more accurately represents the target dynamics during manoeuvre would reduce the necessity to make track updates at great angles from array azimuth broadside. This would reduce the radar time required for tracking with a rotating array multi-function radar. This is proposed as an area of further work.

7 A ROTATING, NARROW BEAMWIDTH MULTI-FUNCTION RADAR SYSTEM

7.1 Introduction

This chapter takes the main findings from chapters 4,5 and 6, and applies them to demonstrating the viability and performance of a narrow beamwidth rotating array multi-function radar with the capability of simultaneous multiple beam processing. The methods for analysis of the search function time developed in chapter 4 are used to compare this system to an equivalent static array system which does not have the ability to process simultaneous multiple beams.

Chapter 4 has shown that multi-function radars utilising rotating arrays are more efficient at performing the search function than those utilising static array faces. It also showed that the use of simultaneous multiple beam processing allowed the possibility of a narrow beamwidth multi-function radar system which did not have excessive search function times. This is important since it shows the feasibility of constructing a narrow beamwidth system which can undertake the surveillance and tracking functions successfully, within the stringent time requirements placed on the multi-function radar.

Chapter 5 then demonstrated the fact that a rotating array multi-function radar system can distribute the radar time resources across the angular coverage in a way that static array systems cannot, and can therefore better support a high loading of radar tasks in a confined angular sector. This gives the rotating array system an advantage in the operationally likely scenario that targets of interest are clustered around a certain direction, rather than equally distributed throughout the radar coverage volume.

Finally chapter 6 went on to show that manoeuvring targets can be successfully tracked with a narrow beamwidth multi-function radar utilising either a static or rotating array antenna. Track robustness can be attained through the use of multiple beam track updates at little cost in terms of radar time.

This final chapter goes on to present a candidate narrow beamwidth multi-function radar system, and assesses and compares its performance to single beam, static systems. Since narrow beamwidth systems imply a larger array, which in turn implies a greater number of elements in each face and greater cost, the number of elements allowed in the different systems considered was fixed. This allowed the comparison an element of realism, and to demonstrate the principle of a narrow beamwidth multi-function radar within current cost constraints.

The following section defines a common requirement for the systems considered in this chapter, akin to that of a naval air defence weapons system radar (or radar suite). The static and rotating systems considered are then presented in section 7.3. The radar time-budget that each of these systems must support to fulfill the proposed requirement, and the associated detection performances they achieve is then given in section 7.4. The final section presents the conclusions of the chapter.

7.2 Requirement

An example requirement, akin to that of a naval air defence radar system, is used to compare the different multi-function radar systems. The requirement is to perform both volume surveillance and tracking out to a range of 50 km. The surveillance volume is subdivided into three regions with different clutter cancellation requirements, shown in Figure 7-1.

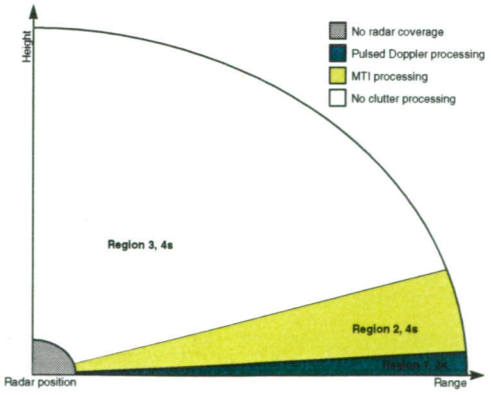

Figure 7-1 Requirement search volume for the static and rotating array systems

Region 1 consists of the bottom beam only, used to search the horizon. This region will experience the severest levels of clutter since it will illuminate the sea and land. Pulsed Doppler waveforms are required to give adequate isolation of the target from the clutter.

Also this region requires the highest search rate, since targets may pop up over the horizon at short range. Region 2 extends from the top of region 1 to an elevation of 10°, and requires MTI Doppler processing for cancellation of rain clutter. Region 3 requires no Doppler processing. Table 7-1 shows the surveillance waveforms and frame times of the example requirement.

Region	Elevation Extent	Frame Time	Waveform Type	Azimuth Broadside Waveform Duration
1	Bottom beam	2 s	Pulsed Doppler - 2 bursts of pulses (8 pulses plus 3 guard pulses)	2(3+8)/2KHz = 11ms
2	Second beam to 10°	4 s	MTI - 3 bursts of pulses (3 pulses plus 2 guard pulses)	3(2+3)/2KHz = 7.5ms
3	10° - 90°	4 s	Non Doppler Processed (1 pulse)	1/2KHz = 0.5ms

Table 7-1 Surveillance frame time and waveform requirements for the example search volume

These waveforms are increased in length to account for the decrease in gain with azimuth scan off that occurs in the static systems, assuming coherent integration is used to offset the $\cos^3(\theta)$ scan off loss. It is assumed that the rotating system performs all surveillance on azimuth array broadside, and thus no increase in the waveform length is required. This will be the case for a multi-function radar with a total occupancy of 100% or less as described in section 5.4.

A peak total of 30 high priority targets must be tracked using dedicated waveforms. It is assumed for simplicity that all low priority targets will be tracked using track while scan, and thus have no impact on the radar resources. The 30 high priority targets will be spread evenly between regions 1 and 2.

7.3 Antenna configurations considered

Chapter 5 showed that a rotating array multi-function radar performed the search function more efficiently than the equivalent static array systems. Also, Billam [Billam, 1997] has shown that a single faced array antenna is the most efficient arrangement of a fixed number of elements in an array antenna. Thus a single face, rotating array system has been chosen here, and compared to both three and four faced static array systems.

Each multi-function radar system will contain a total of 10,000 elements to be distributed equally between the array faces. This has been arbitrarily chosen, to allow a relative comparison of the systems. Obviously a greater number of total elements would

give greater performance and conversely a smaller number would give worse peformance, but it is not absolute performance against the requirement that is of interest.

The static systems have the advantage of having independent steerable beams from each array face, giving 3 or 4 simultaneous beams compared to just one beam for the single array rotating system. Conversely the ERP of the static systems is considerably less than the rotating system due to the distribution of the elements amongst the faces. The antenna characteristics of the systems are given in Table 7-2. A frequency of 3GHz is assumed, and a power feeding each element of 10W.

System	Independent Beams	Elements per face	Beamwidth (deg)	Gain (dB)	Relative ERP
Four Faced Static Array	4	2,500	2	39.0	1
Three Faced Static Array	3	3,333	1.76	40.2	1.78
Single Faced Rotating Array	1	10,000	1	45.0	16

Table 7-2 Antenna characteristics of the different array configurations

7.4 Analysis of time budget and free space detection performance

7.4.1 Surveillance

This section presents the results of applying the UV space and rotating UV space methods for estimation of the surveillance time-budget requirements. It also gives a comparison of the likely detection performance of the different systems using the radar equation.

We start by considering the radar time-budget and performance aspects for the surveillance function. Table 7-3 below shows the results from applying the UV space estimation technique developed in chapter 4 to the four faced static array multi-function radar system.

Region	Number of Beams	Dwell Time	Function Time	Frame Time	Occupancy
1	192	15.7ms	3.0229	2	152%
2	771	10.6ms	8.1697	4	204%
3	4356	0.616ms	2.6854	4	67%
				Total Occupancy	**423%**

Table 7-3 Search time-budget requirements of the 4 faced static array multi-function radar

The 2° beamwidth of the static arrays gives a total of 5319 beams to search, requiring a total radar time of 13.88s. Given the frame time requirements of the three regions, this translates into a total required surveillance occupancy of 423%. Thus an occupancy of

106% is required from each of the multi-function radar array faces to meet the surveillance requirement.

Clearly this is not possible, and in practice the requirement would be alleviated in some way to bring the surveillance occupancy below 100%, allowing enough time for other functions such as tracking. This could be achieved for example by increasing the frame times of the regions somewhat. However this figure is close enough to 100% to allow the requirement to be used for a comparison of the different antenna configurations.

Using the radar equation expressed in [7-1] below we can calculate the broadside signal to noise ratio, SNR_0, against a target in free space. If we assume a duty cycle of 30% for the radar then for a target at a range of 50km, with a radar cross section of $0.1m^2$, a single pulse signal to noise ratio of 11.5dB is achieved. Assuming Swerling 3 target characteristics this equates to a single pulse probability of detection of 0.4.

$$SNR_0 = \frac{P_{av} G_t G_r \lambda^2 \sigma}{(4\pi)^3 R^4 kTB} \qquad [7\text{-}1]$$

where P_{av} is the average transmitted power
G_t is the gain of the antenna on transmit
G_r is the gain of the antenna on receive
λ is the wavelength of the transmitted signal
σ is the radar cross section of the target
R is the target slant range
k is the Boltzmann constant, 1.38 x 10-23 J/deg
T is the temperature in degrees Kelvin
B is the receiver bandwidth in Hertz

For comparison, the occupancy requirements of an equivalent four faced rotating system are shown in Table 7-4.

Region	Number of Beams	Dwell Time	Function Time	Frame Time	Occupancy
1	213	11ms	2.35	2	117%
2	853	7.5ms	6.40	4	160%
3	4721	0.5ms	2.36	4	59%
				Total Occupancy	**336%**

Table 7-4 Search time-budget requirements of the 4 faced rotating array multi-function radar

As was shown in chapter 4, the rotating system requires significantly less radar time to complete the search since it can perform surveillance on azimuth array broadside. For this particular requirement, the rotating system requires just 79% of the radar time of the equivalent static system, whilst achieving the same detection performance.

This system is therefore more efficient than the static 10,000 element system, and can meet the requirement within the time-budget constraints, requiring a surveillance occupancy of just 84% per face. However it has the same 2° beamwidth as the static system, which we wish to reduce.

Table 7-5 shows the situation if all 10,000 elements are configured into a single, rotating array. The decrease in beamwidth gives rise to a vast total number of surveillance beams of 23149. This total surveillance occupancy required for the single array face to perform the volume search rises to 1190%, which is clearly totally impossible. Table 7-5 shows in a striking way the reason the beamwidth of a multi-function radar is compromised between the surveillance and tracking functions.

The large increase in gain, and the increased total power output, however give a significantly increased detection performance. The single pulse signal to noise ratio against the $0.1m^2$ target at 50km rises to 29.6dB, some 18dB greater than that of the four faced array.

Region	Number of Beams	Dwell Time	Function Time	Frame Time	Occupancy
1	425	11ms	4.68	2	234%
2	3840	7.5ms	28.80	4	720%
3	18884	0.5ms	9.44	4	236%
				Total Occupancy	**1190%**

Table 7-5 Search time-budget requirements of the single faced rotating array multi-function radar, with no capability for simultaneous multiple beam processing

Table 7-5 shows the radar time constraints that must be overcome through the use of simultaneous multiple beam processing. To enable the timely surveillance of regions 2 and 3, we consider a quadrupling of the transmit beamwidth, coupled with narrow receive beams, shown in Figure 7-2(a), below.

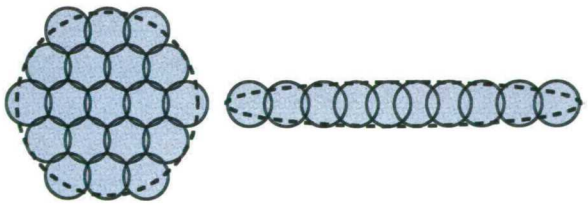

(a) (b)

Figure 7-2(a,b) Simultaneous multiple beam configurations for (a) Regions 2 and 3, (b) Region 1. Dashed line shows transmit beam pattern, filled circles show possible receive beam positions

This allows the search of these regions to be undertaken with a 16^{th} of the number of beams. It will give a comparable search occupancy to that of the four faced systems,

since those systems have a ¼ of the total occupancy per face, and ¼ of number of search beams, thus a 16^{th} of the occupancy of the single array.

For the same reasons, a broadening of a factor of 8 is applied to the search of the single beam in elevation of region 1, shown in Figure 7-2(b). This again will give a comparable surveillance occupancy to the four faced system, but will also give the narrowest beamwidth in elevation which is important to minimise the effects of multipath in the bottom beam.

Table 7-6 shows the time-budget requirements for the 10,000 element array applying this scheme of simultaneous multiple beam processing. The use of the broadened transmit beam patterns enables a reduction in the total required surveillance occupancy to 89%.

The free space detection performance of the surveillance regions is now different since the transmit beam used for region 1 has a higher gain than that used for regions 2 and 3. A signal to noise ratio of 20.6dB is achieved against the $0.1m^2$ target at 50km in region 1, and 17.6dB in regions 2 and 3.

Thus the single array system utilising multiple beam processing can successfully conduct the surveillance of the volume within the multi-function radar time resource constraints, and achieve a satisfactory free space detection performance. This system requires just 84% of the radar time that the four faced static system requires, whilst achieving a signal to noise ratio 9dB higher in region 1 and 6 dB higher in regions 2 & 3.

Region	Number of Beams	Dwell Time	Function Time	Frame Time	Occupancy
1	53	11ms	0.5855	2	29%
2	240	7.5ms	1.8008	4	45%
3	1181	0.5ms	0.5903	4	15%
				Total Occupancy	**89%**

Table 7-6 Search time-budget requirements of the single faced rotating array multi-function radar, with the capability for simultaneous multiple beam processing

7.4.2 Tracking

In this section we compare the tracking performance of the single array rotating system utilising simultaneous multiple beam processing to the four faced static system which does not have the capability to perform simultaneous multiple beam processing.

The comparison is made difficult by the variation in the radar time requirements of both the static and rotating array tracker systems with the trajectory characteristics. As discussed in section 6.5.6, a target trajectory which is close to the edges of the array coverage when compared to a similar trajectory close to array azimuth broadside will require a considerably greater amount of radar time in the static array system. Conversely in the rotating case, although the general azimuthal direction of the trajectory does not affect the total radar time requirements, a target which is manoeuvring for much of its trajectory will require a greater amount of radar time than one which follows mostly a constant velocity trajectory.

This is reflected in the fact that the constant velocity target required less radar time for tracking in the rotating case than the static case, whereas for benchmark trajectory 6 the rotating array system required more than double that of the static array system (see results in Appendices B & C). Taking an average of the radar time required for tracking all of the 7 targets considered, the static system required 60% of the radar time used by the single array system rotating with a period of 1s. This figure will be used as a comparison here, but the dependency on the likely target trajectories must be noted. It is also important to note that the use of multiple Kalman filtering techniques such as IMM may reduce the radar time requirements of the rotating array tracker against manoeuvring targets.

Tracking benefits from knowledge of the target direction, and so broadened beams need only occasionally be used. The rotating array system can therefore obtain maximum gain in both transmit and receive for most track updates. This will give a free space detection performance some 18dB higher than the static system if no beam broadening is used. Since the minimum length of the transmitted waveform that must be used for tracking will be defined by the clutter conditions, the difference in the radar time that will be required by the two systems for tracking will be dependent on the clutter environment in which the system operates. The case of benign clutter and severe clutter are discussed below.

7.4.2.1 Benign clutter environment

In the absence of severe clutter the waveforms may be reduced in length, since Doppler discrimination of the target and the clutter is not required. If the tracking waveforms are to aim to achieve a signal to noise ratio of around 20dB against the target, as

recommended in chapter 6 for efficient tracking, then the difference in radar time the two systems will require for tracking will depend on the following factors;

i. *increase in track update rates for narrow beam tracking*
ii. *increase in radar time to track manoeuvring targets with a rotating array tracker*
iii. *decrease in track waveform length due to higher free space detection performance*

Chapter 6 quantified the first of these factors. The increase in radar time necessary to track using a narrower beamwidth is shown in Figure 6-77. An increase of around 15% in radar time is required to track using a 1° beamwidth rather than a 2° beamwidth.

The second factor, has been discussed in section 7.4.2 above, and is dependent on the specific target trajectory assumed. The single array system rotating with a period of 1s required a factor of 1.67 times the radar time of the static array system, based upon an average of the 7 target trajectories considered in this study.

These two factors suggest a radar time requirement for the rotating array system of almost double that of the static system. This combined with the fact that the static system has four times the total occupancy available for tracking from its four faces, suggests the static system should be able to track almost 8 times as many targets. However, the waveform length requirements of the rotating array system will be considerably less than the static system, since the free space detection performance of the rotating system is 18dB greater. This potentially allows a reduction in the transmitted waveform energy by a factor of 64 to allow tracking to occur at the same signal to noise ratio as in the static case. In practise the savings made in radar time by reducing the transmitted waveform length will be limited by the need to transmit and receive at least one pulse, and will therefore depend upon the target range (assuming range unambiguous operation), but they should certainly outweigh the increase in radar time required for factors discussed above.

It is concluded that in a benign clutter environment, the rotating array system is likely to be able to track at least as many, if not more, high priority targets than the static system, and with a better resolution and accuracy.

7.4.2.2 Severe clutter environment

In a severe clutter environment the length of the waveforms used for tracking is likely to be dominated by the requirement for Doppler resolution. In this situation the waveform length will not be able to be reduced in the rotating array tracker, resulting in tracking taking place at a signal to noise ratio higher than that necessary, and a greater radar time requirement for the rotating system. This is the more stressful of the two clutter situations in terms of radar time, and thus we consider the tracking requirement outlined in section 7.2 for this case.

Waveforms assumed for tracking the 30 targets are based on those for surveillance of regions 1 and 2. In the case of tracking however, where the target velocity is known, only a single Doppler pulse burst need to be transmitted to cover the required velocities of interest. The tracking dwell time for region 1 is thus half of that for surveillance, and for region 2 one third of the for surveillance.

The tracking occupancy requirements for the static and rotating array systems are shown in Table 7-7 and Table 7-8 below. An average update rate of 1Hz has been assumed for the rotating system, which is decreased by 15% for the static system to account for tracking with a broader beamwidth. The update rate is reflected in the frame time in each table.

The rotating array system requires an occupancy of 12% to cope with the peak loading of tracks given by the requirement. The static array system requires nearly 15%, however this is shared amongst the four faces, and thus the tracking occupancy required per face is just 3.7%.

Region	Dwell Time	Number of targets	Function time	Frame Time	Occupancy
1	5.5ms	15	82.5ms	1s	8.25%
2	2.5ms	15	37.5ms	1s	3.75%
				Total Occupancy	**12%**

Table 7-7 Tracking time-budget requirements of the single faced rotating array multi-function radar

Region	Dwell Time	Number of targets	Function time	Frame Time	Occupancy
1	7.85ms	15	117.75ms	1.15s	10.23%
2	3.53ms	15	52.95ms	1.15s	4.6%
				Total Occupancy	**14.8%**

Table 7-8 Tracking time-budget requirements of the four faced array multi-function radar

In this severe clutter environment, for a given total radar tracking occupancy, the static system will be able to track at least four times the number of targets as the rotating array

system. The signal to noise ratio at which tracking would occur would be 18dB higher in the rotating array system.

The rotating array system could reduce the occupancy required for tracking through the use of cluster tracking techniques. Simultaneous multiple beam processing may be used for the updating of multiple tracks closely spaced in angle. This is beyond the scope of this study and is proposed as an area of further investigation.

7.4.3 Summary

The rotating array requires a greater occupancy for tracking of high priority targets against the target trajectories considered within this study. However, against the example requirement, this was more than offset by the efficiency with which this antenna configuration is able to perform the search function.

The rotating array system, utilising multiple beam processing, required an occupancy of 89% to meet the search requirement, and 12% to meet the tracking requirement set. Thus within the limits of the accuracy of the simple analysis performed, the total occupancy of 101% indicates that the rotating array system was able to meet the example requirement.

The static array system required an occupancy of 106% per face to meet the search requirement and 3.7% per face to meet the tracking requirement. Thus in total the four faced static system required an occupancy around 9% greater than the rotating system in order to meet the requirement set.

The rotating system achieved a higher signal to noise ratio in all cases due to the increased antenna gain. In surveillance, a free space signal to noise ratio of 9dB and 6dB greater was achieved in regions 1 and 2 respectively. In tracking, since the maximum antenna gain is achieved in both transmit and receive, an 18dB better free space signal to noise ratio was achieved. However, to achieve timely surveillance, a considerable broadening of the transmit beam was considered, resulting in illumination of a greater area of clutter. The impact of this must be considered carefully before such a strategy may be adopted.

7.5 Conclusions

This chapter has compared two different multi-function radar systems against a simple, but realistic requirement. A fixed number of active array modules have been considered, since to a large degree the cost of an active array multi-function radar is dependent on this factor. These have been distributed differently in each of the two systems.

The first system is a multi-function radar utilising four fixed antenna faces. This has traditionally been regarded as the best system if it can be afforded. The second system considered takes on the findings of chapters 4, 5 and 6, and utilises a single rotating array with the capability of performing simultaneous multiple receive beam processing. This system has a narrower beamwidth than the static array system, and would ordinarily have difficulty in meeting the time-budget constraints placed on the multi-function radar.

The analysis shows that the single rotating array multi-function radar is able to meet the example requirement for surveillance and tracking within the radar time-budget constraints, through the use of simultaneous multiple beam processing. A total occupancy of 101% is required, which to within the accuracy of the analysis made, is achievable. The static system requires a total occupancy of 110% to meet the same requirement, which is not achievable, and would thus require a small reduction in the requirement specified.

The rotating array system requires more radar time resources for tracking than the static array system. However in the case of the example requirement, the extra time needed was more than compensated for by the efficiency with which the rotating array system performed the search.

The benefits and drawbacks of the narrow beamwidth rotating array system compared to the static array system considered are summarised below.

Advantages	Disadvantages
• Increased free space detection performance in surveillance • Increased free space detection performance in tracking • Better plot resolution in tracking and surveillance • Better smoothed track accuracy • Better performance in multipath conditions • Increased resistance to main lobe jamming • Greater ability to cope with an uneven loading of tasks, or tasks confined to a narrow angular sector	• Increased radar time requirement for tracking in some cases • Increased illumination of clutter • Increased receiver or digital beamformer complexity

Essentially, the use of simultaneous multiple beam processing may be regarded as another degree of freedom in the control of the multi-function radar. It allows the time and energy resources to be more closely fitted to the requirement. A multi-function radar with a narrow beam searching in clutter may have a free space detection performance in excess of that required, but clutter cancellation below that required within the time constraints. The use of multiple beams allows the adjustment of time and energy resources allocated in a given direction independently, and therefore to trade off the free space detection performance with the Doppler cancellation.

8 CONCLUSIONS AND FURTHER WORK

8.1 Summary

A phased array antenna can electronically steer the direction of the antenna beam near instantaneously. In a multifunction radar this capability is used to allow the system to multiplex its time between many different functions, the primary functions usually being volume surveillance and multiple target tracking. Potentially the use of automated digital control of the multi-function radar system allows the tasks it is performing to be dynamically adjusted. Savings in radar time made in meeting the requirement of one function allow that time to be devoted beneficially to other functions. It is important therefore to ensure that the multi-function radar's resources are efficiently allocated between the functions, and that each function is performed with the minimum use of radar time and energy possible. The aim of the work presented in this thesis has been to investigate and improve techniques for multi-function radar control and tracking. The research has been focused particularly on coping with the effects of utilising rotating arrays and on the use of techniques such as beam broadening and simultaneous multiple receive beam processing, that will be available in future multi-function radars with advanced digital beamforming capabilities.

A fundamental disadvantage of the multi-function radar is the compromise that must be made on the radar beamwidth. To allow surveillance of the volume to occur at a useful rate whilst supporting the required levels of clutter suppression through Doppler processing, a broad radar beamwidth must be utilised. However, the requirements for good plot accuracy and resolution for the tracking function conflict with this, desiring a narrow radar beamwidth. The result is that many current multi-function radar systems have a radar beamwidth larger than is ideal for the tracking function to allow timely volume surveillance, and as a result have poor performance when compared to dedicated tracking radars. By applying novel methods for estimation of the search time requirements of different multi-function radar configurations, it has been concluded that this compromise on radar beamwidth may be avoided through the use of simultaneous multiple beam processing. This allows the surveillance of the volume to be achieved

inside the surveillance frame time requirements with a narrow radar beamwidth. This in turn allows the benefits of a narrow radar beamwidth to be accrued by the tracking function.

A second important conclusion from the research is that the traditional view of four fixed array faces as the 'ideal' antenna configuration for a multi-function radar is not supported. It has been shown that multi-function radars which utilise rotating array antennas are considerably more efficient at performing the surveillance function in their use of radar resources than their static array counterparts.

There are also benefits in the resource management and scheduling of a rotating array system. A multi-function radar utilising a rotating array antenna has the ability to distribute radar time across the angular coverage in a way that a static array antenna system cannot. This allows better support for a high loading of surveillance and tracking tasks in a confined angular sector, which is a likely operating environment for the multi-function radar. A novel task scheduling strategy for a rotating array multi-function radar which achieves this has been presented, and its performance assessed through computer simulation.

The utilisation of a narrow beamwidth in the multi-function radar brings disadvantages as well as advantages. The coupling of a narrow radar beamwidth with a low track update rate, enforced by the radar time-budget constraints, increases the difficulty in tracking of manoeuvring targets. This is particularly the case for the rotating array which has blind arcs in the antenna coverage.

Efficient tracking strategies have been developed which address this problem for both static array and rotating array multi-function radars. Successful tracking of highly manoeuvrable targets with a narrow beam multi-function radar has been demonstrated though simulation. High levels of track robustness can be attained through the use of multiple beam track updating strategies which cost little radar time.

These findings have been summarised by presenting a simple assessment of a narrow beamwidth, rotating array multi-function radar utilising simultaneous multiple beam processing against a realistic, fictional, requirement. This system has been compared to a four faced static array system using the same total number of array elements/active array modules. The rotating system has been shown to be able to meet the requirement

within the radar time-budget constraints successfully, at the cost of increasing the clutter illuminated by the transmit beam. When compared to the four faced static system, the rotating system required less radar time resources to meet the requirement, and achieved a higher free space detection performance in both surveillance and tracking.

Thus the possibility of a multi-function utilising a narrow radar beamwidth has been demonstrated within the radar time and energy resources available. Coupled with the use of a rotating array antenna, such a system would be both efficient, and give good performance for the surveillance and tracking functions. However, if significant beam broadening is required, then the implications of illuminating more clutter than is illuminated by current systems must be assessed. The advantages and disadvantages of such a system are summarised below.

Advantages	Disadvantages
• Increased free space detection performance in surveillance and tracking • Increased efficiency in use of radar time/energy resources • Better plot resolution in tracking and surveillance • Better smoothed track accuracy • Better performance in multipath conditions • Increased resistance to main lobe jamming • Greater ability to cope with an uneven loading of tasks, or tasks confined to a narrow angular sector	• Increased radar time requirement for tracking in some cases • Increased illumination of clutter • Increased receiver or digital beamformer complexity

8.2 Evaluation of static array, rotating array and variable beam pattern multi-function radar

A novel method of calculating the search function time for a static radar has been

developed. This gives analytical expressions which may be quickly evaluated for a range of beamwidths and search sectors, without explicitly calculating each beam direction and dwell time. This will allow surveillance configurations of a multi-function radar to be evaluated rapidly using simple equations. The method is based upon estimating the number of beams and the dwell times required in each beam direction in UV space, in which the beam area remains invariant.

By creating a similar projection to the UV space projection, involving a transformation onto the surface of a 3D cylinder, another spatial system may be created in which the beam area of a rotating multi-function radar system remains invariant. This projection is somewhat akin to the Sanson-Flamsteed sinusoidal and Mollweid projections used in the field of cartography. The above methodology for estimating the beam directions and dwell times, and thus the search function time, may be applied in this spatial system for the rotating system.

The above methods for static and rotating multi-function radars have been compared with the process of calculating beam directions and dwell times exactly, and have found answers within a few percent. The accuracy decreased somewhat as the beamwidth considered increased (to around 8% for a 10° beamwidth), due to the exact number of beams required to exactly cover the edges of a given region.

A comparison of the search function for different configurations of static and rotating array multi-function radars has been made. It was found that the static systems require 20% (4 faced) and nearly 50% (3 faced) more radar time to execute a complete search of the same volume. When comparing the 3 faced static system with a 2 faced rotating system, it was found that nearly the same amount of radar time must be dedicated from each of the 3 faces as is required from just 2 faces in the rotating case. Thus this comparison suggests one of the 3 faces could be eliminated if rotation was employed with very little detriment to the search. These figures will vary to some degree, depending upon the exact volume that is to be surveyed, and the tilt angle of the arrays.

The impact of using a broadened beam both in transmit and receive on the multi-function radar system has been made. For any significant broadening of the beam there is a heavy penalty to be paid both in the tracking and surveillance functions.

The impact of using a broadened beam in transmit, coupled with narrow receive beams has also been made. The variation of surveillance search time has been determined as a function of transmit beamwidth both in thermal noise and in clutter conditions, assuming multiple narrow receive beams. When target detection is limited by thermal noise the result is as predicted by the familiar search radar equation; the search time is invariant with transmit beamwidth, since a wider beam requires a longer dwell time to regain the signal to noise ratio.

When target detection is limited by clutter, the search time may be decreased by broadening of the transmit beam. This is because the dwell time in that instance is determined by the resolution required in the Doppler domain, governed by the length, of the transmit waveform. The greater quantity of clutter illuminated is far outweighed by the Doppler discrimination possible.

The implication from these arguments is that the compromise on beamwidth usually associated with air defence multi-function radar systems does not necessarily hold if the multi-function radar has the capability of processing multiple receive beams. Systems may be built with narrower receive beamwidths than those currently, whilst still retaining the ability to cancel clutter through Doppler processing within the time-budget constraints of the multi-function radar. From the tracking perspective all the benefits of a dedicated tracking radar may be realised, such as excellent monopulse accuracy, resolution of closely spaced targets, and resistance to main beam jamming.

8.3 Resource management of static and rotating array multi-function radar

A set of objectives which a scheduling algorithm should attempt to meet have been proposed. It is immediately clear that not all objectives can be perfectly met in a practical situation, thus the importance of each objective to the multi-function radar system must be reflected in the scheduling algorithm.

A simulation model of a static multi-function radar, centred upon the task scheduler has been implemented. This allows design of multi-function radar search coverage volumes and analysis of the performance at a macroscopic and a microscopic level. Three static task scheduler algorithms have been incorporated into the simulation and tested. The

first is a simulation of the MESAR look based scheduler. The other two work on the same principle, but are modified to calculate and reset time balances in a different way. Of these, one is a look based scheduler as per MESAR, the other is a simplified version which assumes that tasks are not broken down into looks, having some execution time advantage.

The simulation has been tested and validated using the MESAR search region parameters as a test case. A detailed assessment of the MESAR scheduler has been made. This was important since there was some question over whether this algorithm was performing as expected in the MESAR radar.

The results show that the scheduler algorithms achieve 100% utilisation of the multi-function radar antenna in all circumstances. This was the second of the three objectives which applied to a static multi-function radar, and reflects the importance attached to full utilisation of the multi-function radar antenna. This objective is achieved at the expense of scheduling tasks as close as is possible to their desired time (the first objective). Tasks are always scheduled after their desired update time to some extent. This is minimised in the scheduling architecture, by splitting waveforms up into smaller looks so that the scheduling of a long waveform may be interrupted by a higher priority function. This entails however some extra complication in the signal processing since data from the interrupted waveform must be buffered to allow the interruption.

The MESAR algorithm is not optimal, in that better algorithms could be devised which give 100% radar utilisation and schedule tasks closer to their desired time by allowing tasks to be scheduled early. However, although relatively simple, the current algorithm meets the requirements for timely scheduling adequately. The algorithm has therefore been validated against the proposed objectives as far as is possible within this study.

An analysis of the differences between static and rotating multi-function radars has drawn out the complications that the scheduling algorithms must overcome for efficient operation of the multi-function radar. These are summarised;

i. blind arcs in the antenna coverage

ii. tasks must be scheduled close to array azimuth broadside where possible

iii. radar occupancy may be distributed non-uniformly with azimuth

It is concluded that a rotating scheduler algorithm should include some form of prediction of the radar load over one or more successive scans in order to allocate resources efficiently in situations of high radar loading. For resources to be allocated correctly in this situation a rotating multi-function radar scheduler must allow the use of forward and backward scanning of tasks to enable distribution of resources with angle. The theoretical extent to which this can be achieved has been determined for a multi-function radar which does not compensate the transmitted energy in surveillance with scan angle, and for a multi-function radar which does.

An algorithm has been presented for the scheduling of tasks in a rotating radar that copes with the problems outlined in (i) to (iii) above. It is highly efficient in distributing the radar occupancy to the angular sectors which require it most. It will automatically adjust from a situation in which tasks are uniformly distributed throughout the multi-function radar coverage to a situation in which the threat may come from a particular angular sector, so that many of the tasks are concentrated in a small azimuthal sector.

The cost of unnecessarily scheduling tasks away from array broadside in rotating multi-function radar systems has been determined in terms of the decrease in detection performance and in terms of the decrease in angular estimation accuracy when using monopulse. It was found that dwell times must be increased by $1/\cos^3(\varphi)$ in order to maintain detection performance, but by $1/\cos^5(\varphi)$ in order to maintain plot accuracy. The total increase in the radar time for surveillance will therefore increase, however this is offset somewhat by the increase in beamwidth (so a reduced number of search beams). Therefore the search function time needs only be increased by a factor of $1/\cos^2(\varphi)$ in order to maintain detection performance, and by $1/\cos^4(\varphi)$ in order to maintain plot accuracy.

The use of fuzzy logic and penalty functions has been suggested as a simple and effective technique for the resource management of a multi-function radar. Such techniques would allow a flexibility in the time at which tasks are scheduled, resulting in a more efficient allocation of the multi-function radar resources. Also, these techniques have the capability of allowing simple, adaptable and comprehensible control rules to be used in the radar resource management. Fuzzy logic has been successfully applied to the control of an airborne intercept radar by Popoli [Popoli & Blackman, 1987]. This is considered a fruitful area for further work.

8.4 Adaptive tracking in multi-function radar

The problems of tracking manoeuvring targets with a narrow beamwidth multi-function radar system and a rotating array multi-function radar system have been addressed through computer simulation and Monte Carlo analysis. Computer simulations of both static array and rotating array multi-function radars have been constructed, and have been applied to the target trajectories given in the benchmark tracking problem [Blair et al, 1994].

Most importantly these results have shown the viability of a narrow beam multi-function radar tracker for the tracking of manoeuvring targets, for both static and rotating array systems. They have indicated the most efficient values of signal to noise ratio to aim for in the updating of tracks, and have shown that the robustness of track can be maintained through the use of multiple beam track updates. The extra radar time for such updates is not prohibitive, requiring less than a 10% increase in radar time in most cases.

The results have shown that the signal to noise ratio that is aimed for use in the MESAR radar for tracking is unnecessarily high. The signal to noise ratio may be reduced considerably (by at least 6dB), without decreasing the track robustness below a reasonable level, or the tracking accuracy below that desired.

The study has quantified the variation in both radar time and track robustness when the radar beamwidth is varied. At narrow beamwidths the use of multiple beam track updates is imperative to allow robust tracking. An efficient strategy for the use of multiple beam track updates has been proposed, and the increase in track robustness made using this update strategy has been quantified.

A rotating array adaptive tracker has been constructed based upon the same track updating strategy as that used in the MESAR static array tracker. The rotating array tracker uses roughly the same amount of radar time as the static array tracker for constant velocity targets, close to array azimuth broadside. However, it requires considerably more radar time than the static array system in periods when the target executes a strong manoeuvre. This is due to the necessity for track updates to made at large scan angles from array azimuth broadside. In the case of the most stressful target trajectory considered, benchmark target trajectory 6, the rotating array system required roughly 2½ times the radar time of the static array system.

However, the increase in radar time is heavily dependent on the exact target trajectory; on the period of the manoeuvres, and on the azimuth angle of the target. This is due to the amount of track updates which must be made at large scan angles from array azimuth broadside, necessitating long dwell times to offset the loss in antenna gain. A manoeuvring target trajectory, remaining mainly close to array azimuth broadside of the static array, would require a greater radar time for tracking in rotating array case. Conversely, for a target trajectory close to 60° away from azimuth broadside of the static array, the situation is likely to be reversed, the rotating array system requiring less radar time for tracking.

It is thought that the implementation of a multiple model tracker which more accurately represents the target dynamics during manoeuvre would reduce the necessity to make track updates at great angles from array azimuth broadside. This would reduce the radar time required for tracking with a rotating array multi-function radar, as well as increase the smoothed track accuracy during target manoeuvre. This is proposed as an area of further work.

Another method by which the radar time required for the tracking function may be reduced in a system which utilised simultaneous multiple beam processing would be to utilise group tracking methods, i.e. synchronising track updates on closely spaced targets. This may also be worth further study, although the benefit that will be accrued will depend upon the likely target density in relation to the radar beamwidth.

9 REFERENCES

Adams, M.: 'The Little Book of Map Projections', G. Phillip and Son, 1914

Applebaum, S.P.: 'Adaptive Arrays', *IEEE Trans. AP-24*, 1976. pp 650-662

Barbato,A. & Giustiniani, P.: 'An Improved Scheduling Algorithm for a Naval Phased Array Radar', *Proc. of Radar 92*, IEE Conf. Publ., No. 365, 1992 , pp 42-45

Barton, D.K.: 'Modern Radar System Analysis', Artech House, 1988

Bayliss, E.T.: 'Design of Monopulse Antenna Difference Patterns with Low Sidelobes', Bell System Technical Journal 47, No.5, 1968

Best, J.H.: 'Phased Array Co-ordinate Transformations', *The Microwave Journal*, July 1962

Billam, E.R.: 'Design and Performance Considerations in Modern Phased Array Radar', *Proc. of Radar 82*, IEE Conf. Publ. No. 216, 1982 , pp 15-29

Billam E.R.: 'New Techniques in Phased Array Radar', *Proc. of 15th European Microwave Conference*, 1985 , pp 15-19

Billam, E.R.: 'The Optimisation of Beam Position Separation in Phased Array Radar', *Proc. CIE International Conference on Radar*, 1986 , pp 359-370

Billam, E.R.: 'Phased Array Radar and the Royal Navy', *Journal of Naval Science*, Vol. 12, No. 2, 1986

Billam, E.R. & Harvey, D.H.: 'MESAR - An Advanced Experimental Phased Array Radar', *Proc. Radar 87*, IEE Conf. Publ. No. 281, 1987 , pp 37-40

Billam, E.R.: 'Phased Array Radar and the Detection of Low Cross Section Targets', *Proc. of European Military Microwave Conference*, 1989a, pp 55-65

Billam, E.R.: 'MESAR - The Application of Modern Technology to Phased Array

Radar', IEE Tutorial Meeting on Phased Array Radar, September 1989b

Billam, E.R.: 'Parameter Optimisation in Phased Array Radar', *Proc. of Radar 92*, IEE Conf. Publ., No. 365, 1992 pp 34-37

Billam, E.R.: 'Parameter Optimisation in Phased Array Radar', Ph.D. Thesis, University of Birmingham, 1994

Billam, E.R.: 'The Problem of Time in Phased Array Radar', *Proc. of Radar 97*, IEE Conf. Publ., No. 449, 1997a pp 565-567

Billam, E.R.: 'Rotating versus Fixed Active Arrays for Multifunction Radar', *Proc. of Radar 97*, IEE Conf. Publ., No. 449, 1997b, pp 573-575

Billeter, D.R.: 'Multifunction Array Radar', Artech House, 1989

Birch, P.: 'MESAR Task Scheduler', MESAR Technical Design Note No. 240, Siemens Plessey Radar Technical Note, 1990

Blackman, S. S.: 'Multiple Target Tracking with Radar Applications', Artech House, 1986

Blair, W.D. & Watson, G.A. 'Benchmark Problem for Radar Resource Allocation and Tracking Manoeuvring Targets in the Presence of False Alarms and ECM', Naval Surface Warfare Center, Dahlgren Division, Technical Report No. NSWCDD/TR-96/10, 1996

Blair, W.D. & Watson, G.A.: 'IMM Algorithm Solution to Benchmark Problem for Tracking Manoeuvring Targets', *Proc. SPIE 2221*, 1994 pp 476-488

Blair, W.D., Watson, G.A. & Hoffman, S.A.: 'Benchmark Problem for Beam Pointing Control of Phased Array Radar Against Manoeuvring Targets', *Proc. of American Control Conference*, 1994 , pp 2071-2075

Blair, W.D., Watson, G.A., Gentry, G.L. & Hoffman, S.A.: 'Benchmark Problem for Beam Pointing Control of Phased Array Radar Against Manoeuvring Targets in the Presence of False Alarms and ECM', *Proc. of American Control Conference*, 1995, pp 2601-2605

Butler, J.M.: 'UK/US MESAR Trials Report', Defence Research Agency Technical

Report, No. DRA/AW/AWI/AWIR/CR/Cr95306/1.0, 1995

Butler, J.: 'Beam Pointing Errors in Tracking Manoeuvring Targets', Defence Research Agency Technical Report, No. DRA/AW/AWI/AWIS/WP/Wp94210/1.0, 1994

Butler, J.M., Moore, A.R., & Griffiths, H.D., 'Resource Management for a Rotating Array Multi-Function Radar', *Proc. of Radar 97*, IEE Conf. Publ., No. 449, 1997

Castella, F.R.: 'An Adaptive 2-Dimensional Kalman Tracking Filter', *IEEE Trans. AES*, Vol. AES-16, No. 6, Nov. 1980 pp 821-829

Chamberlin, W.: 'The Round Earth on Flat Paper: Map Projections used by Cartographers', National Geographic Society Press, 1947

Chestnutt, J.: 'Overview of the MESAR Task Scheduler Subsystem', MESAR Technical Design Note No. 131, Siemens Plessey Radar Technical Note, 1984

Cohen, S.A.: 'Adaptive Variable Update Rate Algorithm for Tracking Targets with a Phased Array Radar', *IEE Proc. F*, Vol. 133, No. 3, 1986 pp 127-280

Daeipour, E., Bar-Shalom, Y., Li, X.: 'Adaptive Beam Pointing Control of a Phased Array Radar using an IMM Estimator', *Proc. of American Control Conference*, 1994 pp 2093-2097

Daum, F.E & Fitzgerald, R.J.: 'Decoupled Kalman Filters for Phased Array Radar Tracking', *IEEE Trans. on Automatic Control*, Vol. 28, No. 3, 1983 pp 269-283

Dolph, C.L.: 'A Current Distribution for Broadside Arrays which Optimises the relationship between Beamwidth and Sidelobe Level', *Proc. IRE*, Vol. 34, 1946

Gardner, L.A. & Mullen, R.J.: 'Constant Gain Tracker with Variable Frame Time', *IEEE Trans. on Aerospace and Electronic Systems*, Vol. 24, No. 4, 1988, pp 322-336

Godbehere, D.B.: 'The MESAR Scheduler Investigation', Private Communication between Siemens Plessey Systems, Cowes and Defence Research Agency, Portsdown, 1996

Harris, F.J.: 'On The Use Of Window Functions For Harmonic Analysis With The Discrete Fourier Transform', *Proc. IEEE*, Vol. 66, No.1, 1978

Kahrilas, P.J.: 'Electronic Scanning Radar Systems Design Handbook', Artech House, 1976

Kingsley S. & Quegan,S .: 'Understanding Radar Systems', McGraw-Hill Book Company, 1992

Kirubarajan, T., Bar-Shalom, Y., Blair & W.D., Watson: 'IMMPDAF Solution to Benchmark for Radar Resource Allocation and Tracking Targets in the Presence of ECM', *IEEE Trans. on Aerospace and Electronic Systems*, Scheduled to appear in October 1998

Levanon, N.: 'Radar Principles', John Wiley & Sons, 1988

Milne, K.: 'Synthesis of Power Radiation Patterns for Linear Array Antennas', *IEE Proc.*, Vol. 134, Pt. H, No.3, June 1987 , pp 285-296

Money, D.G.: 'Naval Environment Clutter, Attenuation and Propagation Specifications', Defence Research Agency Technical Report, No. DRA/SS/SSWI/WP95016/1.0, 1995

Moore, A.R. & Butler, J.M.: 'Digital Adaptive Beamforming Progress', Defence Research Agency Technical Report, No. DRA/AW/AWI/AWIS/CR94304/1.0, 1994

Moore, A.R., Levett, W.A., & Butler, J.M.: 'Active Multifunction Radar in Theatre Missile Defence', *Proc. 8th Int. Conference on Theatre Missile Defence*, 1995

Moore, A.R., Salter, D.M.: 'Multifunction Radar for Naval Weapons System Applications', *Proc. International Maritime Defence Exhibition 95*, 1995

Munu, M., Harrison, I., Wilkin, D. & Woolfson, M.S.: 'Comparison of Adaptive Target Tracking Algorithms for Phased Array Radar', *IEE Proc. F*, Vol. 139, No.5, 1992 pp 336-342

Noyes, S.P.: 'Finding the Time of Next Update', MESAR Technical Design Note No. 243, Siemens Plessey Radar Technical Note, 1990

Noyes, S.P.: 'Plot to Track Association', MESAR Technical Design Note No. 246, Siemens Plessey Radar Technical Note, 1990

Noyes, S.P.: 'Track Smoothing Algorithms', MESAR Technical Design Note No. 242, Siemens Plessey Radar Technical Note, 1990

Orman A.J. & Potts C.N.: 'On the Complexity of Coupled-Task Scheduling', Discrete Applied Mathematics, No. 72, 1997

Orman A.J., Potts C.N., Shahani A.K. & Moore A.R.: 'Scheduling for a Multifunction Phased Array Radar System', *European Journal of Operational Research*, No. 90, 1996

Popoli, R. & Blackman, S.S.: 'Expert System Allocation for the Electronically Scanned Antenna Radar', *Proc. of American Control Conference*, 1987, pp 1821-1826

Quigley, A.L.C. & Holmes, J.E.: 'The Development of Algorithms for the Formation and Updating of Tracks', Admiralty Signals and Weapons Establishment Technical Report (Classification Unlimited), 1975

Rhatigan, B.R., Kalata, P.R., Chmielewski, T.A.: 'An α–β Target Tracking Approach to the Benchmark Tracking Problem', *Proc. of American Control Conference*, 1994 pp 1076-1080

Rhodes, D.R., An introduction to monopulse, McGraw-Hill Book Company, 1959

Sabatini, S. and Tarantino, T.: 'Multifunction Array Radar, System Design and Analysis', Artech House, 1994

Salter, D.M.: 'MESAR - The Plessey/Admiralty Research Establishment Adaptive Phased Array Demonstrator', *Proc. Military Microwaves 88*, 1988 pp 55-59

Salter, D.M.: 'IS&T Final Report', Roke Manor Research Technical Report, No. 72/96/R/63C, 1992

Sastry, C.R., Slocumb, B.J., West, P.D., Kamen, E.W., Stalford, H.L.: 'Tracking a Manoeuvring Target Using Jump Filters', *Proc. of American Control Conference*, 1994 pp 2031 - 2087

Shin, H.J., Hong, S.M., Hong, D.H.: 'Adaptive Update Rate Target Tracking for Phased Array Radar', *IEE Proc. Radar, Sonar and Navigation*, Vol. 142, No. 3, June 1995 pp 137-143

Skolnik, M. I.: 'Radar Handbook', McGraw-Hill, 1970

Skolnik, M.I.: 'An Introduction to Radar Systems', McGraw-Hill, 1981

Stafford, W.K.: 'Real-time Control of a Multifunction Electronically Scanned Adaptive Radar (MESAR)', IEE Colloquium on Real Time Management of Adaptive Radar Systems, June 1990

Stafford, W.K.: 'Tracking Waveform Selection', MESAR Technical Design Note No. 248, Siemens Plessey Radar Technical Note, 1991

Sworder, D.D. & Boyd, J.E.: 'Dual-Path Algorithms for the Bench Mark Tracking Problem', Proc. of American Control Conference, 1994, pp 1080-2092

Taylor, T.T.: 'Design Of Line-Source Antennas for Narrow Beamwidth and Low Sidelobes', *IRE Trans. Antennas and Propagation*, Vol. AP7, 1955

Tsaknakis, H. & Athans, M.: 'Tracking Manoeuvring Targets Using H_∞ Filters', *Proc. of American Control Conference*, 1994, pp 1796-1803

Tunnicliff, J.: 'The MESAR Tracking Algorithm', MESAR Technical Design Note, No. 23, Admiralty Signals and Weapons Establishment Technical Note, 1980

Van Keuk, G. & Blackman, S.S.: 'On Phased Tracking and Array Parameter Control', *IEEE Trans. on Aerospace and Electronic Systems*, Vol. 29, No. 1, 1993, pp 186-194

Van Keuk, G.: 'Software Structure and Sampling Strategy for Automatic Tracking with a Phased Array Radar', *AGARD Conf. Proceedings*, No. 252, 1978

Villeneuve, A.T.: 'Taylor Patterns for Discrete Arrays', *IEEE Trans. Antennas and Propagation*, Vol. Ap-32, 1984 pp 1089-1093

Von Aulock, W.: 'Properties of Phased Arrays', *Proc. IRE*, Vol. 48, 1960

Watson, G.A. & Blair, W.D.: 'Multiple Model Estimation for Control of a Phased Array Radar', *SPIE*, Vol. 1954, 1993 pp 456-461

Wilkin, D.J., Harrison, I. & Woolfson, M.S.: 'Target Tracking Algorithms for Phased Array Radar', *IEE Proc. F*, Vol. 138, No. 3, 1991 pp 255-262

Woodward, P.M.: 'Method of Calculating the Field Over a Plane Aperture Required to Produce a Given Polar Diagram', *J. IEE*, Vol. 93, Pt. IIIa, 1947

Wray, M.: 'Software Architecture for Real Time Control of the Radar Beam within MESAR', *Proc. of Radar 92*, IEE Conf. Publ., No. 365, 1992 pp 38-41

APPENDIX A

THE BENCHMARK TRACKING PROBLEM

The benchmark tracking problem was proposed in 1994 [Blair et al, 1994] to cope with the lack of a common means of comparing different tracker systems. The benchmark problem addressed beam pointing control of a phased array radar against highly manoeuvring targets, and has been widely applied in the U.S. ([Rhatigan et al, 1994], [Sastry et al, 1994], [Sworder & Boyd, 1994], [Daeipour et al, 1994], [Tsaknakis & Athans, 1994], [Blair & Watson, 1994], [Kirubarajan et al, 1998]). The bench mark problem specified;

i. a set of target trajectories against which to assess the tracker
ii. a model of the radar measurement process
iii. a set of metrics by which the tracker may be assessed

It has since been used, especially in the U.S., as a standard against which different phased array tracker systems may be compared, and has been revised subsequently in 1995 [Blair et al, 1995] and 1996 [Blair & Watson, 1996].

It was intended to employ part of the benchmark for further work in this area. However, it was necessary to extend the benchmark model extensively to study this problem, since it applies only to a static face phased array multi-function radar, and also, does not allow for the generation of multiple receive beams. Also, the model is provided in MATLAB, which would have proved to slow to allow the parameter investigation that was required to be undertaken. The entire model would thus have needed to be translated into a compilable language such as C or Fortran to enable the Montecarlo analysis undertaken.

Therefore, employing the entire Benchmark model is proposed as an area of further work. In this study only the Benchmark target trajectories are included within the investigation.

Target Scenarios

Six target scenarios are specified within the benchmark problem. The benchmark scenarios have been reproduced from [Blair & Watson, 1996], and are shown in Figure A-1 to Figure A-3 below. The start point of each trajectory is marked with a circle. The targets exhibit cross sectional fluctuations according to the Swerling Case 3 model and perform up to 7g lateral acceleration, and 2g longitudinal acceleration. Target ranges vary between 20 - 120 km, and target elevations vary between 0° to 80°. Since the model considers only a static single faced multi-function radar, the target azimuth varied between ±60°. The six target scenarios each represent a different target type.

The first trajectory is representative of a large aircraft, such as a military cargo aircraft. The aircraft flies with a constant speed of 290 m/s and performs a 2g turn, and then a 3g turn.

The second trajectory is representative of a smaller, more manoeuverable, high performance commercial aircraft. The aircraft flies with a speed of 305m/s and performs a 2.5g turn through 90°, before descending and performing a second 4g manoeuvre.

The third and fourth trajectories are both representative of medium, high speed bombers, with good manoeuverability. The third trajectory aircraft flies at a constant height, and initial speed of 457m/s. A 45° 4g turn is made, followed by a second 4g turn of 90°. In the subsequent period of straight and level flight the aircraft decelerates to a speed of 274m/s.

The fourth trajectory has an initial speed of 251m/s and height of 2.29km. The first 4g, 45° manoeuvre is followed a period of straight and level, constant velocity flight. A 6g turn is then made, and the aircraft accelerates to a height of 4.57km, where the aircraft levels out and flies at constant velocity.

The final two trajectories are representative of fighter/attack aircraft. Trajectory five begins with a period of longitudinal maximum thrust acceleration (<1g) at a height of 1.5km. A 5g turn is made, whilst the throttle is maintained. 20s later a 7g turn is made, after which straight and level, constant velocity flight occurs. A 6g turn is then made, whilst the aircraft pitches up concurrently, and climbs to an altitude of 4.45km, where the aircraft levels out and flies at constant velocity.

The sixth trajectory begins with straight and level, constant velocity flight at a speed of 426m/s and height of 1.55km. A 7g turn is made, followed later by a 6g turn, in which the aircraft is turned nose down to decrease its altitude to a height of 0.79km. A period of constant height, low longitudinal acceleration flight follows, before a 6g turn is made. A period of full thrust acceleration (<1g) is followed by a 7g turn, and constant velocity flight.

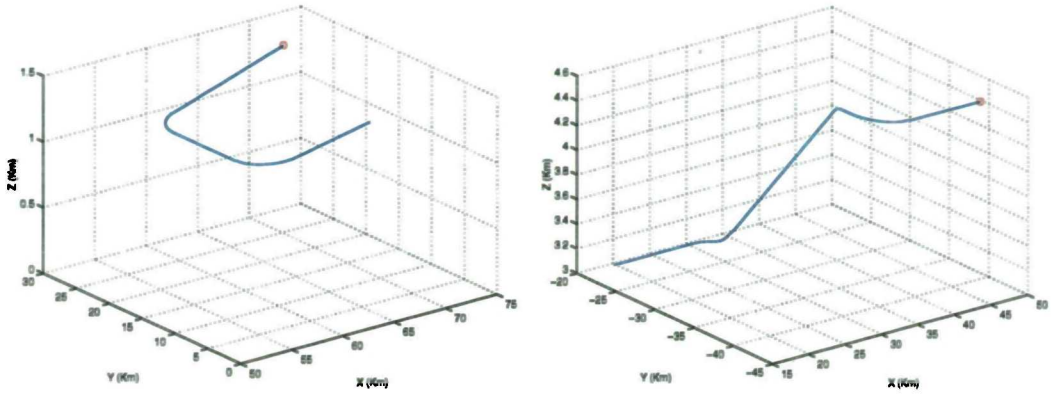

Figure A-1(a,b) Benchmark tracking problem trajectories 1 (a) and 2 (b)

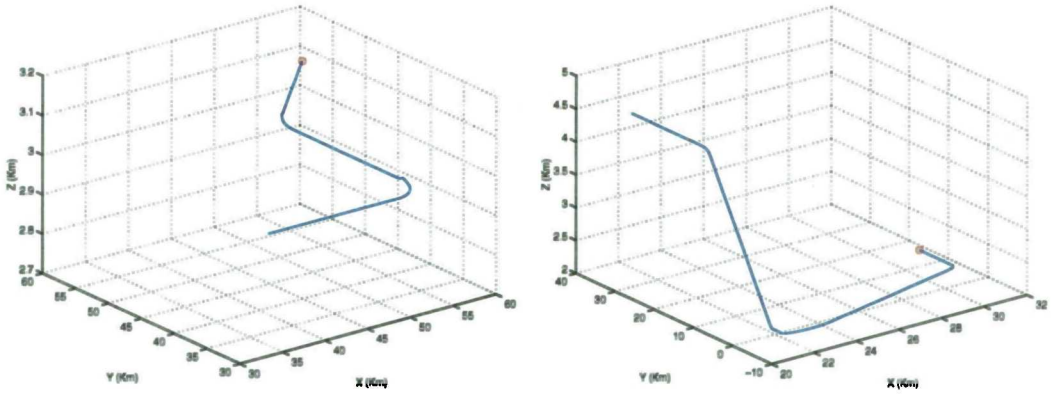

Figure A-2(a,b) Benchmark tracking problem trajectories 3 (a) and 4 (b)

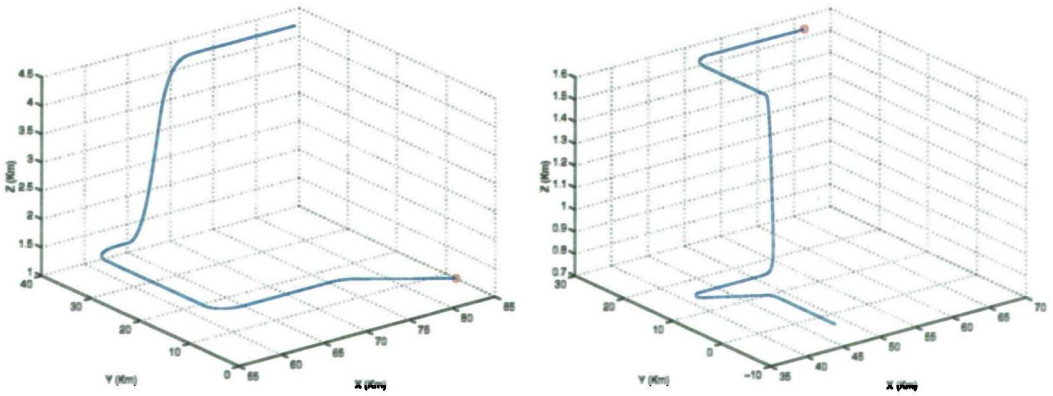

Figure A-3(a,b) Benchmark tracking problem trajectories 5 (a) and 6 (b)

Modeling of the Target Measurement Process

The radar that is specified in the Benchmark Problem is a 4 GHz phased array using amplitude comparison monopulse. The array consists of 3025 elements, and is tilted back 15° from vertical. Each track update consists of one phase/frequency coded pulse, from a selection of eight specified waveforms. The range gate is approximately 1.6km for a track dwell and 10km for a search dwell. The radar 3dB beamwidth is 2.4° on broadside, and broadens to 4.5° at maximum scan. The radar has a maximum scan angle of 60°, and a single pencil beam.

The model uses the radar equation to model target detection. The output signal to noise ratio for the compressed pulse, SNR_c, is given by equation [A-1], and the radar parameters in Table A-1.

$$SNR_c = \frac{P_t G_t G_r \lambda^2 F_t^2 F_r^2 \sigma_o}{(4\pi)^3 L_{tot}} \left(\frac{N_s \tau_c}{k_o T_o F_n} \right) \left(\frac{G_{stc}\{R\}}{R^4} \right) \qquad [A\text{-}1]$$

where F_t is the transmit propagation factor
F_r is the receive propagation factor
σ_o is the target rcs
L_{tot} are the total losses for the radar system
N_s is the number of discrete sub-pulses in the transmitted pulse
τ_c is the sub-pulse width, assumed to be equal to the compressed pulse width
k_o is the Boltzmann constant
T_o is the reference temperature
F_n is the receiver noise figure
$G_{stc}\{R\}$ is the sensitivity time control gain with range

P_t	1 MW
G_t , G_r	36.8 dB
λ	7.5 cm
F_t , F_r	0 dB
L_{tot}	21.6 dB
T_o	290 K
F_n	3 dB

Table A-1 Radar equation parameters for the Benchmark Problem

Eight sets of waveform parameters are specified, as is the sensitivity time control function with range. Functions are specified for the calculation of antenna gain patterns, sum and difference channel voltages and monopulse angular estimation.

The RCS of the target is modeled as Swerling 3, where the average RCS, σ_{ave}, varies between target scenarios. It may be computed by solving equation [A-2] below, where

x is a random number, uniformly distributed between 0 and 1.

$$\left(1+\frac{2\sigma_o}{\sigma_{ave}}\right)\exp\left(-\frac{2\sigma_o}{\sigma_{ave}}\right)=1-x \qquad [A\text{-}2]$$

Metrics

The primary measure of tracking performance in the Benchmark Problem is a weighted sum of the average radar energy per second and the average radar time per second. The average energy per second, E_{ave}, is the sum of the energy of the track dwells scheduled by the tracking algorithm divided by the number of seconds of the trajectory. The average radar time per second, T_{ave}, is the sum of the radar time of the track dwells scheduled by the tracking algorithm, divided by the number of seconds of the trajectory. Two cost functions are then defined;

$$C_1 = E_{ave} + 10^3 T_{ave}$$

$$C_2 = E_{ave} + 10^5 T_{ave} \qquad [A\text{-}3]$$

C_1 corresponds to a period of operation when radar energy is critical, and C_2 corresponds to a period of operation when radar time is critical. The objective is to minimise one of the cost functions on request. The best algorithm is determined as the one that minimised the appropriate cost function, while satisfying a constraint of 4% on the maximum number of tracks lost during the Monte Carlo simulation.

A secondary metric is the computer resources that are required for implementation of each algorithm. The number of floating point operations per second that the algorithm requires in its final implementation is to be calculated.

APPENDIX B

STATIC ARRAY TRACKER MONTECARLO SIMULATION RESULTS: BENCHMARK TARGETS 1 TO 6 & CONSTANT VELOCITY TRAJECTORY

A complete set of Montecarlo simulation results is presented here of the multiple beam, static array tracker that was developed. A beamwidth of 2.5° has been used.

Static Array Multi-function Radar

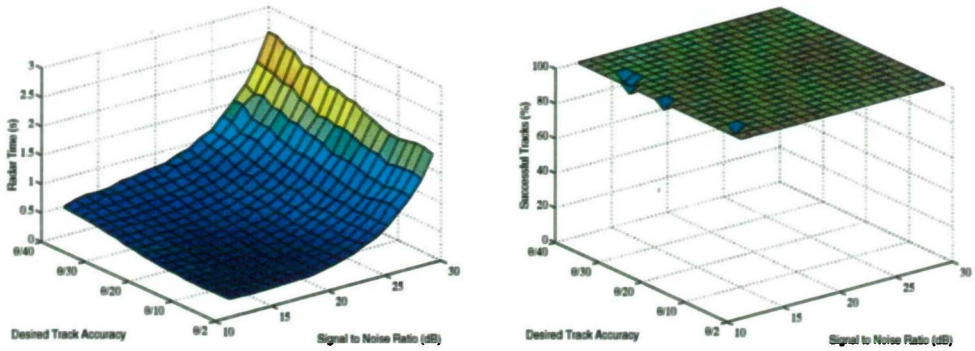

Figure B-1(a,b) Total radar time required to maintain track on Benchmark target trajectory 1, and (b) the percentage of successful tracks. Static array system with a beamwidth of 2.5°

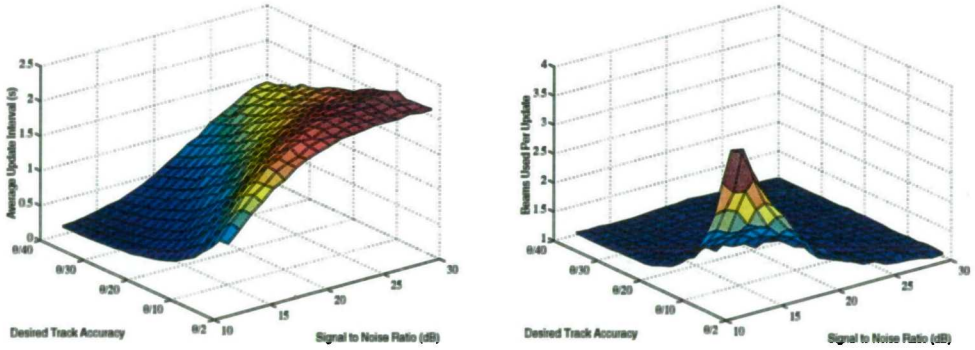

Figure B-2 (a,b) Average track update interval required to maintain track on Benchmark target trajectory 1, (b) Average number of beams required for each track update. Static array system with a beamwidth of 2.5°

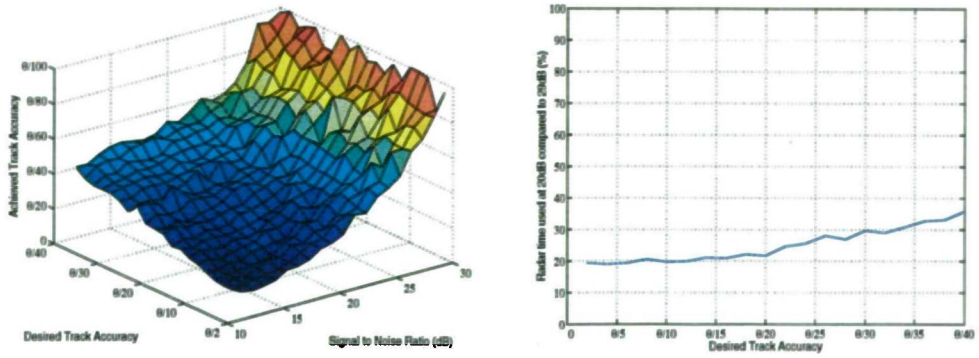

Figure B-3(a,b) Achieved smoothed track accuracy for Benchmark target trajectory 1, excluding periods of manoeuvre, and (b) Percentage of radar time required for tracking Benchmark target trajectory 1 using only a 20dB signal to noise ratio instead of a 29dB signal to noise ratio. Static array system with a beamwidth of 2.5°

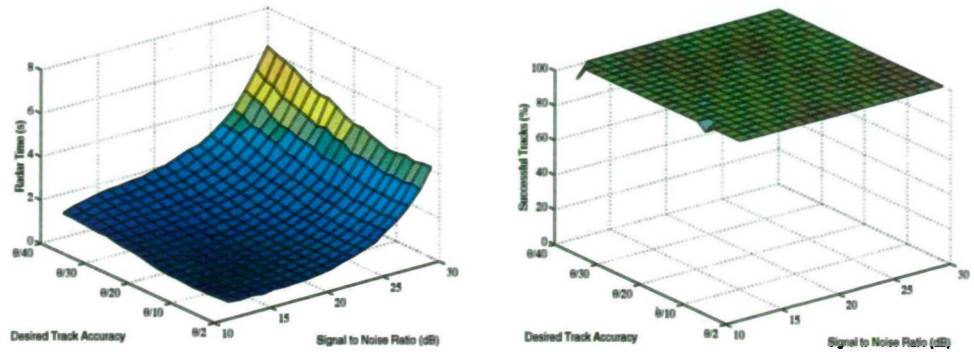

Figure B-4(a,b) Total radar time required to maintain track on Benchmark target trajectory 2, and (b) the percentage of successful tracks. Static array system with a beamwidth of 2.5°

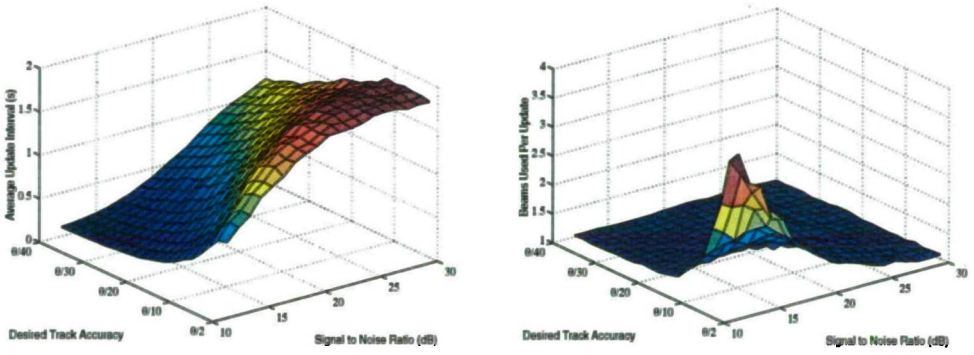

Figure B-5(a,b) Average track update interval required to maintain track on Benchmark target trajectory 2, (b) Average number of beams required for each track update. Static array system with a beamwidth of 2.5°

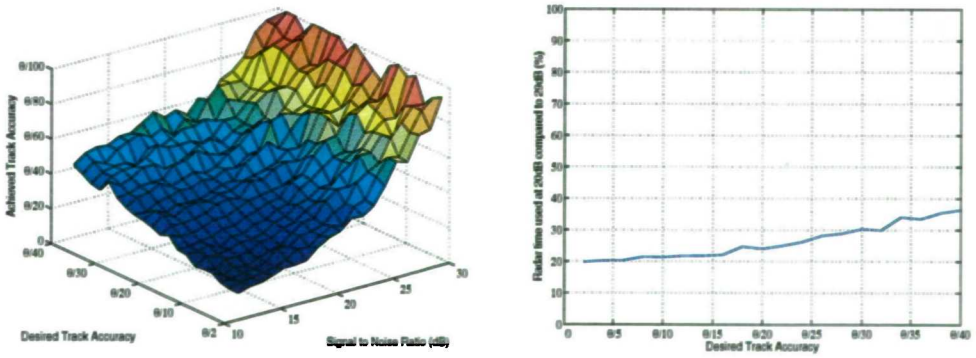

Figure B-6(a,b) Achieved smoothed track accuracy for Benchmark target trajectory 2, excluding periods of manoeuvre, and (b) Percentage of radar time required for tracking Benchmark target trajectory 2 using only a 20dB signal to noise ratio instead of a 29dB signal to noise ratio. Static array system with a beamwidth of 2.5°

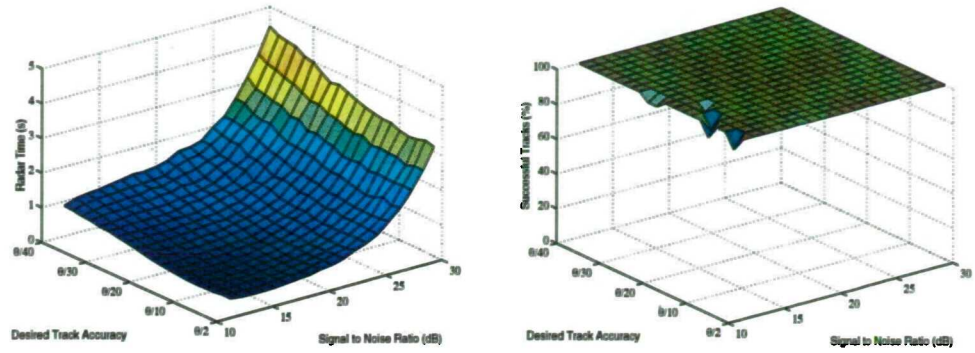

Figure B-7(a,b) Total radar time required to maintain track on Benchmark target trajectory 3, and (b) the percentage of successful tracks. Static array system with a beamwidth of 2.5°

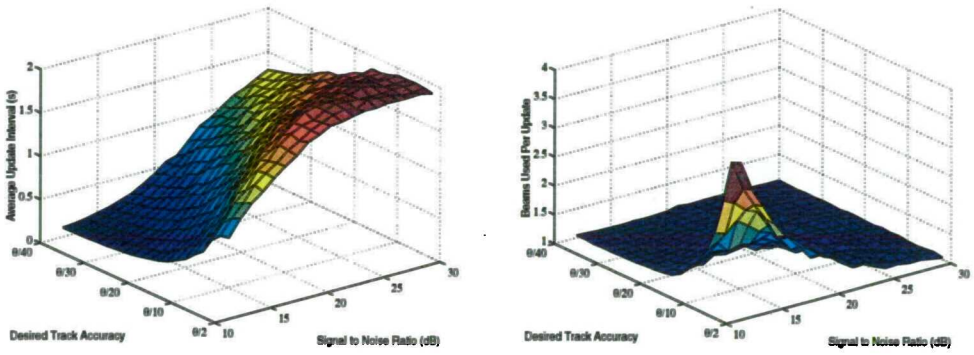

Figure B-8(a,b) Average track update interval required to maintain track on Benchmark target trajectory 3, (b) Average number of beams required for each track update. Static array system with a beamwidth of 2.5°

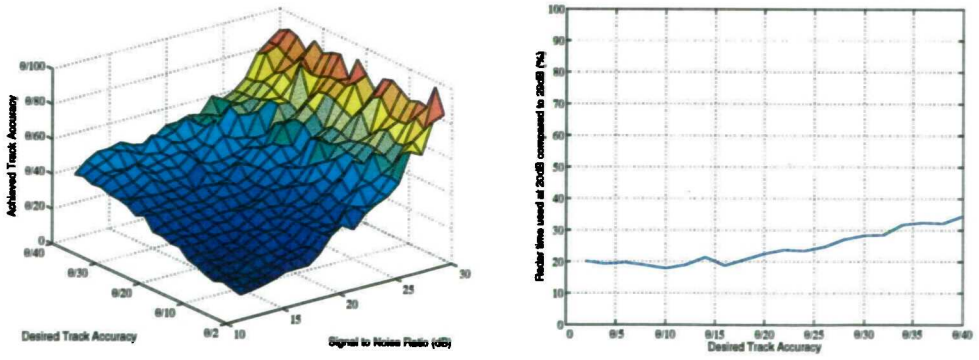

Figure B-9(a,b) Achieved smoothed track accuracy for Benchmark target trajectory 3, excluding periods of manoeuvre, and (b) Percentage of radar time required for tracking Benchmark target trajectory 3 using only a 20dB signal to noise ratio instead of a 29dB signal to noise ratio. Static array system with a beamwidth of 2.5°

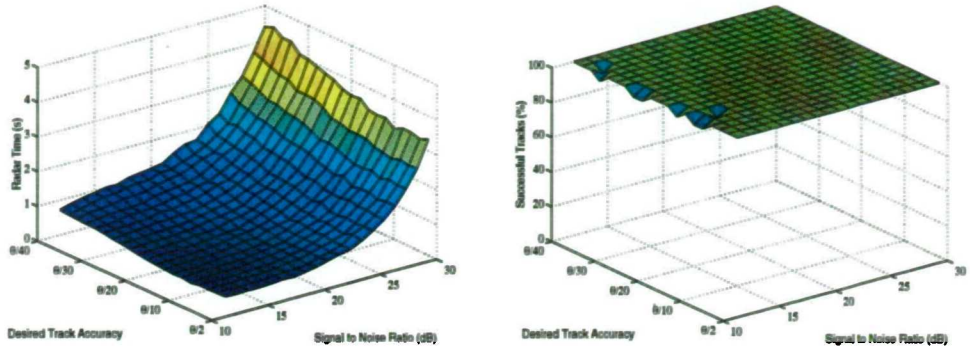

Figure B-10(a,b) Total radar time required to maintain track on Benchmark target trajectory 4, and (b) the percentage of successful tracks. Static array system with a beamwidth of 2.5°

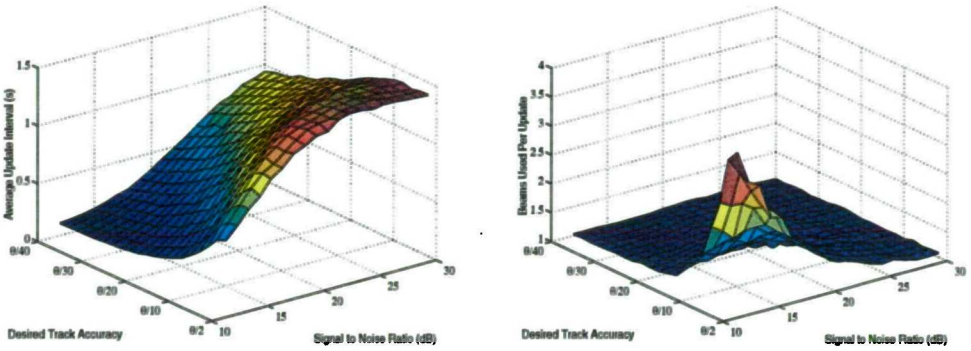

Figure B-11(a,b) Average track update interval required to maintain track on Benchmark target trajectory 4, (b) Average number of beams required for each track update. Static array system with a beamwidth of 2.5°

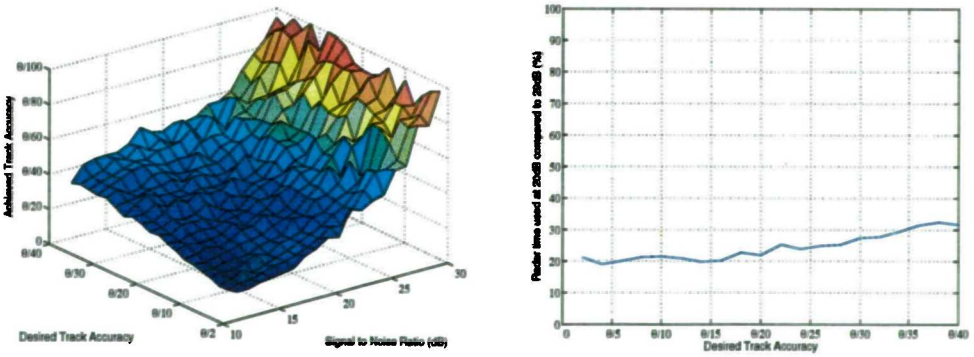

Figure B-12(a,b) Achieved smoothed track accuracy for Benchmark target trajectory 4, excluding periods of manoeuvre, and (b) Percentage of radar time required for tracking Benchmark target trajectory 4 using only a 20dB signal to noise ratio instead of a 29dB signal to noise ratio. Static array system with a beamwidth of 2.5°

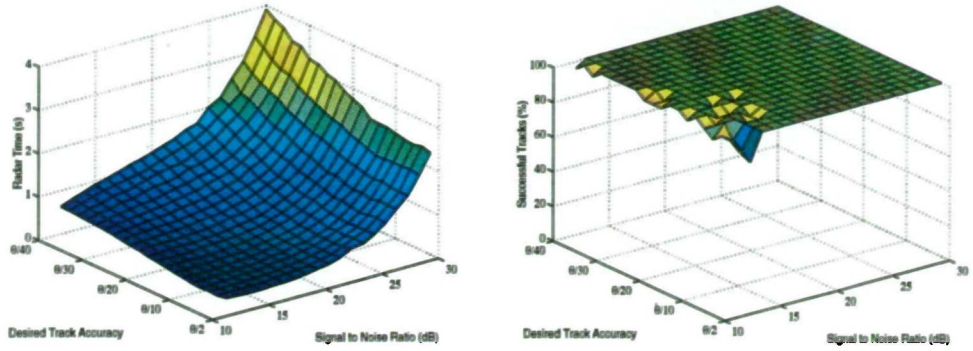

Figure B-13(a,b) Total radar time required to maintain track on Benchmark target trajectory 5, and (b) the percentage of successful tracks. Static array system with a beamwidth of 2.5°

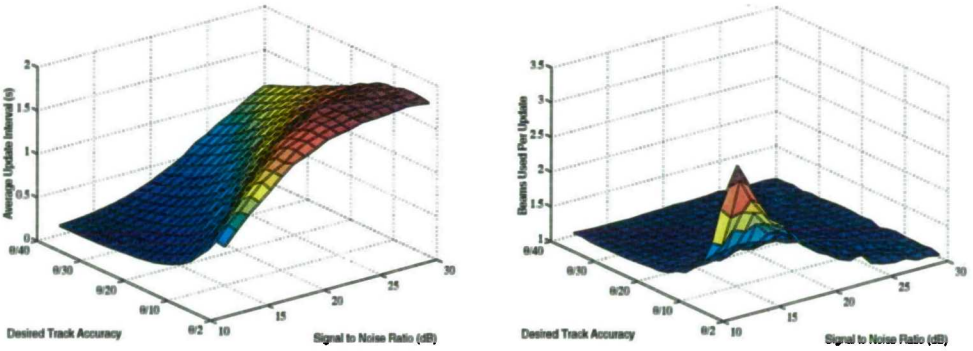

Figure B-14(a,b) Average track update interval required to maintain track on Benchmark target trajectory 5, (b) Average number of beams required for each track update. Static array system with a beamwidth of 2.5°

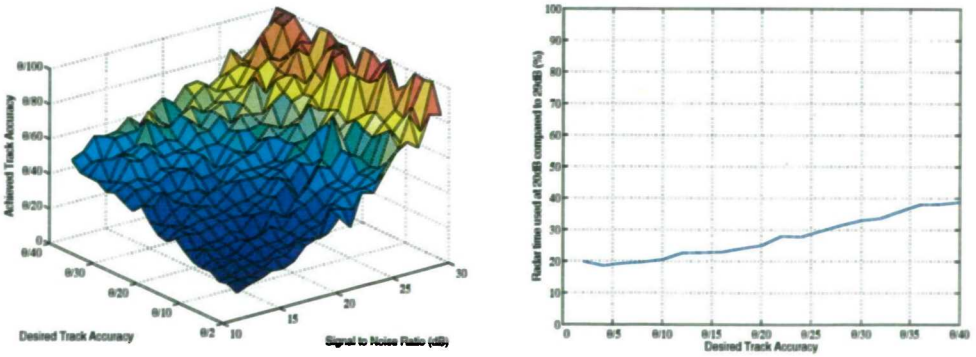

Figure B-15(a,b) Achieved smoothed track accuracy for Benchmark target trajectory 5, excluding periods of manoeuvre, and (b) Percentage of radar time required for tracking Benchmark target trajectory 5 using only a 20dB signal to noise ratio instead of a 29dB signal to noise ratio. Static array system with a beamwidth of 2.5°

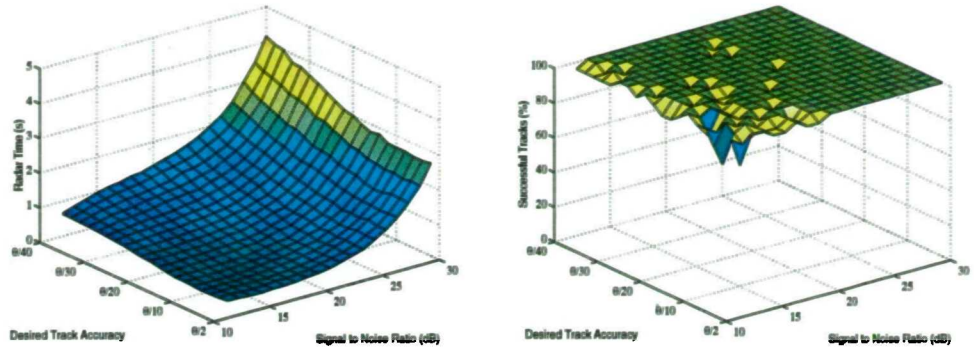

Figure B-16(a,b) Total radar time required to maintain track on Benchmark target trajectory 6, and (b) the percentage of successful tracks. Static array system with a beamwidth of 2.5°

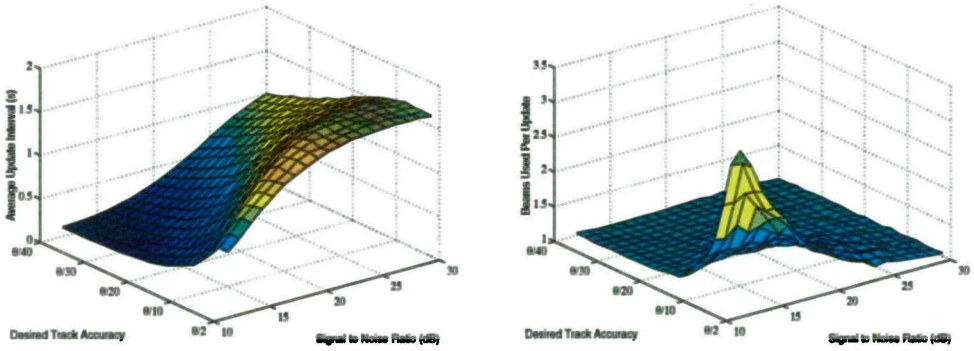

Figure B-17(a,b) Average track update interval required to maintain track on Benchmark target trajectory 6, (b) Average number of beams required for each track update. Static array system with a beamwidth of 2.5°

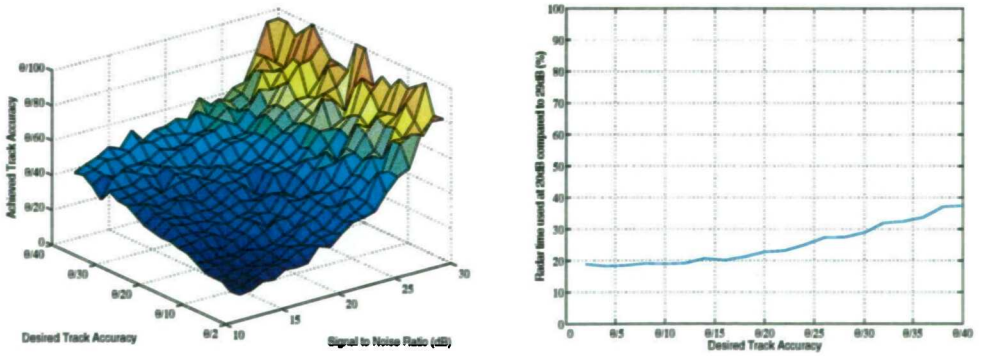

Figure B-18(a,b) Achieved smoothed track accuracy for Benchmark target trajectory 6, excluding periods of manoeuvre, and (b) Percentage of radar time required for tracking Benchmark target trajectory 6 using only a 20dB signal to noise ratio instead of a 29dB signal to noise ratio. Static array system with a beamwidth of 2.5°

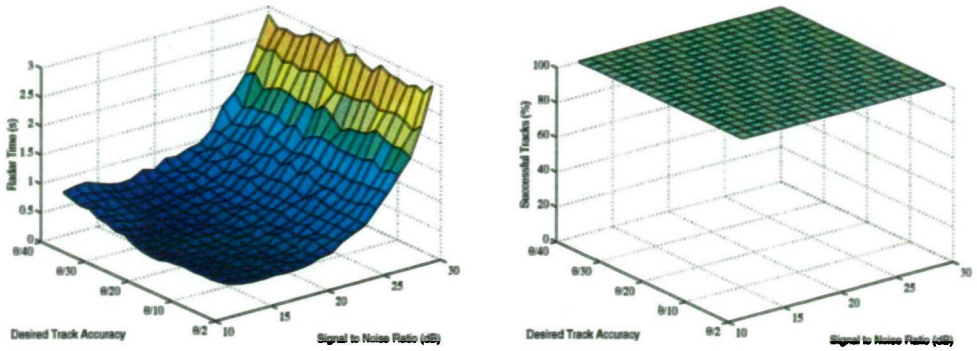

Figure B-19(a,b) Total radar time required to maintain track on the constant velocity trajectory, and (b) the percentage of successful tracks. Static array system with a beamwidth of 2.5°

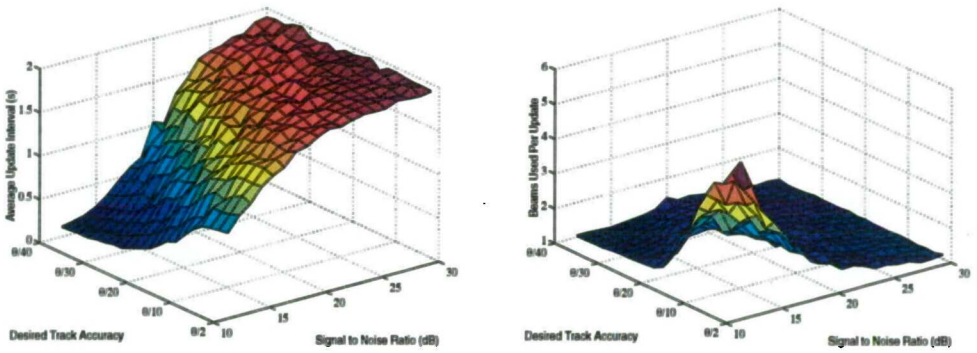

Figure B-20(a,b) Average track update interval required to maintain track on the constant velocity trajectory, (b) Average number of beams required for each track update. Static array system with a beamwidth of 2.5°

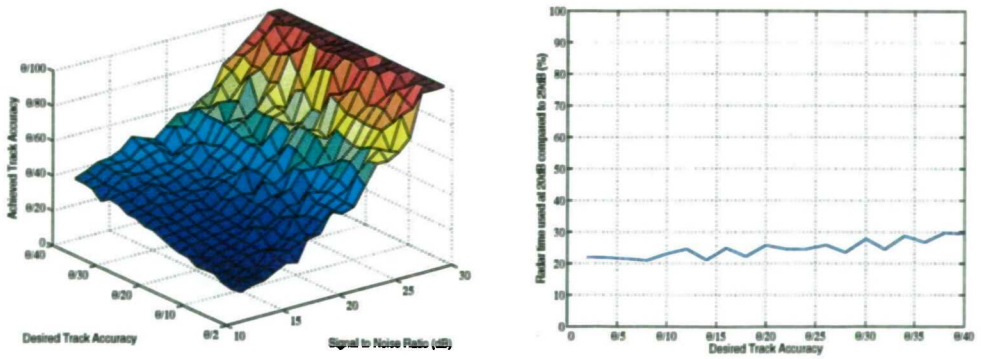

Figure B-21(a,b) Achieved smoothed track accuracy for the constant velocity trajectory, excluding periods of manoeuvre, and (b) Percentage of radar time required for tracking the constant velocity trajectory using only a 20dB signal to noise ratio instead of a 29dB signal to noise ratio. Static array system with a beamwidth of 2.5°

APPENDIX C

ROTATING ARRAY TRACKER MONTECARLO SIMULATION RESULTS: BENCHMARK TARGETS 1 TO 6 & CONSTANT VELOCITY TRAJECTORY

Montecarlo simulation results are presented here of the multiple beam, rotating array tracker developed. A beamwidth of 2.5° was used. A complete set of results are presented for the case of single array multi-function radar rotating with periods of 1s. For the remaining three systems considered, only results for benchmark target trajectory 6 are given for comparison.

Single Array Multi-function Radar, Period 1s

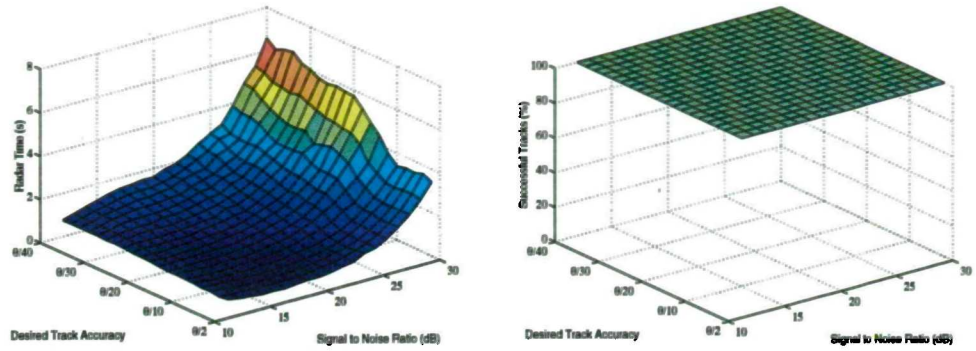

Figure C-1(a,b) Total radar time required to maintain track on Benchmark target trajectory 1, and (b) the percentage of successful tracks. Single faced rotating system with a beamwidth of 2.5°

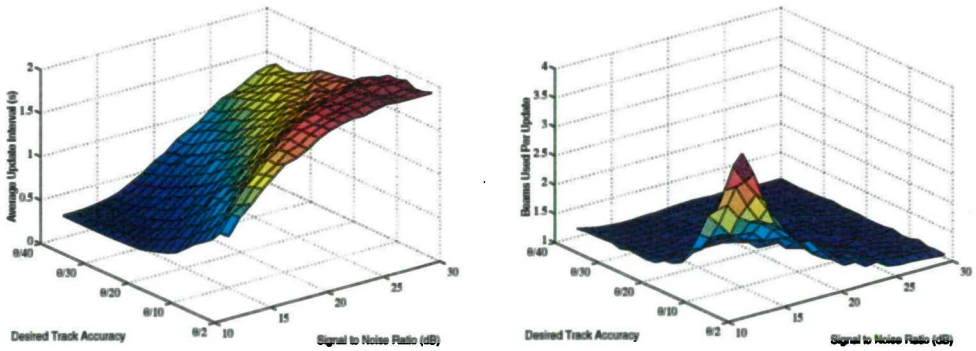

Figure C-2(a,b) Average track update interval required to maintain track on Benchmark target trajectory 1, (b) Average number of beams required for each track update. Single faced rotating system with a beamwidth of 2.5°

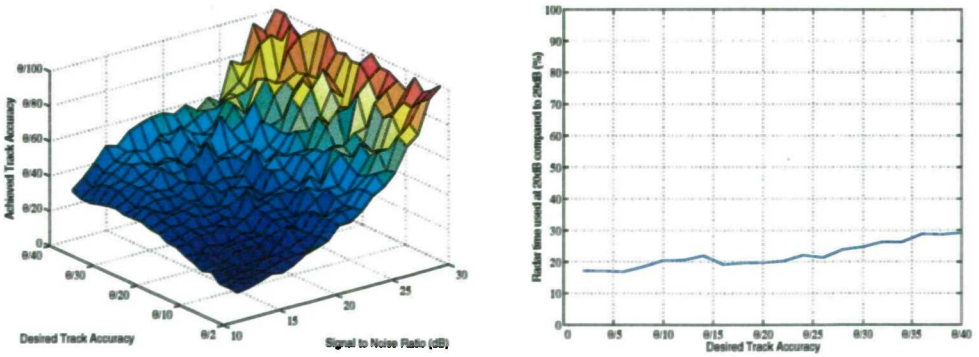

Figure C-3(a,b) Achieved smoothed track accuracy for Benchmark target trajectory 1, excluding periods of manoeuvre, and (b) Percentage of radar time required for tracking Benchmark target trajectory 1 using only a 20dB signal to noise ratio instead of a 29dB signal to noise ratio. Single faced rotating system with a beamwidth of 2.5°

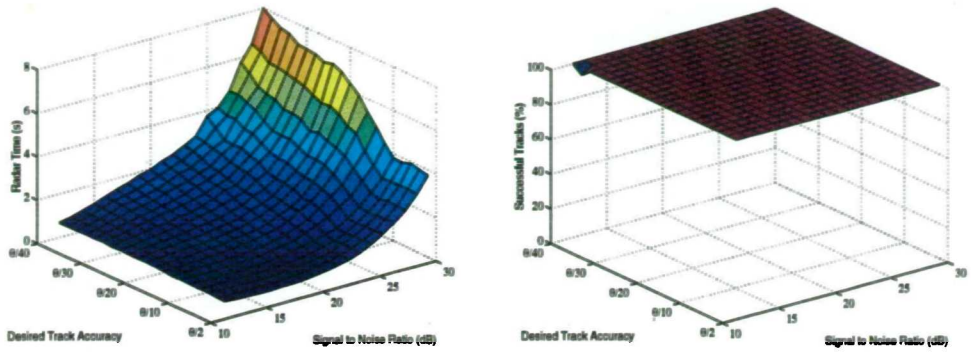

Figure C-4(a,b) Total radar time required to maintain track on Benchmark target trajectory 2, and (b) the percentage of successful tracks. Single faced rotating system with a beamwidth of 2.5°

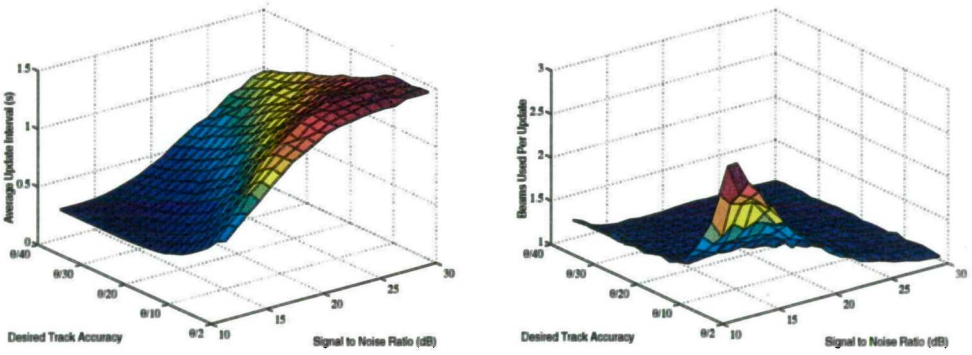

Figure C-5(a,b) Average track update interval required to maintain track on Benchmark target trajectory 2, (b) Average number of beams required for each track update. Single faced rotating system with a beamwidth of 2.5°

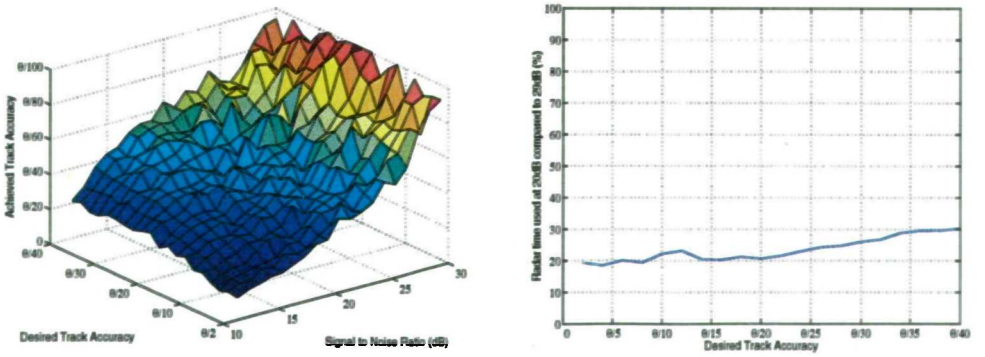

Figure C-6(a,b) Achieved smoothed track accuracy for Benchmark target trajectory 2, excluding periods of manoeuvre, and (b) Percentage of radar time required for tracking Benchmark target trajectory 2 using only a 20dB signal to noise ratio instead of a 29dB signal to noise ratio. Single faced rotating system with a beamwidth of 2.5°

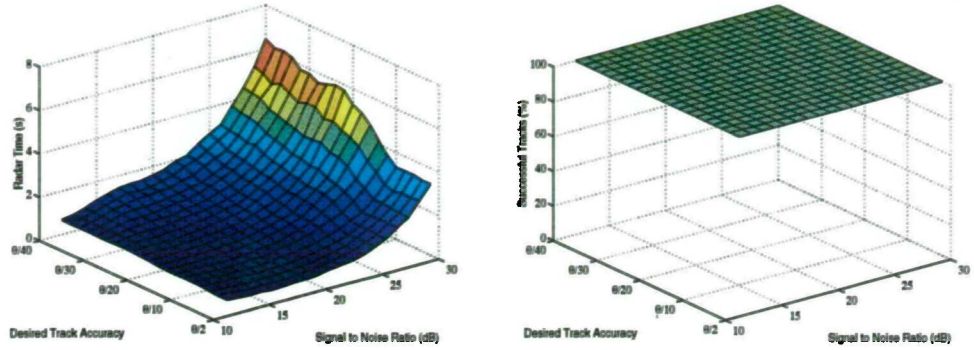

Figure C-7(a,b) Total radar time required to maintain track on Benchmark target trajectory 3, and (b) the percentage of successful tracks. Single faced rotating system with a beamwidth of 2.5°

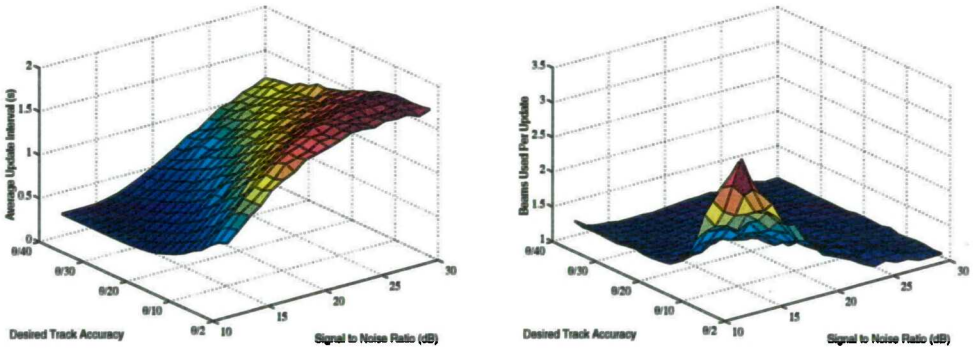

Figure C-8(a,b) Average track update interval required to maintain track on Benchmark target trajectory 3, (b) Average number of beams required for each track update. Single faced rotating system with a beamwidth of 2.5°

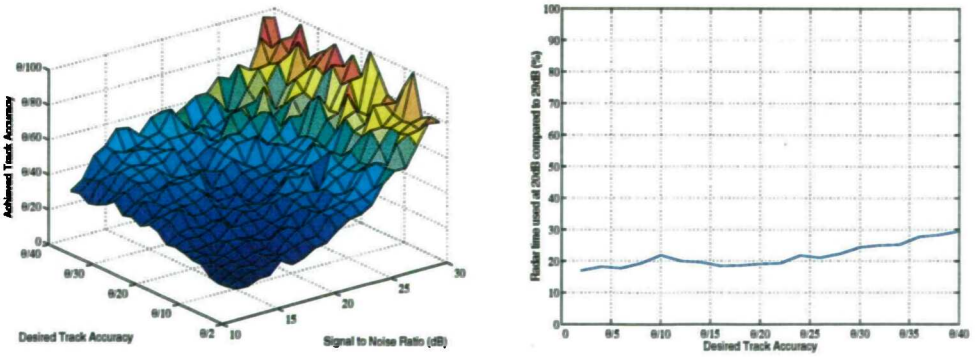

Figure C-9(a,b) Achieved smoothed track accuracy for Benchmark target trajectory 3, excluding periods of manoeuvre, and (b) Percentage of radar time required for tracking Benchmark target trajectory 3 using only a 20dB signal to noise ratio instead of a 29dB signal to noise ratio. Single faced rotating system with a beamwidth of 2.5°

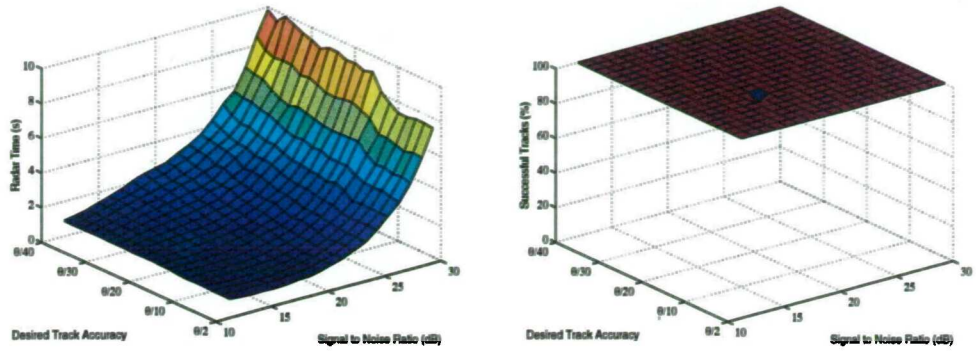

Figure C-10(a,b) Total radar time required to maintain track on Benchmark target trajectory 4, and (b) the percentage of successful tracks. Single faced rotating system with a beamwidth of 2.5°

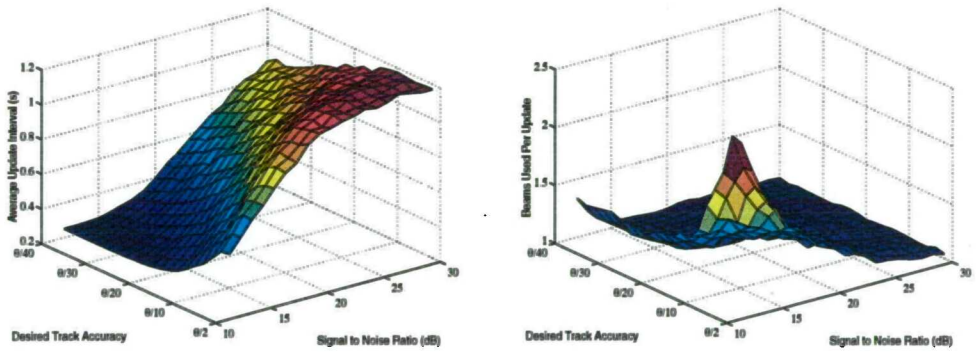

Figure C-11(a,b) Average track update interval required to maintain track on Benchmark target trajectory 4, (b) Average number of beams required for each track update. Single faced rotating system with a beamwidth of 2.5°

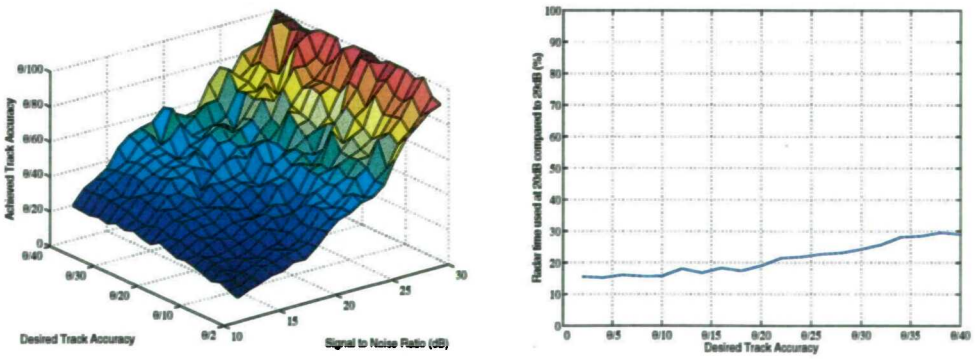

Figure C-12(a,b) Achieved smoothed track accuracy for Benchmark target trajectory 4, excluding periods of manoeuvre, and (b) Percentage of radar time required for tracking Benchmark target trajectory 4 using only a 20dB signal to noise ratio instead of a 29dB signal to noise ratio. Single faced rotating system with a beamwidth of 2.5°

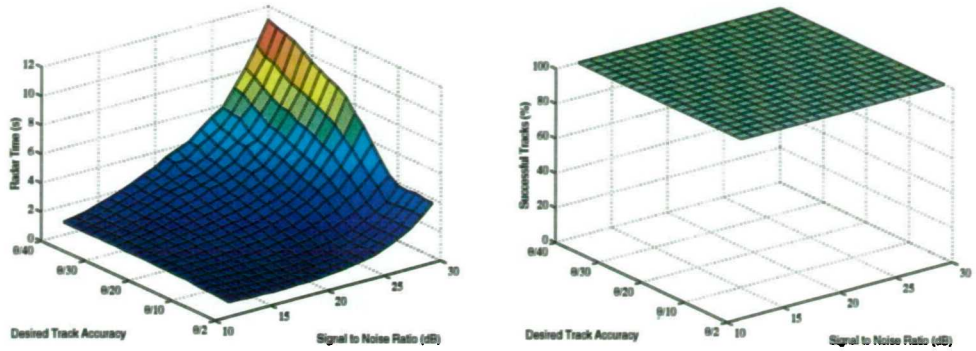

Figure C-13(a,b) Total radar time required to maintain track on Benchmark target trajectory 5, and (b) the percentage of successful tracks. Single faced rotating system with a beamwidth of 2.5°

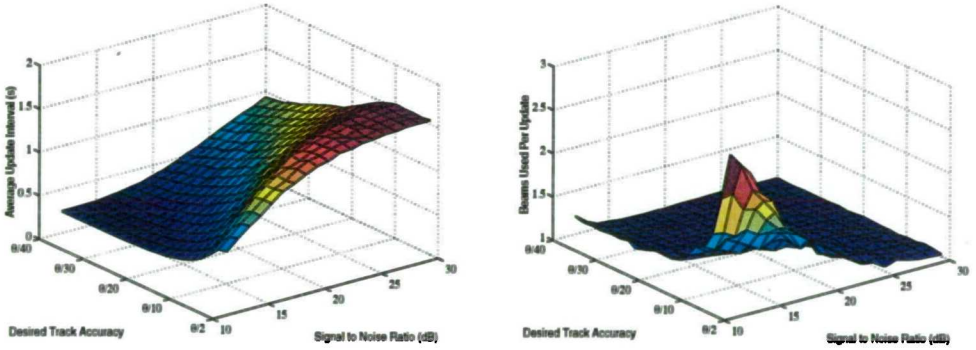

Figure C-14(a,b) Average track update interval required to maintain track on Benchmark target trajectory 5, (b) Average number of beams required for each track update. Single faced rotating system with a beamwidth of 2.5°

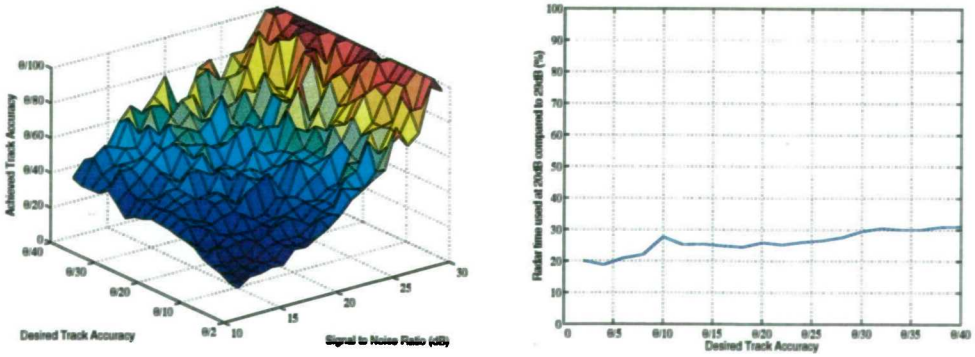

Figure C-15(a,b) Achieved smoothed track accuracy for Benchmark target trajectory 5, excluding periods of manoeuvre, and (b) Percentage of radar time required for tracking Benchmark target trajectory 5 using only a 20dB signal to noise ratio instead of a 29dB signal to noise ratio. Single faced rotating system with a beamwidth of 2.5°

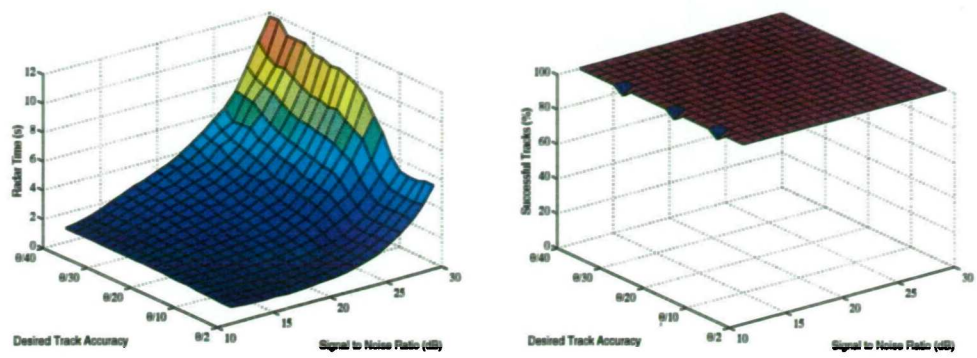

Figure C-16(a,b) Total radar time required to maintain track on Benchmark target trajectory 6, and (b) the percentage of successful tracks. Single faced rotating system with a beamwidth of 2.5°

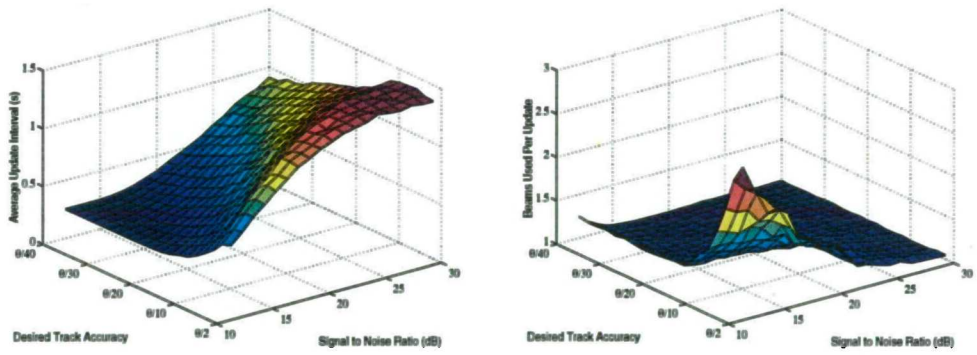

Figure C-17(a,b) Average track update interval required to maintain track on Benchmark target trajectory 6, (b) Average number of beams required for each track update. Single faced rotating system with a beamwidth of 2.5°

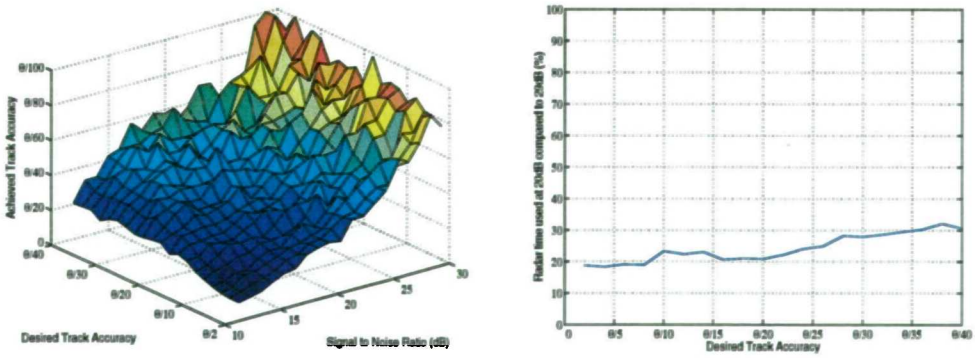

Figure C-18(a,b) Achieved smoothed track accuracy for Benchmark target trajectory 6, excluding periods of manoeuvre, and (b) Percentage of radar time required for tracking Benchmark target trajectory 6 using only a 20dB signal to noise ratio instead of a 29dB signal to noise ratio. Single faced rotating system with a beamwidth of 2.5°

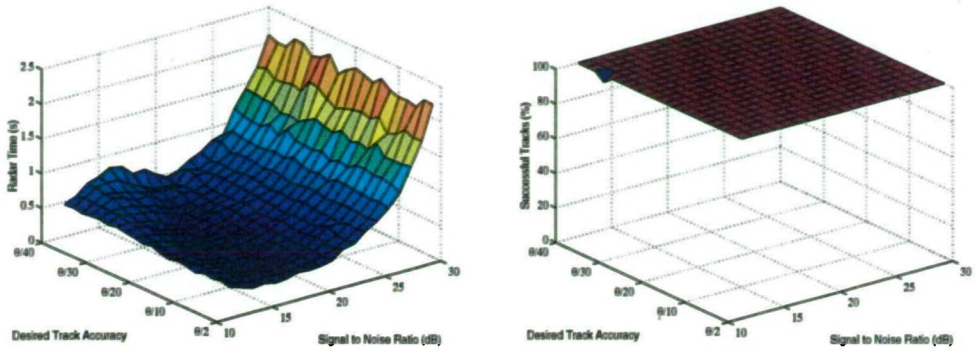

Figure C-19(a,b) Total radar time required to maintain track on the constant velocity trajectory, and (b) the percentage of successful tracks. Single faced rotating system with a beamwidth of 2.5°

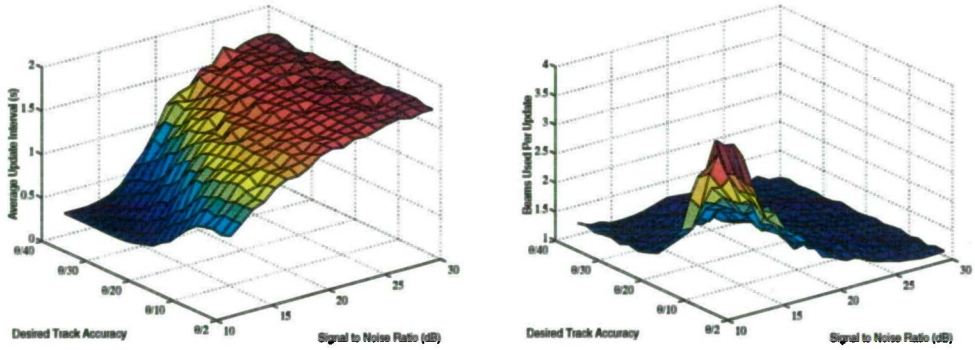

Figure C-20(a,b) Average track update interval required to maintain track on the constant velocity trajectory, (b) Average number of beams required for each track update. Single faced rotating system with a beamwidth of 2.5°

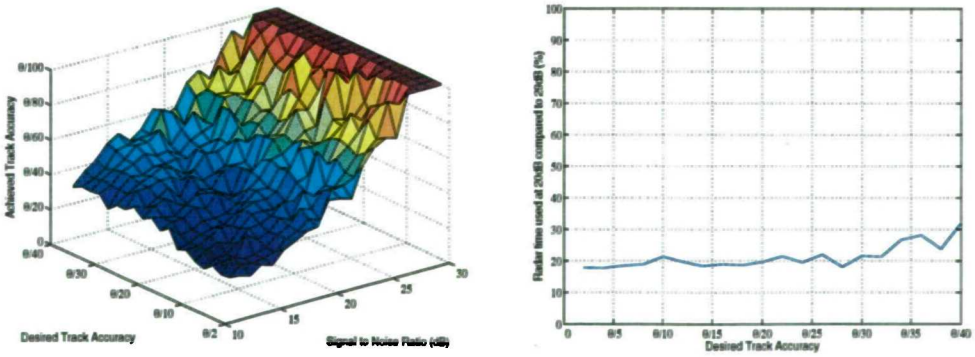

Figure C-21(a,b) Achieved smoothed track accuracy for the constant velocity trajectory, excluding periods of manoeuvre, and (b) Percentage of radar time required for tracking the constant velocity trajectory using only a 20dB signal to noise ratio instead of a 29dB signal to noise ratio. Single faced rotating system with a beamwidth of 2.5°

Single Array Multi-function Radar, Period 2s

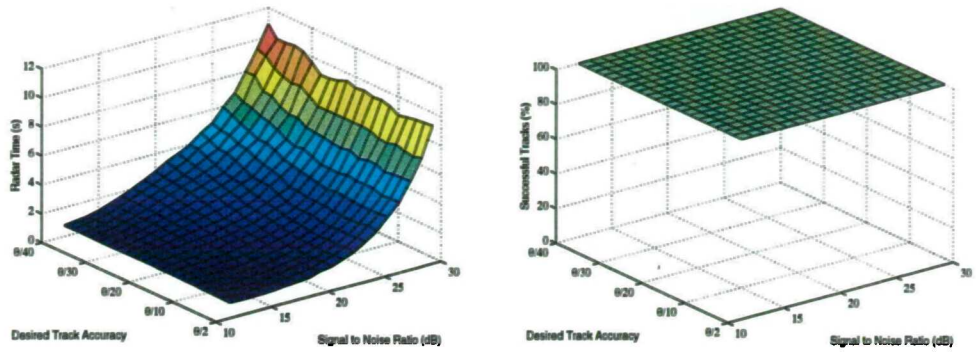

Figure C-22(a,b) Total radar time required to maintain track on Benchmark target trajectory 6, and (b) the percentage of successful tracks. Single faced rotating system with a beamwidth of 2.5°

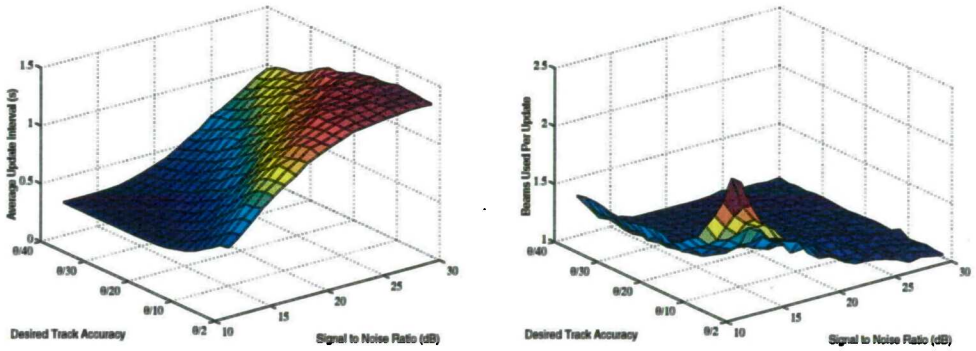

Figure C-23(a,b) Average track update interval required to maintain track on Benchmark target trajectory 6, (b) Average number of beams required for each track update. Single faced rotating system with a beamwidth of 2.5°

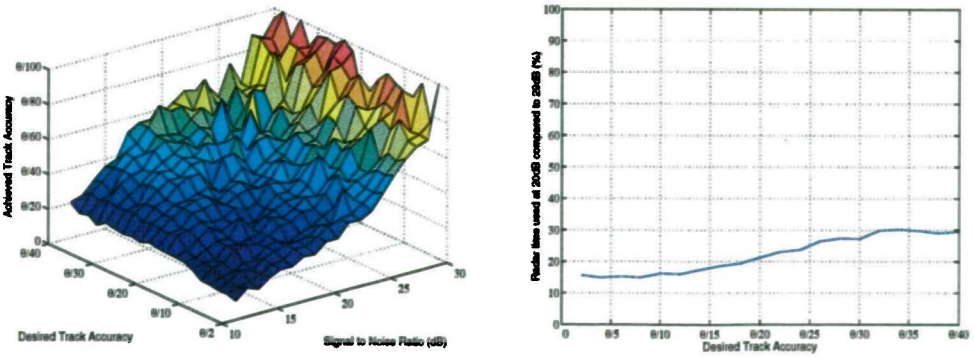

Figure C-24(a,b) Achieved smoothed track accuracy for Benchmark target trajectory 6, excluding periods of manoeuvre, and (b) Percentage of radar time required for tracking Benchmark target trajectory 6 using only a 20dB signal to noise ratio instead of a 29dB signal to noise ratio. Single faced rotating system with a beamwidth of 2.5°

Twin Array Multi-function Radar, Period 1s

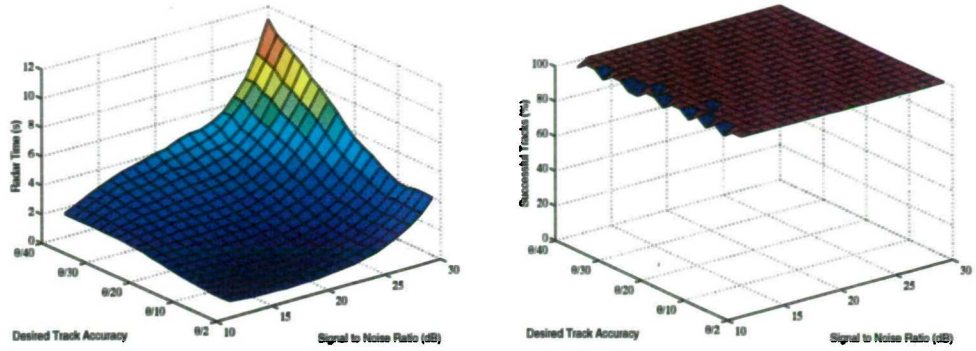

Figure C-25(a,b) Total radar time required to maintain track on Benchmark target trajectory 6, and (b) the percentage of successful tracks. Single faced rotating system with a beamwidth of 2.5°

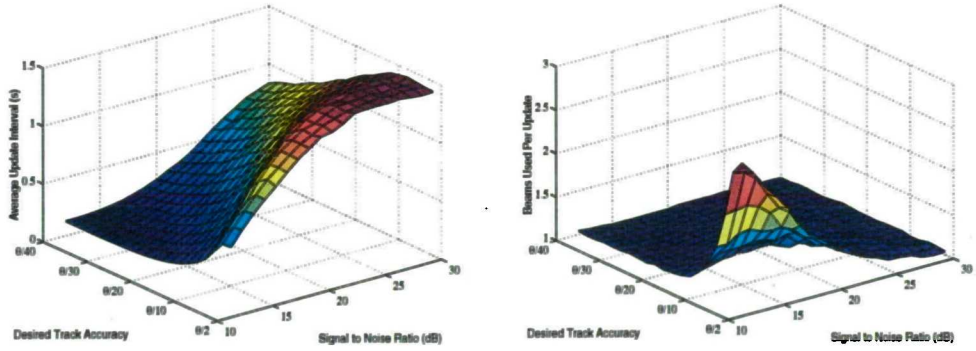

Figure C-26(a,b) Average track update interval required to maintain track on Benchmark target trajectory 6, (b) Average number of beams required for each track update. Single faced rotating system with a beamwidth of 2.5°

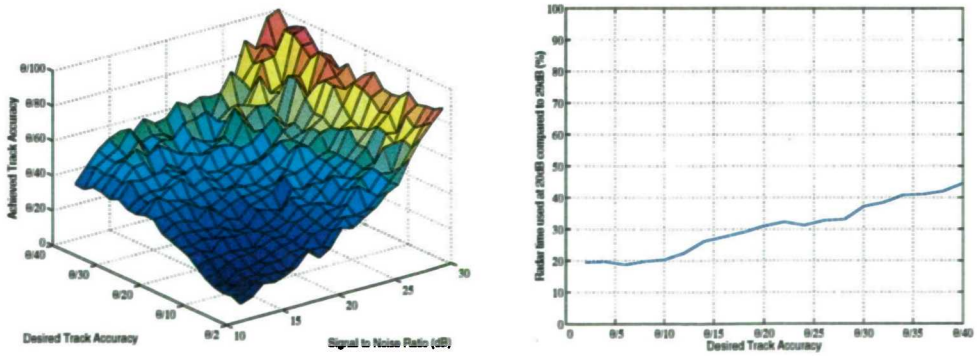

Figure C-27(a,b) Achieved smoothed track accuracy for Benchmark target trajectory 6, excluding periods of manoeuvre, and (b) Percentage of radar time required for tracking Benchmark target trajectory 6 using only a 20dB signal to noise ratio instead of a 29dB signal to noise ratio. Single faced rotating system with a beamwidth of 2.5°

Twin Array Multi-function Radar, Period 2s

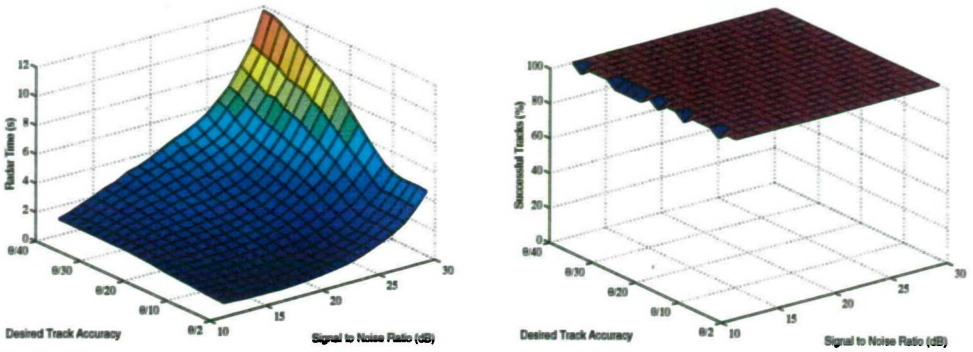

Figure C-28(a,b) Total radar time required to maintain track on Benchmark target trajectory 6, and (b) the percentage of successful tracks. Single faced rotating system with a beamwidth of 2.5°

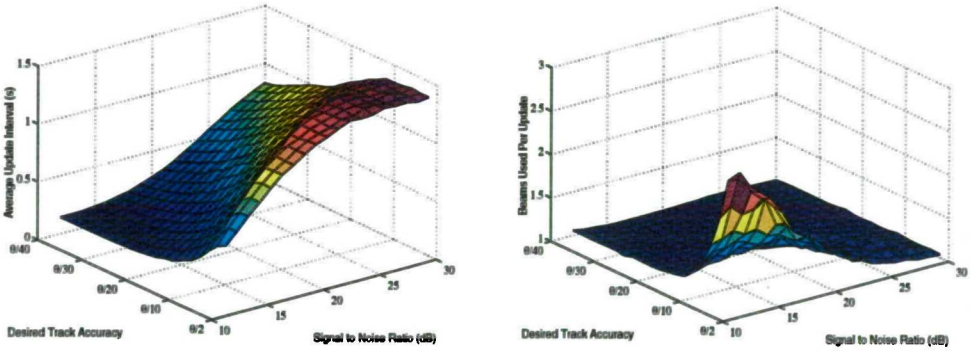

Figure C-29(a,b) Average track update interval required to maintain track on Benchmark target trajectory 6, (b) Average number of beams required for each track update. Single faced rotating system with a beamwidth of 2.5°

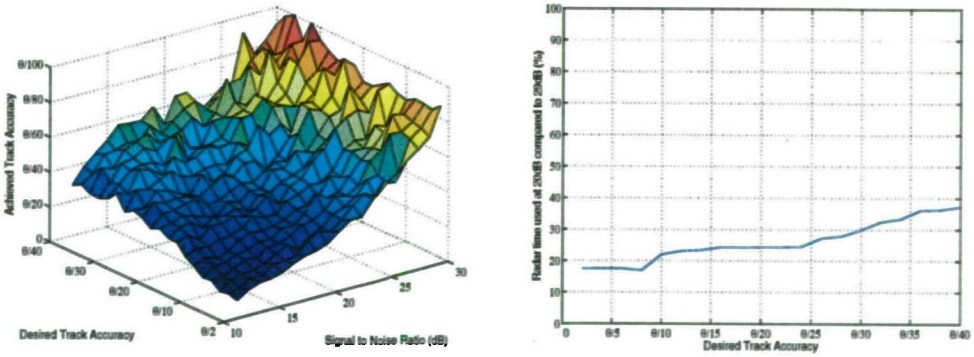

Figure C-30(a,b) Achieved smoothed track accuracy for Benchmark target trajectory 6, excluding periods of manoeuvre, and (b) Percentage of radar time required for tracking Benchmark target trajectory 6 using only a 20dB signal to noise ratio instead of a 29dB signal to noise ratio. Single faced rotating system with a beamwidth of 2.5°